Dark Matter: Galaxy Formation, Small Scale Crisis, and WDM

N. Menci
Osservatorio Astronomico di Roma - INAF

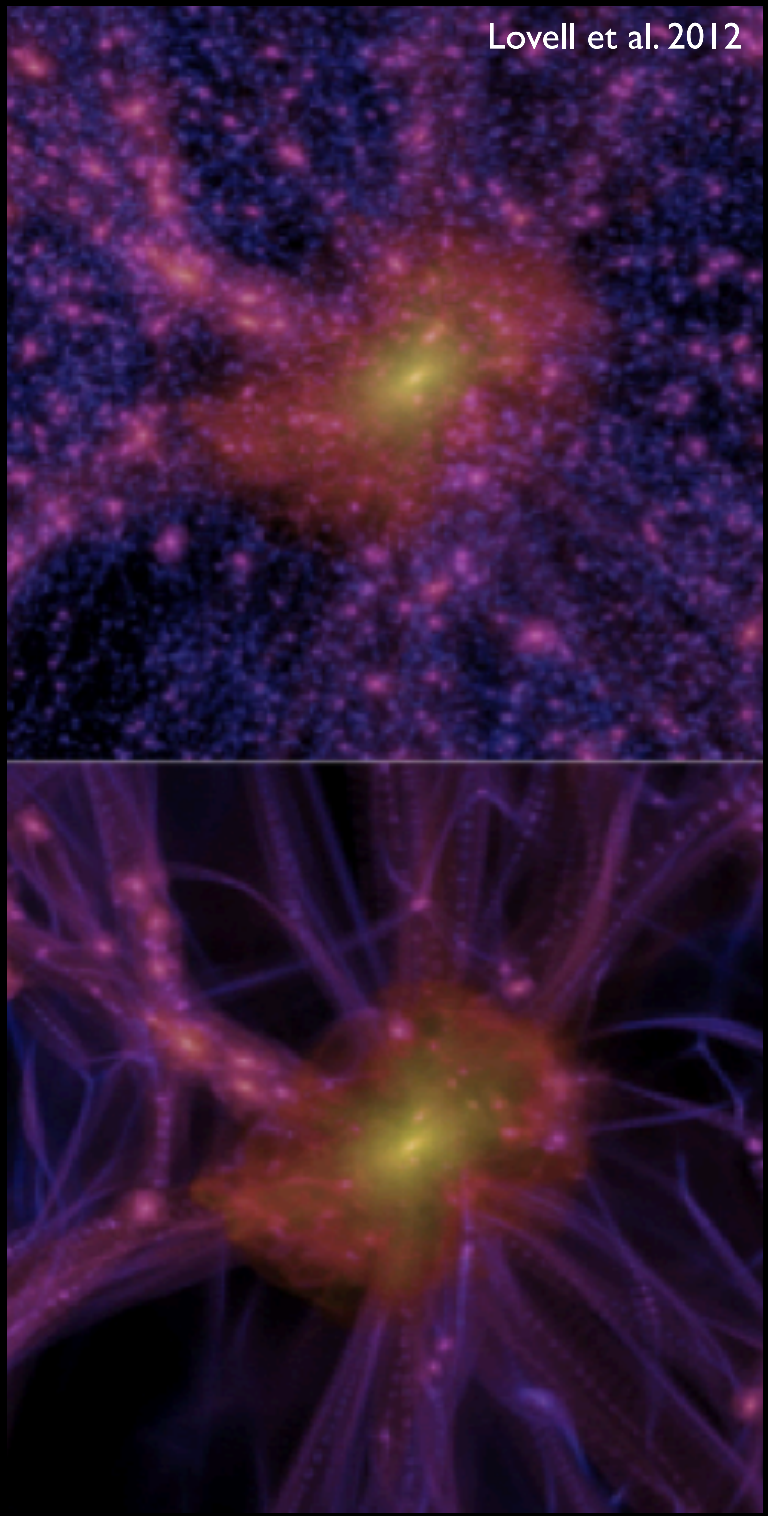

Outline

"Ab Initio" Galaxy Formation in DM dominated Universe
- Power Spectrum
- Free Streaming Scale
- Connecting baryon physics to DM haloes: semi-analytic models

Galaxy Formation in Cold Dark Matter:
- Basic properties
- The small-scale crisis: Galaxies and AGN
- Feedback scale
- Is baryon physics a solution ?

Galaxy Formation in Warm Dark Matter scenarios
- Galaxy and AGN luminosity functions
- The luminosity function of satellites
- Hints from abundance matching: the V_{max}-M_* relation

Galaxies are the tip of the iceberg (underlying DM distribution)

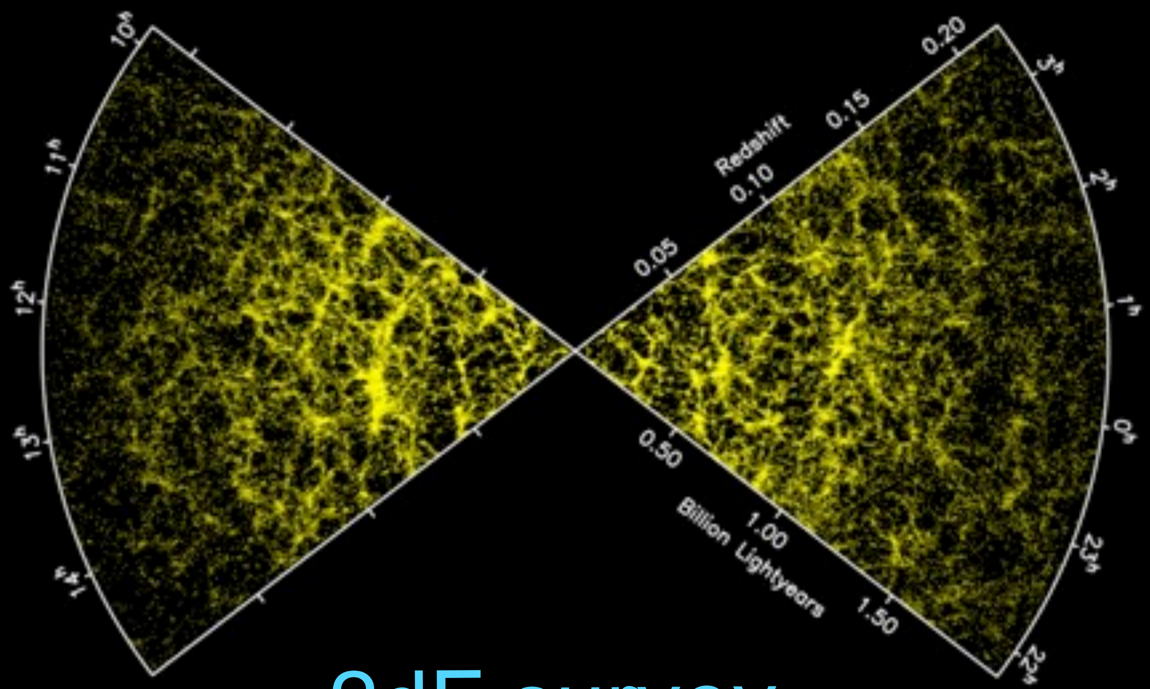

2dF survey

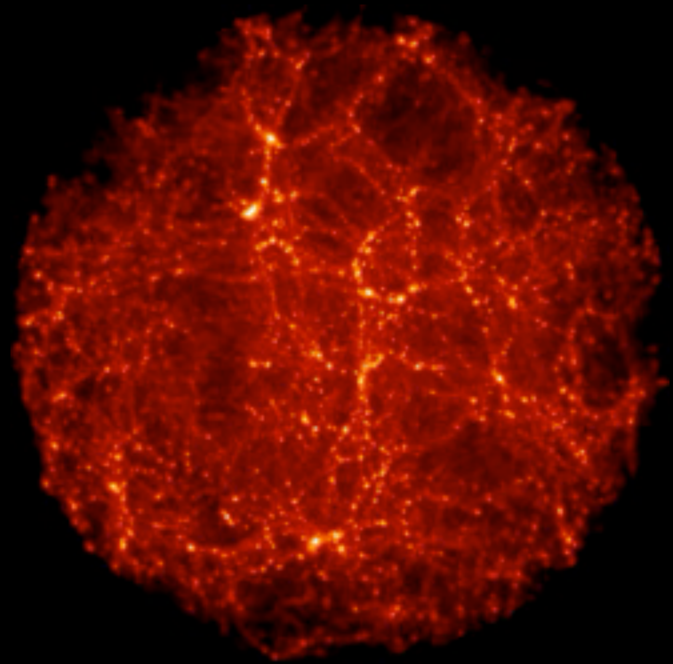

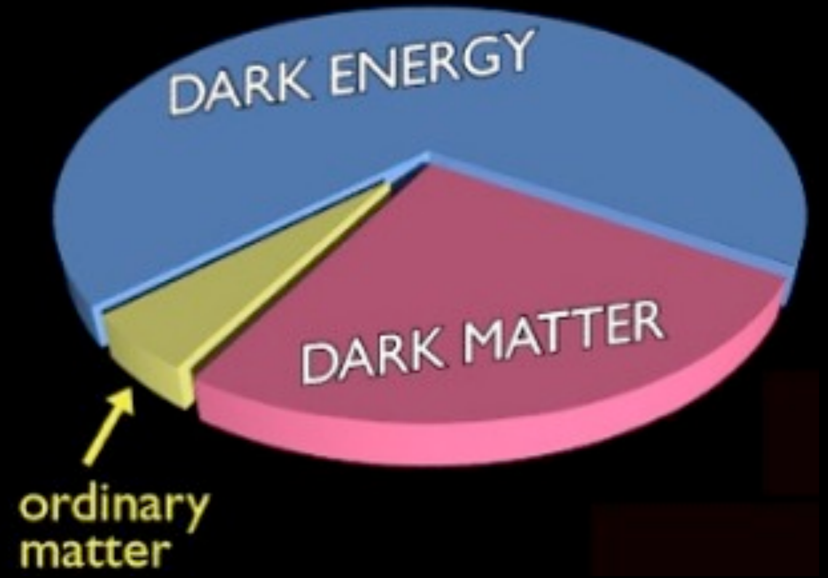

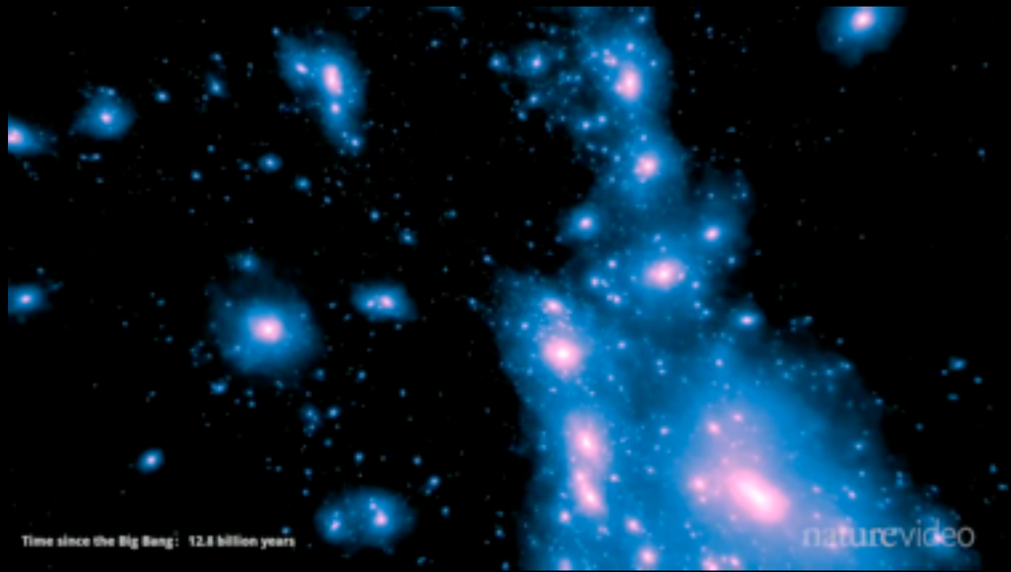

Galaxies are the tip of the iceberg (underlying DM distribution)

Galaxy Formation Theory

Describe the collapse and evolution of the DM clumps dominating the gravitational dynamics

Connect properties of ordinary matter (gas physics, star formation,astrophysical processes) to the potential wells of DM condensations

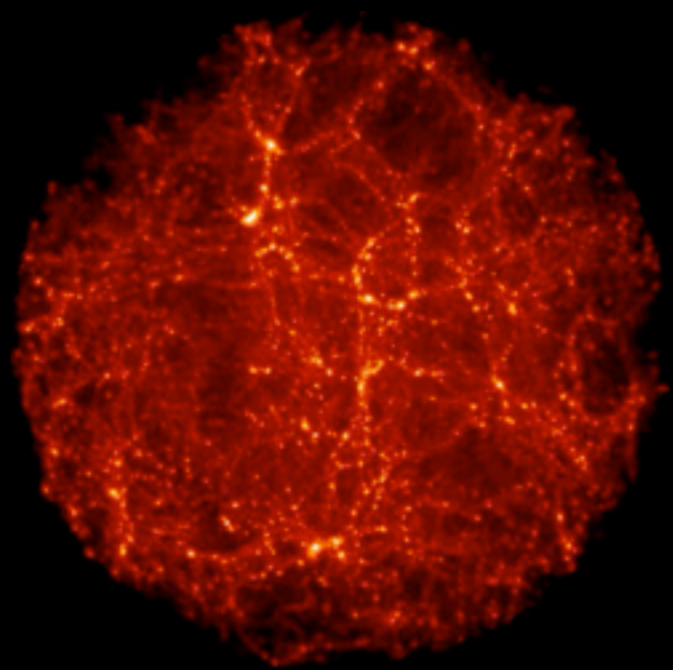

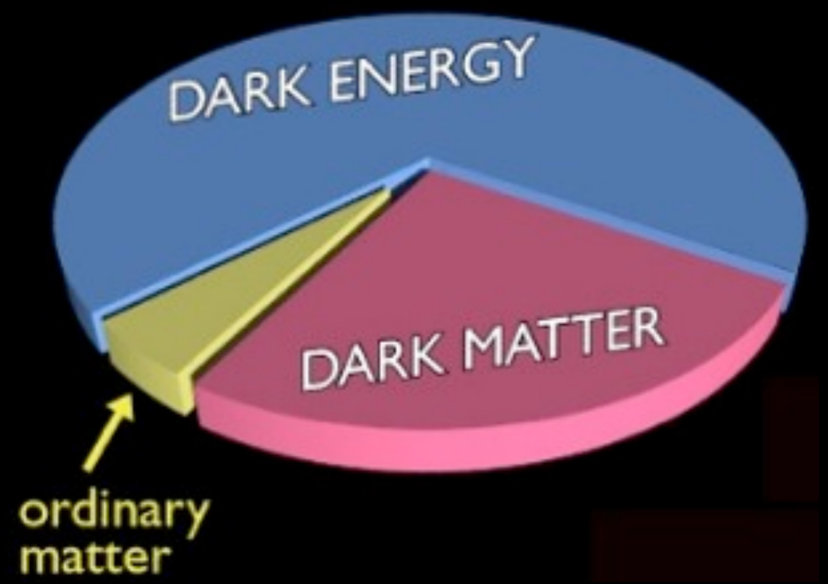

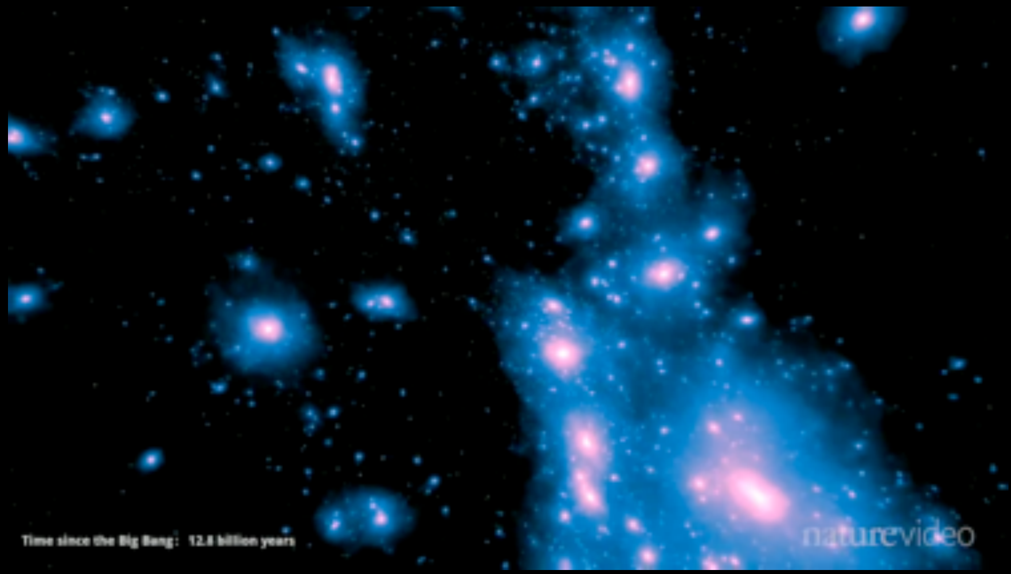

Galaxies are the tip of the iceberg (underlying DM distribution)

Galaxy Formation Theory

Describe the collapse and evolution of the DM clumps dominating the gravitational dynamics

Connect properties of ordinary matter (gas physics, star formation,astrophysical processes) to the potential wells of DM condensations

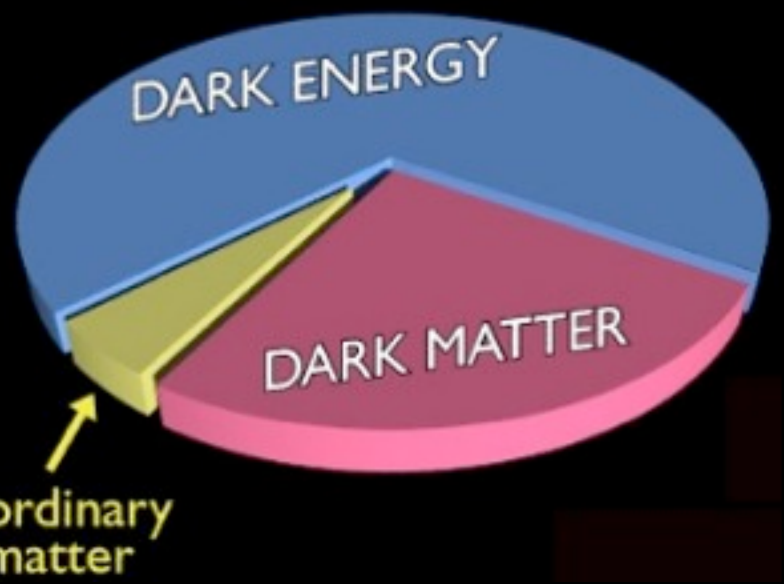

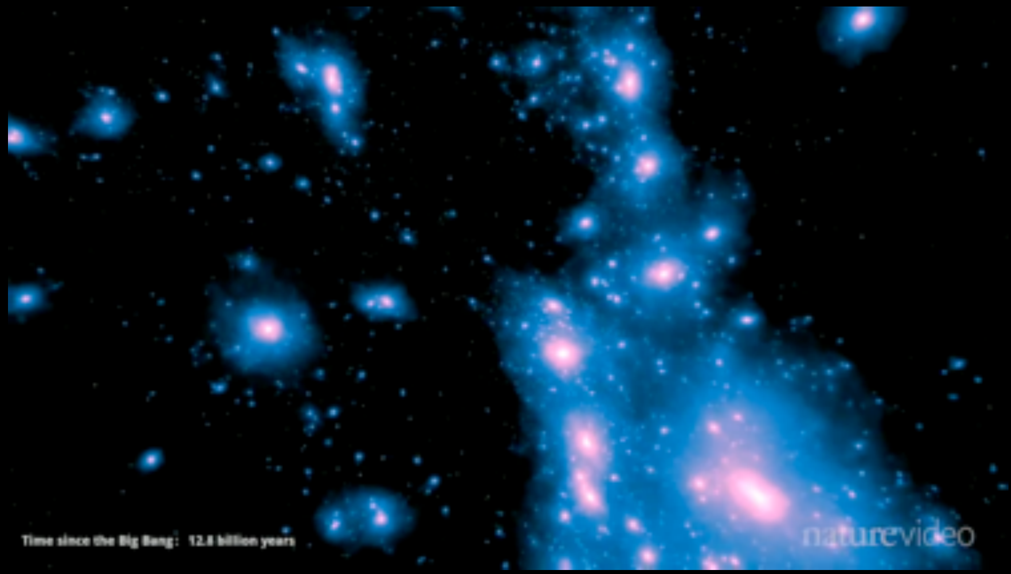

Galaxies are the tip of the iceberg (underlying DM distribution)

Diemand et al. 2008

Galaxy Formation Theory

Describe the collapse and evolution of the DM clumps dominating the gravitational dynamics

Connect properties of ordinary matter (gas physics, star formation,astrophysical processes) to the potential wells of DM condensations

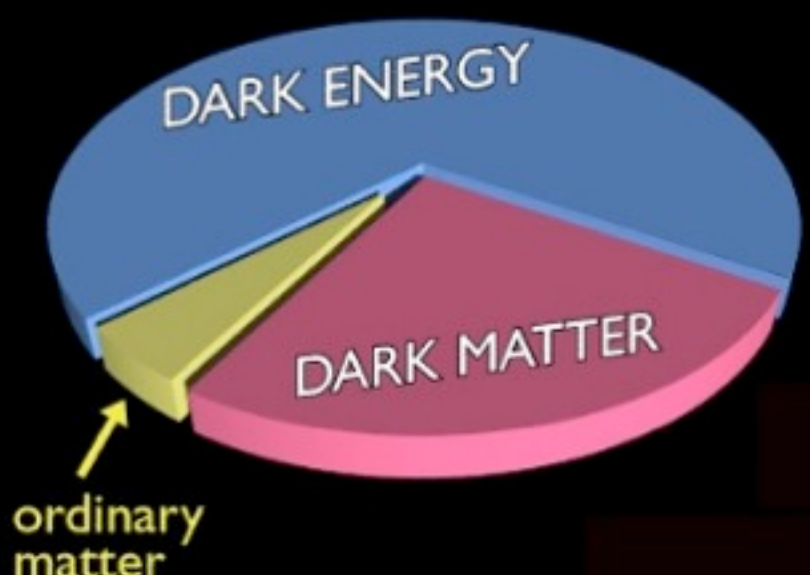

Cosmic Structures form from the collapse of overdense regions in the DM primordial density field, and grow by gravitational instability

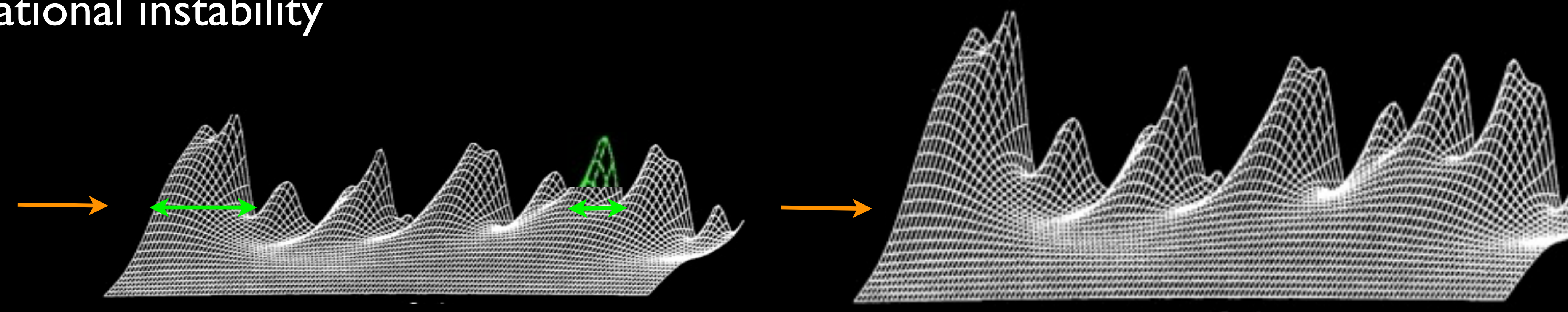

$R=2\pi/k$

$$M = \frac{4\,\pi}{3}\rho\, R^3$$

$$\langle \delta_M^2 \rangle = \sigma^2(M)\, g(t)$$

Gaussian Random field

$$\delta = \frac{\delta\rho}{\rho}$$

$$p(\delta_k) = \frac{1}{\sqrt{2\pi}\,\sigma_k}\, e^{\frac{\delta_k^2}{2\,\sigma_k^2}}$$

Mean (square) value of perturbations of size R(~1/k) enclosing a mass M

$$P(k) = \frac{1}{V}\langle|\delta_k|^2\rangle$$

$$\sigma_M^2 = \frac{1}{(2\pi)^3\, V}\int^{M\leftrightarrow k} dk\, k^2\, P(k)$$

$$\sigma_M^2 \leftrightarrow P(k)$$

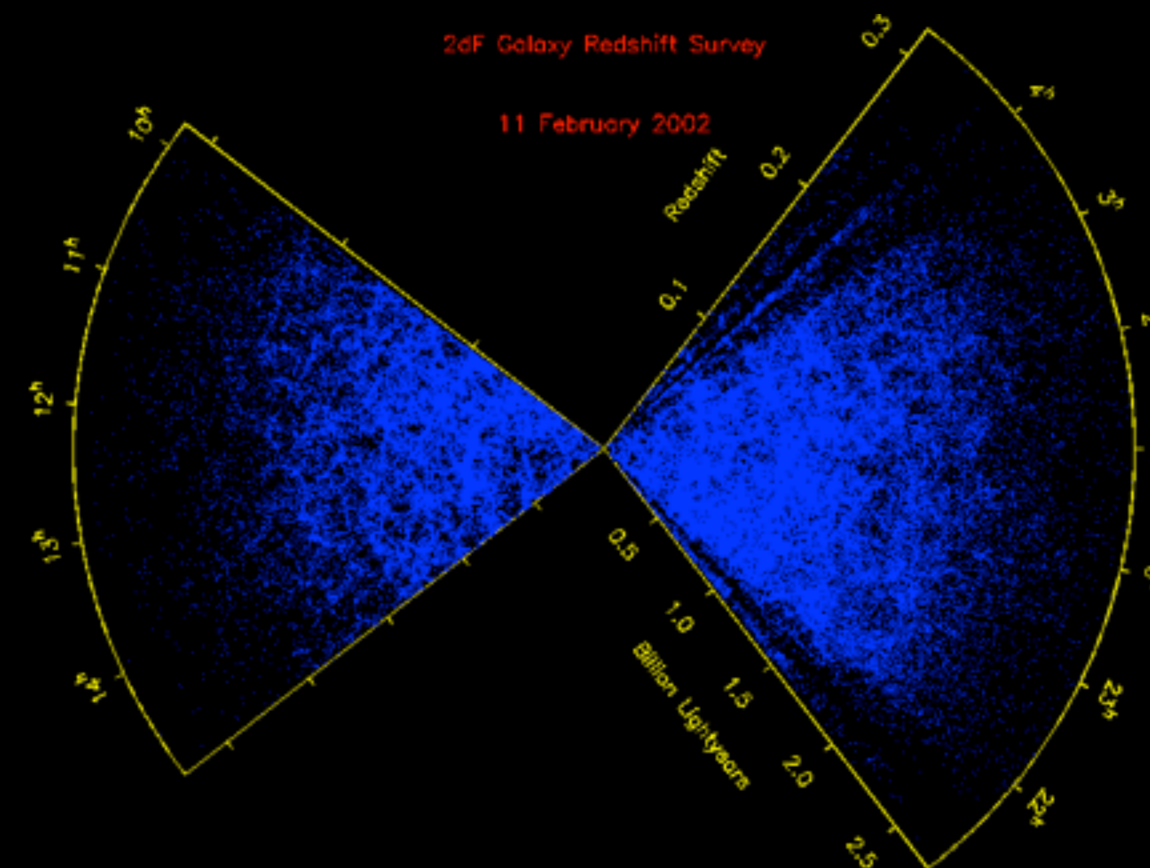

Cosmic Structures form from the collapse of overdense regions in the DM primordial density field, and grow by gravitational instability

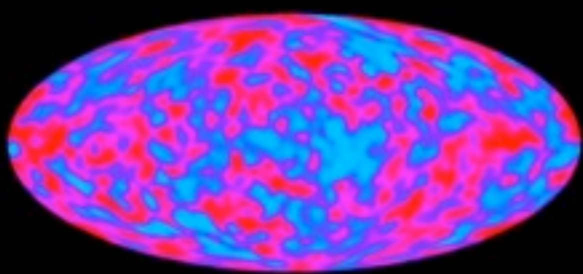

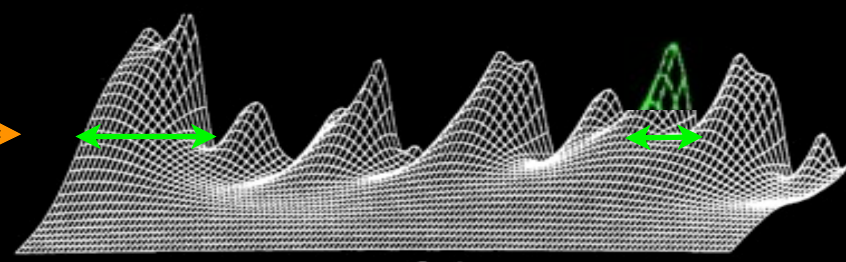

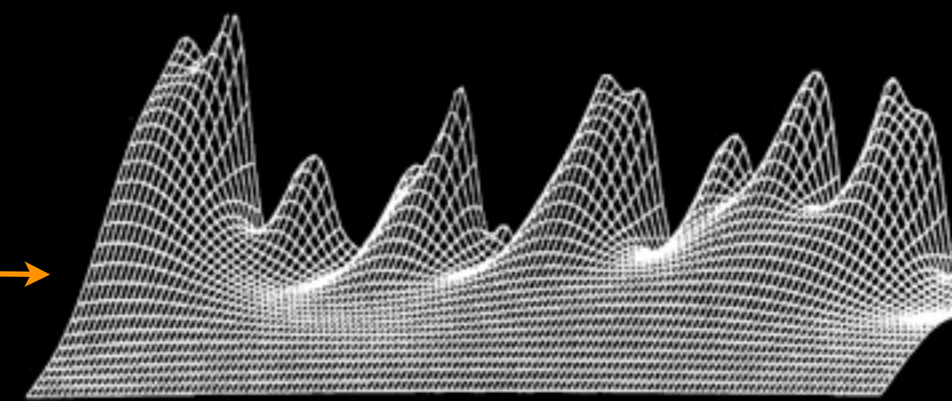

$R=2\pi/k$

$$M = \frac{4\,\pi}{3}\rho\, R^3$$

$$\langle \delta_M^2 \rangle = \sigma^2(M)\, g(t)$$

Gaussian Random field

$$\delta = \frac{\delta\rho}{\rho}$$

$$p(\delta_k) = \frac{1}{\sqrt{2\pi}\,\sigma_k}\, e^{\frac{\delta_k^2}{2\,\sigma_k^2}}$$

Mean (square) value of perturbations of size R(~1/k) enclosing a mass M

$$P(k) = \frac{1}{V}\,\langle|\delta_k|^2\rangle$$

$$\sigma_M^2 = \frac{1}{(2\pi)^3\,V}\int^{M\leftrightarrow k} dk\, k^2\, P(k)$$

$$\sigma_M^2 \leftrightarrow P(k)$$

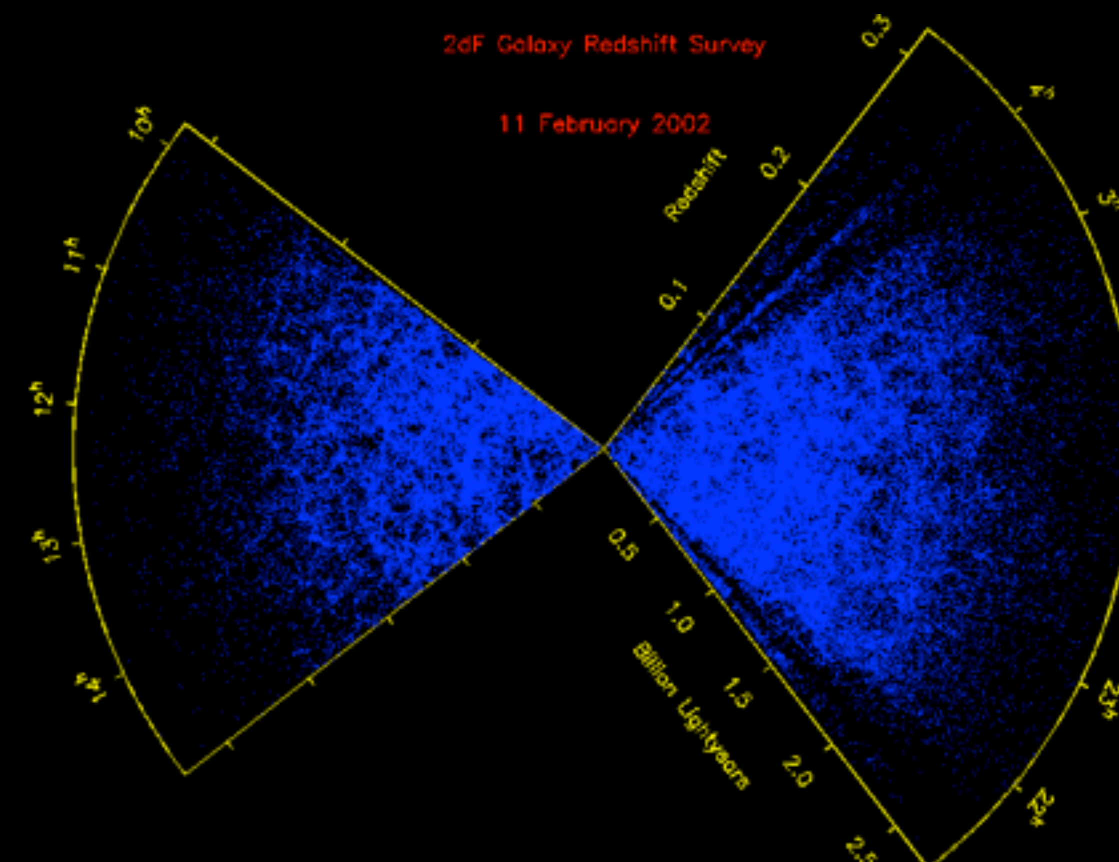

The Variance of the perturbation field

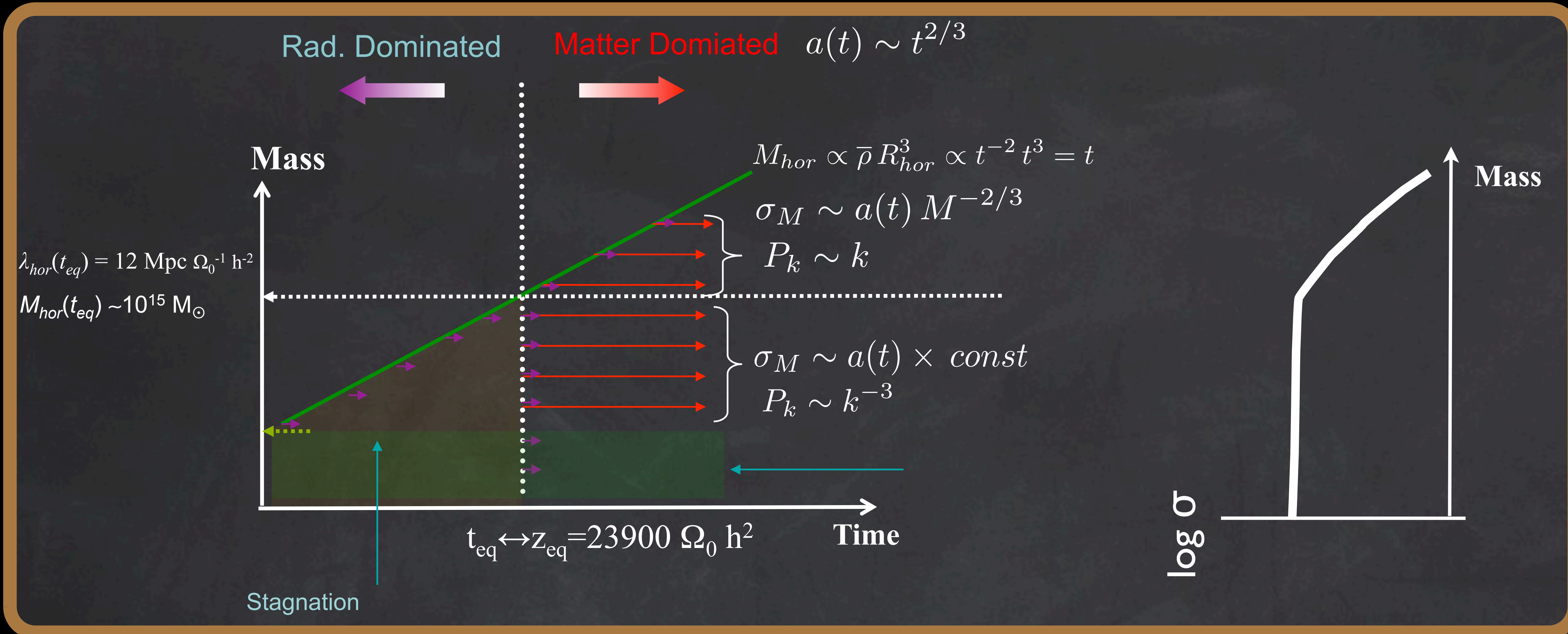

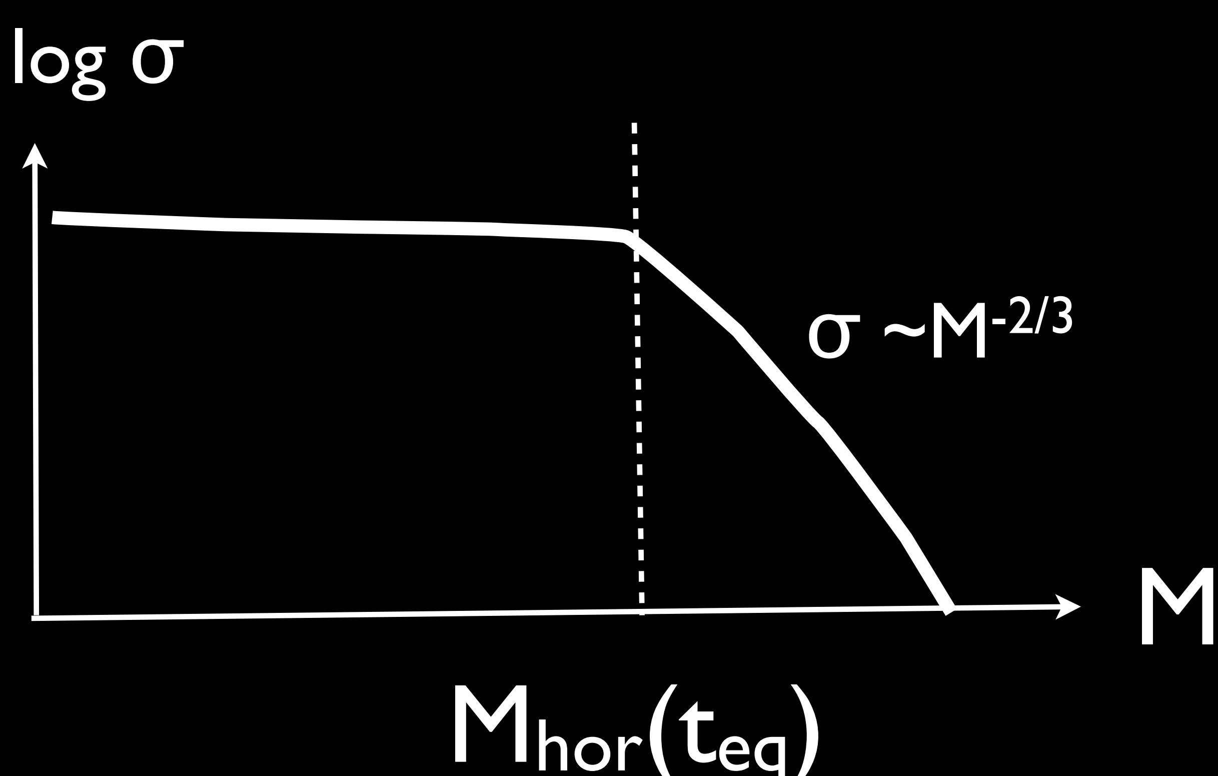

Perturbations involving scales larger than that of the horizon at the equivalence start to grow later

$R_{hor} = 2c\, t_{hor} = 13\ h^{-2}$ *Mpc*
$= 110$ Mpc for $\sigma_0 = 0.3$ $h = 0.7$

In terms of wavenumber k→Power Spectrum

$$\sigma_M^2 = \frac{1}{(2\pi)^3 V} \int^{M \leftrightarrow k} dk\, k^2\, P(k)$$

$$P(k) = \langle |\delta_k|^2 \rangle$$

$$\sigma_M \propto M^{-2/3} \qquad P(k) \propto k$$

$$\sigma_M = const \qquad P(k) \propto k^{-3}$$

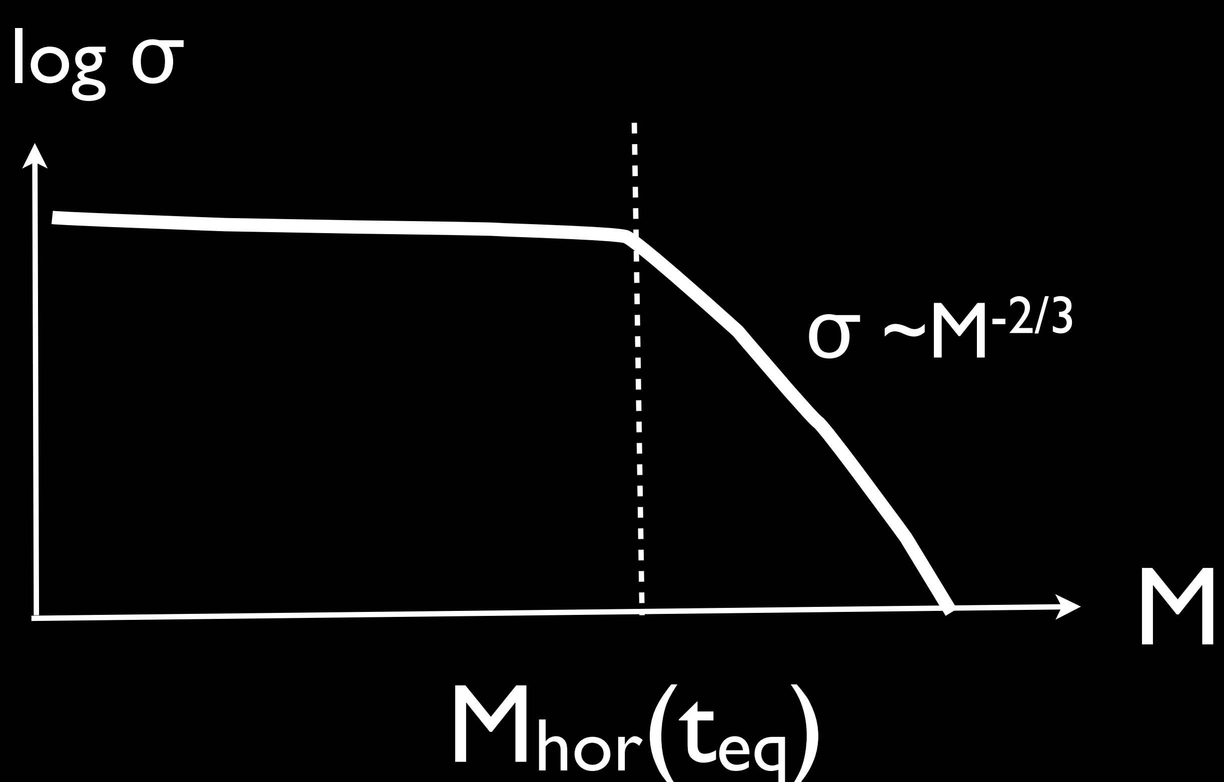

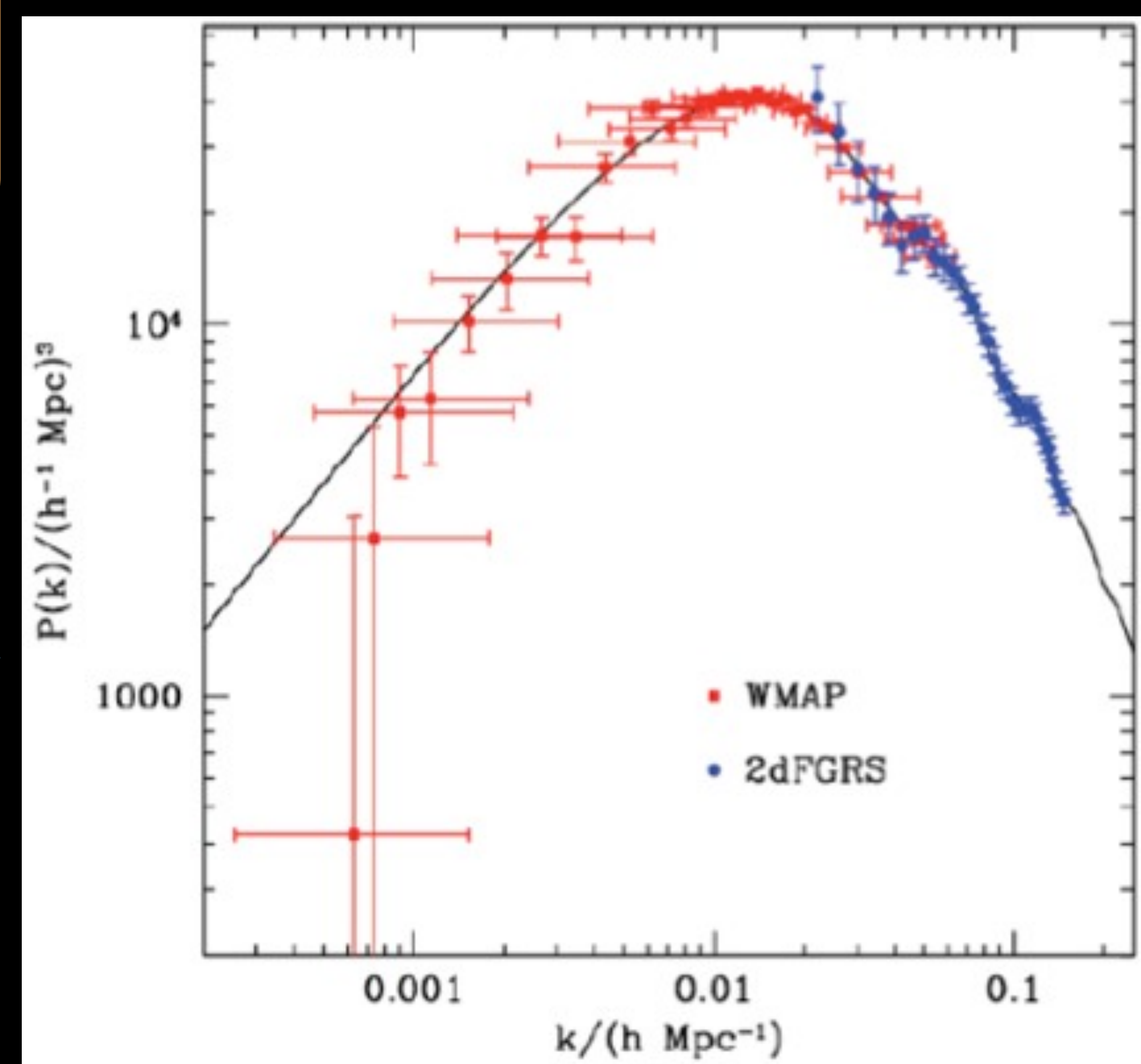

The evolution of DM perturbation

Initial density perturbations constitute a random Gaussian field.

Measurements of the CMB show that its variance is inversely related to their mass scale.

This implies that small scales collapse - on average - at earlier times

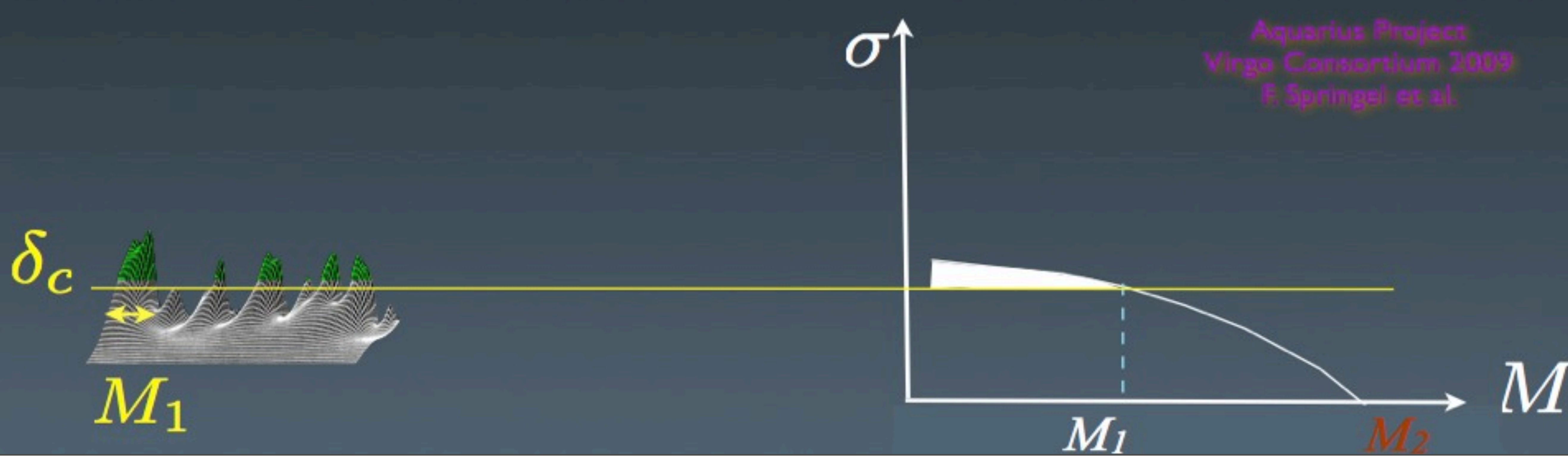

The evolution of DM perturbation

Initial density perturbations constitute a random Gaussian field.

Measurements of the CMB show that its variance is inversely related to their mass scale.

This implies that small scales collapse - on average - at earlier times

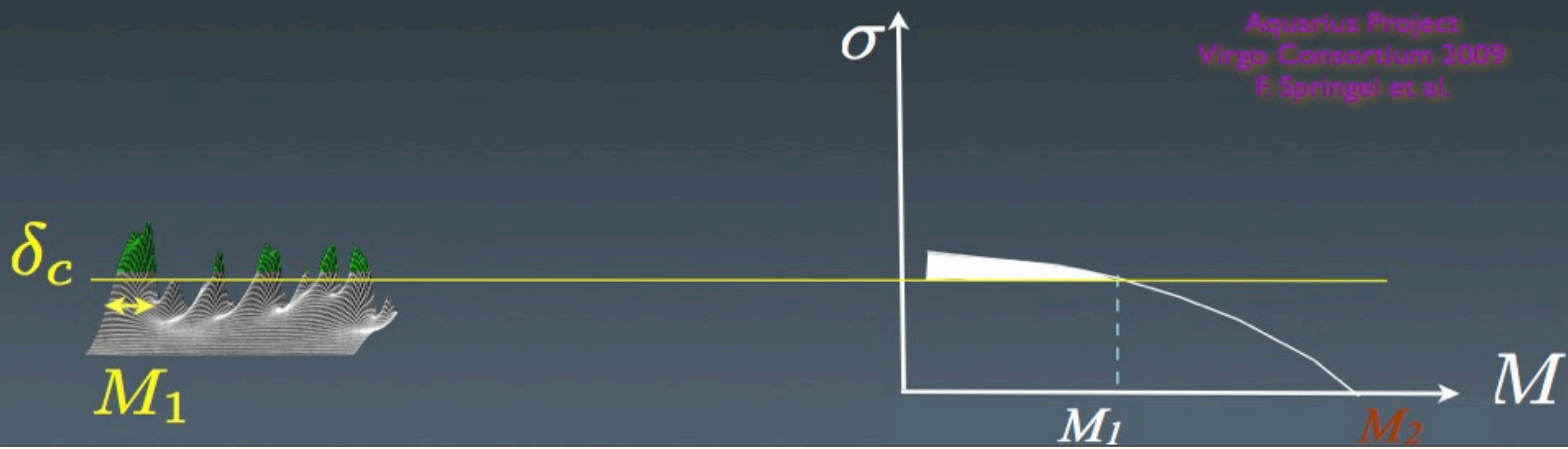

The evolution of DM perturbation

Initial density perturbations constitute a random Gaussian field.

Measurements of the CMB show that its variance is inversely related to their mass scale.

This implies that small scales collapse - on average - at earlier times

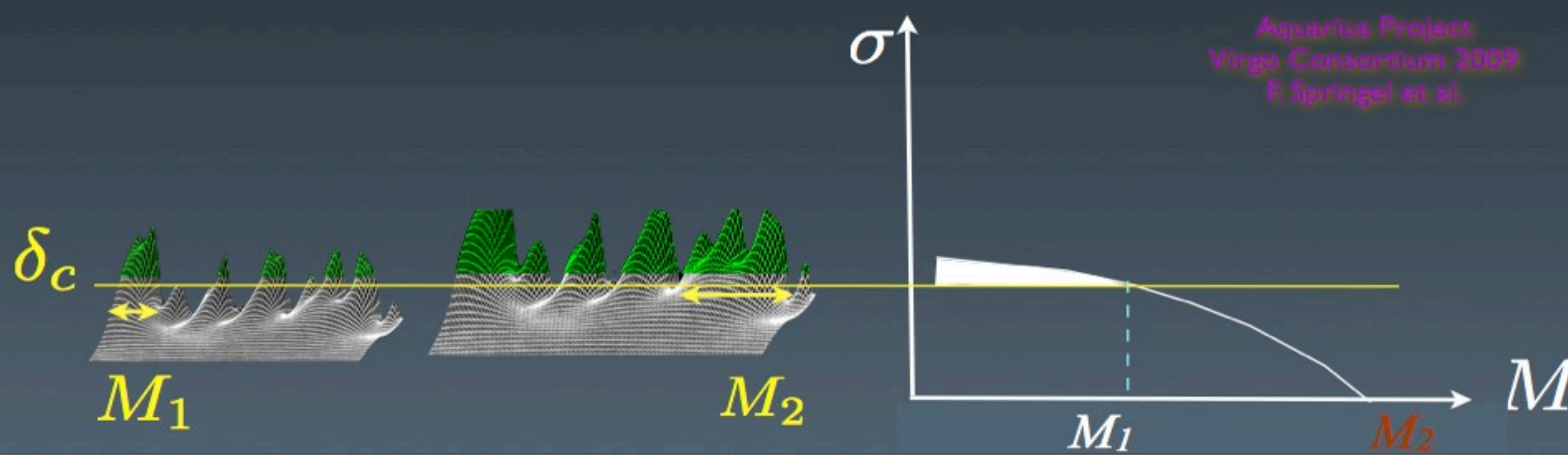

The evolution of DM perturbation

Initial density perturbations constitute a random Gaussian field.

Measurements of the CMB show that its variance is inversely related to their mass scale.

This implies that small scales collapse - on average - at earlier times

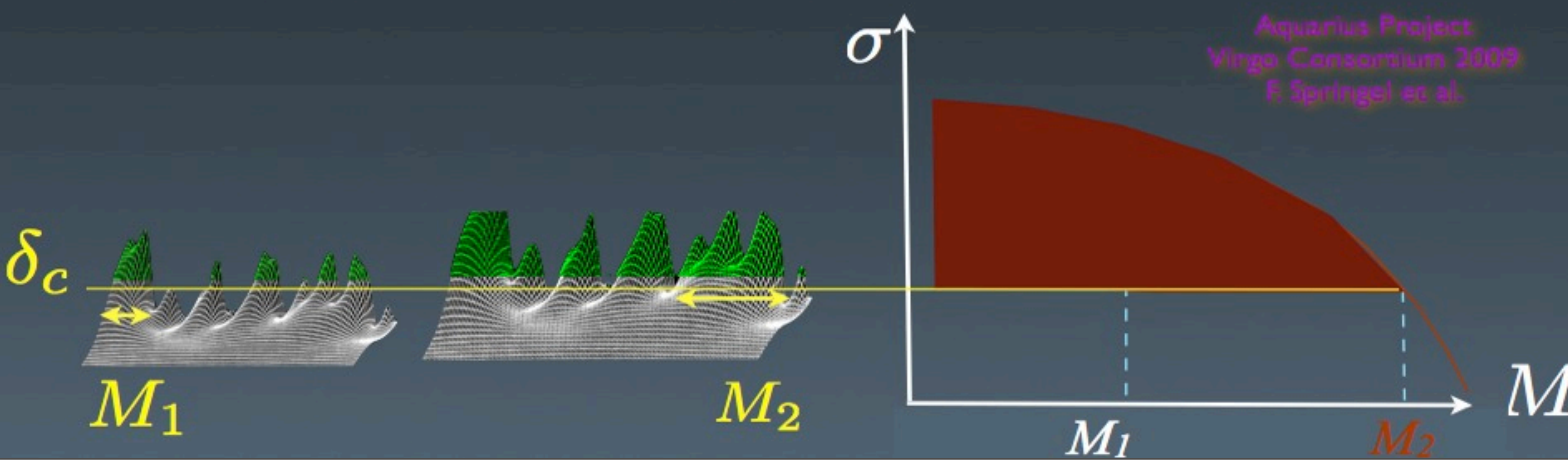

Dissipation, free-streaming scale

$$r_{fs} = \int_0^t \frac{v(t)}{R(t)}$$

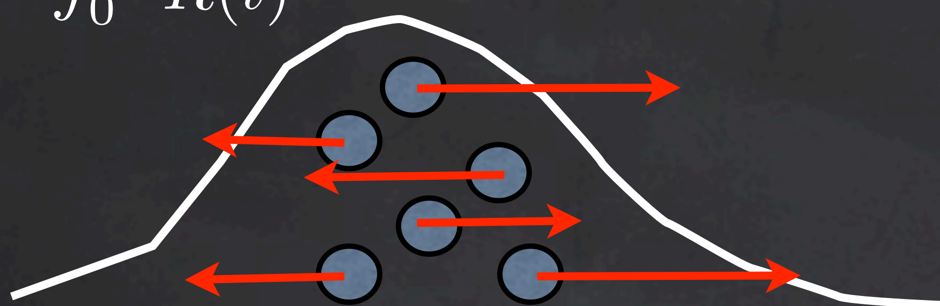

$$\sigma_\chi \propto a^{-1}\, m_\chi^{-1/2}$$

$$M_{fs} = 4 \times 10^{15} \left(\frac{m_\nu}{30\ \mathrm{eV}} \right)^{-2} M_\odot$$

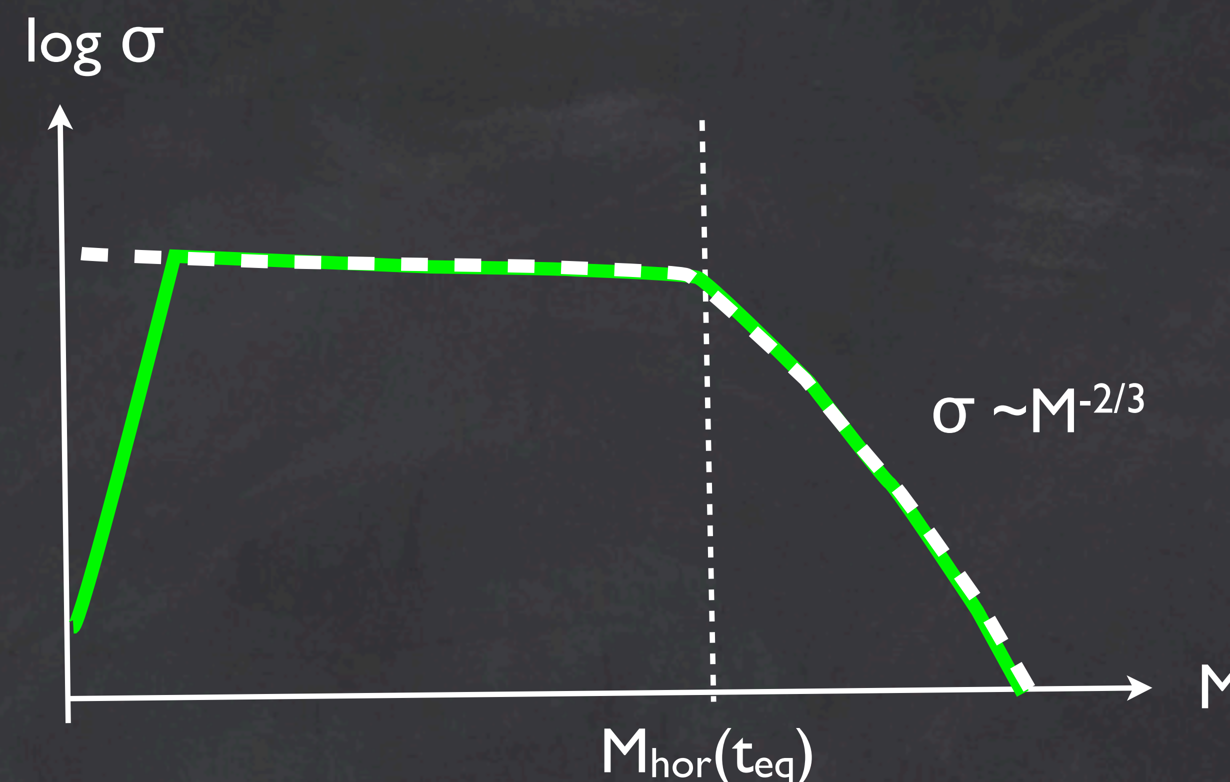

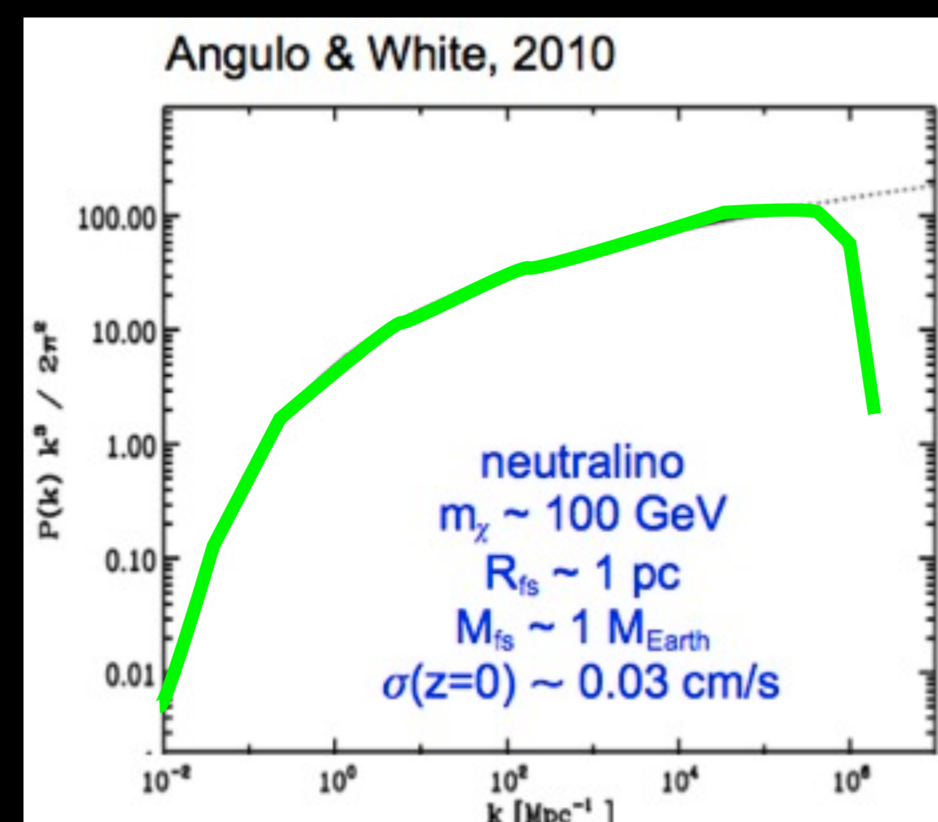

Dissipation, free-streaming scale

$$r_{fs} = \int_0^t \frac{v(t)}{R(t)}$$

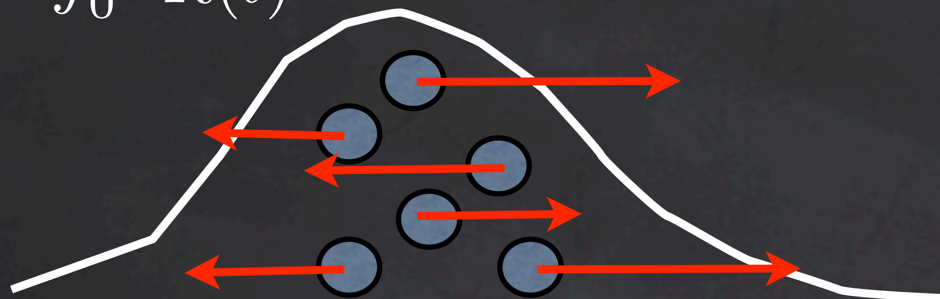

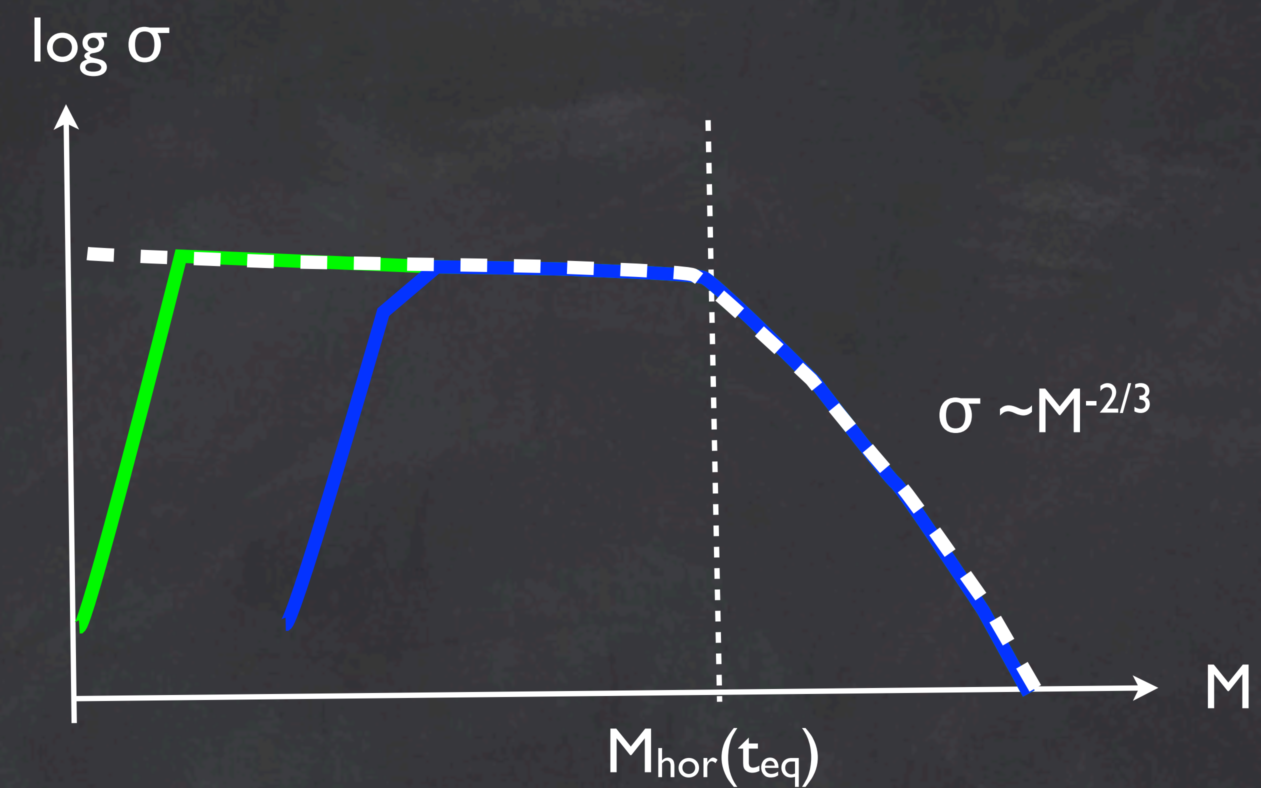

$$\sigma_\chi \propto a^{-1}\, m_\chi^{-1/2}$$

$$M_{fs} = 4 \times 10^{15} \left(\frac{m_\nu}{30\ \mathrm{eV}}\right)^{-2} M_\odot$$

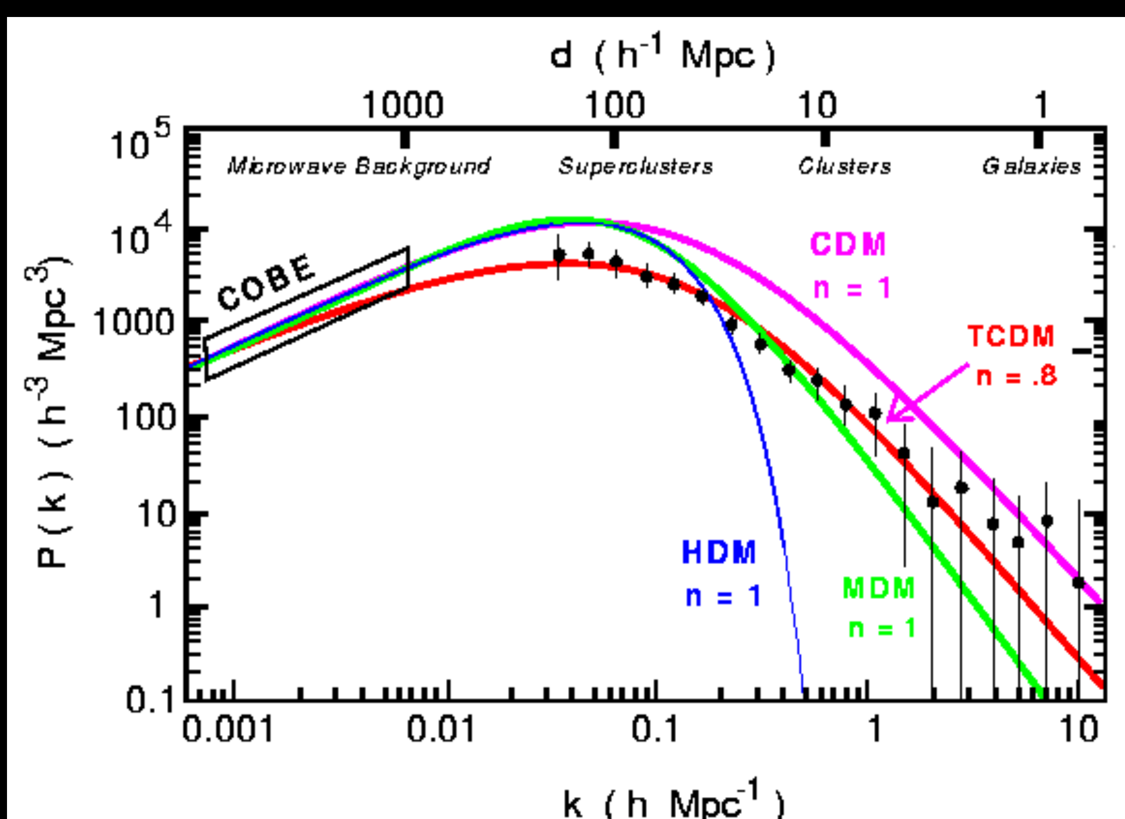

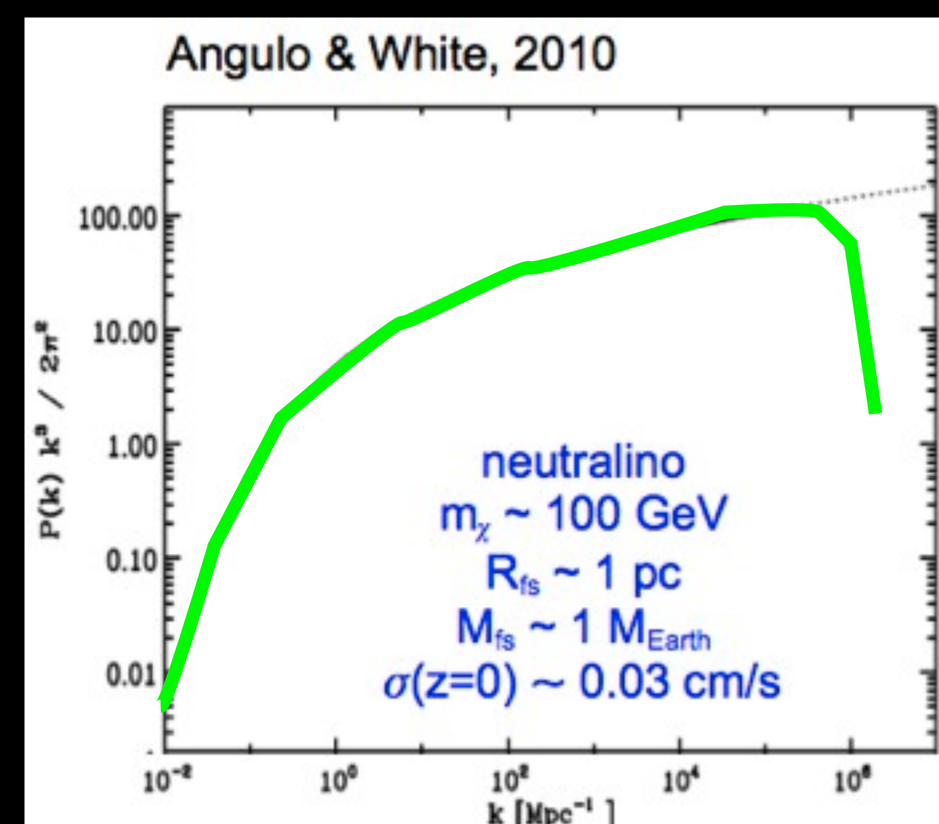

Varying the particle mass

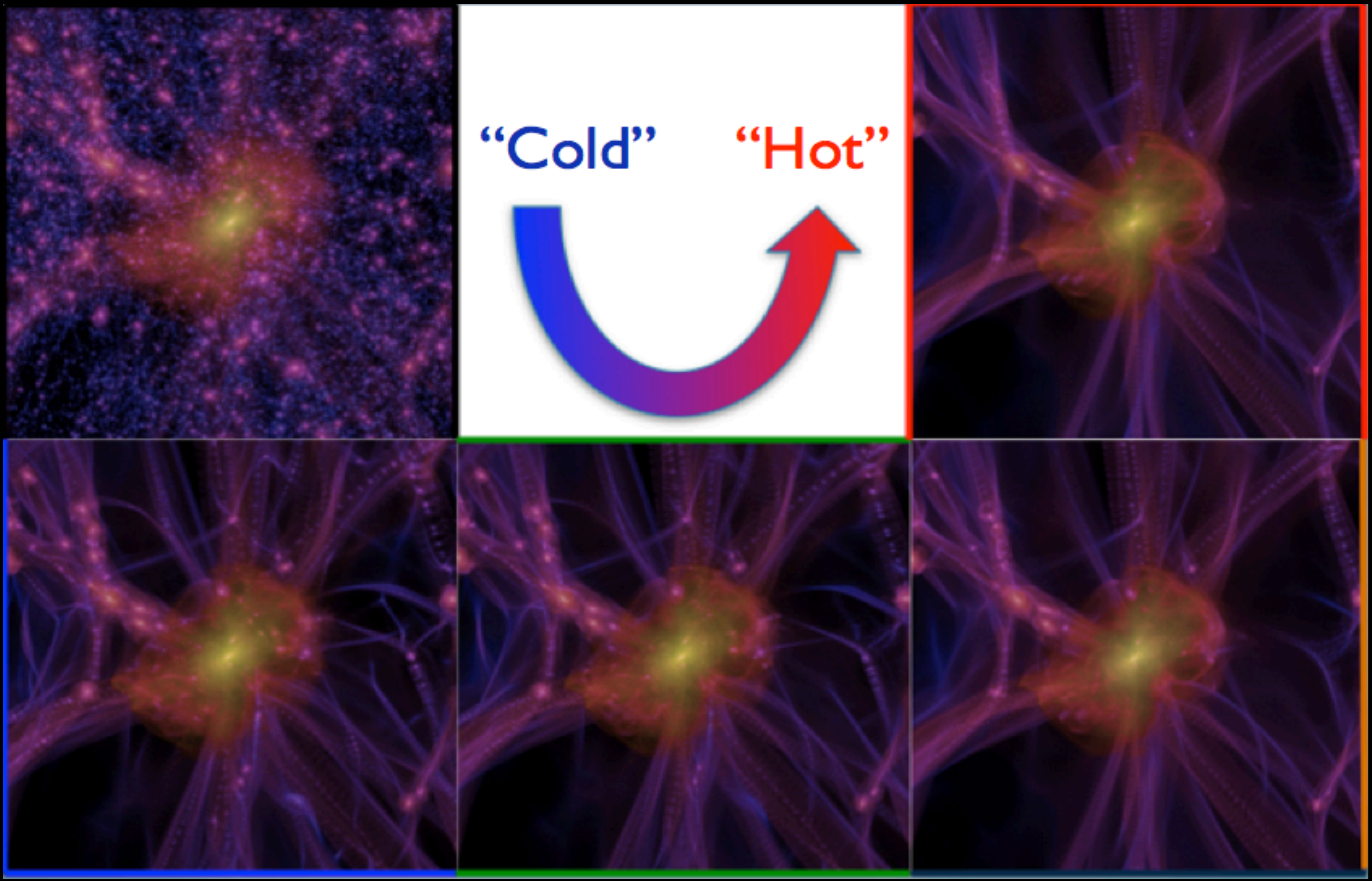

Lovell et al. 2012

What' so cold about CDM

For "thermal relics" such as neutrinos, it is relatively straightforward to compute their present day abundance. Neutrinos relativistic at decoupling → large velocity dispersion.

Candidates for "Hot Dark Matter" -- ruled out by observation.

CDM: Velocity dispersion assumed to be vanishingly small

limit M_{fs} << Masses of Cosmological Relevance

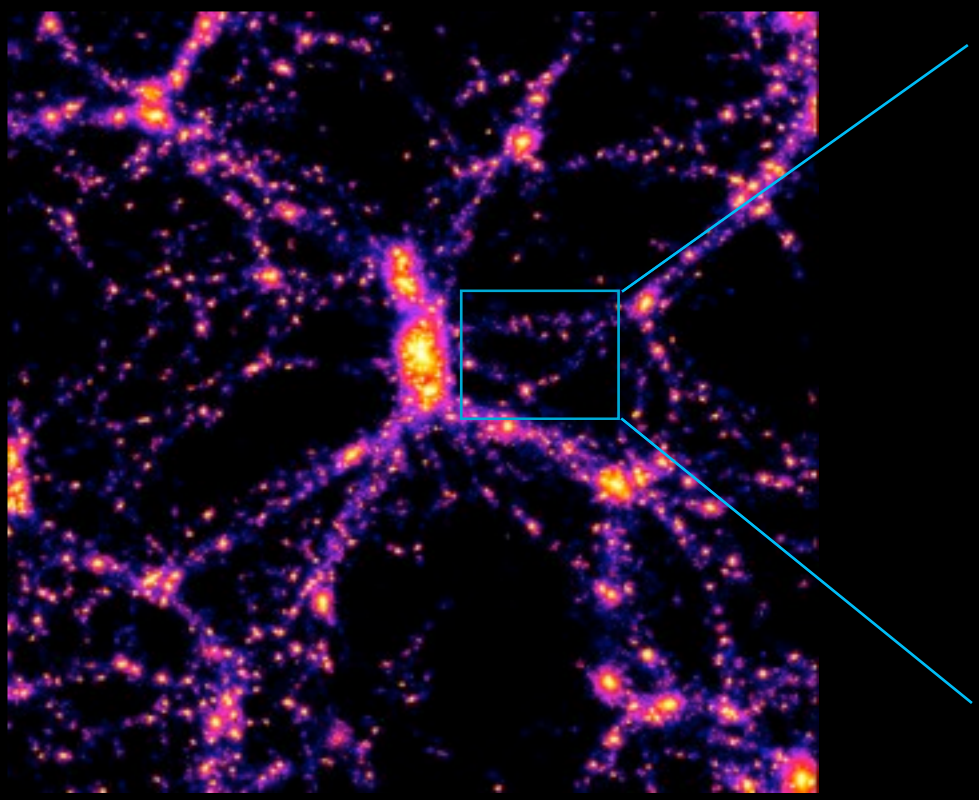

Testing the COLD DARK MATTER scenario against observations: the evolution of galaxies

Requires modelling of baryon physics inside evolving DM potential wells

- gas physis (cooling, heating)
- disk formation
- star formation
-evolution of the stellar population
- injection of energy into the gas
  from SNae

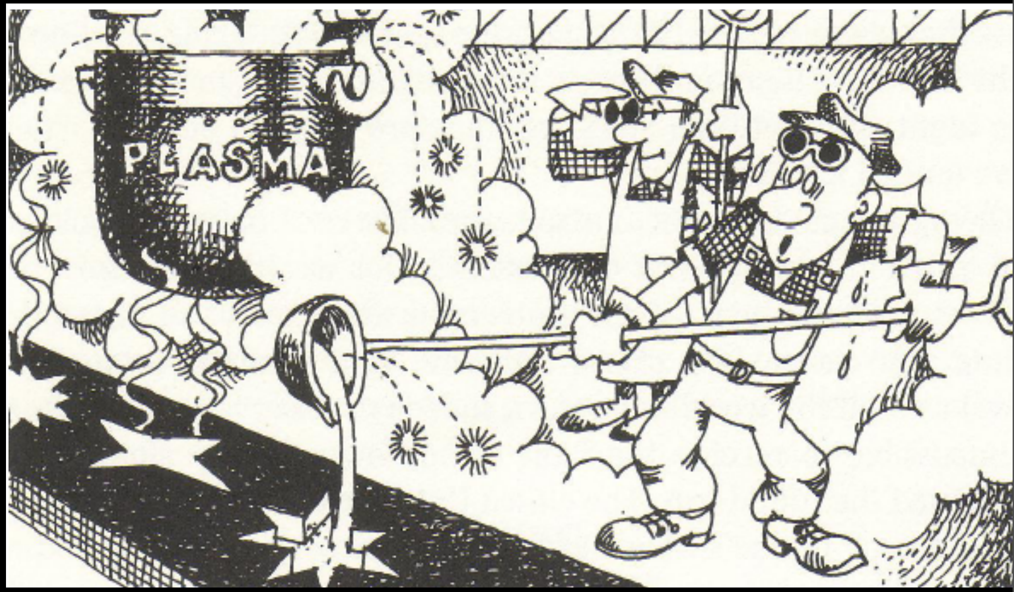

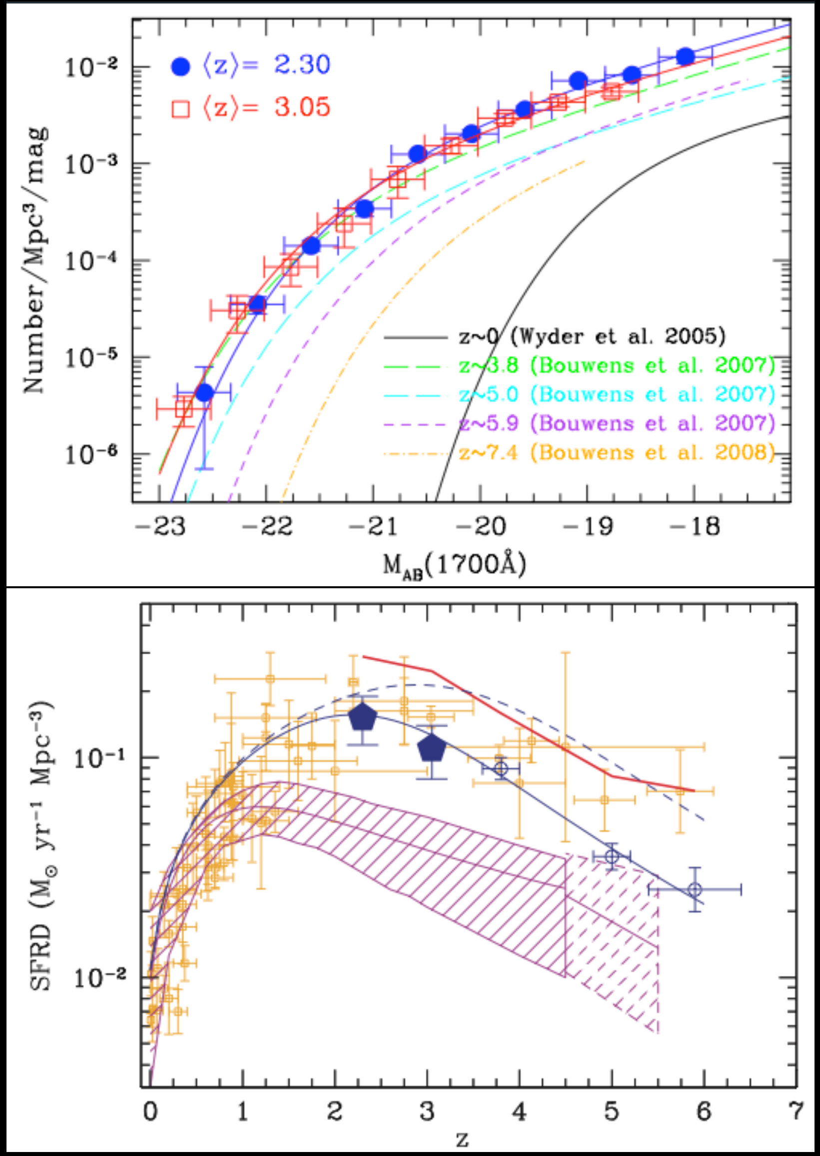

Testing the COLD DARK MATTER scenario against observations: the evolution of galaxies

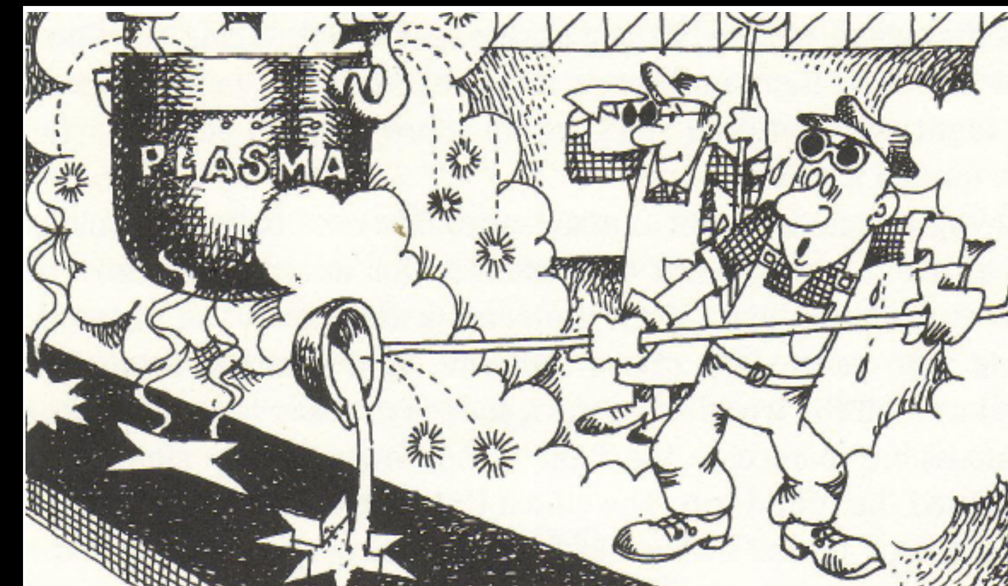

Requires modelling of baryon physics inside evolving DM potential wells

- gas physis (cooling, heating)
- disk formation
- star formation
-evolution of the stellar population
- injection of energy into the gas
  from SNae

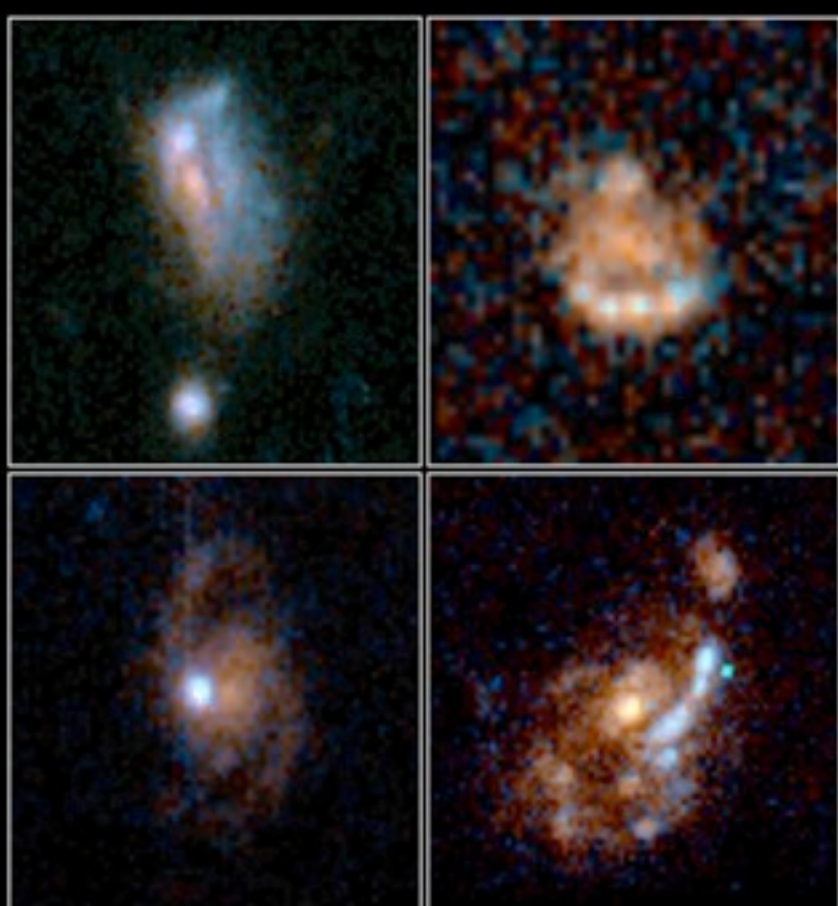

Medium Deep Survey HST • WFPC2

PRC94-39b • ST ScI OPO • R. Griffiths (JHU), NASA

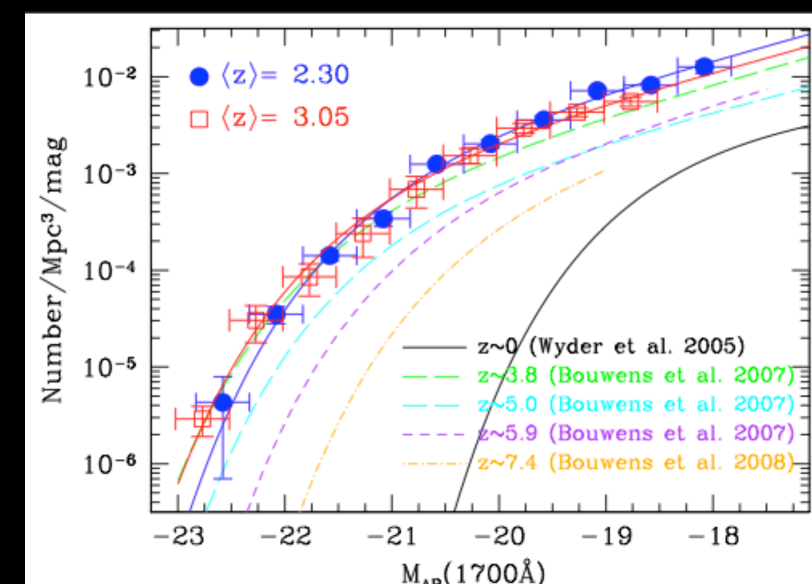

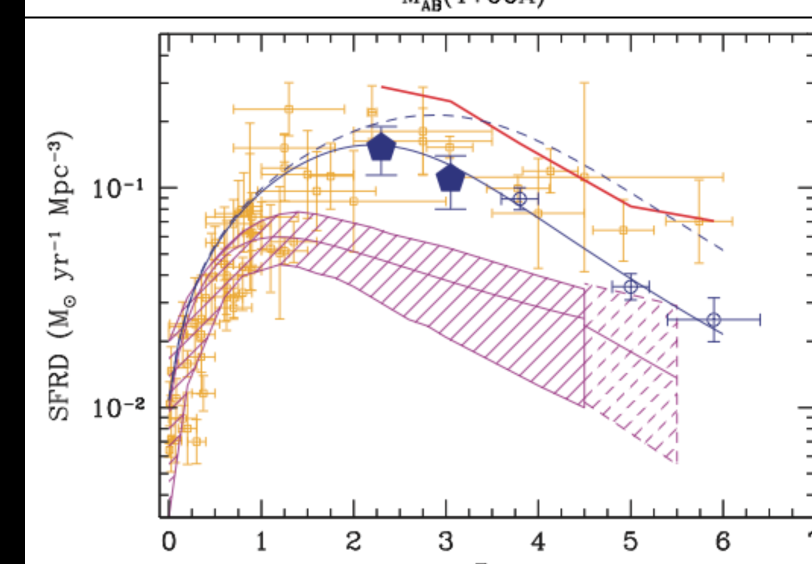

Galaxy Formation in a Cosmological Context

Hydrodynamcal
N-body simulations

Pros
include hydrodynamics of gas
contain spatial information
Cons
numerically expensive
(limited exploration of parameter space)
requires sub-grid physics

Semi-Analytic Models
Monte-Carlo realization of collapse and merging histories

Pros
Physics of baryons linked to DM halos through scaling laws, allows a fast spanning of parameter space
Cons
Simplified description of gas physics
Do not contain spatial informations

Galaxy Formation in a Cosmological Context

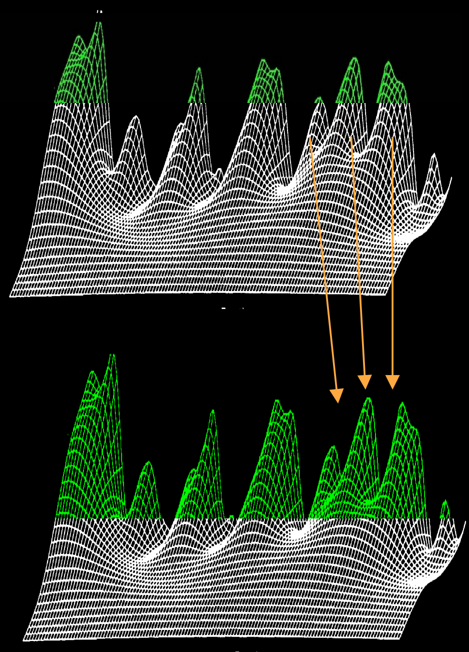

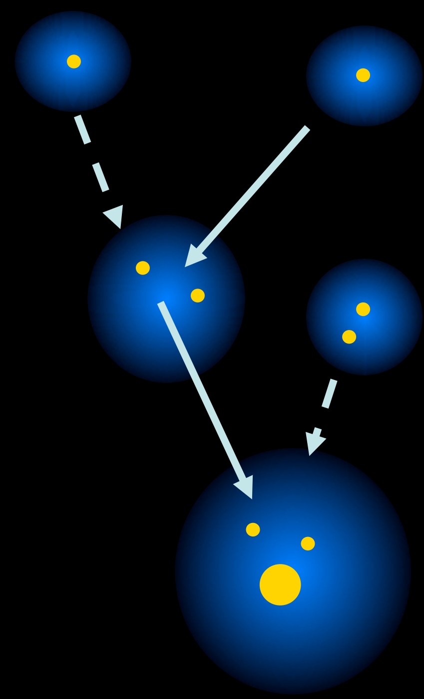

Semi-Analytic Models
Monte-Carlo realization of collapse and merging histories

<u>Pros</u>

Physics of baryons linked to DM halos through scaling laws, allows a fast spanning of parameter space

<u>Cons</u>

Simplified description of gas physics
Do not contain spatial informations

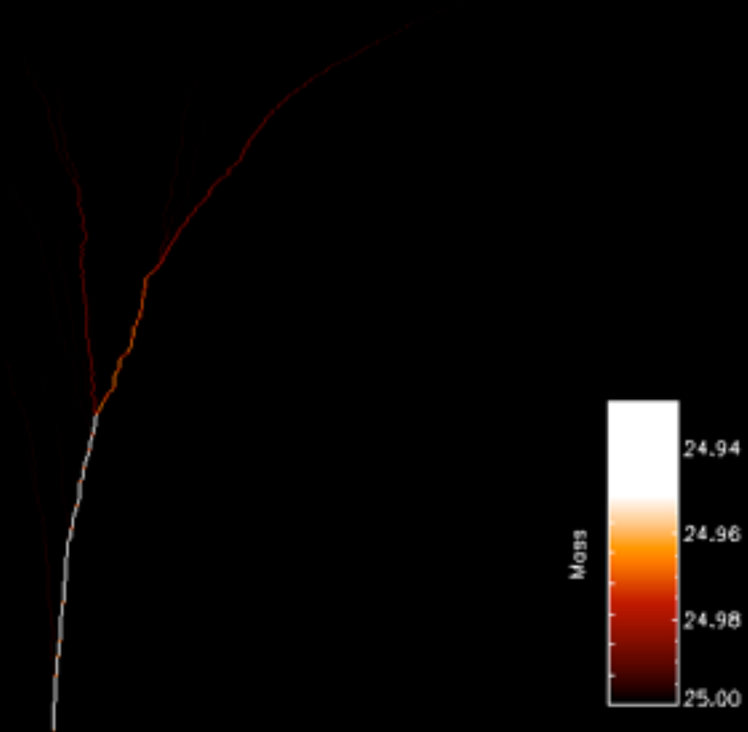

Sub-Halo dymanics:
dynamical friction, binary aggregation

Halo Properties
Density Profiles
Virial Temperature

Gas Properties
Profiles
Cooling - Heating Processes
Collapse, disk formation

Star Formation Rate

Gas Heating (feedback)
SNae
UV background

Evolution of stellar populations

Growth of Supermassive BHs
Evolution of AGNs

Semi-analytic Models

White & Frenk 1991, Kauffmann et al. 1993, Cole et al. 2001, Monaco et al. 2007, NM et al. 2007)

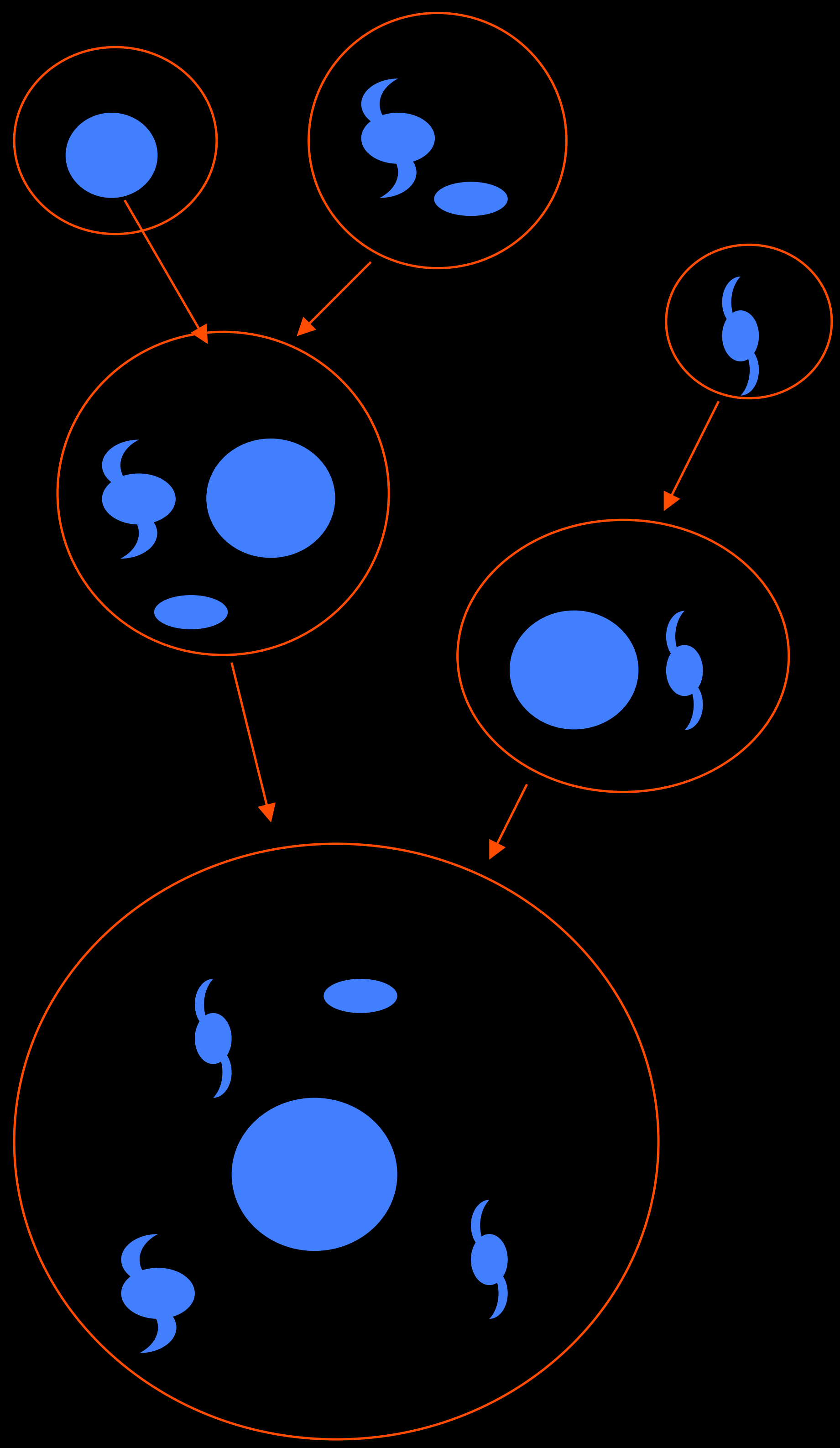

Dynamical Processes affecting sub-haloes

Dynamical Friction
Binary Aggregation
Stripping

Halo Properties

Average Density
Virial Temperature
Virial Radius
Density Profile

Gas Properties

Profiles
Cooling
Disk

Star Formation Rate

SNae feedback

Evolution of Stellar Populations

Semi-analytic Models

White & Frenk 1991, Kauffmann et al. 1993, Cole et al. 2001, Monaco et al. 2007, NM et al. 2007)

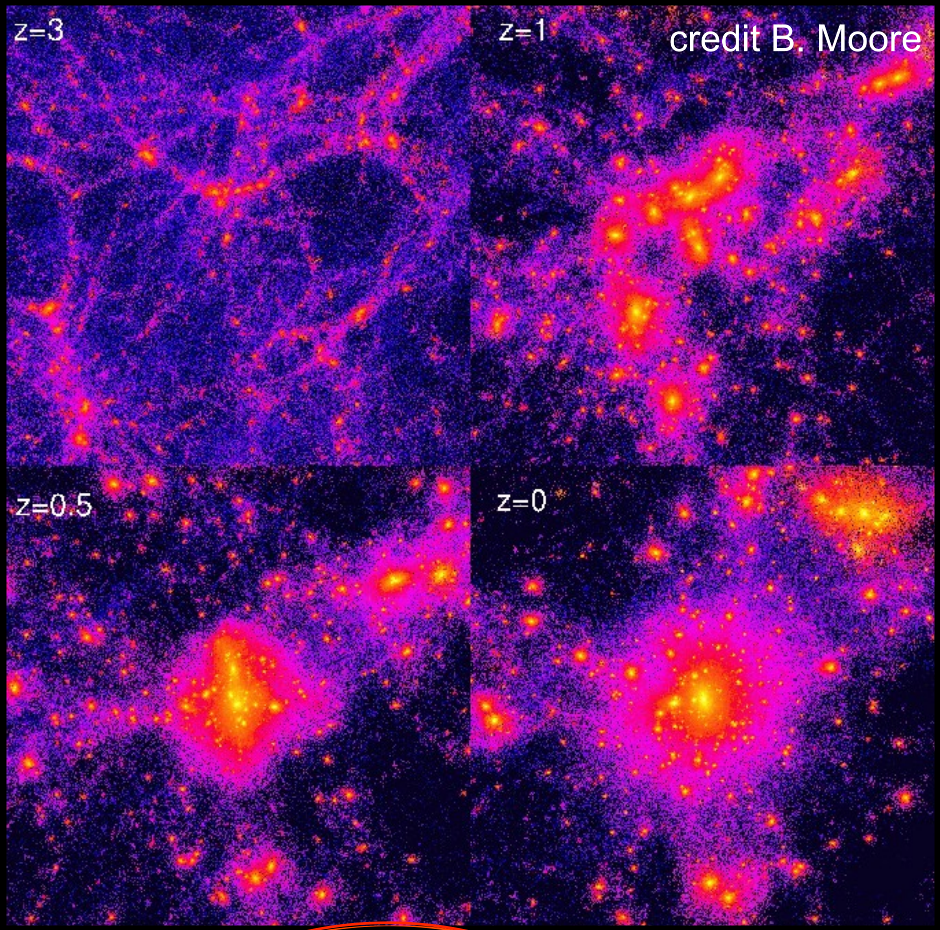

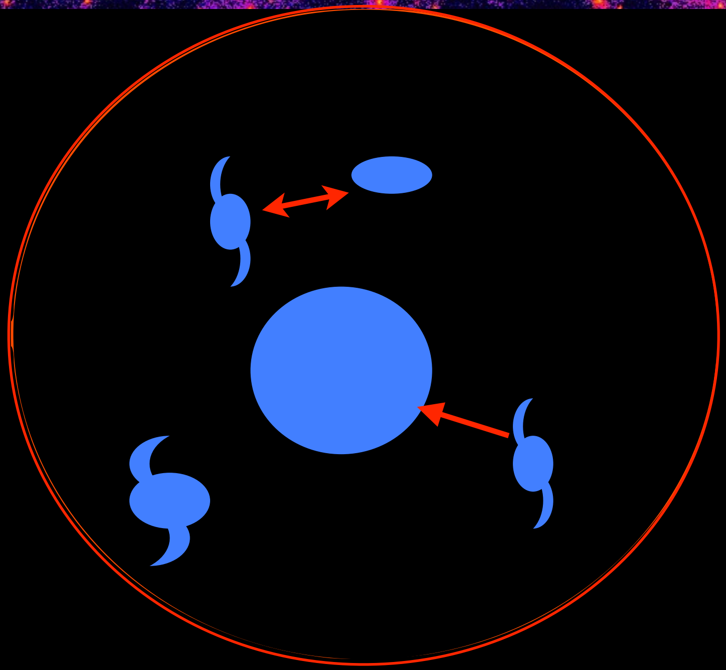

Dynamical Processes affecting sub-haloes

Dynamical Friction
Binary Aggregation
Stripping

Halo Properties

Average Density
Virial Temperature
Virial Radius
Density Profile

Gas Properties

Profiles
Cooling
Disk

Star Formation Rate

SNae feedback

Evolution of Stellar Populations

Compute the structure (density profiles) of DM haloes

$$\bar{\rho} = 180\rho_u$$

$$\rho = \frac{\delta_c \, \rho_{crit}}{(r/r_s)(1+r/r_s)^2}$$

$$r_{vir} = \left(\frac{3M}{4\pi\rho}\right)^{1/3}$$

$$kT_v(M) = \mu \, m_p \frac{GM}{r_{vir}}$$

Dynamical Processes affecting sub-haloes

Dynamical Friction
Binary Aggregation
Stripping

Halo Properties

Average Density
Virial Temperature
Virial Radius
Density Profile

Gas Properties

Profiles
Cooling
Disk

Star Formation Rate

SNae feedback

Evolution of Stellar Populations

Compute the gas hydrostatic equilibrium inside DM haloes

$$\frac{dp}{d\rho} = -\rho \frac{GM}{r^2}$$

GAS $$p_{gas} = \frac{\rho}{\mu m_p} kT$$

DM $$p_{DM} = \rho \sigma^2$$

$$\rho_{gas} \propto \rho_{DM}^{\beta} \qquad \beta = \frac{\mu m_p \sigma^2}{kT}$$

Dynamical Processes affecting sub-haloes

Dynamical Friction
Binary Aggregation
Stripping

Halo Properties

Average Density
Virial Temperature
Virial Radius
Density Profile

Gas Properties

Profiles
Cooling
Disk

Star Formation Rate

SNae feedback

Evolution of Stellar Populations

Gas at the centre of DM haloes radiatively cools due to atomic processes

cooling is faster when
- densities are large → large reddshifts
- and virial T≳10^4 K → low mass glxs

$$\tau_{cool} = \frac{3}{2}\frac{\rho_{gas}(\mathrm{r})}{\mu\,\mathrm{m_p}}\frac{kT}{n_e^2(r)\,\Lambda(T)}$$

r_{cool} = radius enclosing the region where $t_{cool} \leq t_H(z)$

$$\Delta m_{cool}(M) = 4\pi\,\rho_{gas}(r)\,r_{cool}^2\Delta r_{cool}$$

r_{cool} reset to zero after major merging events

Dynamical Processes affecting sub-haloes

Dynamical Friction
Binary Aggregation
Stripping

Halo Properties

Average Density
Virial Temperature
Virial Radius
Density Profile

Gas Properties

Profiles
Cooling
Disk

Star Formation Rate

SNae feedback

Evolution of Stellar Populations

DM angular momentum J aquired from tidal torques due to surrounding perturbations

$$\lambda = J / J_{circ} = JE^{1/2} G^{-1} M^{-5/2} \qquad \lambda \approx 0.01 - 0.08$$

Assume that, durung collapse, the ratio of the ratio $j_{gas} = J_{gas}/J$ is conserved

Assuming an exponential Surf. Density Profile

$$\Sigma(R) = \Sigma_0 \exp(-R / R_d)$$

Assuming centrifugal balance

$$J_{gas} = 2\pi \int V_c(M) \Sigma(R) R^2 dR$$

$$R_d = \frac{1}{\sqrt{2}} \left(\frac{j_{gas}}{m_{gas}} \right) \lambda R_{vir}(M) \qquad m_{gas} \equiv \frac{m_{cold}}{m_{DM}}$$

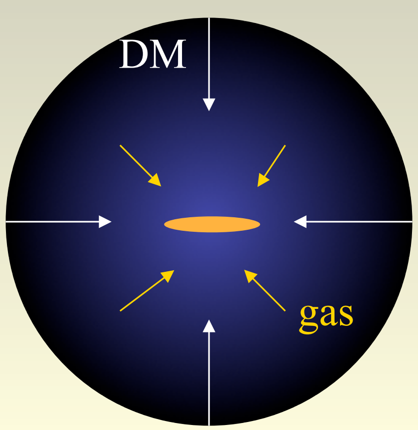

Dynamical Processes affecting sub-haloes

Dynamical Friction
Binary Aggregation
Stripping

Halo Properties

Average Density
Virial Temperature
Virial Radius
Density Profile

Gas Properties

Profiles
Cooling
Disk

Star Formation Rate

SNae feedback

Evolution of Stellar Populations

Cold Gas is gradually converted into stars on a time scale τ_*

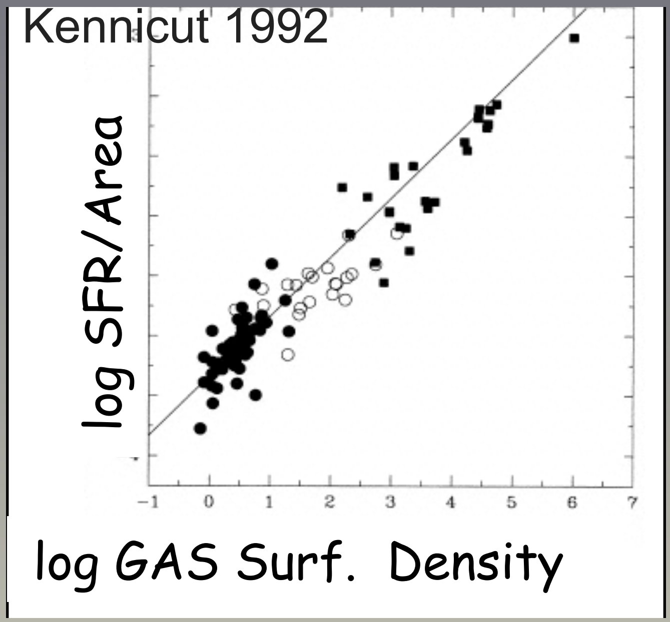

$$\frac{\dot{m}_*}{Area} \approx \left(\frac{m_{cold}}{Area}\right)^{1.5}$$

$$\dot{m}_* \approx \frac{m_{cold}}{\tau_*}$$

$$\tau_* \approx 2Gyr$$

Dynamical Processes affecting sub-haloes

Dynamical Friction
Binary Aggregation
Stripping

Halo Properties

Average Density
Virial Temperature
Virial Radius
Density Profile

Gas Properties

Profiles
Cooling
Disk

Star Formation Rate
quiescent

SNae feedback

Evolution of Stellar Populations

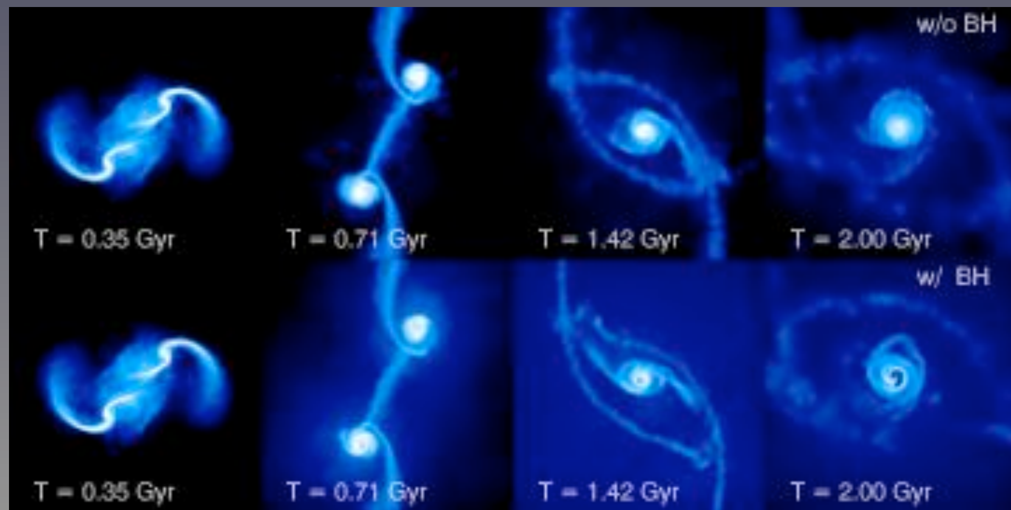

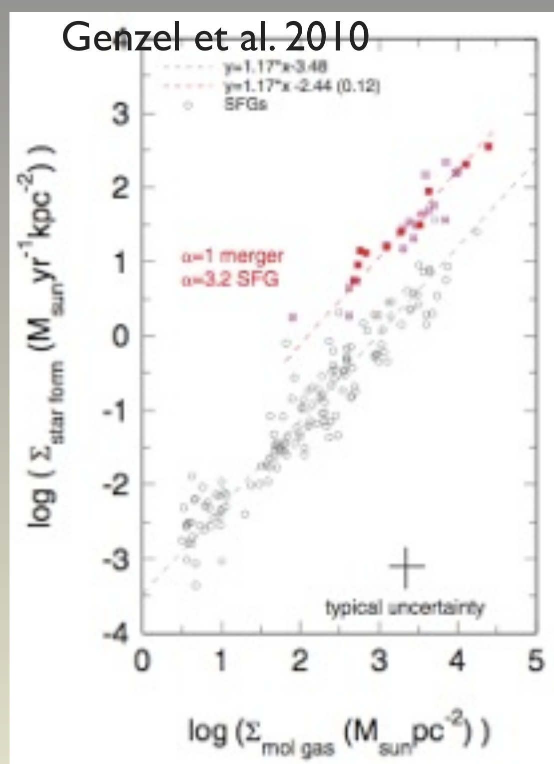

Gas-rich mergers between galaxies funnell large amounts of galactic gas toward the galactic centre

Barnes & Hernquist 1996; Cattaneo, A., Haenhelt, M.G., Rees, M. 1999; Cavaliere, Vittorini 2000; Kauffmann, Haenhelt 2000; ; Wyithe, Loeb 2003; Treister et al. 2010

$$\dot{m}_* \approx \frac{m_{cold}}{\tau_r}$$

$$\tau_r \approx \frac{r_{tidal}}{V_{rel}} \sim 100\ Myr$$

Dynamical Processes affecting sub-haloes

Dynamical Friction
Binary Aggregation
Stripping

Halo Properties

Average Density
Virial Temperature
Virial Radius
Density Profile

Gas Properties

Profiles
Cooling
Disk

Star Formation Rate
starbursts

SNae feedback

Evolution of Stellar Populations

A fraction of the cold gas is re-heated by SNae

$$E_{SN} \approx 10^{51}\, \eta_{IMF}\, \varepsilon_0 \frac{\Delta m_*}{M_\oplus}$$

$$kT_{SN} = E_{SN} / m_{gas} \approx 0.1\ keV$$

Number of SNae produced per unit stellar mass (depends on IMF)

$$\eta_{IMF} = 2 - 5\times 10^{-3}$$

Fraction of energy dumped into gas

$\varepsilon_0 \approx 0.1$

$$\dot{m}_{reheat} \propto \frac{E_{SN}}{\langle v_{esc}^2 \rangle} \propto \frac{\dot{m}_*}{v_c^2}$$

Dynamical Processes affecting sub-haloes

Dynamical Friction
Binary Aggregation
Stripping

Halo Properties

Average Density
Virial Temperature
Virial Radius
Density Profile

Gas Properties

Profiles
Cooling
Disk

Star Formation Rate

SNae feedback

Evolution of Stellar Populations

The integrated emission (wavelength λ) from stellar populations is computed after convolving the Spectral Energy Distributions (Φ_λ, Bruzual & Charlot 1993) with the resulting SFR in all the progenitor haloes of the considered galaxy

$$S_\lambda = \int_0^t \dot{m}_*(t-t')\,\Phi_\lambda(t')\,dt'$$

Dynamical Processes affecting sub-haloes

Dynamical Friction
Binary Aggregation
Stripping

Halo Properties

Average Density
Virial Temperature
Virial Radius
Density Profile

Gas Properties

Profiles
Cooling
Disk

Star Formation Rate

SNae feedback

Evolution of Stellar Populations

Properties of merging trees

Simulation
by Governato 04

Initial (z≈4-6) merging events involve small clumps with comparable size

Rapid merging, frequent encounters

Last major merging at z≈3 for $M \approx 3\,10^{12}\, M_\odot$

At later times, merging rate declines

Accretion of smaller lumps onto the main progenitor

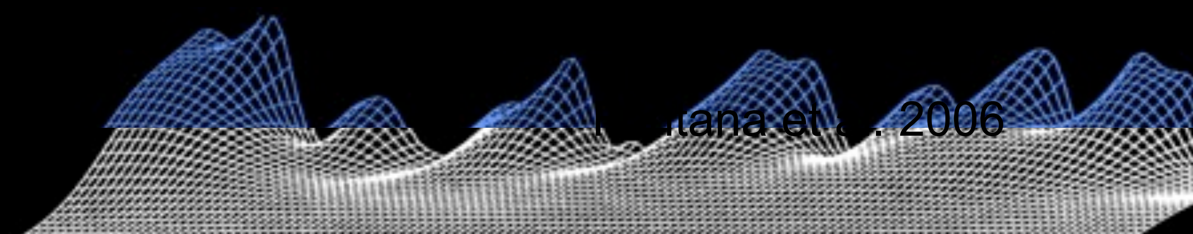

NM et al. 06

Baryonic Processes

Frequent galaxy encounters

Rapid cooling (high gas density)

Starbursts with large fraction of Gas converted into stars

} $z \gtrsim 2$

Decline of cooling rate

Drop of encounter rate

Quiescent and declining star formation

} $z \lesssim 2$

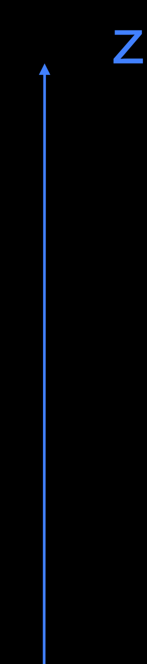

Properties of merging trees

Simulation
by Governato 04

Initial ($z \approx 4$-6) merging events involve small clumps with comparable size

Rapid merging, frequent encounters

Last major merging at $z \approx 3$ for $M \approx 3 10^{12}\ M_{\odot}$

At later times, merging rate declines

Accretion of smaller lumps onto the main progenitor

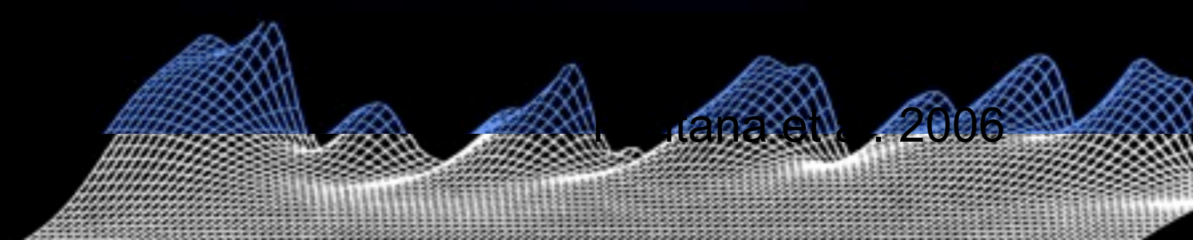

Baryonic Processes

Frequent galaxy encounters

Rapid cooling (high gas density)

Starbursts with large fraction of Gas converted into stars

$z \gtrsim 2$

Decline of cooling rate

Drop of encounter rate

Quiescent and declining star formation

$z \lesssim 2$

NM et al. 06

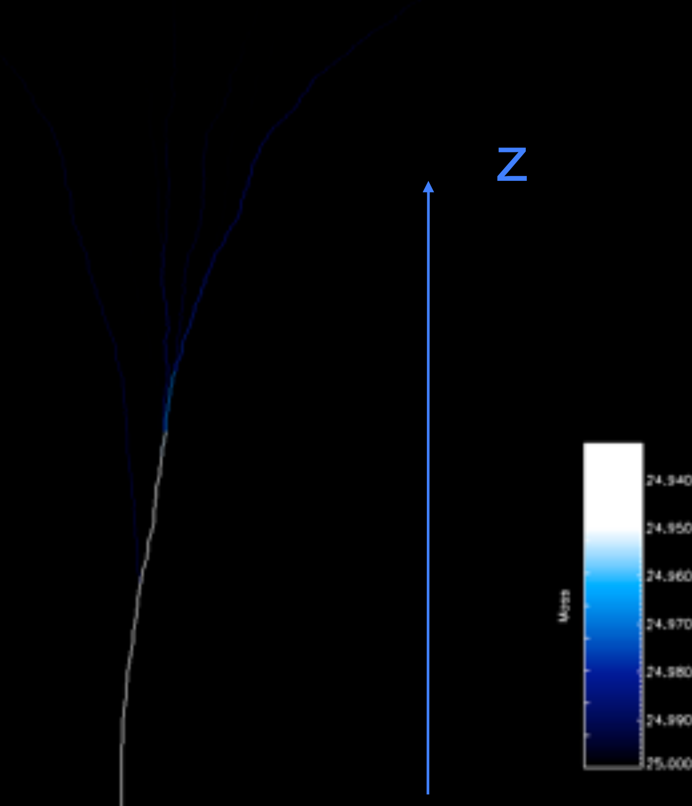

Simulation
by Governato 04

Properties of merging trees

Initial ($z \approx 4$-6) merging events involve small clumps with comparable size

Rapid merging, frequent encounters

Last major merging at $z \approx 3$ for $M \approx 3\,10^{12}\,M_\odot$

At later times, merging rate declines

Accretion of smaller lumps onto the main progenitor

Phase 1

Zhao et al. 2003
Diemand et al. 2007
Hoffman et al. 2007
Ascasibar & Gottloeber 2008

Phase 2

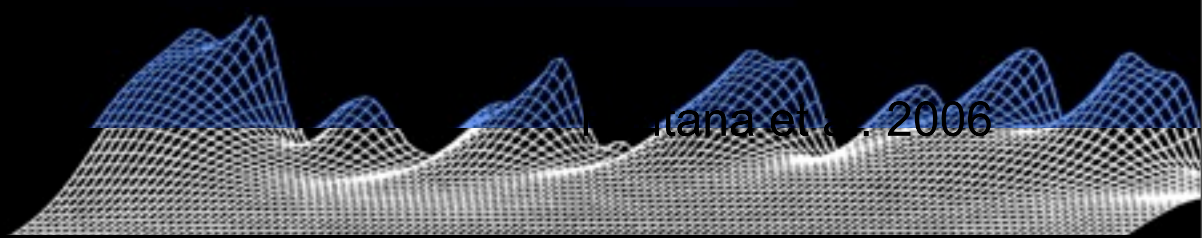

Baryonic Processes

Frequent galaxy encounters

Rapid cooling (high gas density)

Starbursts with large fraction of Gas converted into stars

$z \gtrsim 2$

Decline of cooling rate

Drop of encounter rate

Quiescent and declining star formation

$z \lesssim 2$

NM et al. 06

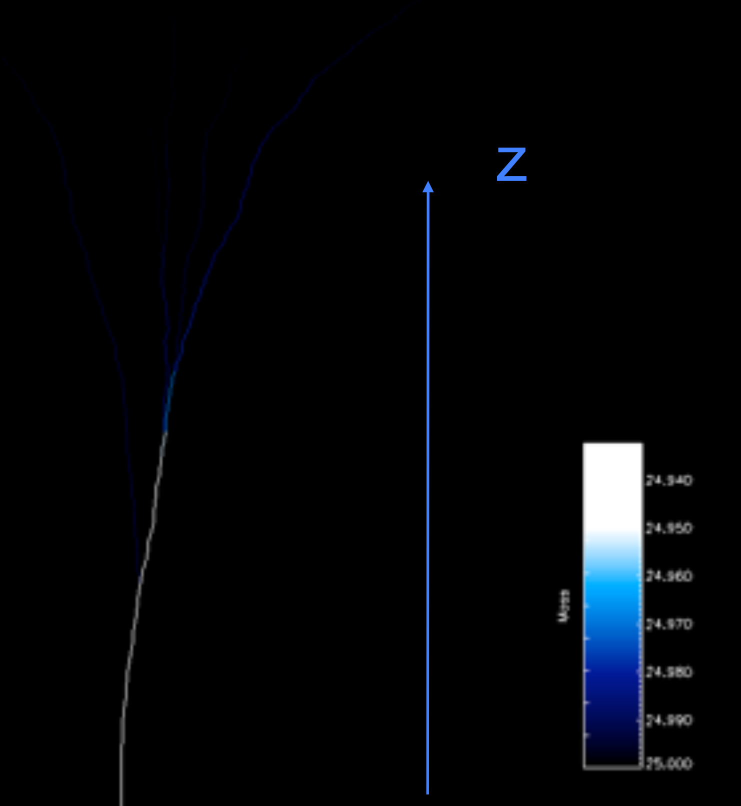

Simulation
by Governato 04

Properties of merging trees

Initial (z≈4-6) merging events involve small clumps with comparable size

Rapid merging, frequent encounters

Last major merging at z≈3 for M≈3 10^{12} $M_\odot$

At later times, merging rate declines

Accretion of smaller lumps onto the main progenitor

Phase 1

Zhao et al. 2003
Diemand et al. 2007
Hoffman et al. 2007
Ascasibar & Gottloeber 2008

Phase 2

Baryonic Processes

Frequent galaxy encounters

Rapid cooling (high gas density)

Starbursts with large fraction of Gas converted into stars

$z \gtrsim 2$

Decline of cooling rate

Drop of encounter rate

Quiescent and declining star formation

$z \lesssim 2$

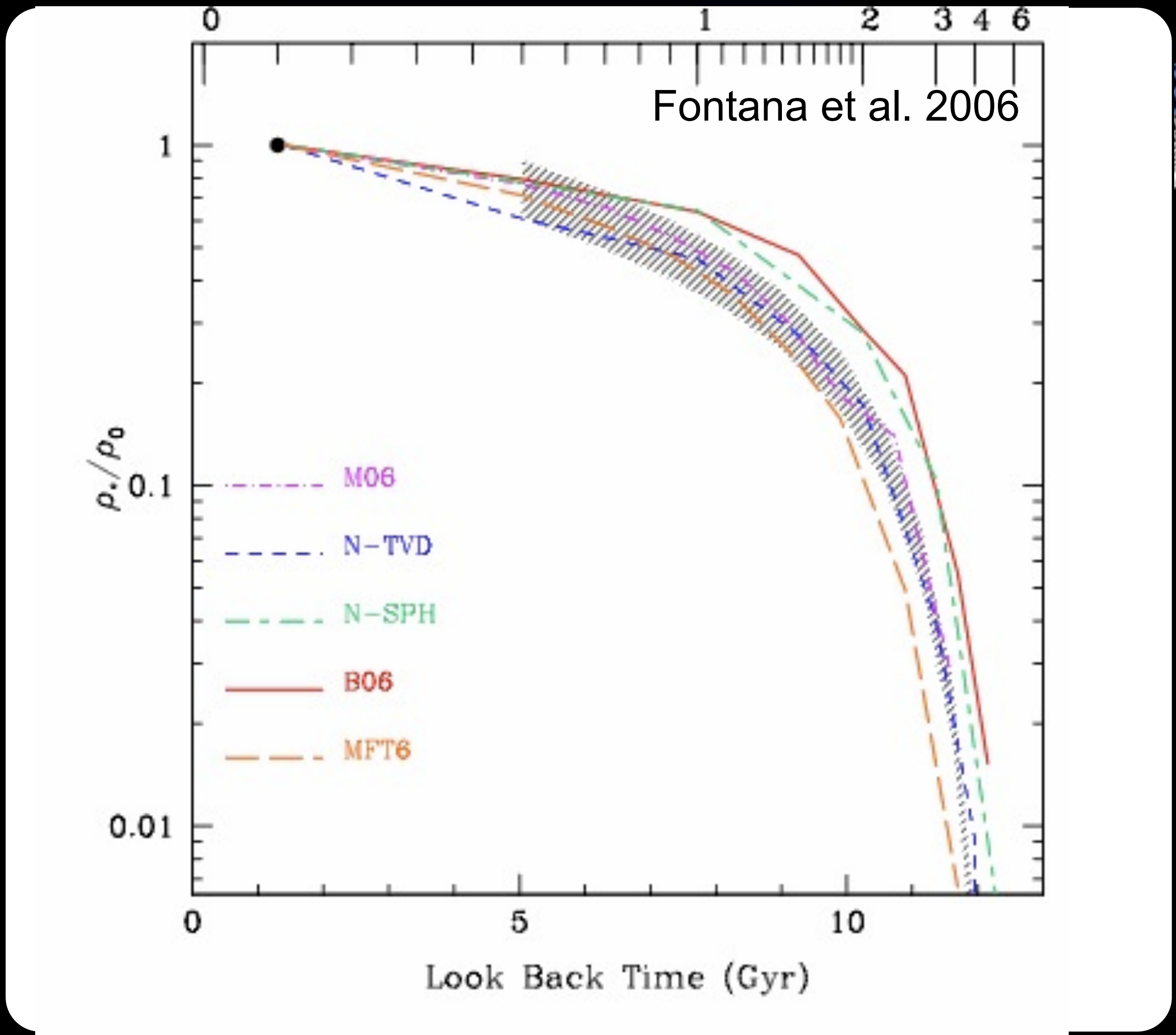

AGN fed by gas destabilized during galaxy encounters

Gas-rich mergers between galaxies of comparable mass have long been advocated to drive quasar activity by funnelling large amounts of galactic gas toward the galactic centre

Barnes & Hernquist 1996; Cattaneo, A., Haenhelt, M.G., Rees, M. 1999; Cavaliere, Vittorini 2000; Kauffmann, Haenhelt 2000; ; Wyithe, Loeb 2003; Treister et al. 2010

Such a picture is supported by hydrodynamical N-body simulations which have shown that tidal torques during galaxy mergers can drive the rapid inflows of gas that are needed to fuel both the intense starbursts and rapid BH accretion associated with ULIRGS and QSOs

Springel et al. 2005; Hernquist 1989; Barnes 1992; Mihos & Hernquist 1994; Barnes & Hernquist 1996; Mihos & Hernquist 1996; Di Matteo, Springel & Hernquist 2005; Springel, Di Matteo & Hernquist 2005

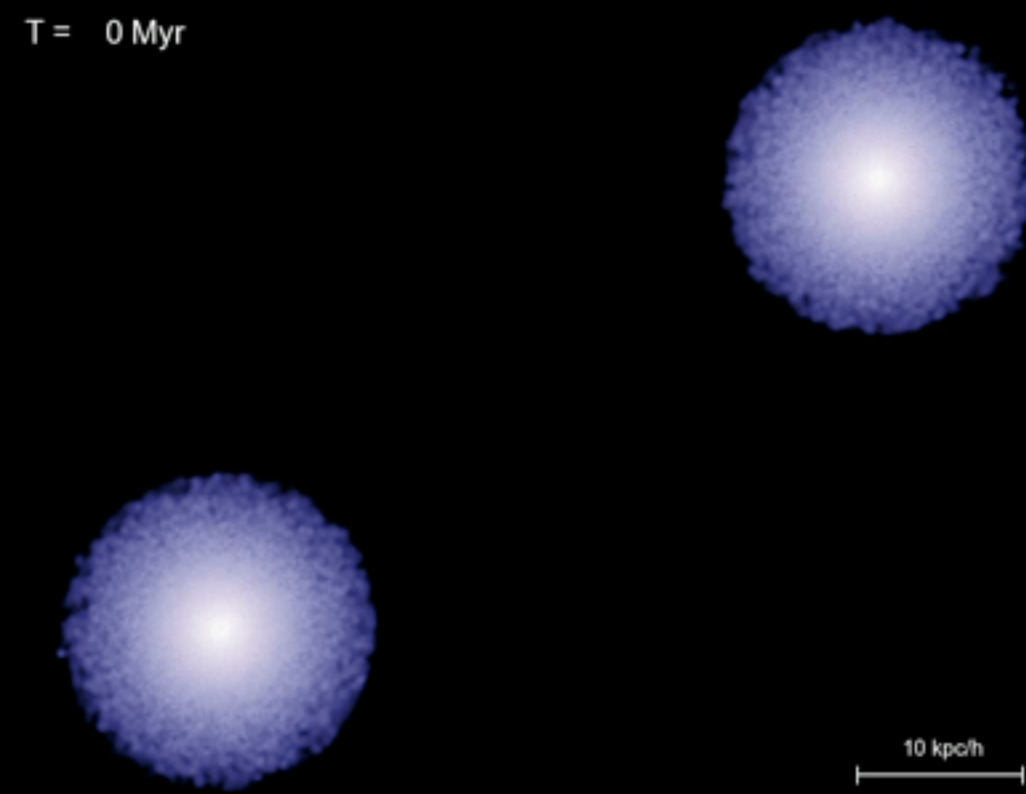

Di Matteo et al. 2005

Gas Angular Momentum

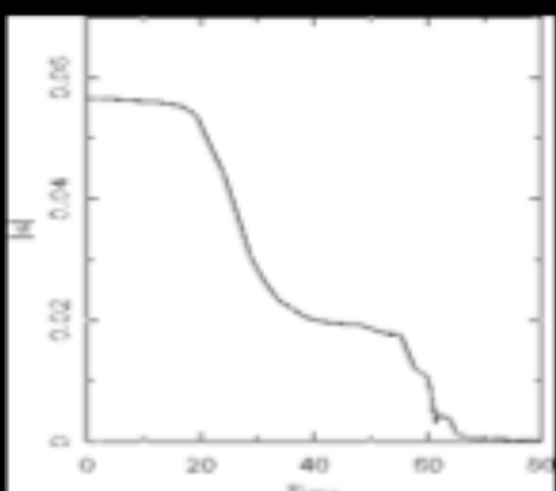

Mihos & Hernquist 1996
See also Noguchi 1987
Barnes & Hernquist 1991

BH accretion is related to starbusrst

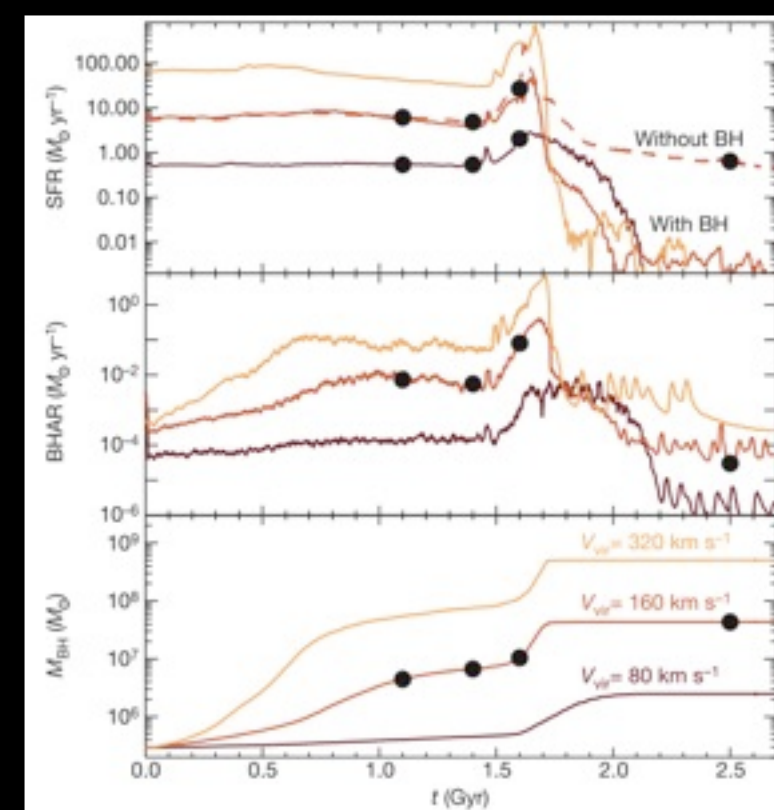

AGN fed by gas destabilized during galaxy encounters

$$\dot{m}_{BH} = f_{acc}\frac{m_{cold}}{\tau_{int}}$$

$$f_{acc} = \frac{1}{8}\frac{\Delta j}{j} \approx \left\langle \frac{m' r_d v_d}{m b V} \right\rangle$$

Larger fraction of accreted gas for major merging events
- high z (m'/m≈1)
- massive haloes (biased, overdense regions)

$$\tau^{-1} = n(z)\Sigma(m, m')\, V_{rel}$$

Higher encounter probability at high z

Part of the avilable galactic cold gas is funnelled toward the centre. The fraction *f* feeding the BH is about 1/4 of the destabilized gas (Sanders & Mirabel 1996)

Gas Angular Momentum

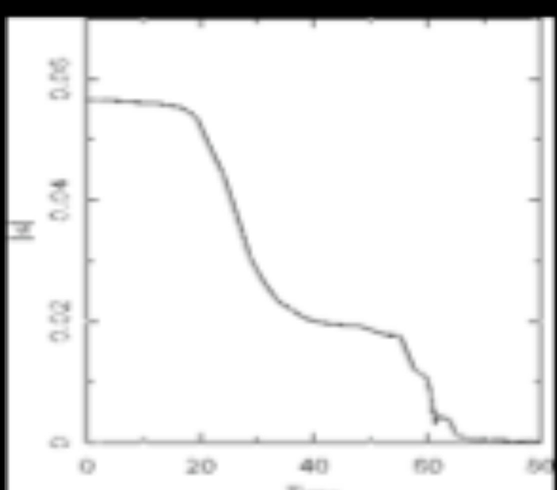

Mihos & Hernquist 1996
See also Noguchi 1987
Barnes & Hernquist 1991

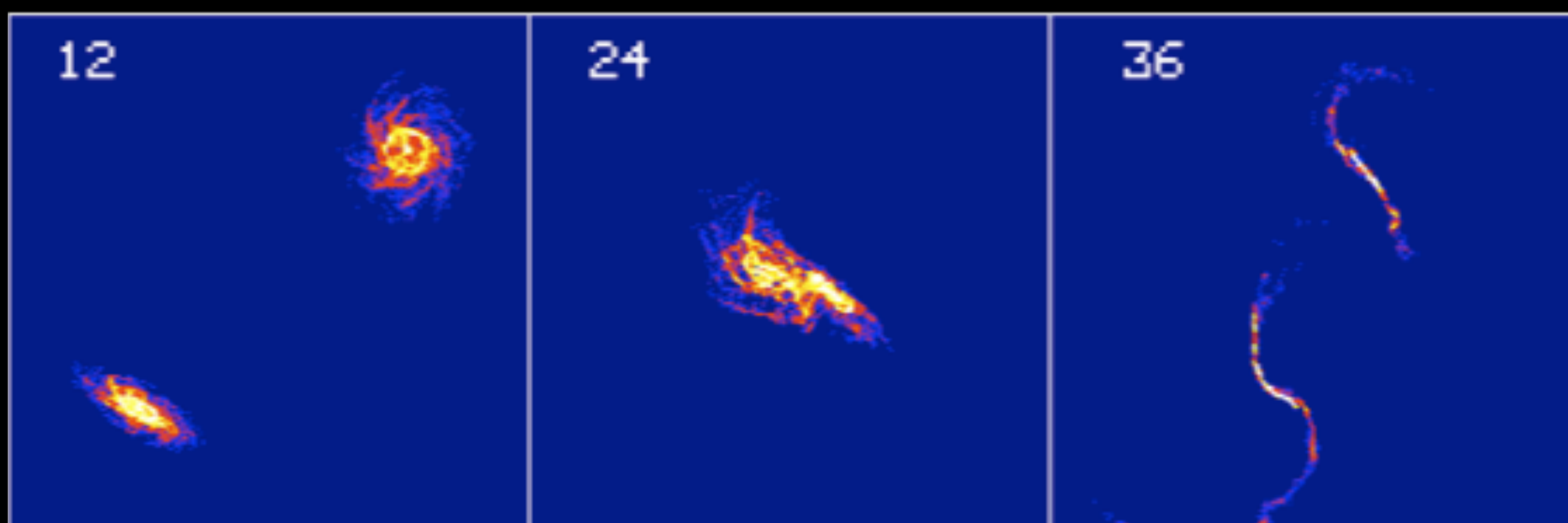

AGN fed by Instability-driven inflows in turbulent disks

Gas rich rotating disks
wildly unstable with giant clumps,
asymetries, rings, etc:

Bournaud Dekel Teyssier Cacciato Daddi Juneau Shankar 2011

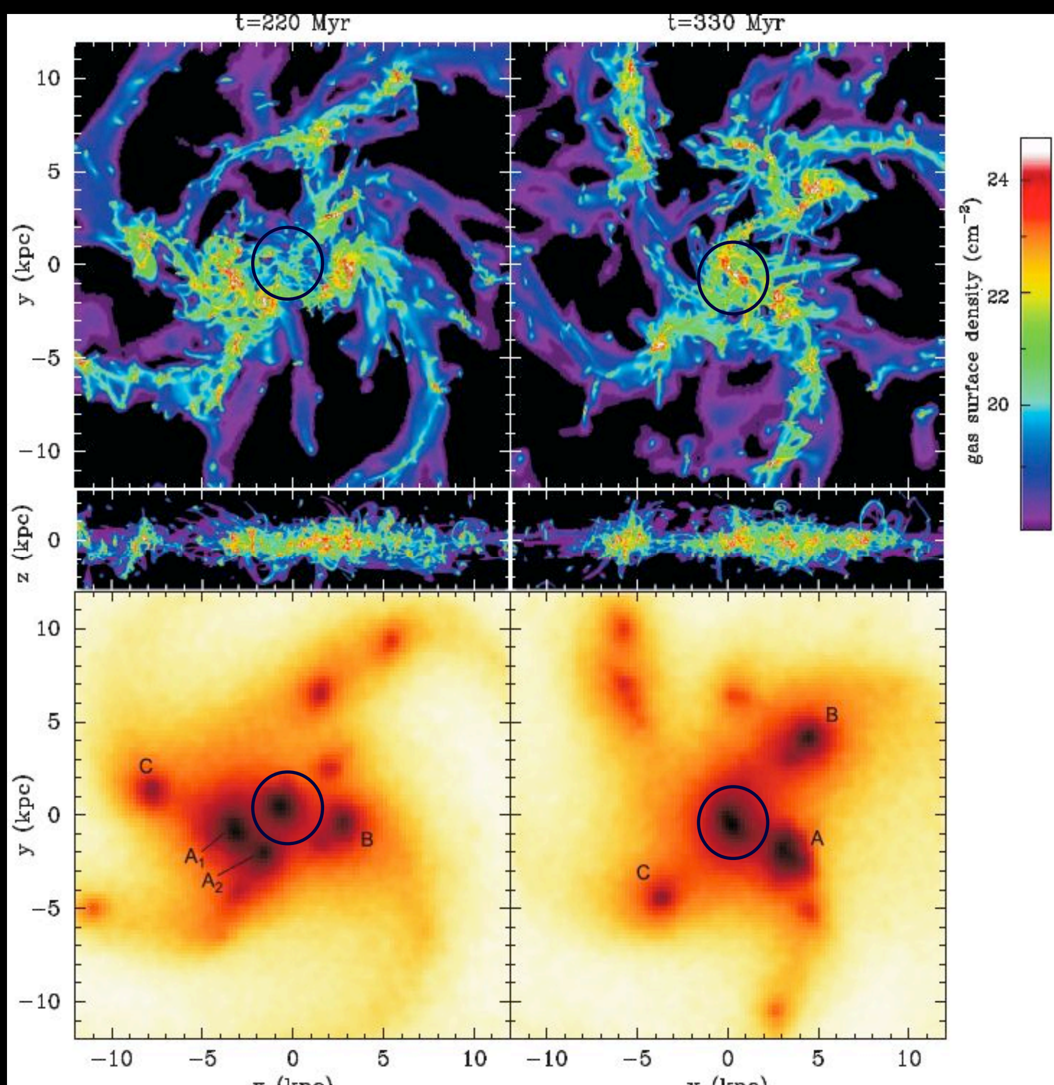

Hopkins Quataert 2012

$$\frac{dM_{BH}}{dt} \equiv \frac{dM_{infl}(R_{acc})}{dt} \approx \frac{\alpha(\eta_k,\eta_d)\, f_d^{4/3}}{1+2.5\, f_d^{-4/3}(1+f_0/f_{gas})}\left(\frac{M_{BH}}{10^8 M_\odot}\right)^{1/6}\left(\frac{M_d(R_0)}{10^9 M_\odot}\right)\left(\frac{R_0}{100pc}\right)^{-3/2}\left(\frac{R_{acc}}{10^{-2}R_{BH}}\right)^{5/6} M_\odot yr^{-1}$$

$$f_0 \approx 0.2 f_d^2 \left[\frac{M_d(R_0)}{10^9 M_\odot}\right]^{-1/3} \qquad f_{gas} \equiv \frac{M_{gas}(R_0)}{M_d(R_0)}$$

Very sensitive to
- gas fraction
- disk fraction

Small dependence on the BH mass

Galaxy Formation models in CDM scenario

Local properties:
gas content
luminosity distribution
disk sizes
distribution of the stellar mass content

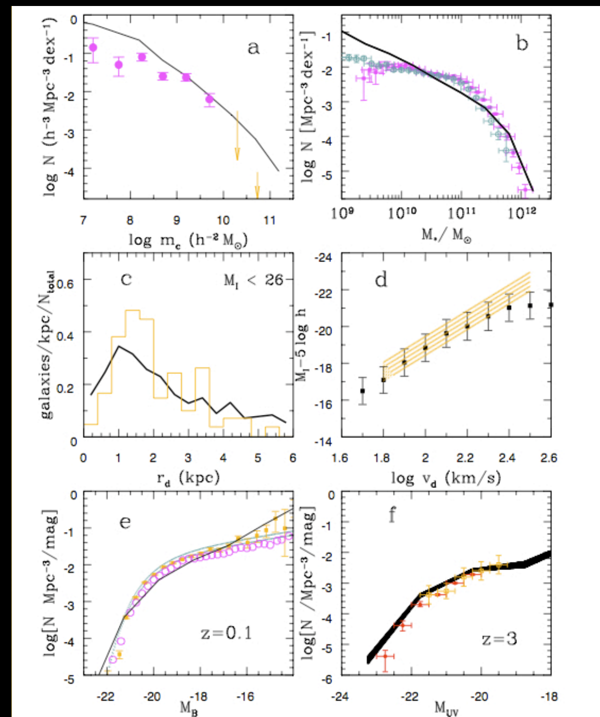

NM et al. 2006

properties of distant galaxies:
luminosity distribution
evolution of the star formation rate

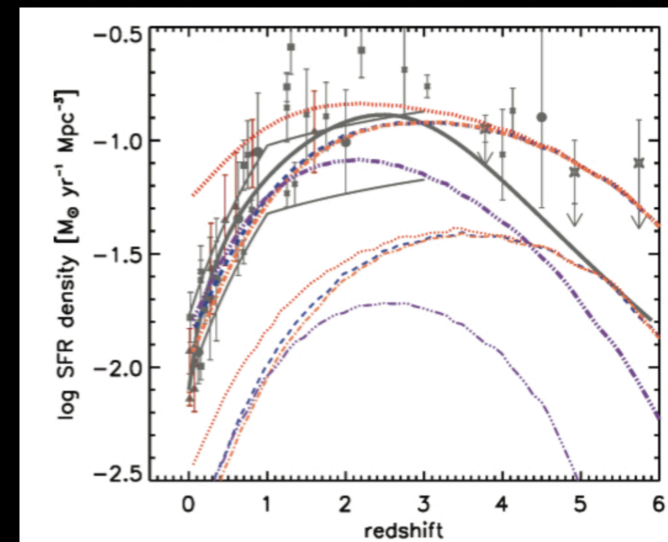

Somerville et al. 2010

NM et al. 2006

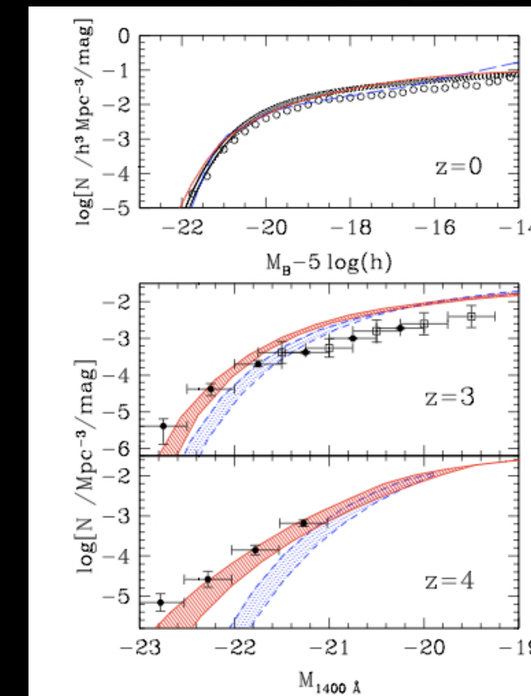

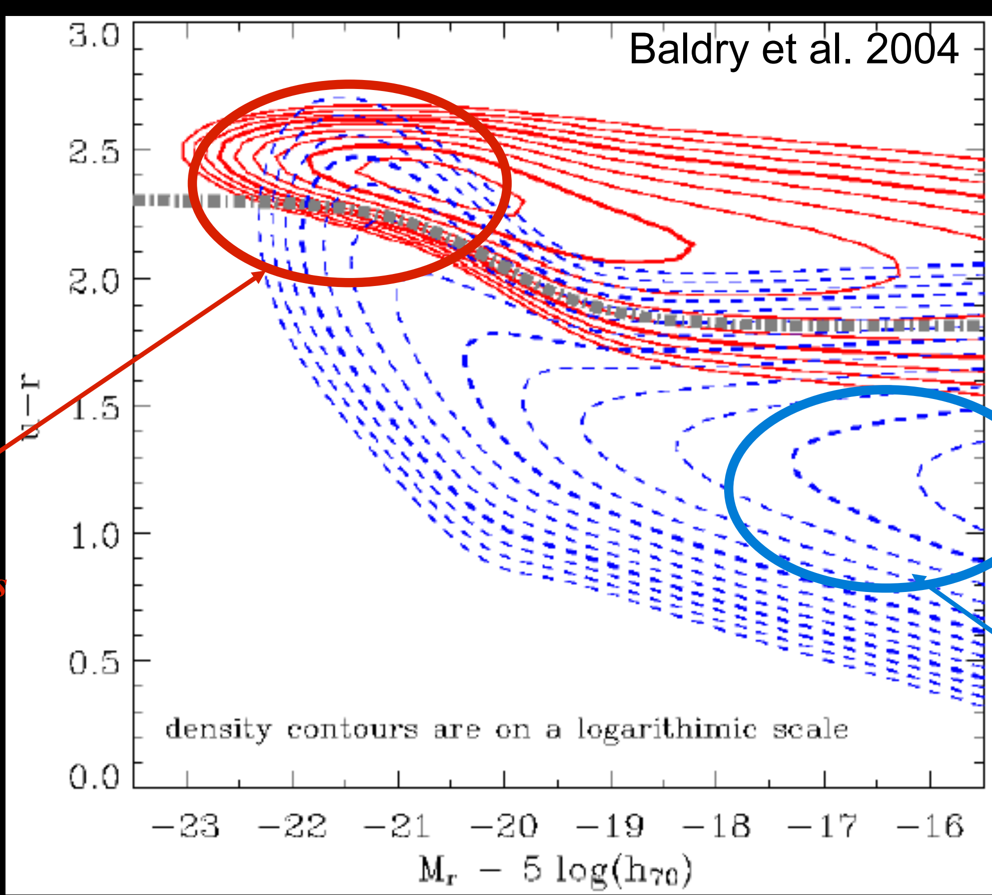

Color Distributions: bimodal distribution (early type vs late type)

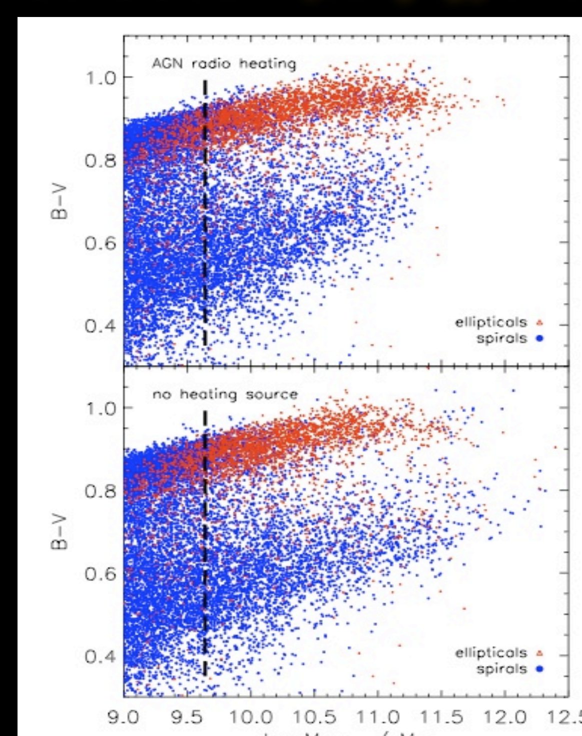

Croton et al. 2006

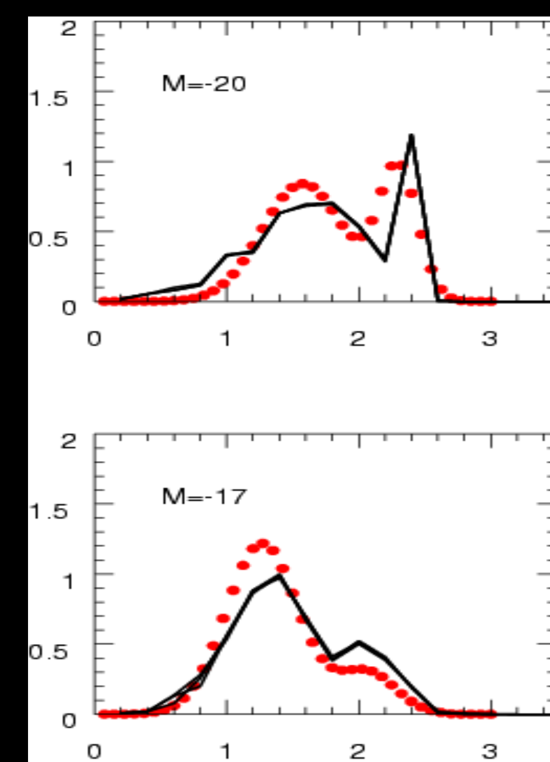

NM et al. 2008

DETAILED PREDICTIONS BASED ON SEMI-ANALYTIC MODEL

(NM et al. 2004, 2005, 2006)

DM merging trees: Monte Carlo realizations

• Dynamical Processes involving galaxies within DM haloes
• Cooling, Disc Properties, Star formation and SNae feedback
• Star bursts triggered by (major+minor) merging and fly-by events

• Growth of SMBH from BH merging + accretion of galactic gas destabilized by galaxy encounters (merging and fly-by events)

Physical, non parametric Model.
Computed from galactic and orbital quantities

Rate of encounters
Fraction of galactic gas accreted by the BH Duty cicle

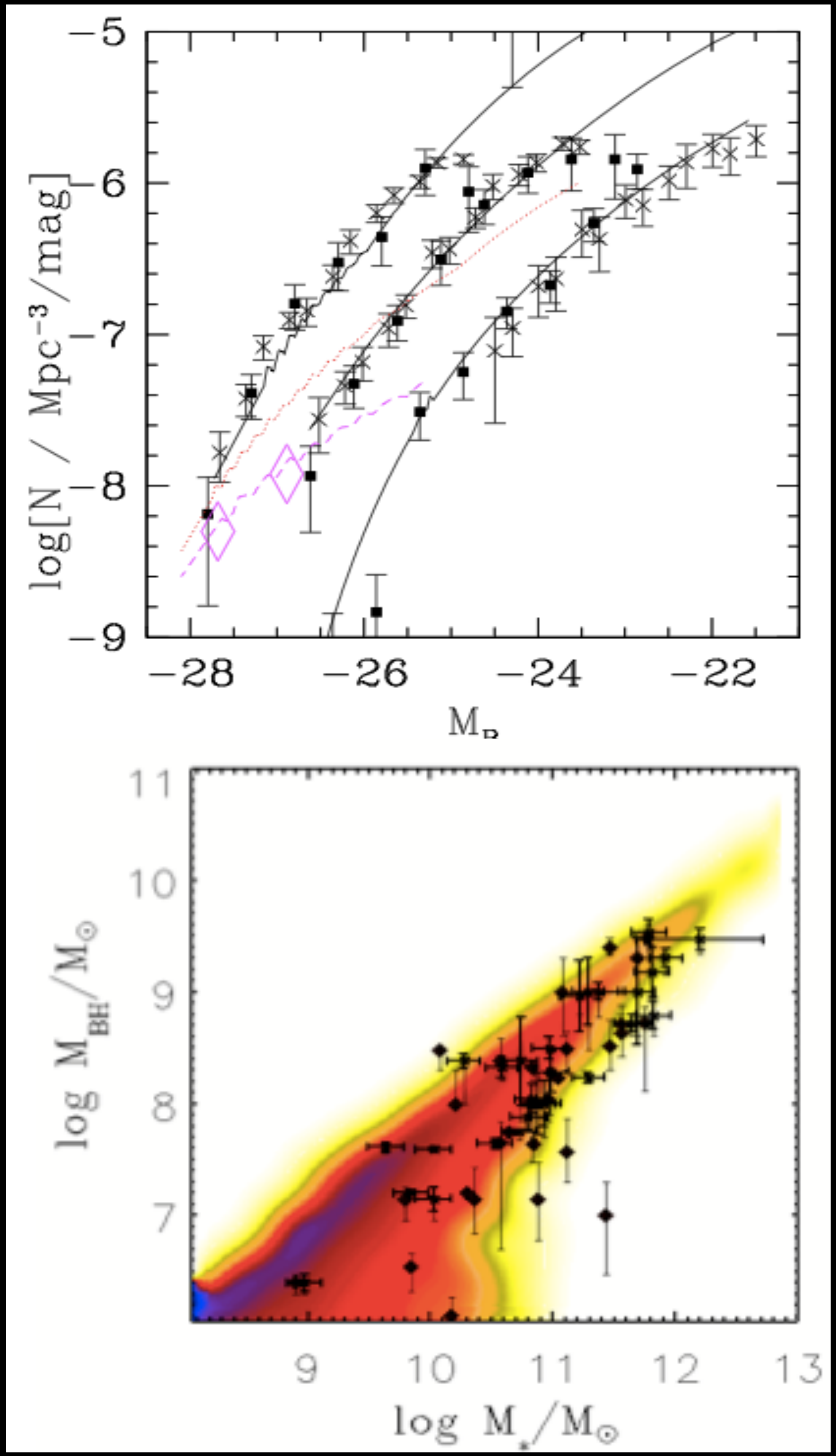

Critical Issues

Overabundance of low-mass objects

i) satellite DM haloes
ii) density profiles
iii) abundance of faint galaxies
iv) abundance of faint AGN

Critical Issues

CDM Substructure in simulated cluster and galaxy haloes look similar.

Expected number of satellites in Milky Way- like galaxies in CDM largely exceeds the observed abundance.

i) satellite DM haloes

Via Lactea simulation of a Milky Way - like galaxy
Diemand et al. 2008

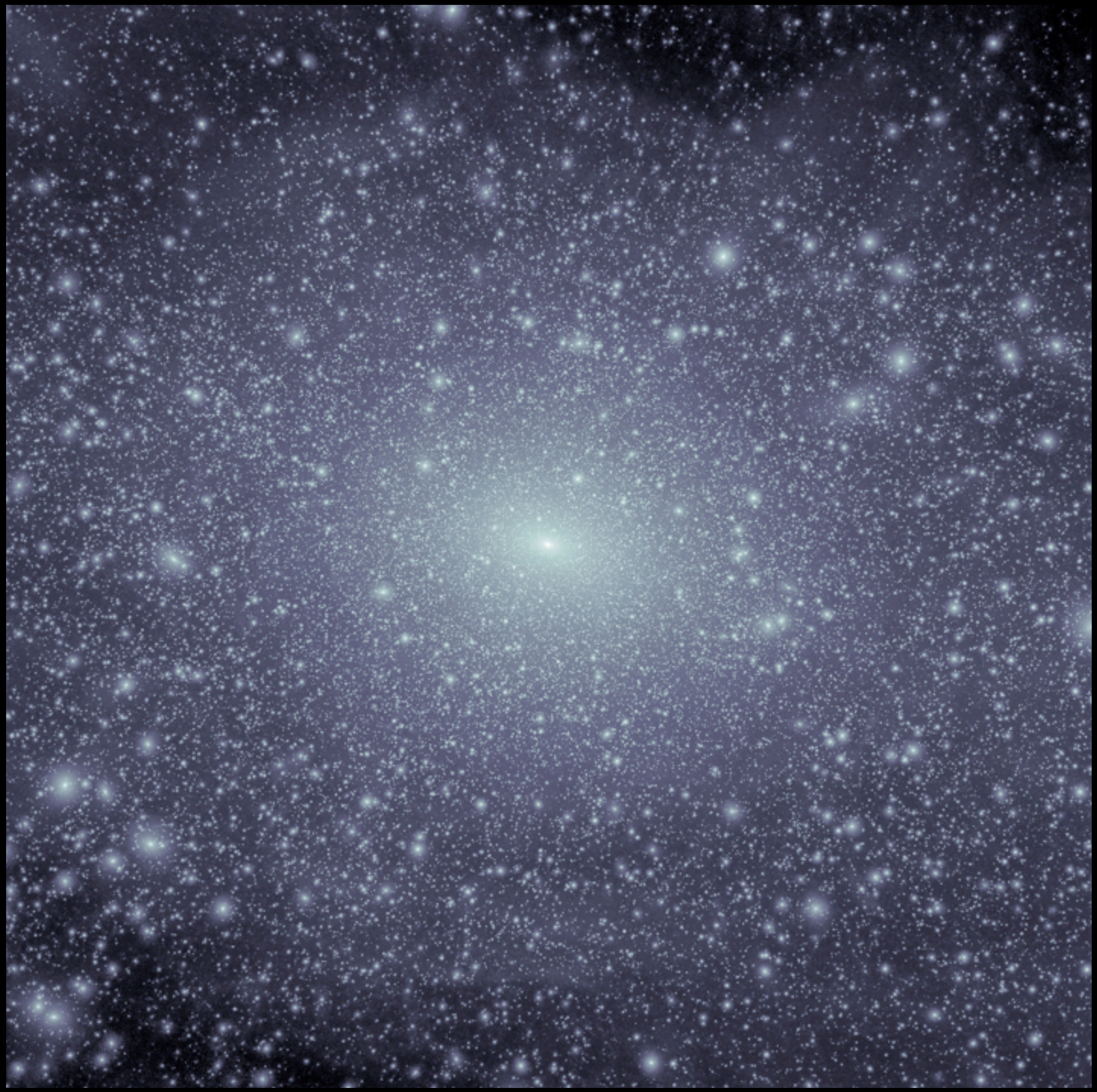

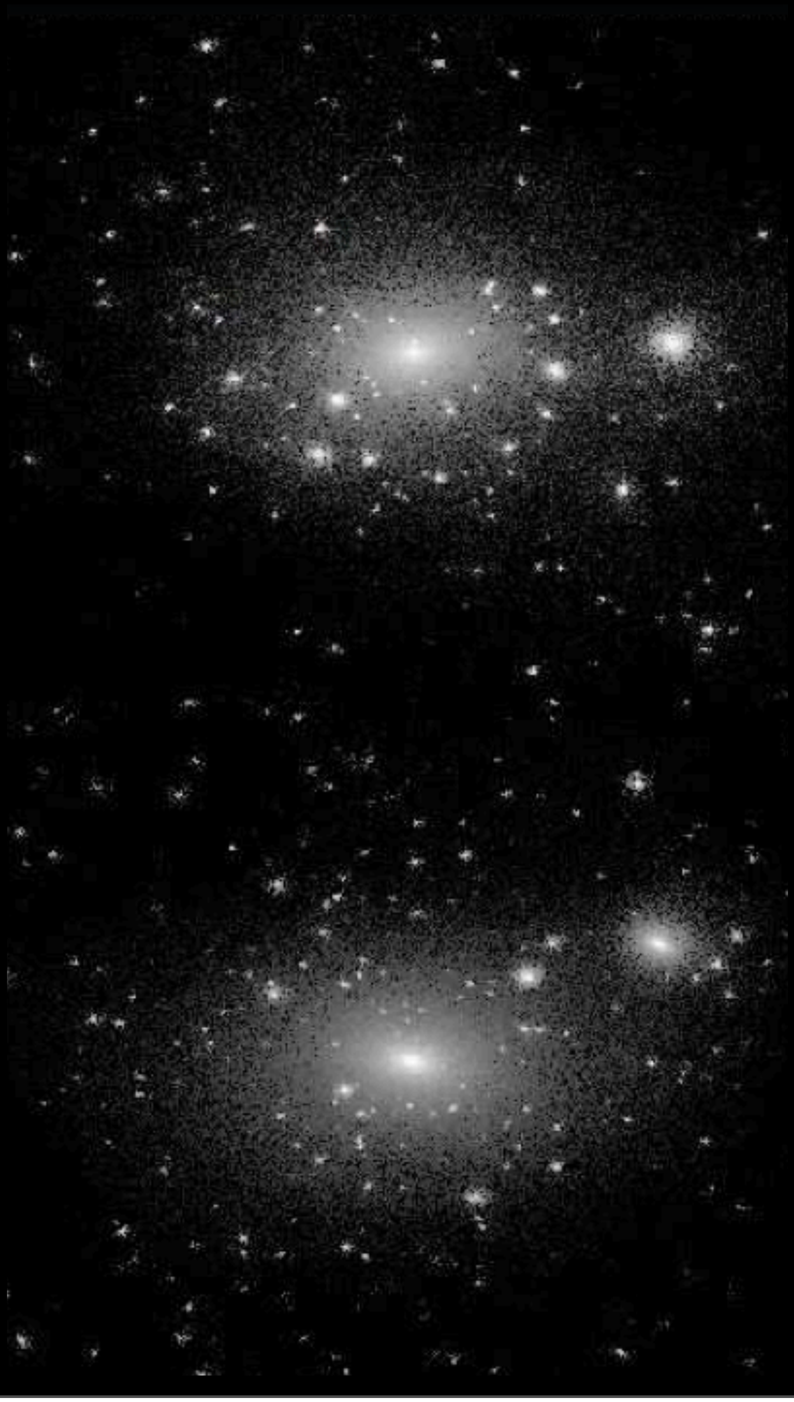

Critical Issues

i) satellite DM haloes

CDM Substructure in simulated cluster and galaxy haloes look similar.

Expected number of satellites in Milky Way- like galaxies in CDM largely exceeds the observed abundance.

Kravtsov, Klypin, Gnedin 2004

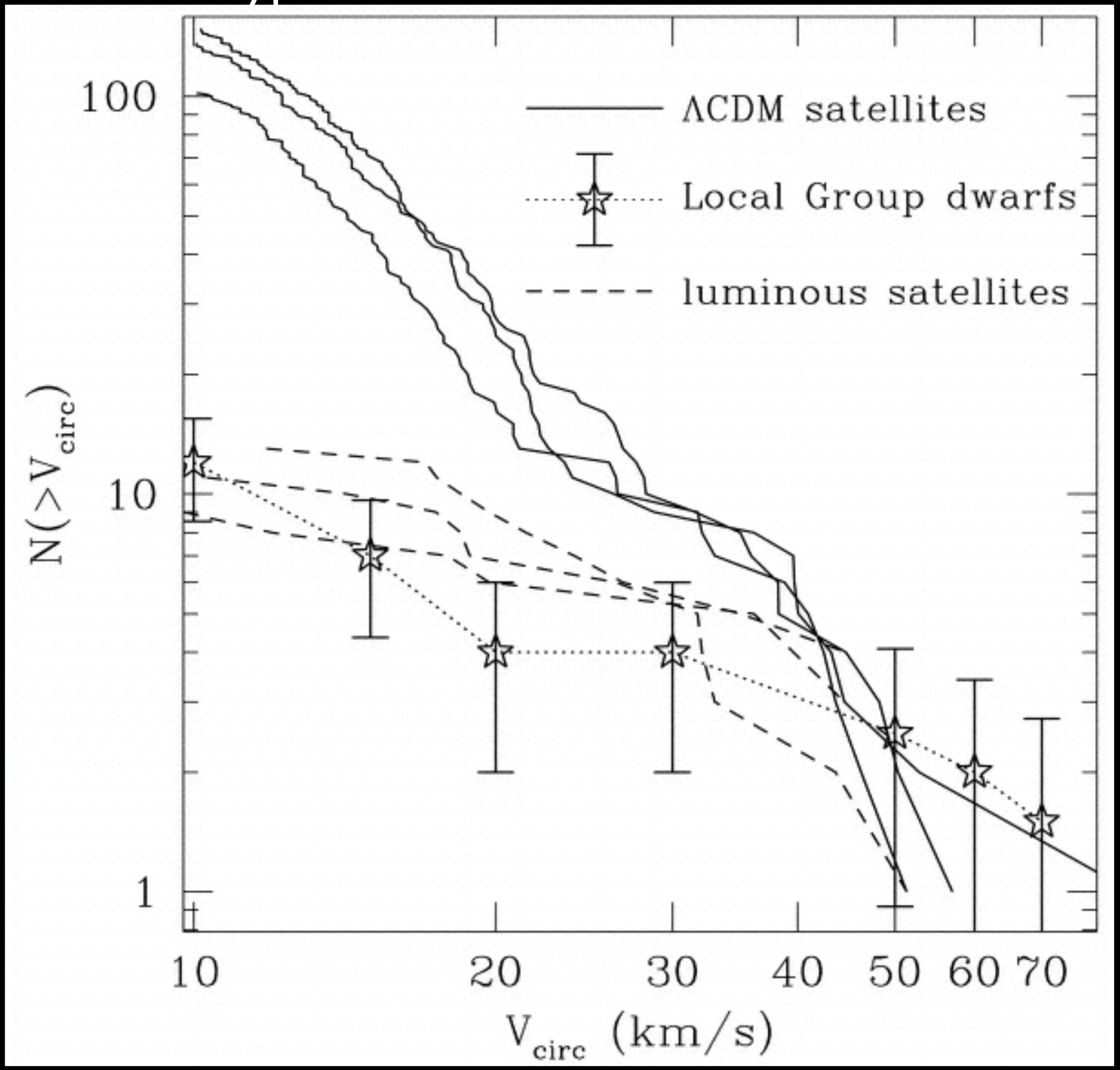

Critical Issues

ii) density profiles

Most observed dwarf galaxies consist of a rotating stellar disk embedded in a massive dark-matter halo with a near-constant-density core. Models based on the dominance of CDM, however, invariably form galaxies with dense spheroidal stellar bulges and steep central dark-matter profiles, because low-angular- momentum baryons and dark matter sink to the centres of galaxies through accretion and repeated mergers.

Moore et al. 2002

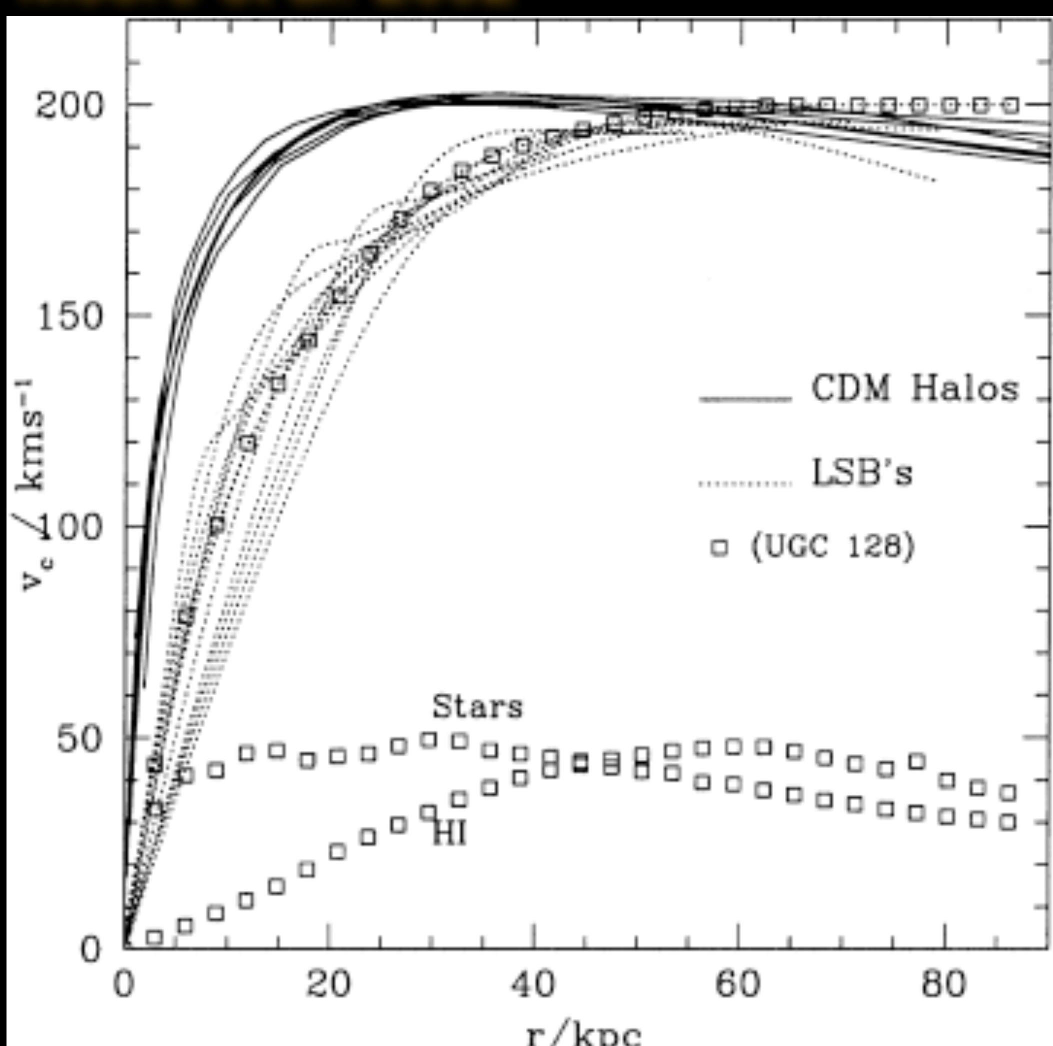

The effect of adopting a cutoff
in the power spectrum for r<8 Mpc

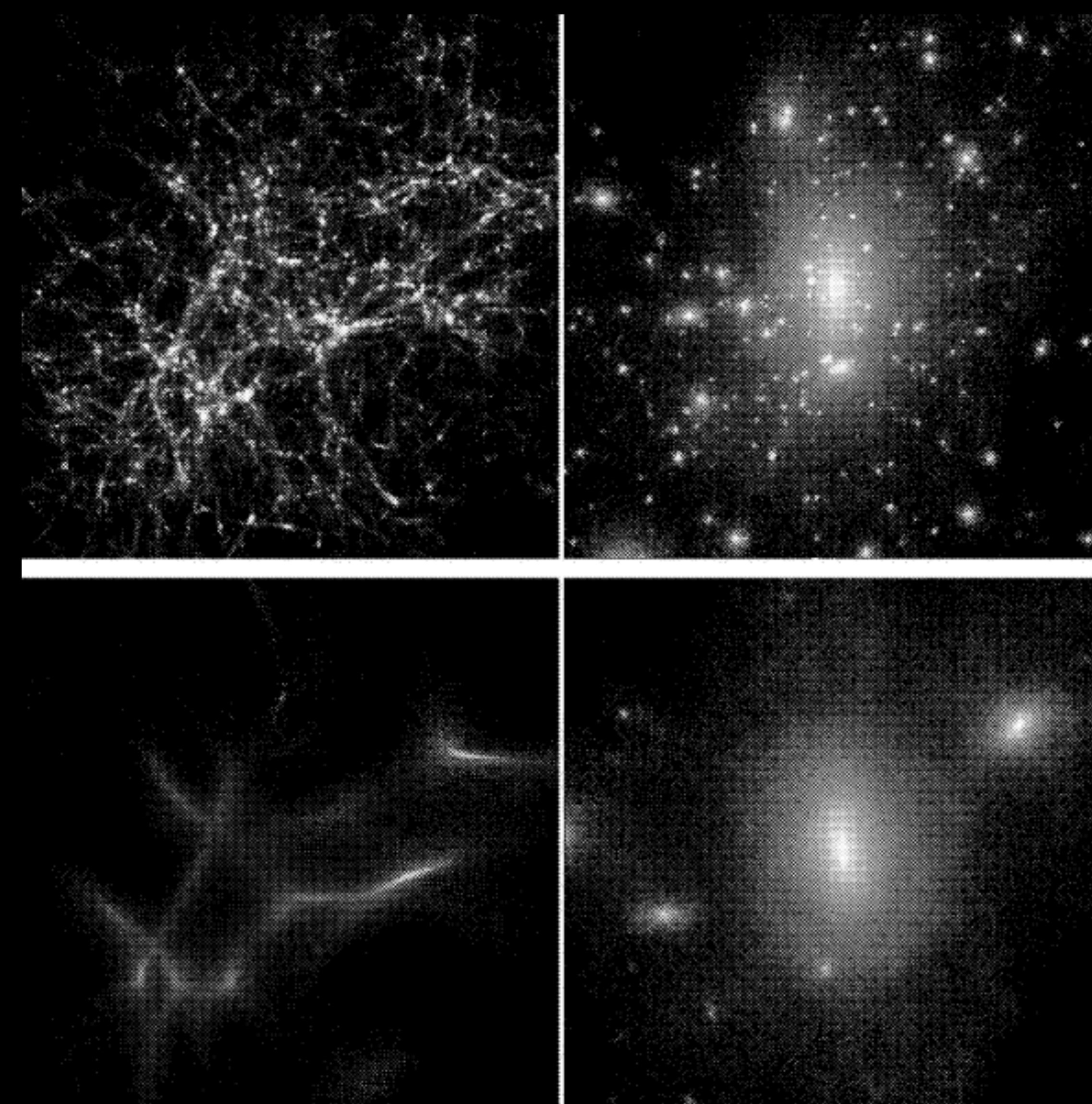

Critical Issues

iii)over-prediction of faint galaxies

In all first-generation SAM the number density of faint (low-mass) galaxies was over-predicted

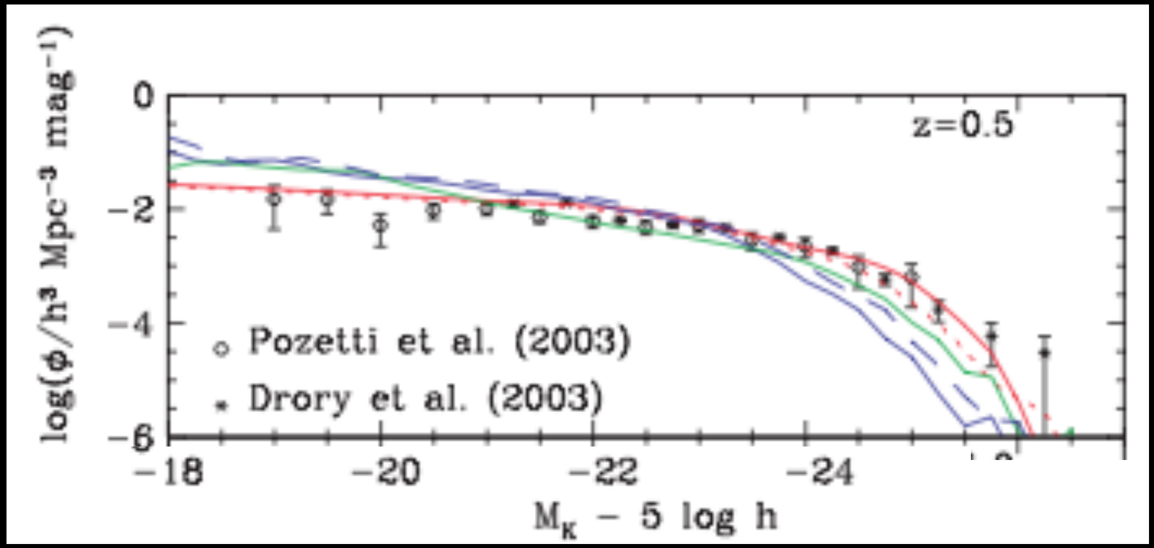

Bower et al. 2006

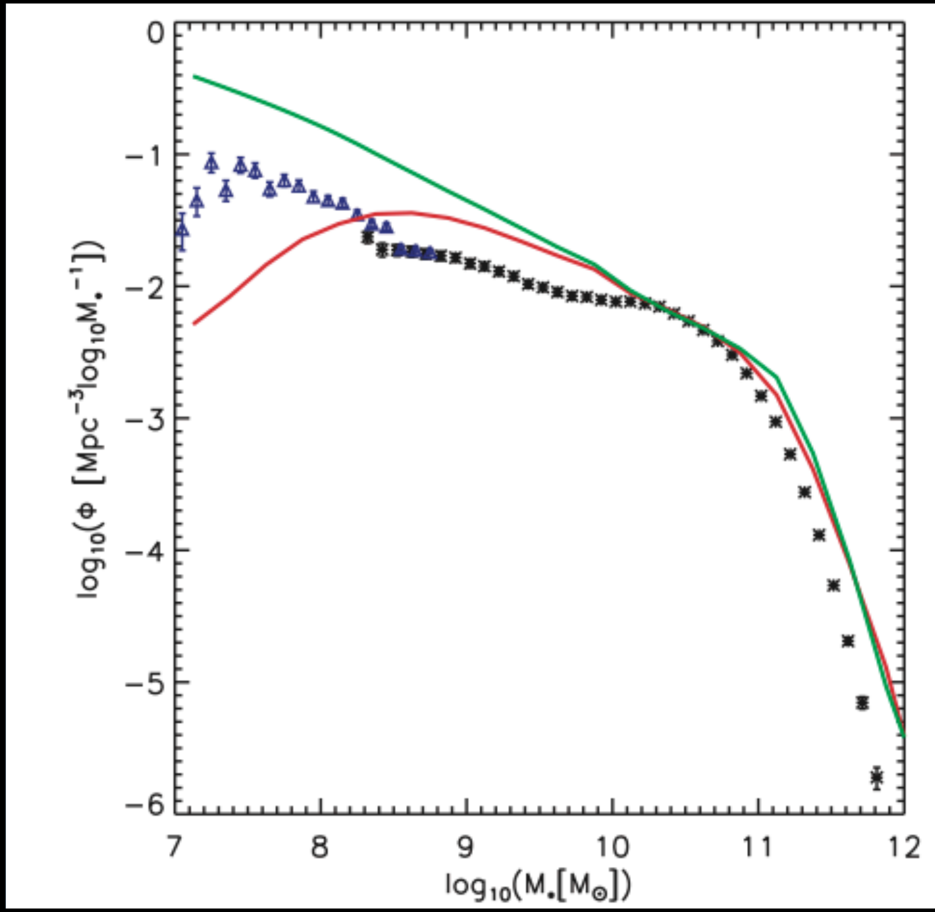

The Stellar Mass Function in the De Lucia et al. SAM based on Millenium merger trees

The K-Band Luminosity Function in the Somerville et al. SAM

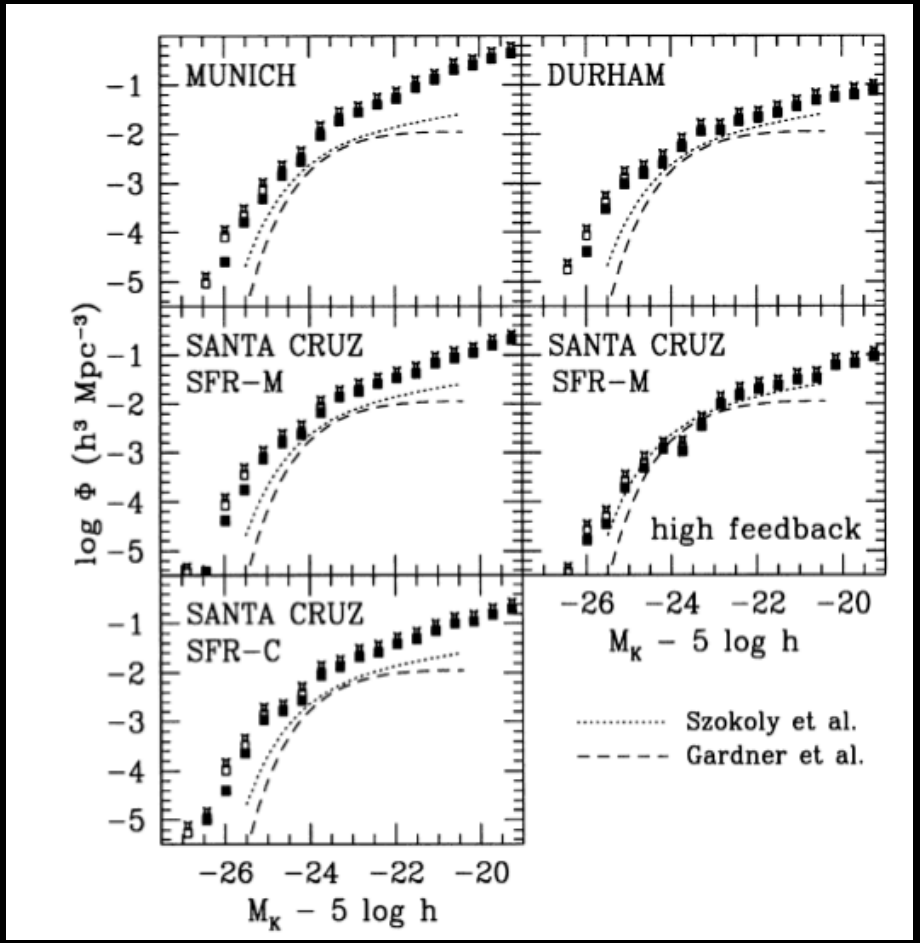

A first-order solution: feedback and UV background

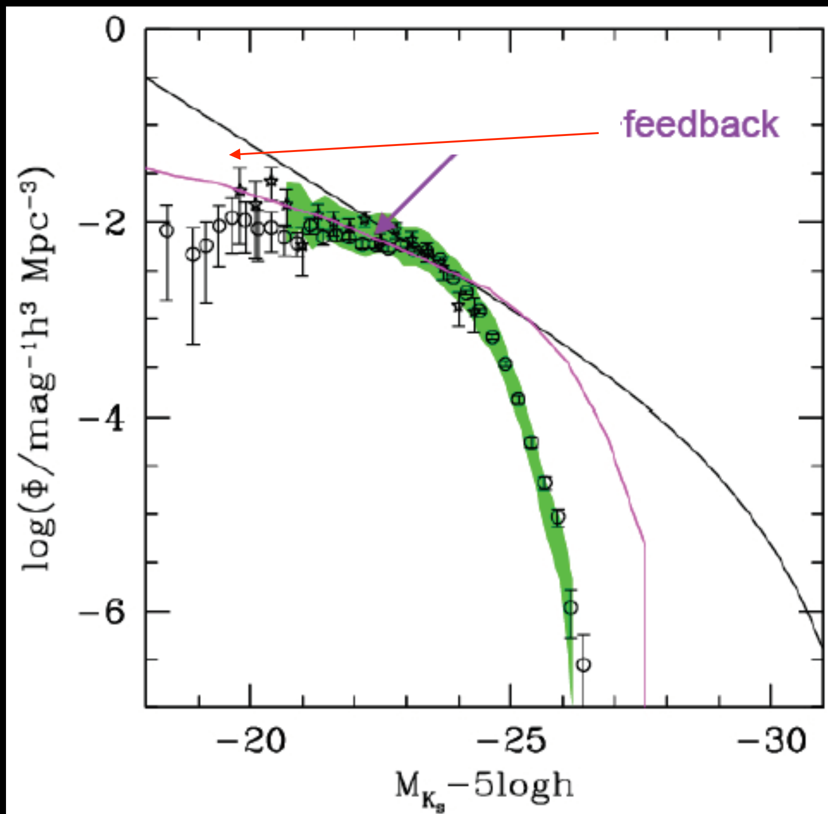

The origin of the problem:

The DM halo Mass function has a steep log slope $N \sim M^{-1.8}$

While the Observed Galaxy Luminosity Function

has a much flattter slope $N \sim L^{-1.2}$

A Possible Solution:

Suppress luminosity (star formation) in low-mass haloes

Heat - Expell Gas from shallow potential wells

- Enhanced SN feedback
- UV background

$$E_{SN} \approx 10^{51}\, \eta_0 \eta_{IMF}\, \Delta M_* erg/s$$

$$v_{SN} = \sqrt{E_{SN}/M_{gas}} \approx 100 \quad km/s$$

At Z=0 the mass scale at which SN can effectively espell gas from DM potential wells

$$M_{SN} \sim 10^{10}\, M_\odot$$

at low z, at higher redshift the density is higher an M_{SN} increases

Vogelsberger et al. 2014

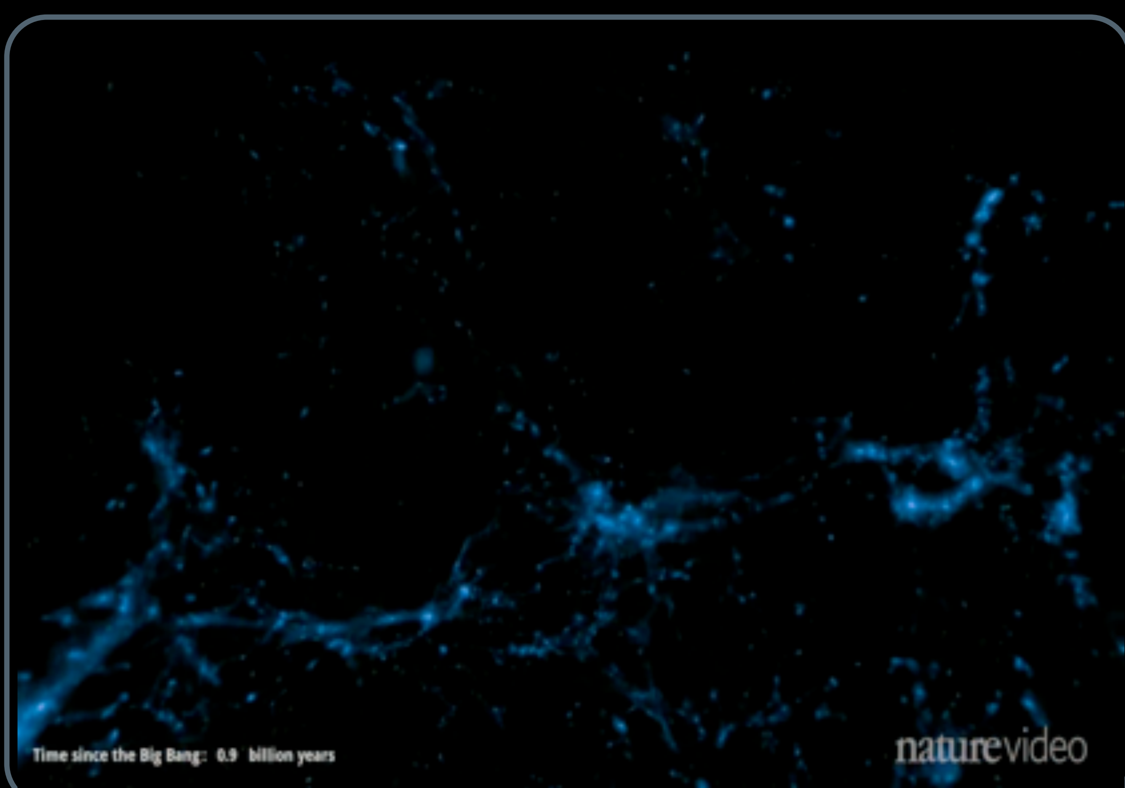

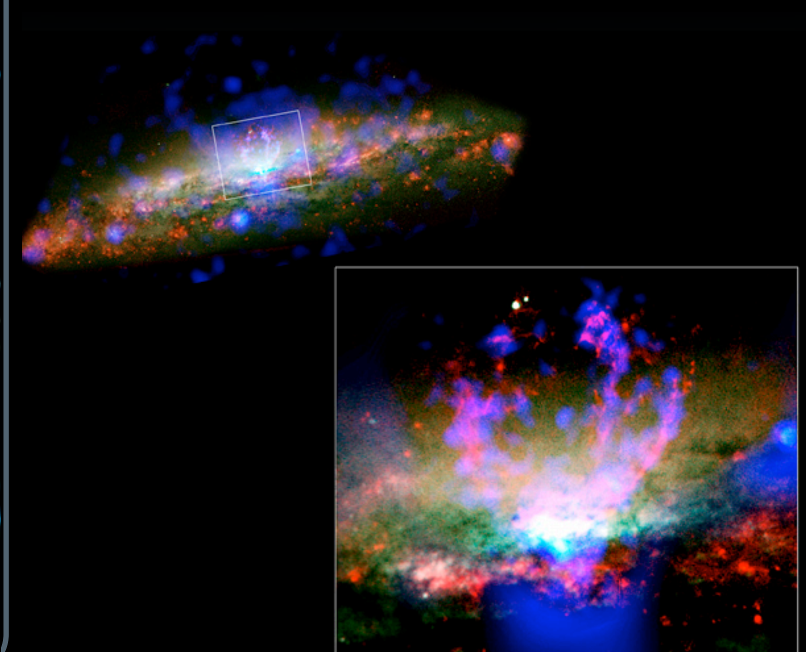

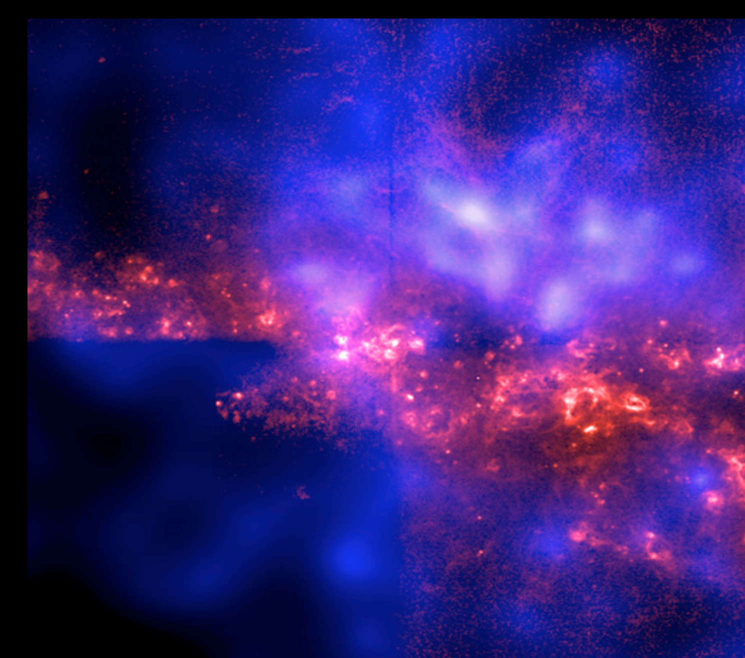

A first-order solution: feedback and UV background

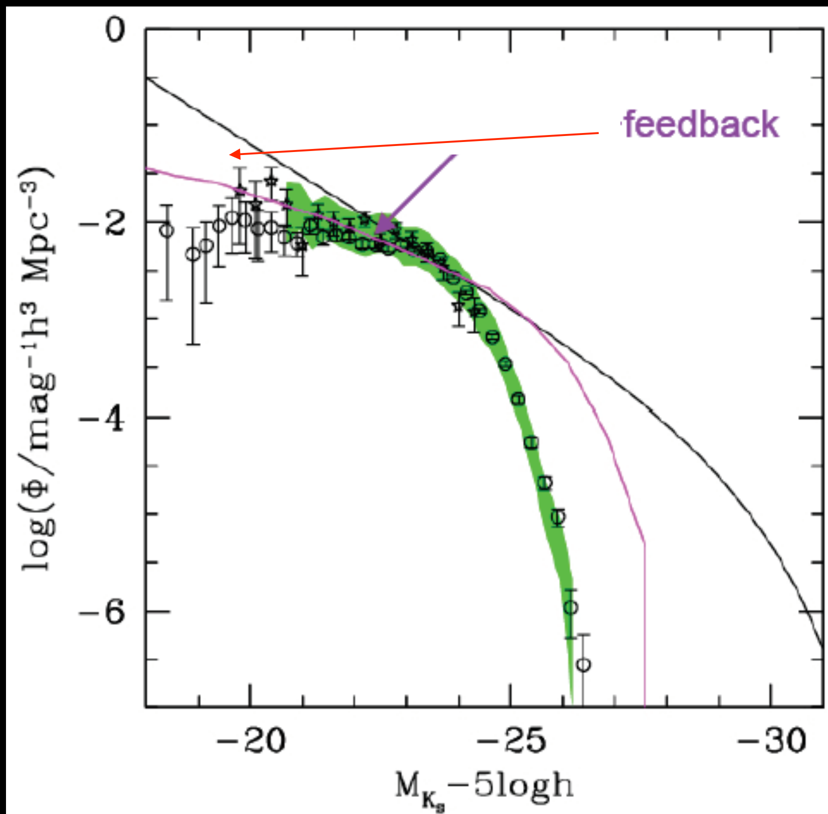

The origin of the problem:
The DM halo Mass function has a steep log slope $N \sim M^{-1.8}$
While the Observed Galaxy Luminosity Function
has a much flattter slope $N \sim L^{-1.2}$

A Possible Solution:
Suppress luminosity (star formation) in low-mass haloes
Heat - Expell Gas from shallow potential wells
- Enhanced SN feedback
- UV background

$$E_{SN} \approx 10^{51}\, \eta_0 \eta_{IMF}\, \Delta M_* erg/s$$

$$v_{SN} = \sqrt{E_{SN}/M_{gas}} \approx 100 \quad km/s$$

At Z=0 the mass scale at which SN can effectively espell gas from DM potential wells

$$M_{SN} \sim 10^{10}\, M_\odot$$

at low z, at higher redshift the density is higher an M_{SN} increases

Vogelsberger et al. 2014

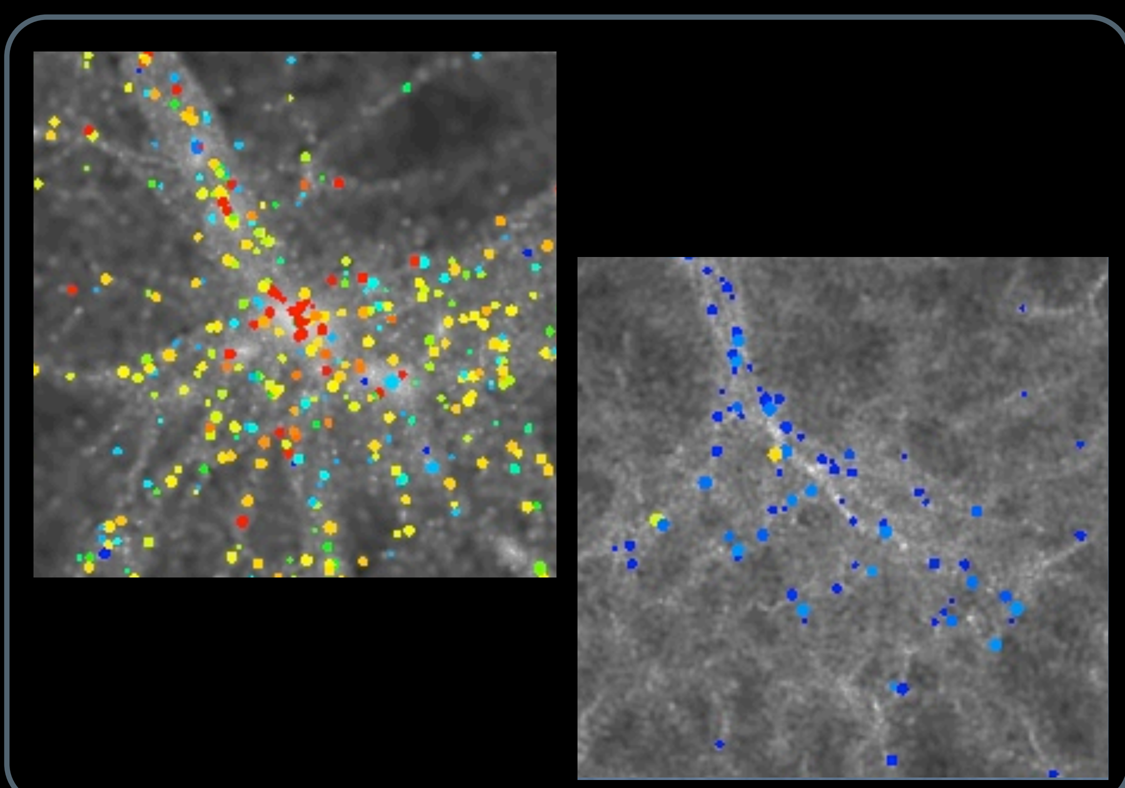

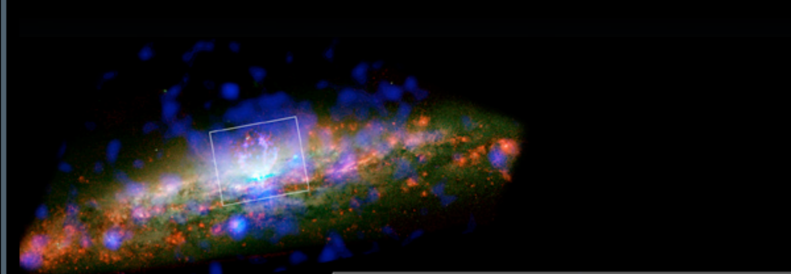

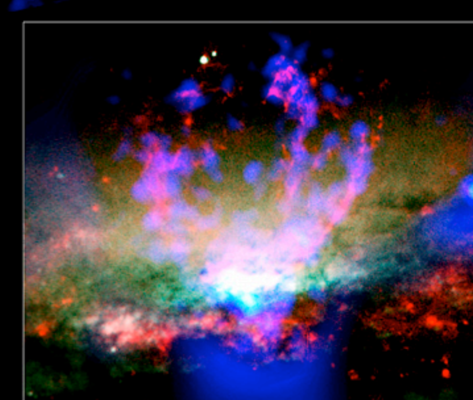

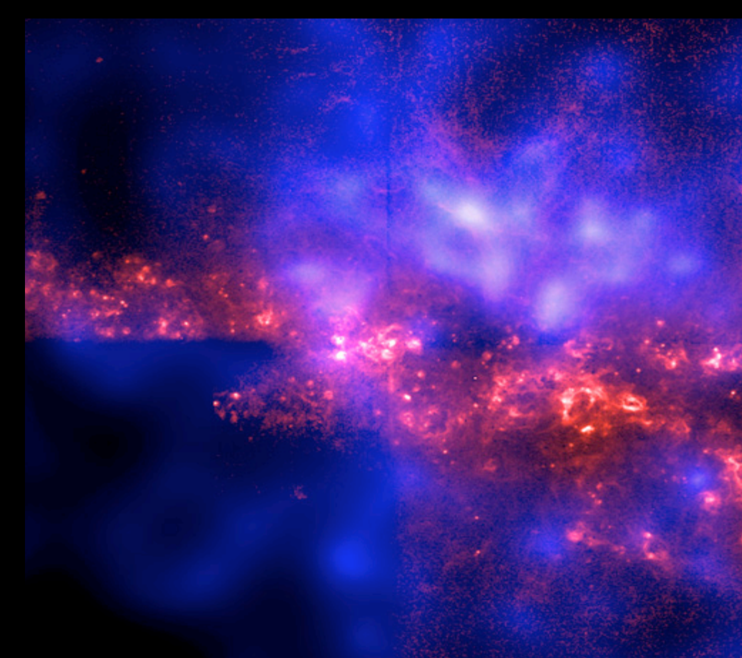

A first-order solution: feedback and UV background

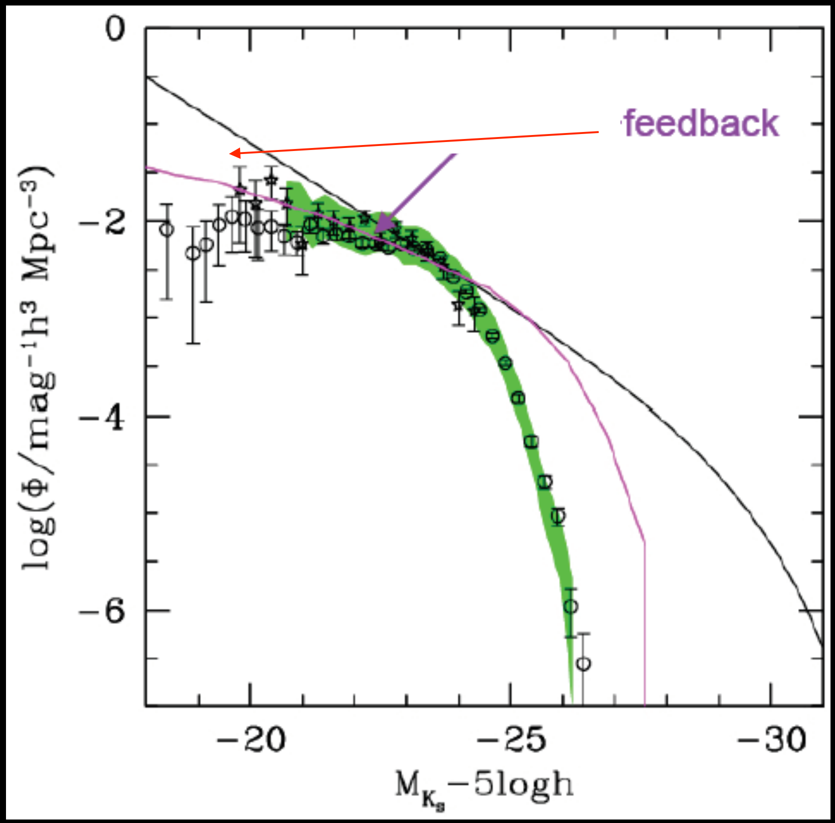

The origin of the problem:
The DM halo Mass function has a steep log slope $N \sim M^{-1.8}$
While the Observed Galaxy Luminosity Function
has a much flattter slope $N \sim L^{-1.2}$

A Possible Solution:
Suppress luminosity (star formation) in low-mass haloes
Heat - Expell Gas from shallow potential wells
- Enhanced SN feedback
- UV background

$$E_{SN} \approx 10^{51}\, \eta_0 \eta_{IMF}\, \Delta M_* erg/s$$

$$v_{SN} = \sqrt{E_{SN}/M_{gas}} \approx 100 \quad km/s$$

Corresponds to a mass scale affected by
non-gravitational SN energy injection

$$M \approx (v_{esc}^2/G)\, r$$

$$M \approx A\, v_{esc}^3\, (1+z)^{-3/2}$$

$$r \propto (M/\rho)^{1/3}$$

$$\rho = 180\, \rho_u = 180\, \rho_u\, (1+z)^3$$

$$A \equiv \sqrt{3/G^3\, 4\pi\, \rho_u}$$

$$v_{esc} = v_{SN} \rightarrow \quad M_{SN} \approx A\, v_{SN}^3\, (1+z)^{-3/2}$$

at $z \approx 0$ $\quad M_{SN} \sim 10^{10}\, M_\odot$

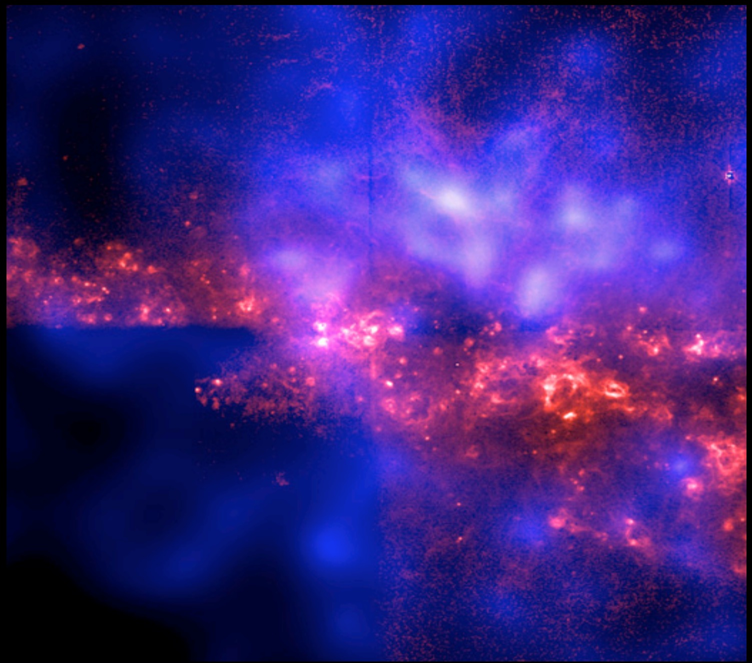

Feedback and UV background
Effect on the density profiles

A proposed solution at low redshift

"... The rapid fluctuations caused by episodic feedback progressively pump energy into the DM particle orbits, so that they no longer penetrate to the centre of the halo" (Winberg et al. 2013, Governato et al. 2012)

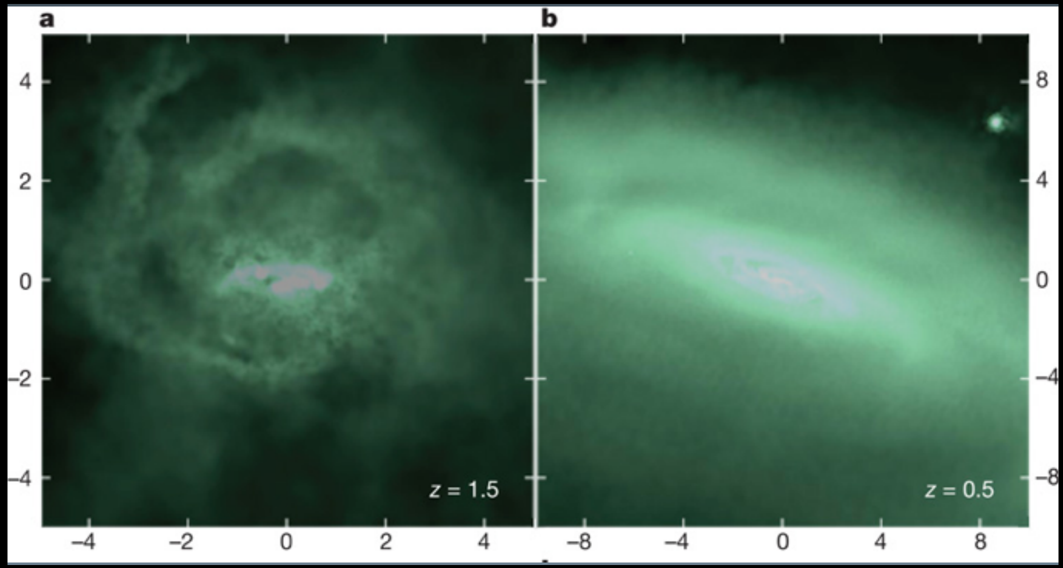

Governato et al. 2012

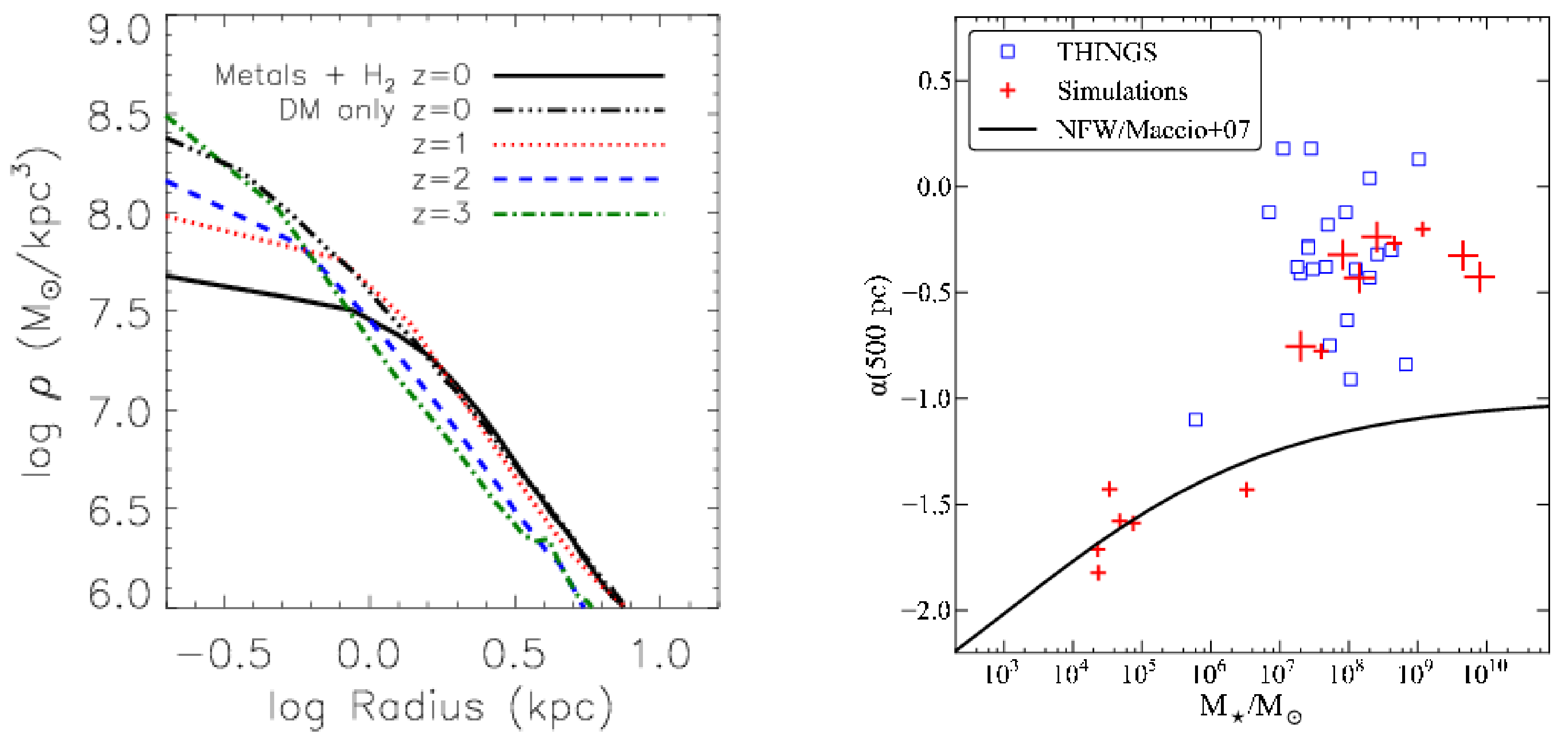

Fig. 3. Baryonic effects on CDM halo profiles in cosmological simulations, from Governato et al. (2012). *(Left)* The upper, dot-dash curve shows the cuspy dark matter density profile resulting from from a collisionless N-body simulation. Other curves show the evolution of the dark matter profile in a simulation from the same initial conditions that includes gas dynamics, star formation, and efficient feedback. By $z = 0$ (solid curve) the perturbations from the fluctuating baryonic potential have flattened the inner profile to a nearly constant density core. *(Right)* Logarithmic slope of the dark matter profile α measured at 0.5 kpc, as a function of galaxy stellar mass. Crosses show results from multiple hydrodynamic simulations. Squares show measurements from rotation curves of observed galaxies. The black curve shows the expectation for pure dark matter simulations, computed from NFW profiles with the appropriate concentration. For $M_* > 10^7 M_\odot$, baryonic effects reduce the halo profile slopes to agree with observations.

Feedback and UV background

i) the abundance of satellites

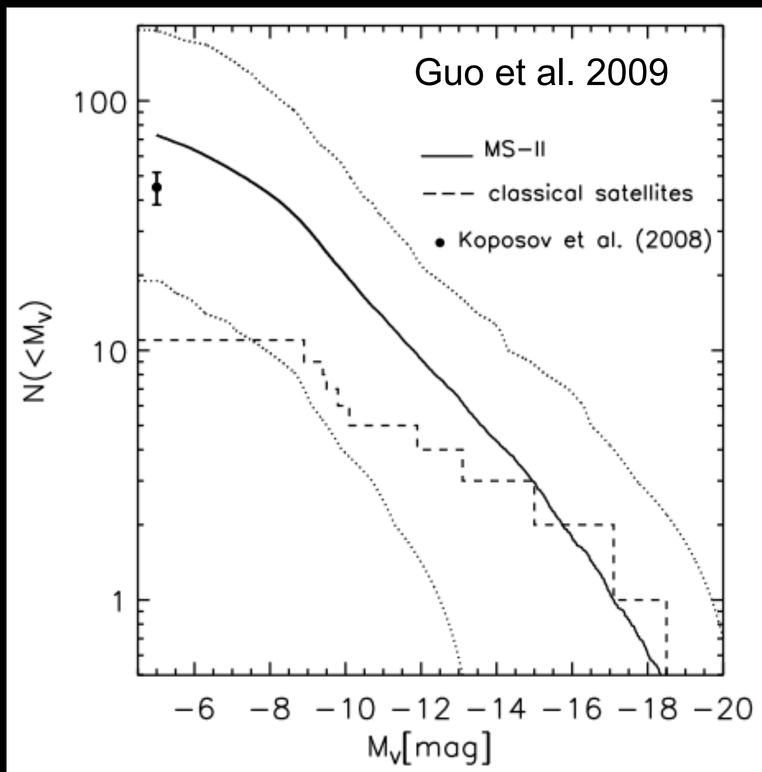

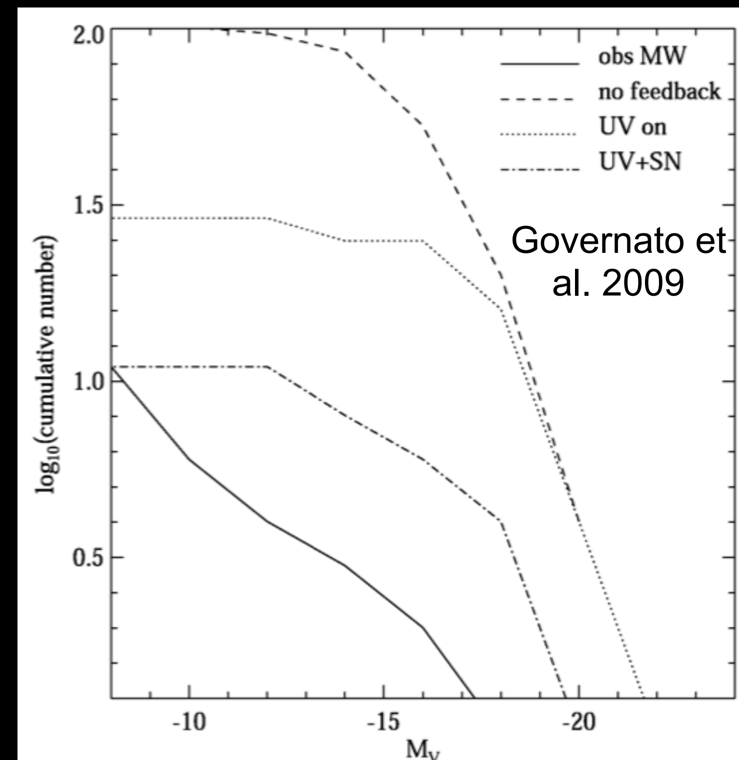

Brooks & Zolotov 2014

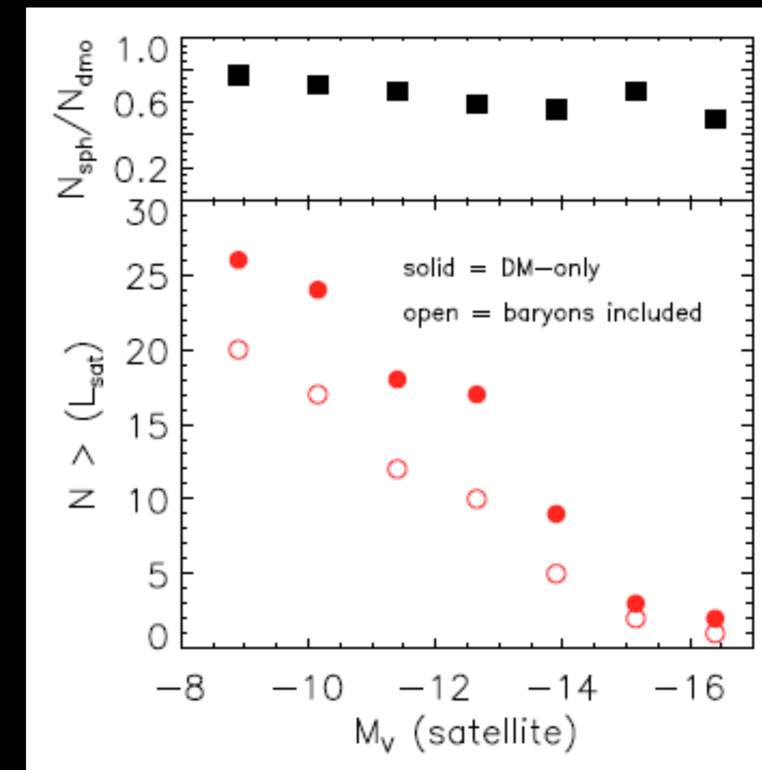

ii) the abundance of faint galaxies

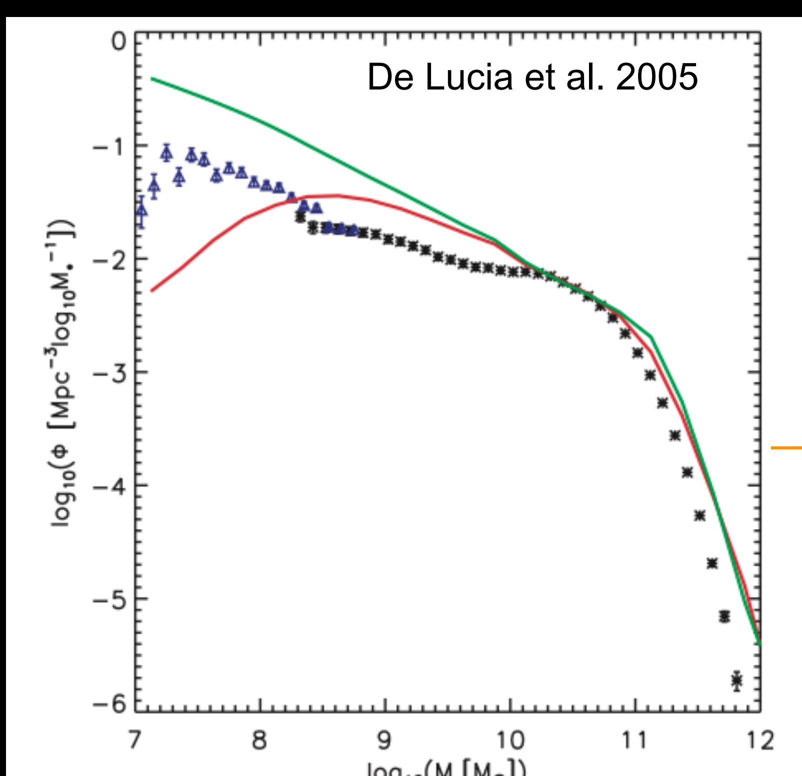

Refined treatment of Gas and Stellar Stripping

Enhanced (tuned) feedback dependence on the circular velocity of the DM halo

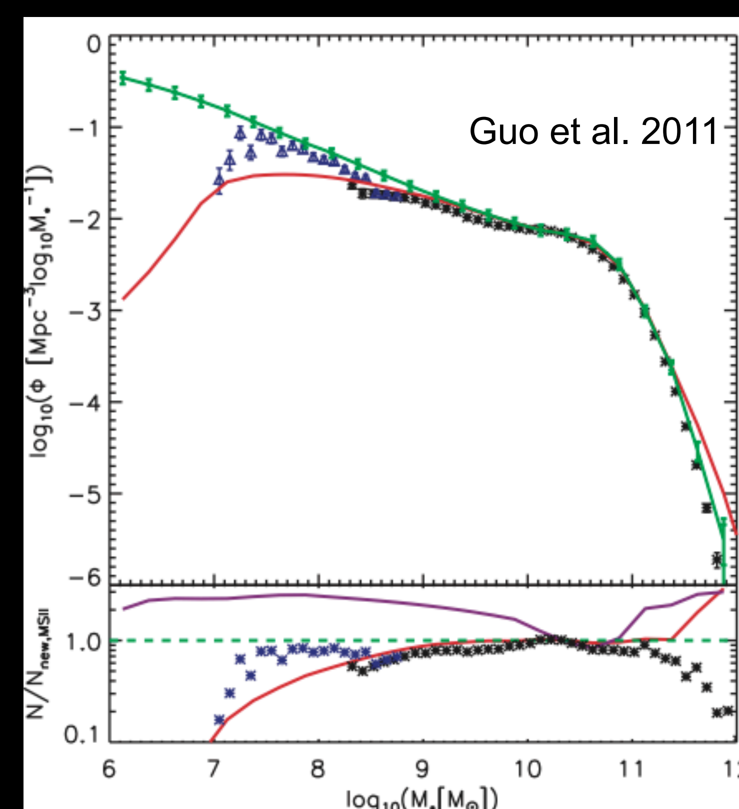

The problem persists at high redshifts

NM et al. 2006

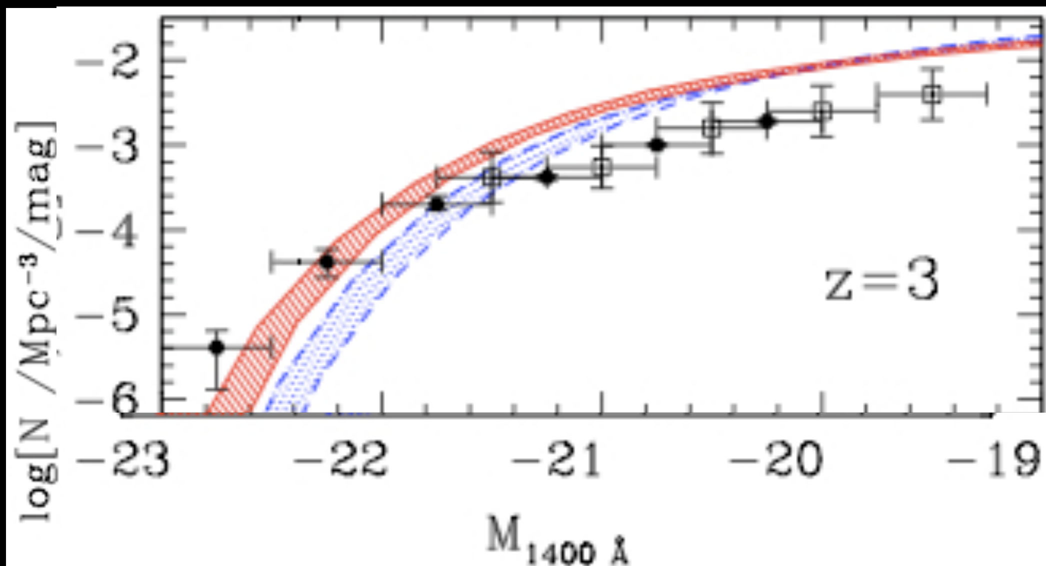

Lo Faro et al. 2009

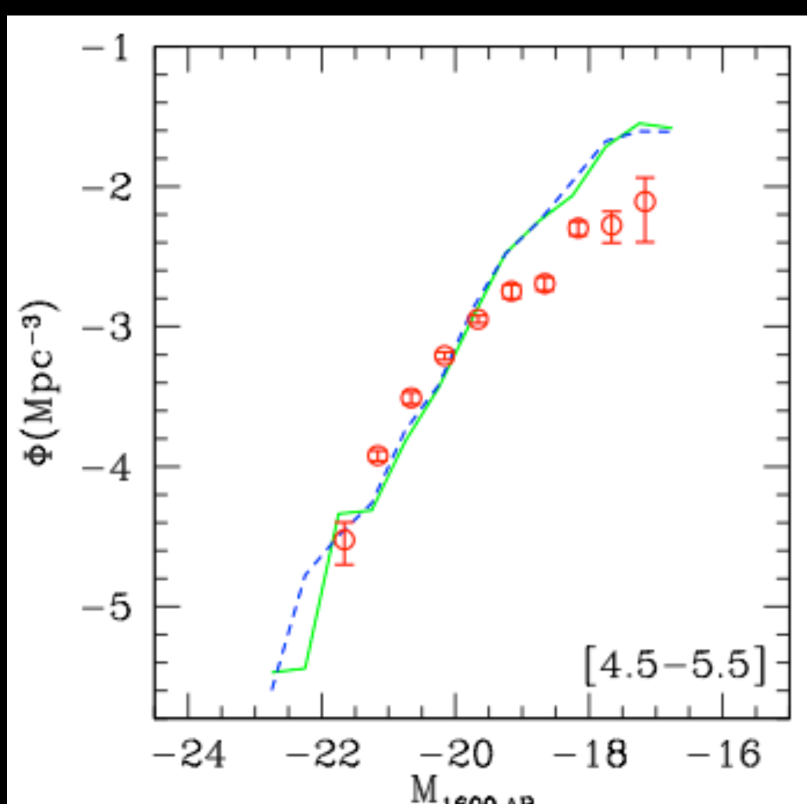

Guo et al. 2011

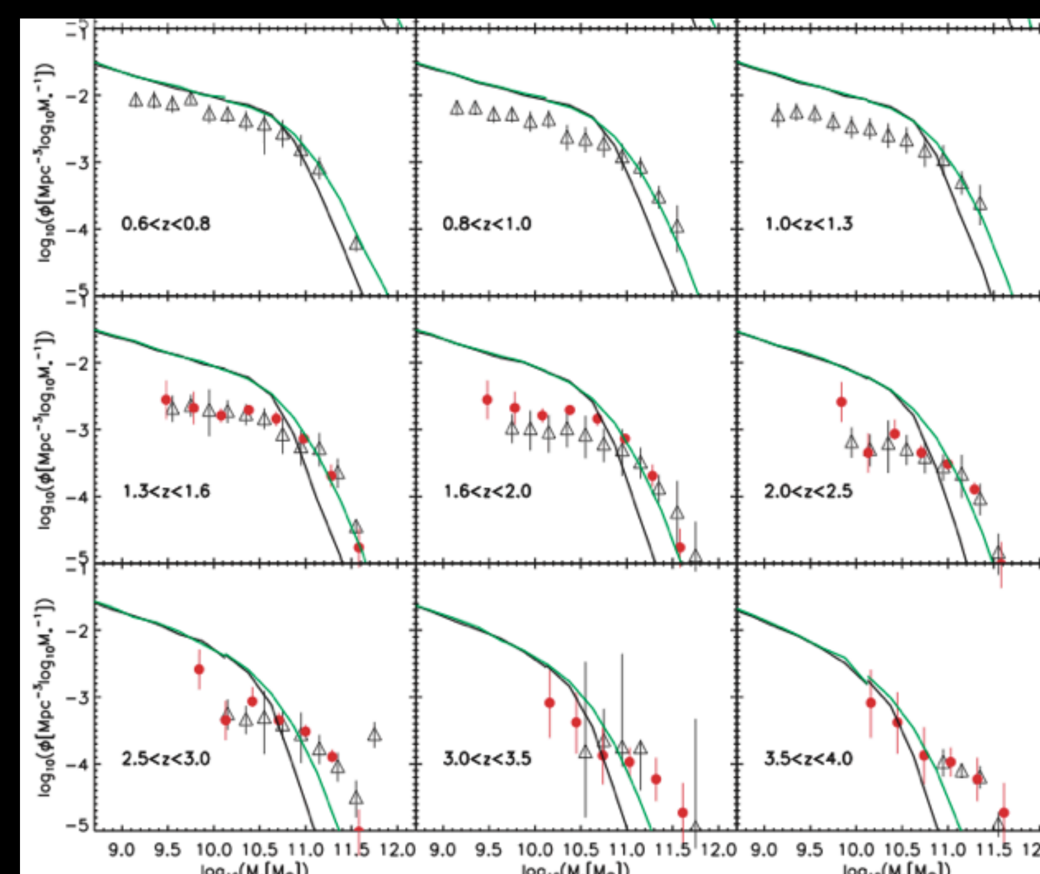

The problem persists at high redshifts

NM et al. 2006

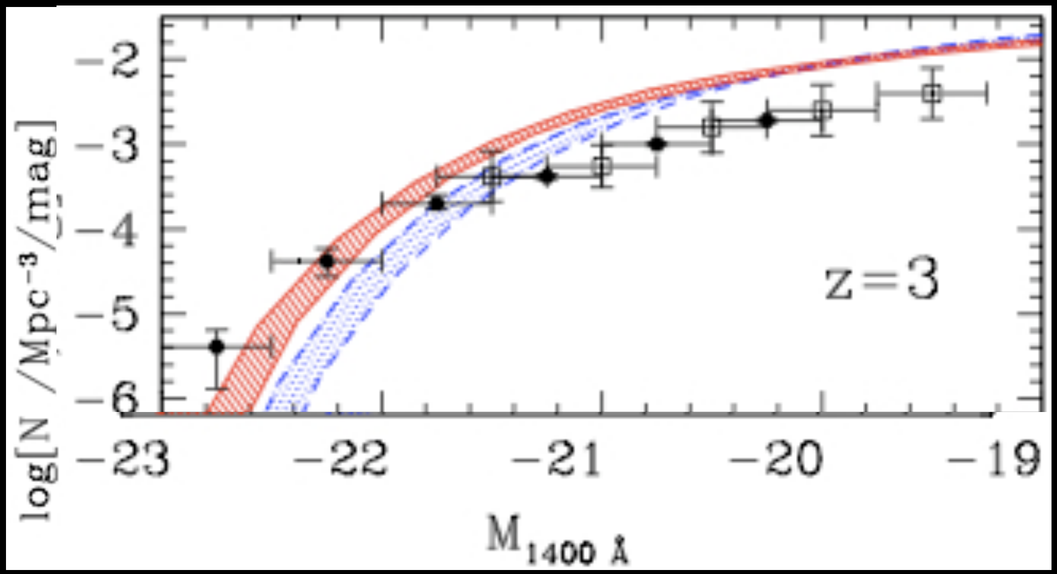

Hirschmann et al. 2012

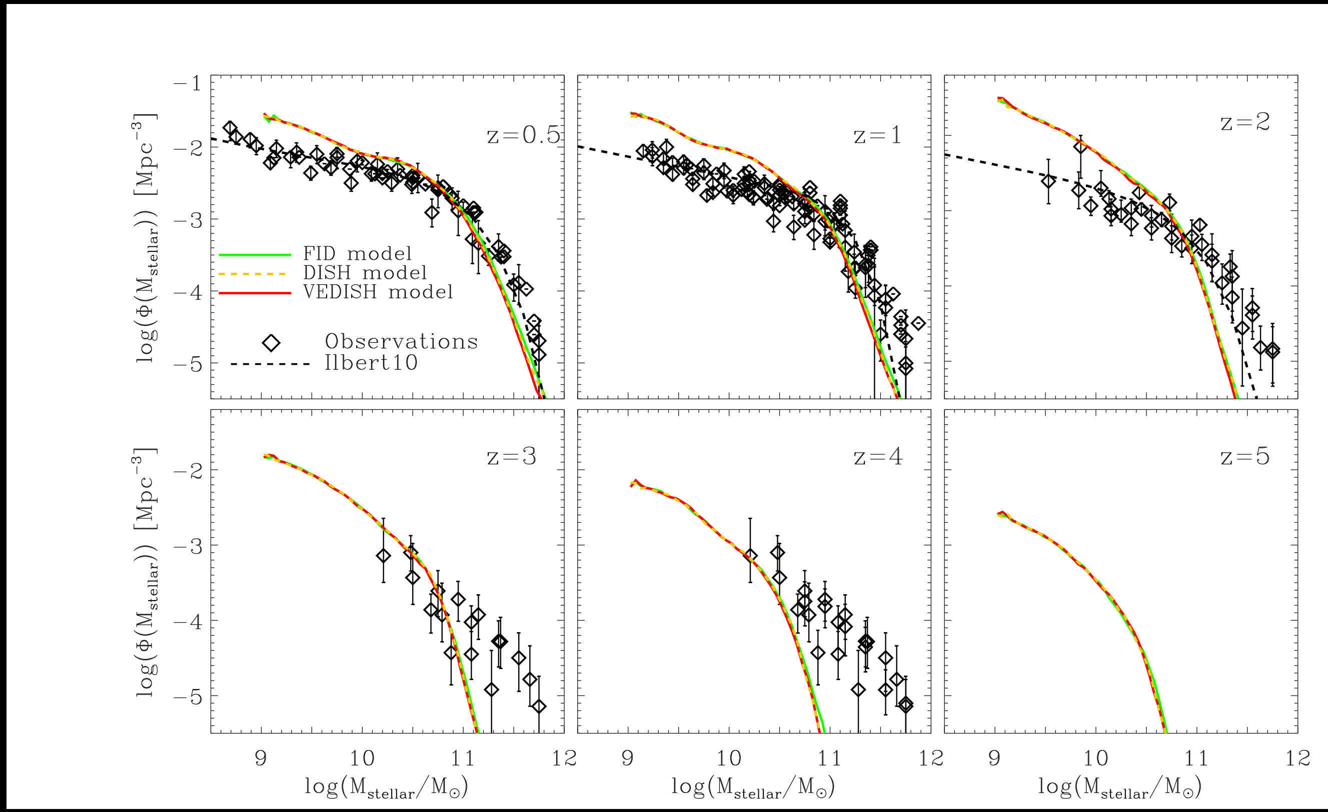

Lo Faro et al. 2009

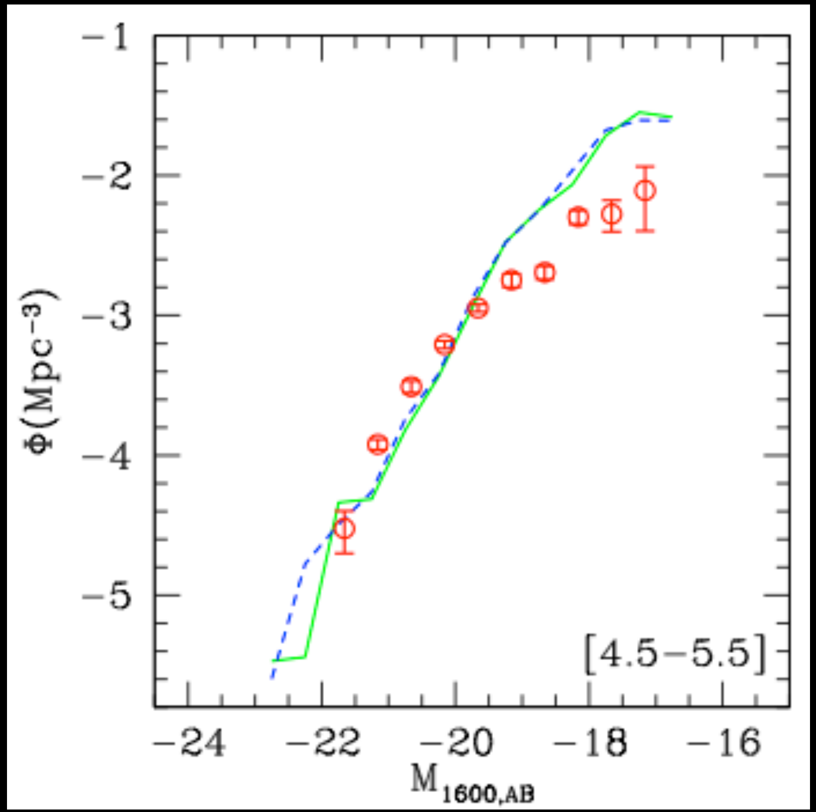

The problem persists at high redshifts

Corresponds to a mass scale affected by non-gravitational SN energy injection

$$M \approx (v_{esc}^2/G)\, r$$

$$r \propto (M/\rho)^{1/3}$$

$$\rho = 180\,\rho_u = 180\,\rho_u\,(1+z)^3$$

$$M \approx A\, v_{esc}^3\,(1+z)^{-3/2}$$

$$A \equiv \sqrt{3/G^3\, 4\,\pi\,\rho_u}$$

$$v_{esc} = v_{SN} \rightarrow \quad M_{SN} \approx A\, v_{SN}^3\,(1+z)^{-3/2}$$

at $z \approx 0$ $\quad M_{SN} \sim 10^{10}\, M_\odot$

Lo Faro et al. 2009

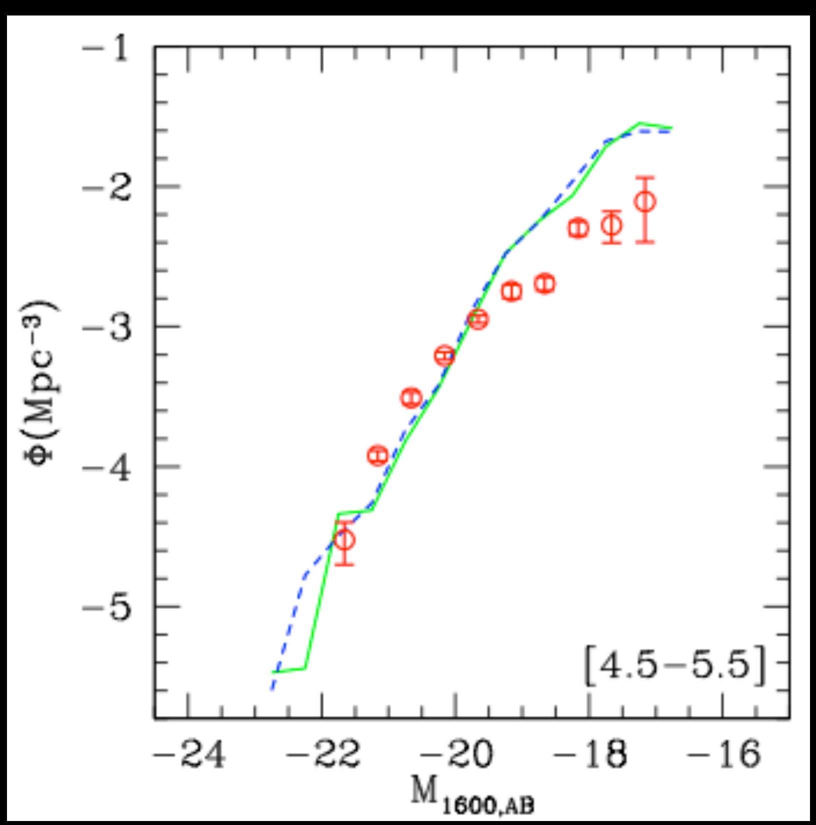

Guo et al. 2011

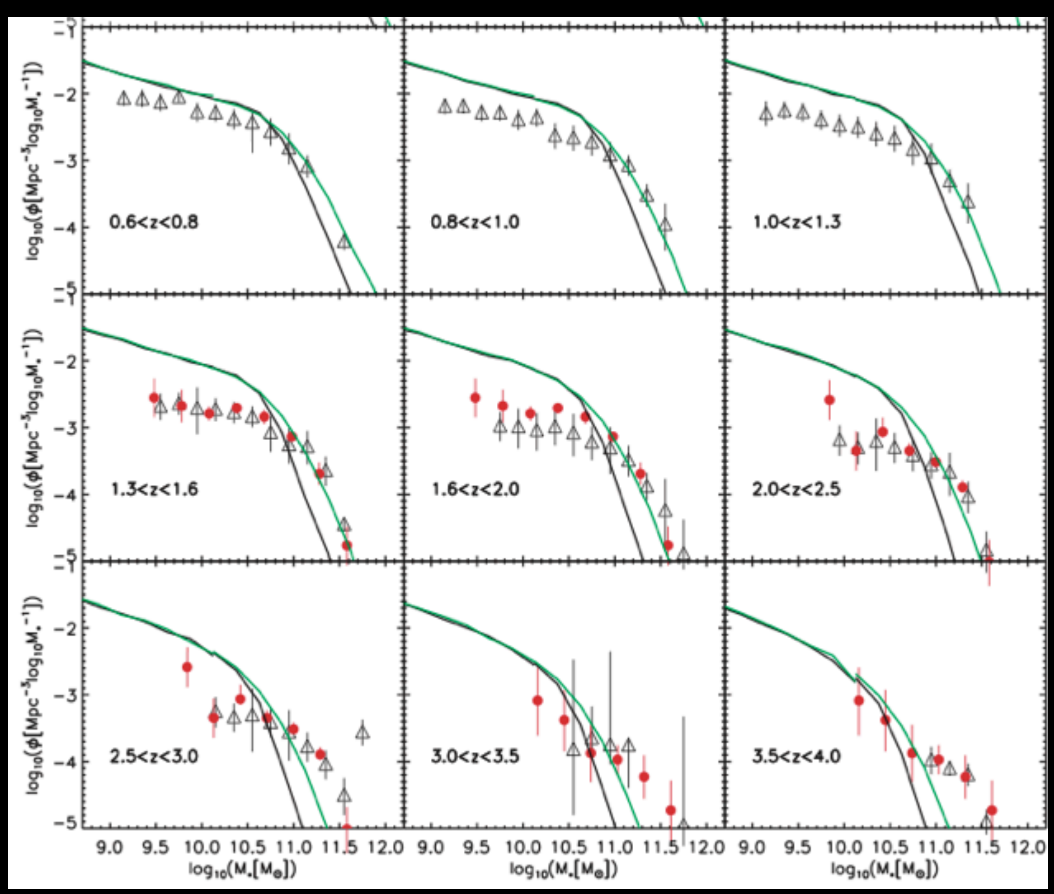

The problem persists at high redshifts

Corresponds to a mass scale affected by non-gravitational SN energy injection

$$M \approx (v_{esc}^2/G)\, r$$

$$r \propto (M/\rho)^{1/3}$$

$$\rho = 180\,\rho_u = 180\,\rho_u\,(1+z)^3$$

$$M \approx A\, v_{esc}^3\,(1+z)^{-3/2}$$

$$A \equiv \sqrt{3/G^3\,4\pi\,\rho_u}$$

$$v_{esc} = v_{SN} \rightarrow \quad M_{SN} \approx A\, v_{SN}^3\,(1+z)^{-3/2}$$

at $z \approx 0$ $\quad M_{SN} \sim 10^{10}\, M_\odot$

Hirschmann et al. 2012

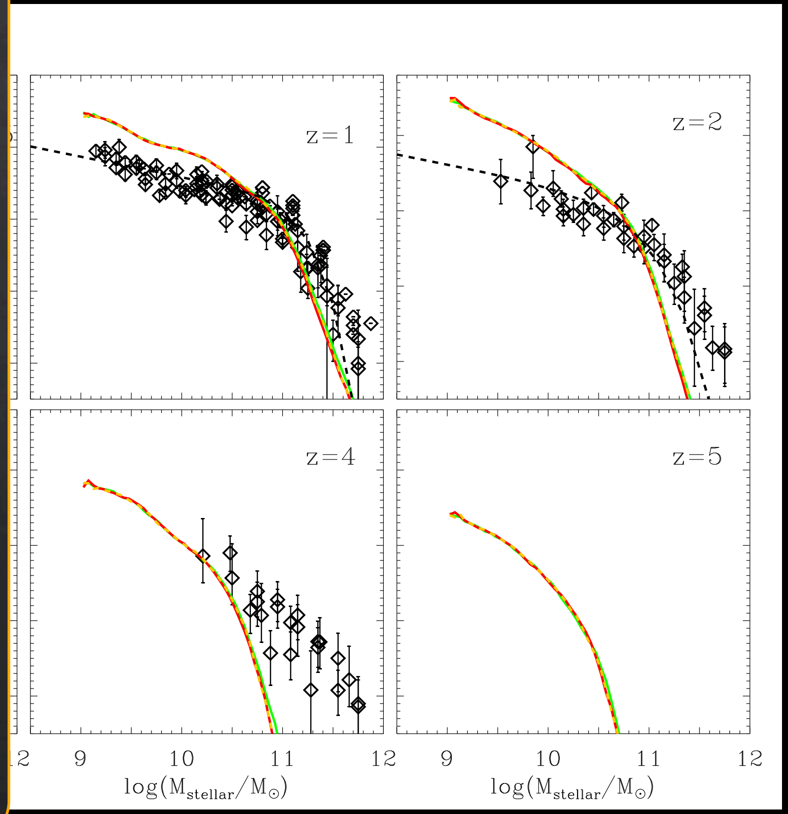

Lo Faro et al. 2009

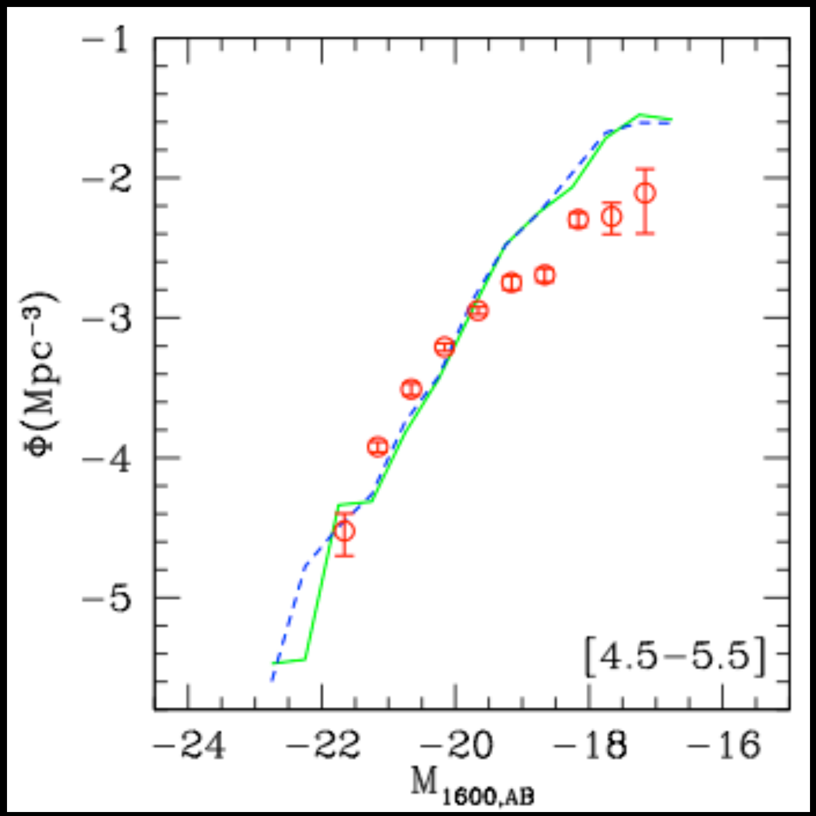

The problem persists at high redshifts
In addition, increasing the feedback yields satellite colors too red

NM et al. 2006

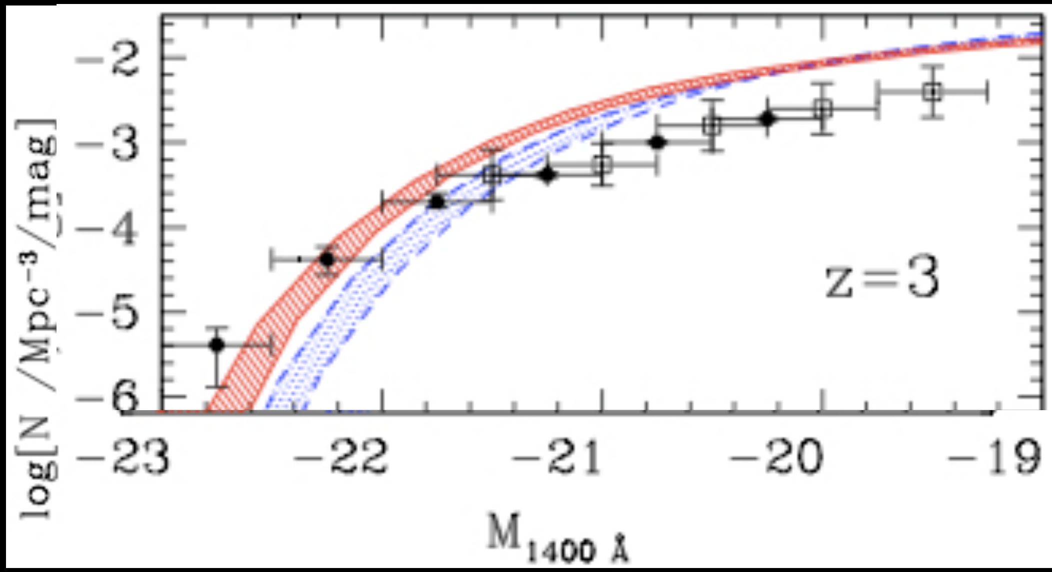

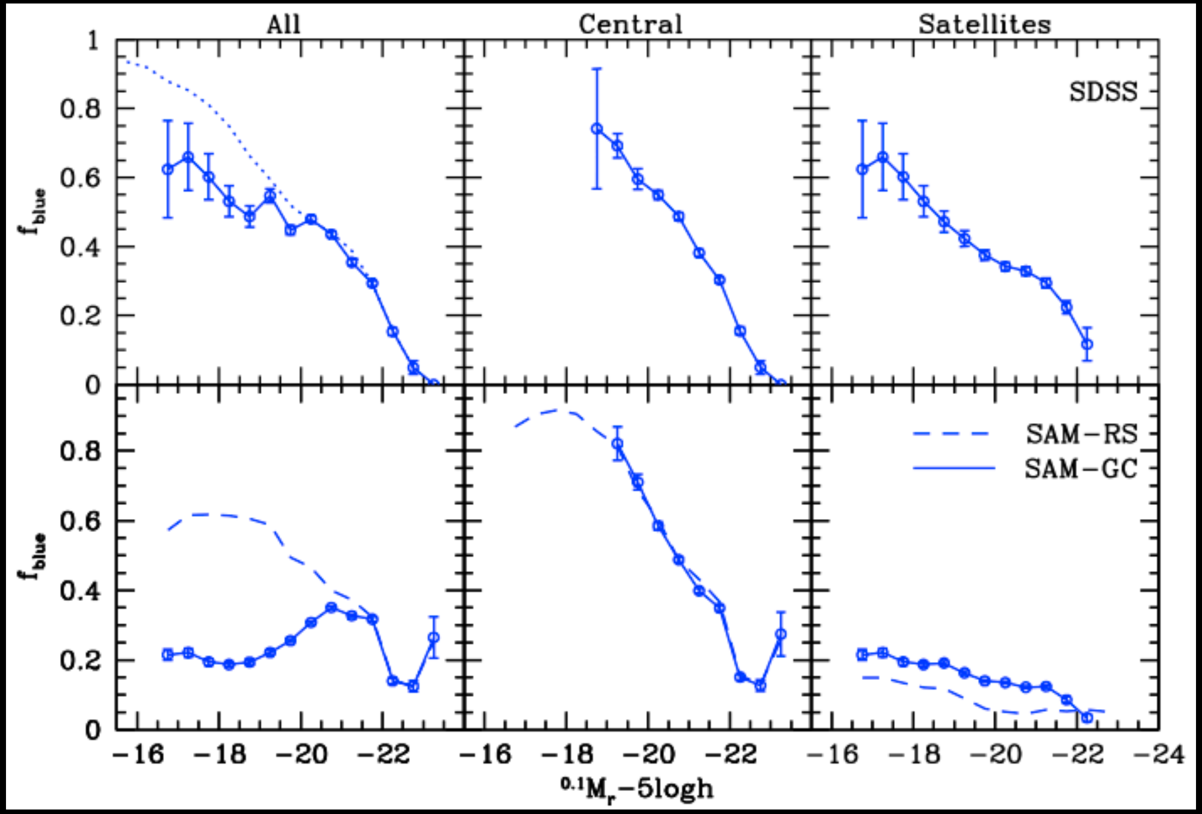

The fraction of Blue Galaxies
g-r < 0.7

The predicted satellites at low redshift are too RED

Increasing the feedback makes low-mass galaxies too red

Weinman et al. 2006

The problem persists at high redshifts
In addition, increasing the feedback yields satellite colors too red

NM et al. 2006

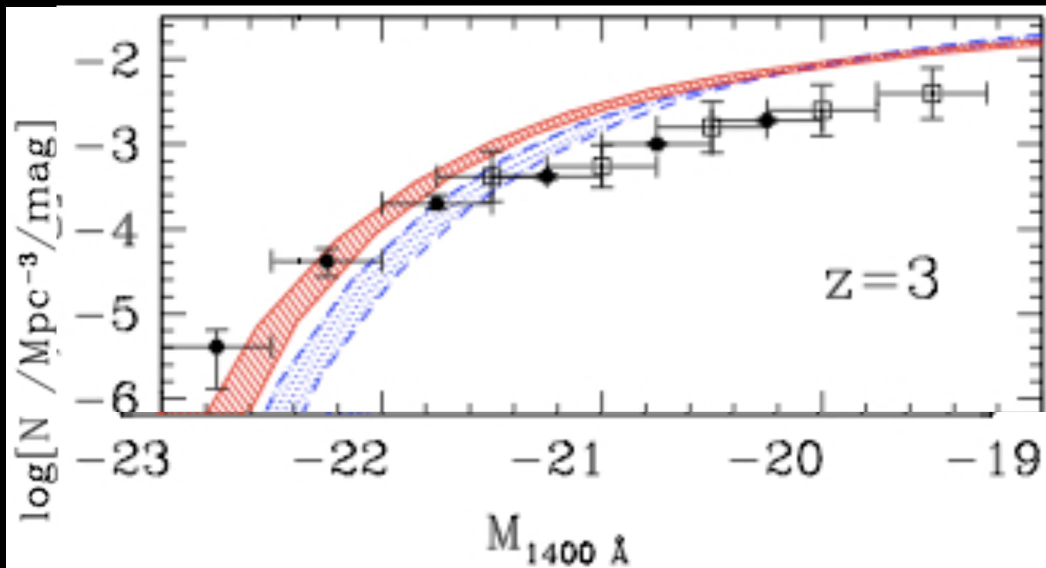

Hirschmann et al. 2012

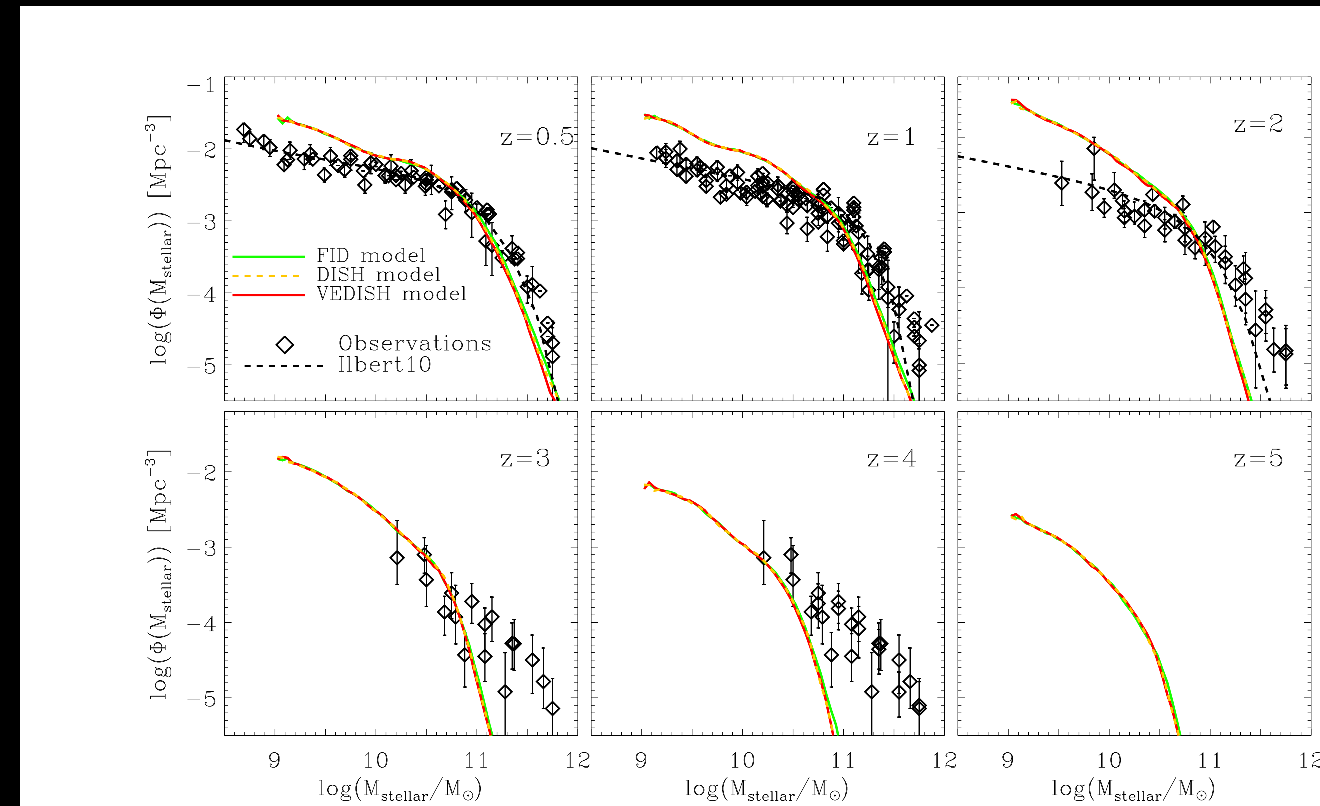

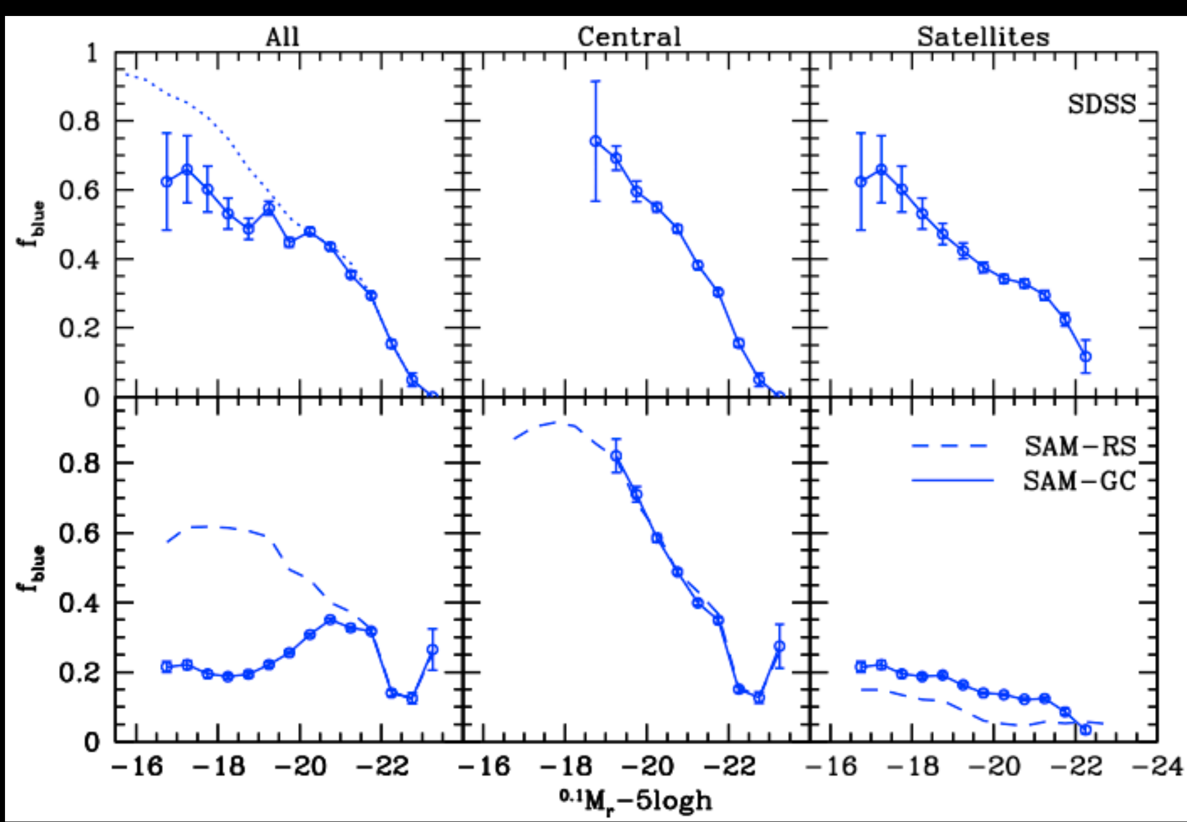

The fraction of Blue Galaxies
g-r < 0.7

The predicted satellites at low redshift are too RED

Increasing the feedback makes low-mass galaxies too red

Weinman et al. 2006

The over-prediction of faint AGNs At High Redshift,ext

NM et al. 2004, 2008
data from La Franca et al. 2005

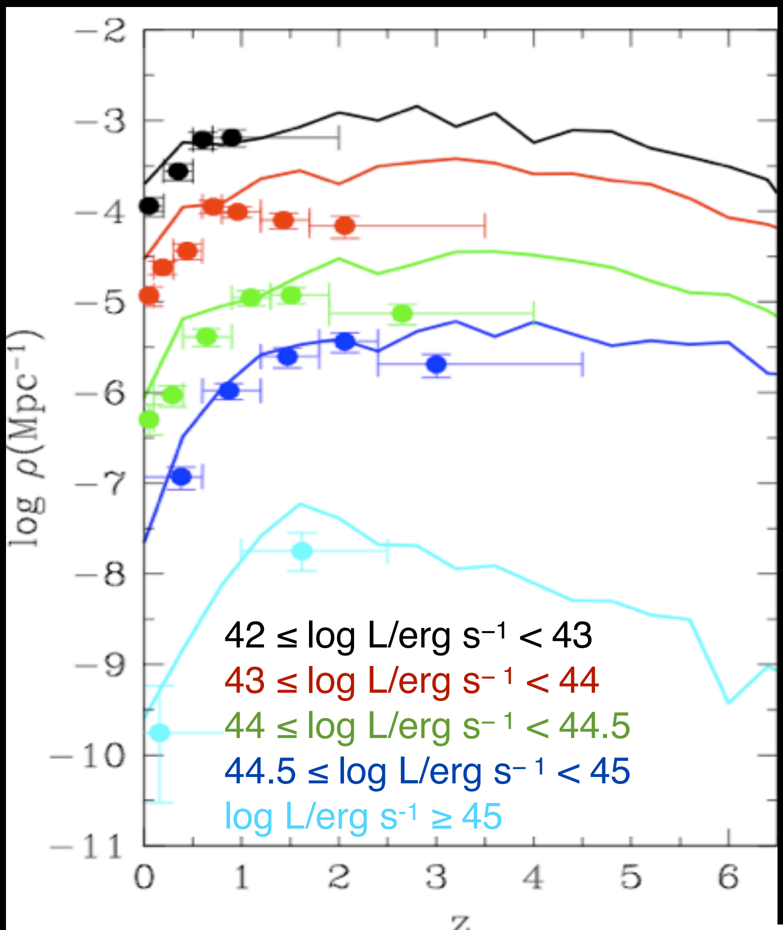

Fiore et al. 2011

models prdictions by NM and
F. Shankar

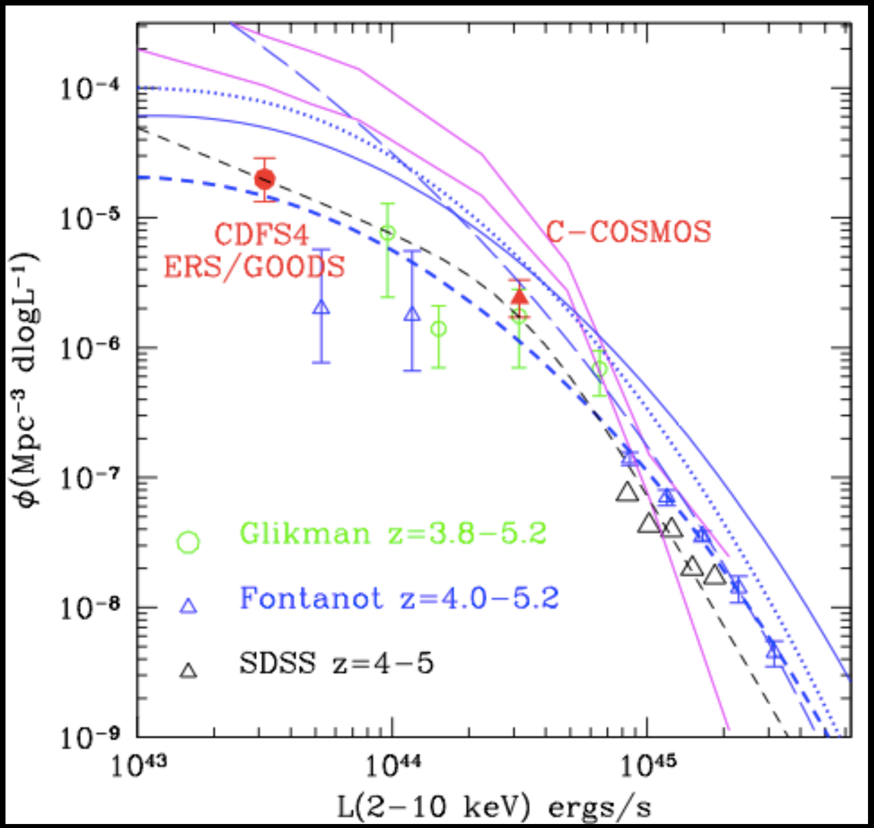

Fanidakis et al. 2012

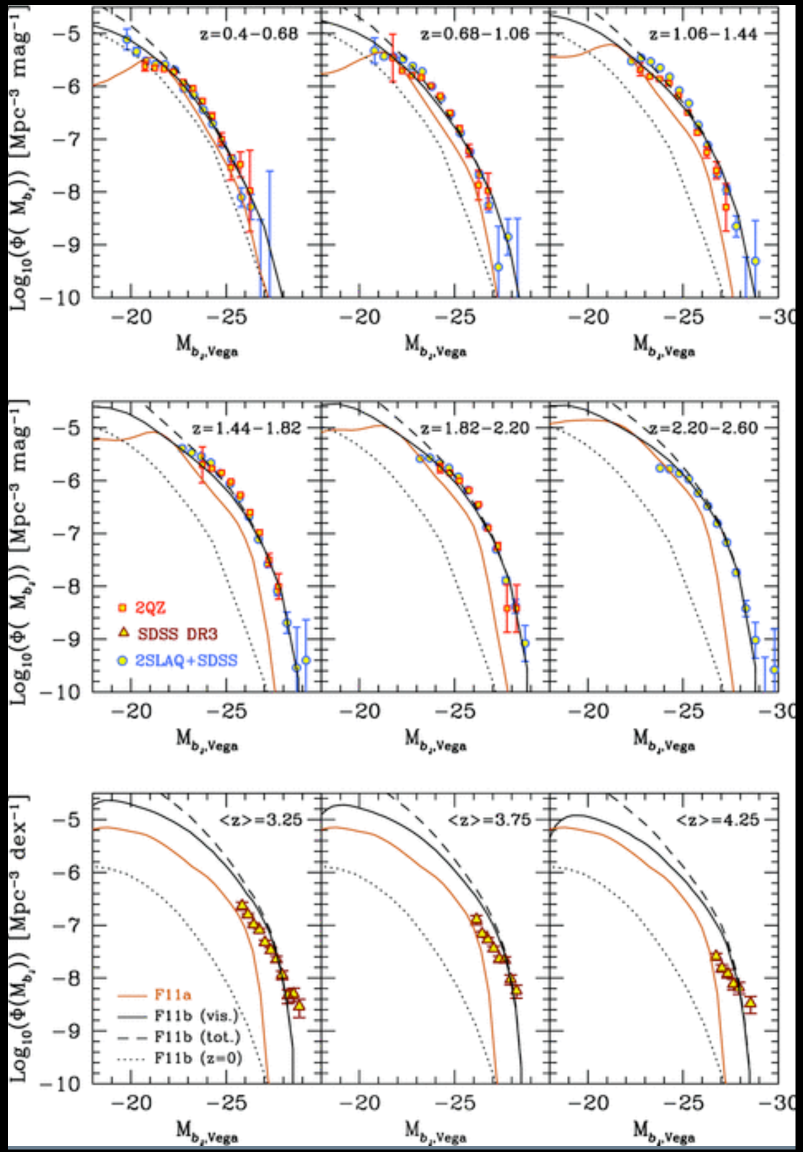

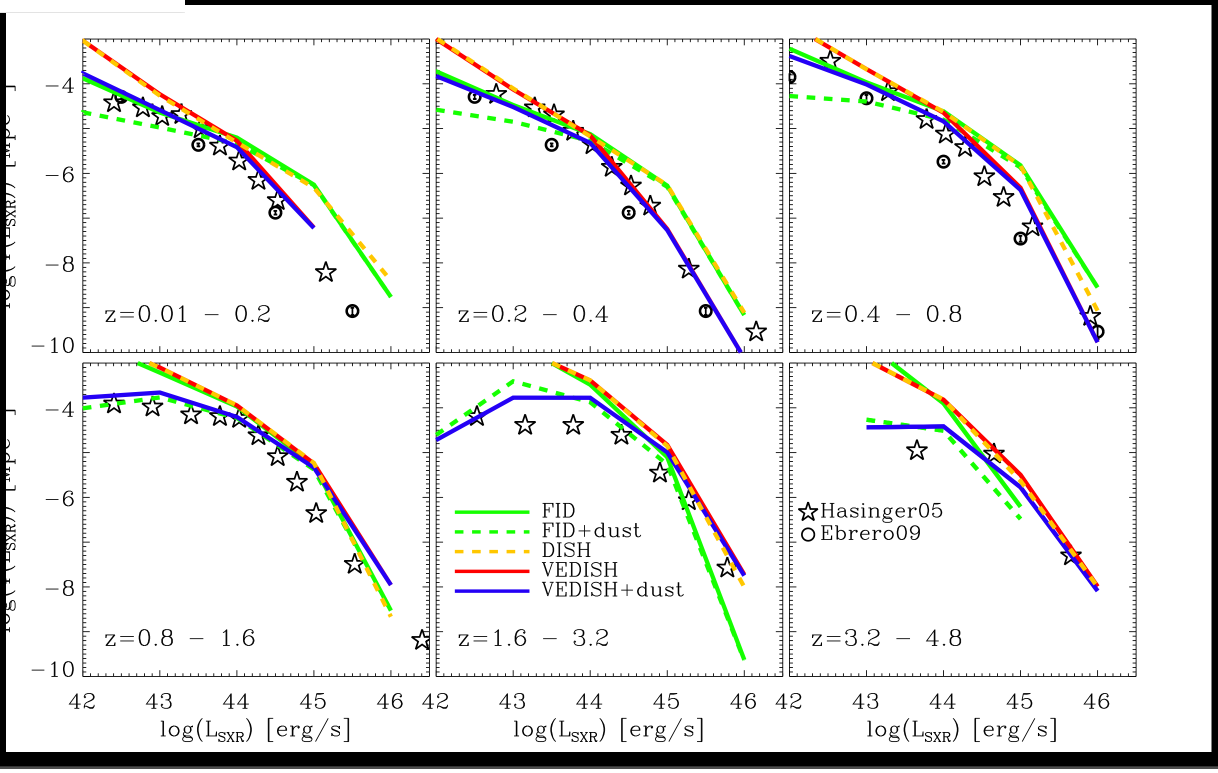

The over-prediction of faint AGNs At High Redshift,ext

NM et al. 2004, 2008
data from La Franca et al. 2005

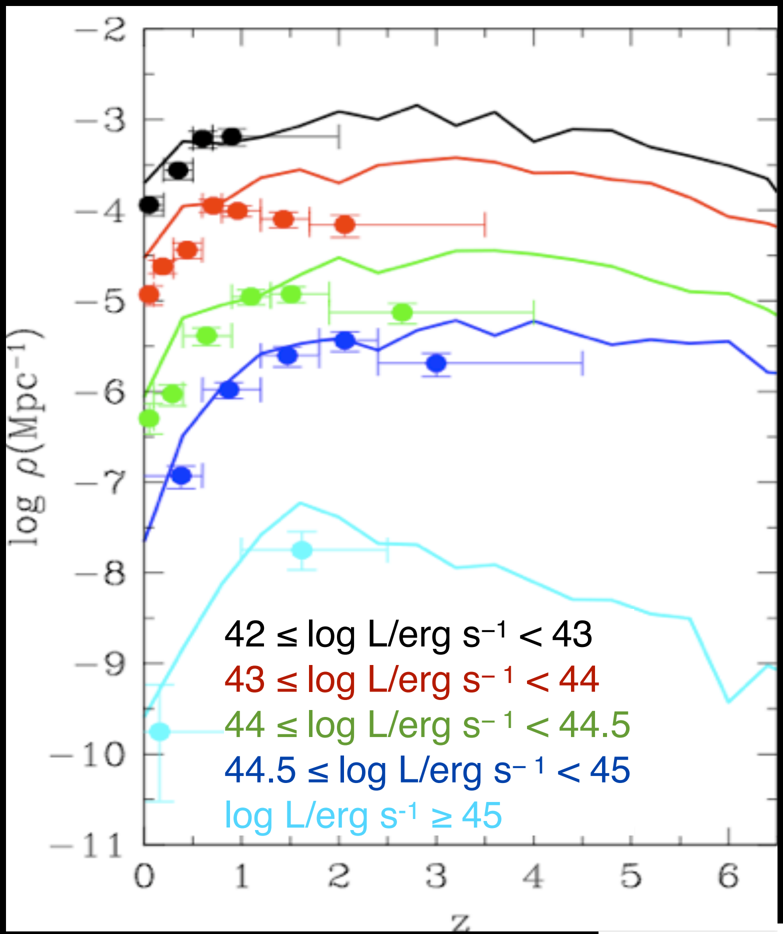

Fiore et al. 2011

models prdictions by NM and F. Shankar

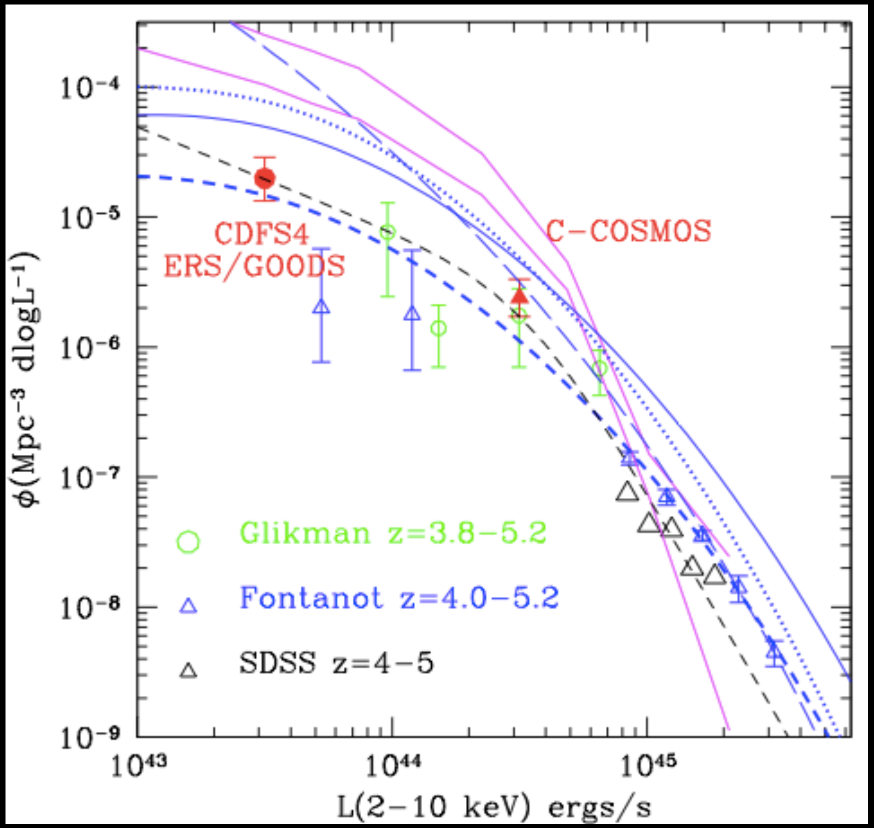

Fanidakis et al. 2012

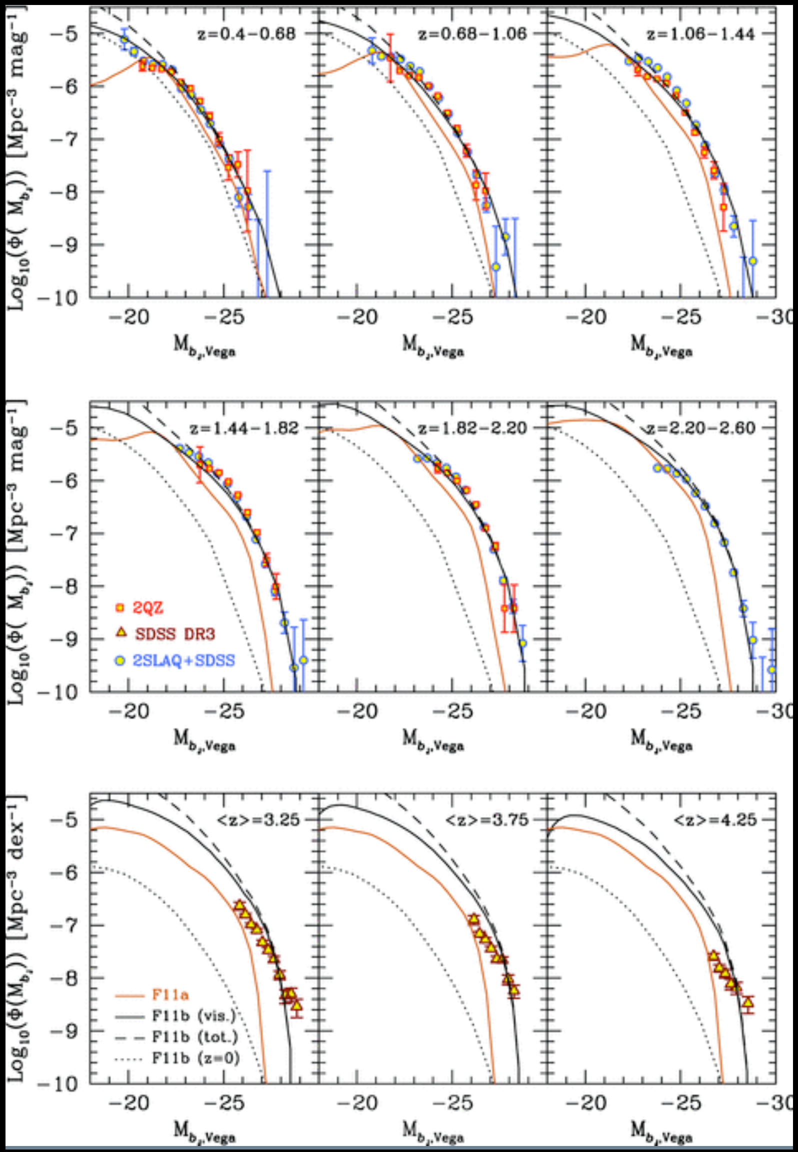

Hirschmann et al. 2012

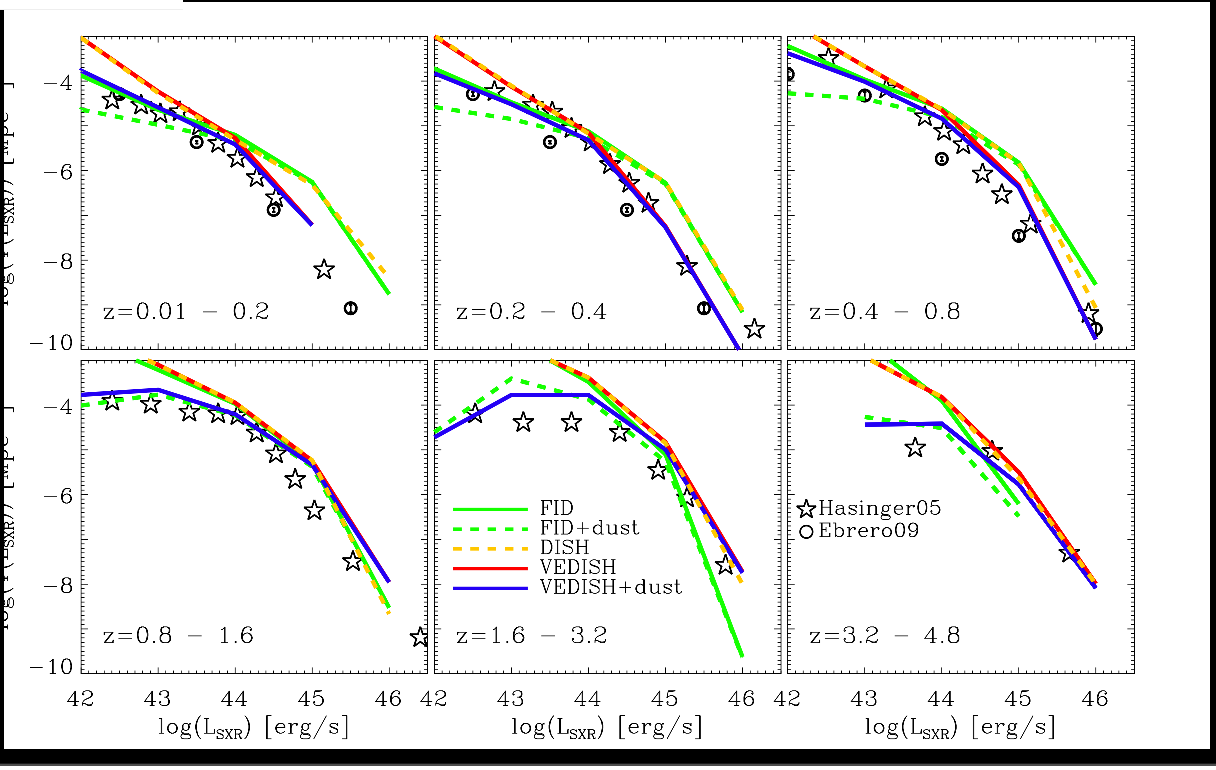

Abundance of galaxies as a function of their velocity width (gas rotation velocity)

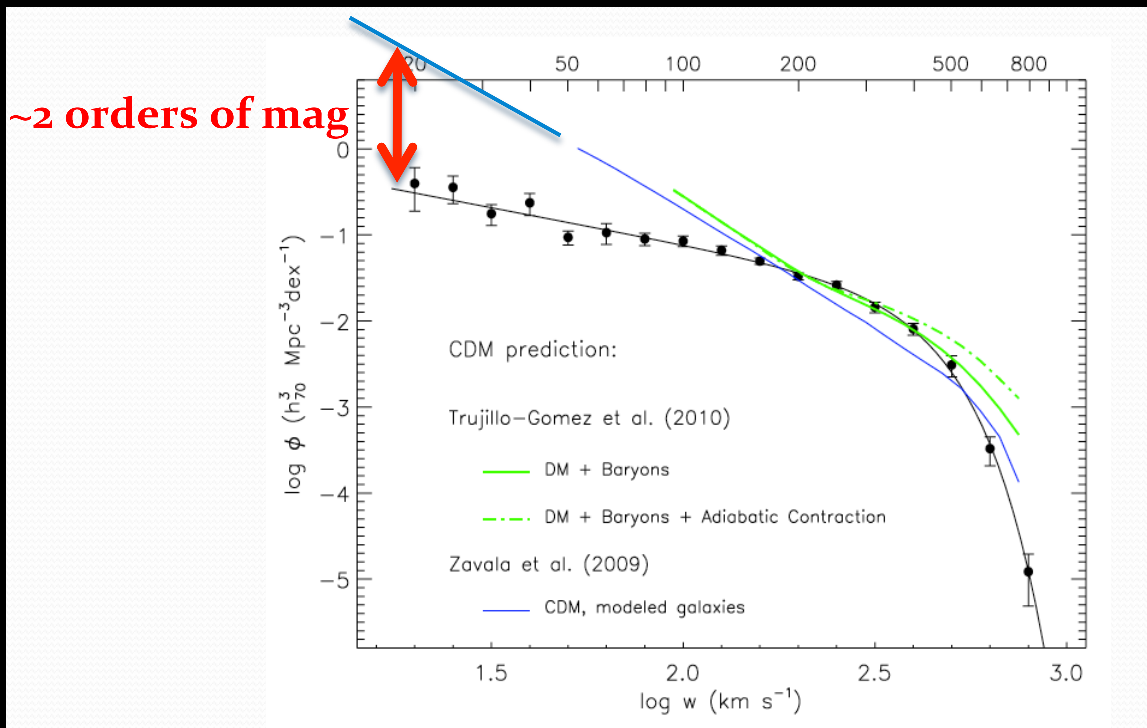

Papastergis+ (2011)

21-cm survey done with Arecibo Telescope: 3000 deg^2; 11000 detections
measures: redshift, velocity width, integrated flux
No spatial resolution (size, inclination, shape)

Directly measures
the depth of the potential well:
less prone to physics of gas (feedback)

Solutions within CDM scenario ?
- large fraction of galaxies with low gas content (below the sensitivity)
-large fraction of galaxies with rising rotation curve

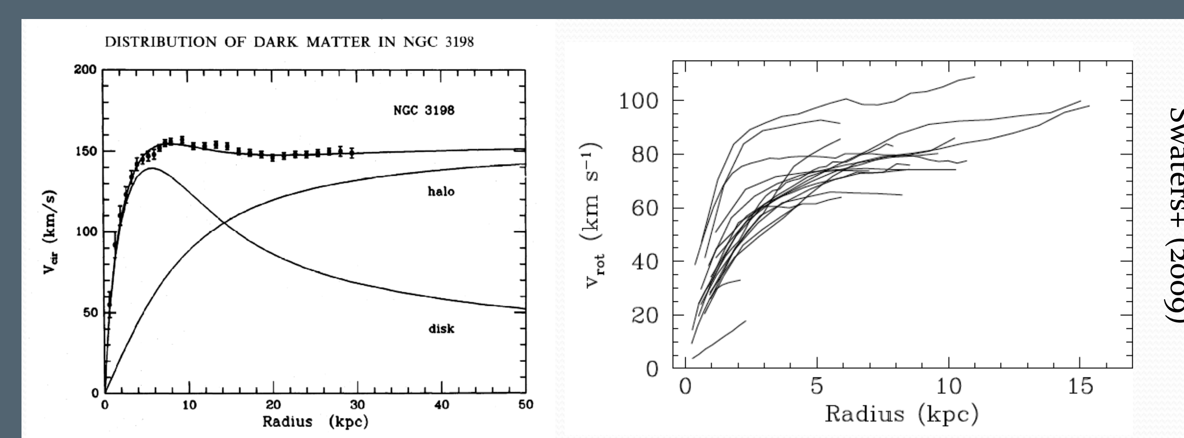

'flat' rotation curve
'rising' rotation curves

Abundance of galaxies as a function of their velocity width (gas rotation velocity)

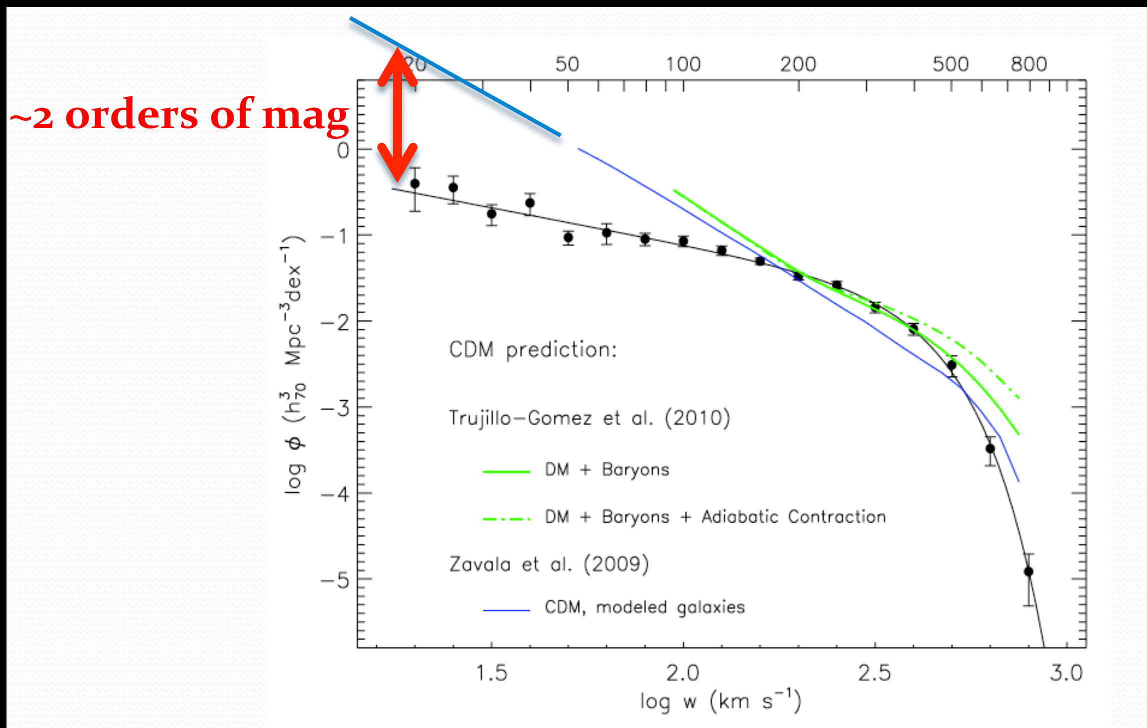

Papastergis+ (2011)

21-cm survey done with Arecibo Telescope: 3000 deg^2; 11000 detections

measures: redshift, velocity width, integrated flux

No spatial resolution (size, inclination, shape)

Directly measures
the depth of the potential well:
less prone to physics of gas (feedback)

At high redshift, galaxies are denser

Difficult to expel gas from such compact objects

Even with maximized feedback, current models still over estimate the number of small mass galaxies

Galaxy formation in WDM Cosmology

Problem Persists at high redshifts

Too many low-mass structures

Need to suppress Power Spectrum at small scales ?

can WDM solve all problems simultaneously ?

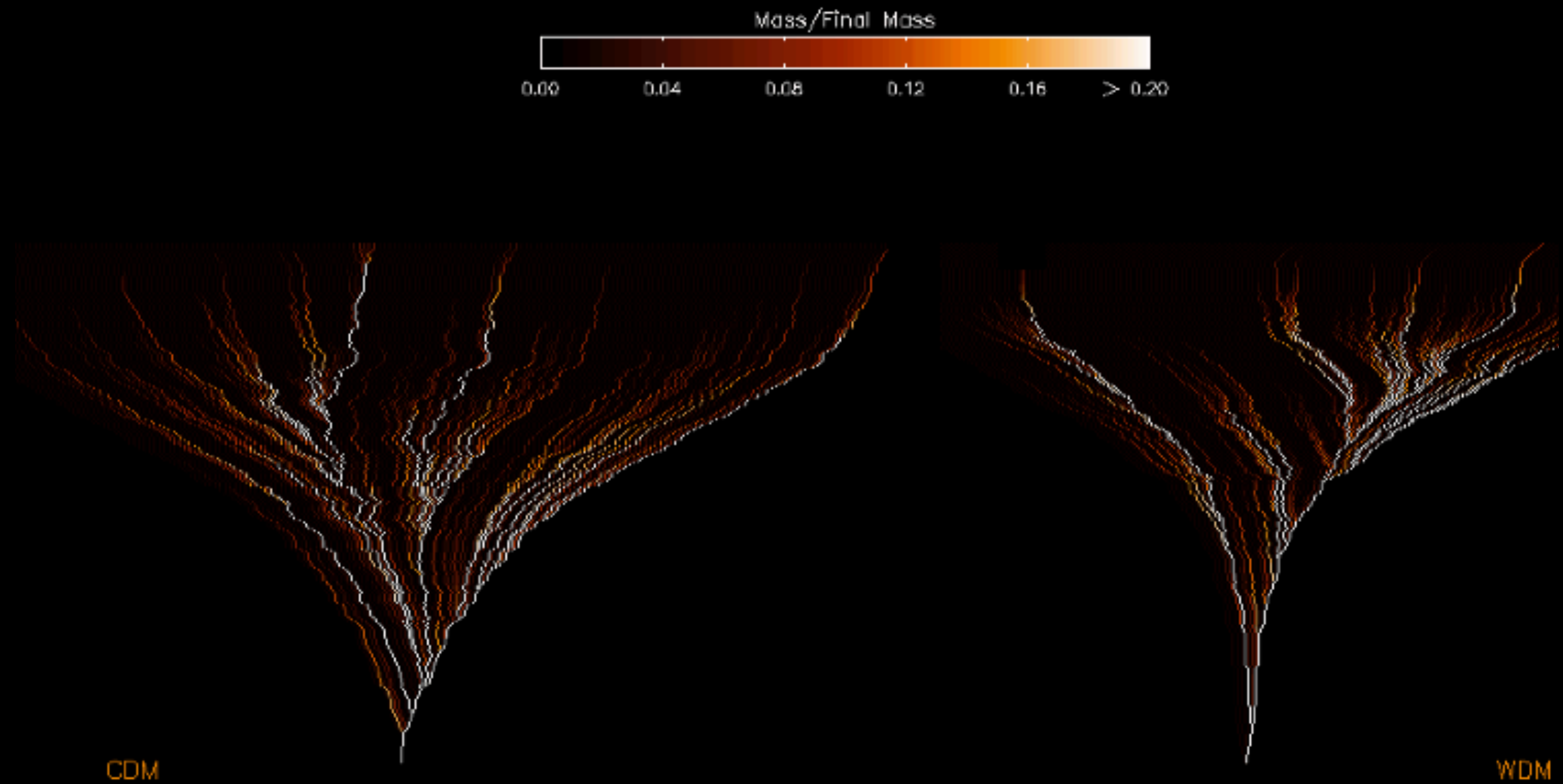

Galaxy formation in WDM Cosmology

Problem Persists at high redshifts

Too many low-mass structures

Need to suppress Power Spectrum at small scales ?

can WDM solve all problems simultaneously ?

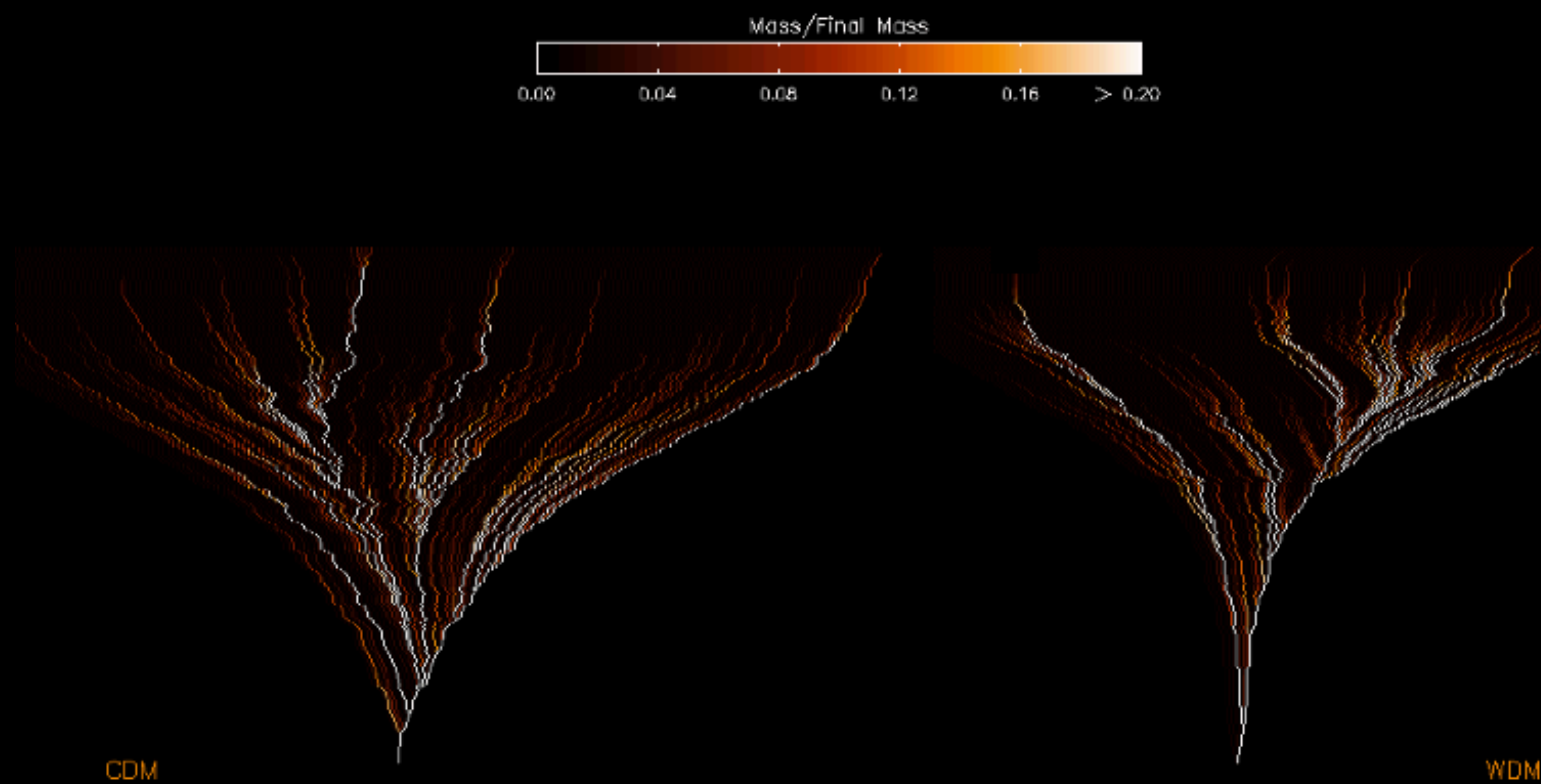

Rome PANDA model

NM, A. Lamstra

Implementing WDM power spectrum in the galaxy formation model

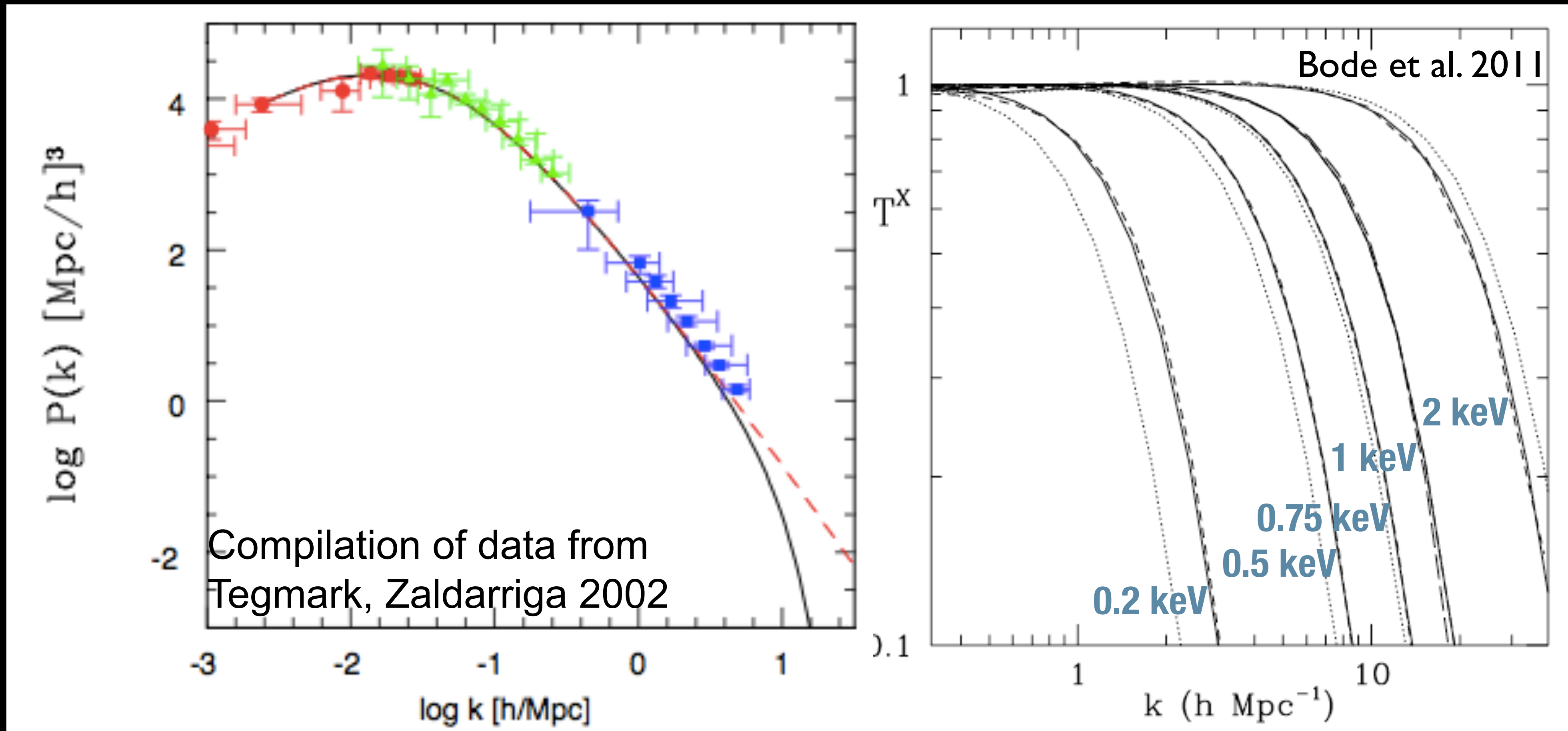

To explore the maximal effect of a power-spectrum cutoff on galaxy formation, we consider a cutoff at scales just below 0.2 Mpc, where data from Lyman-α systems (compared to N-body simulations) yields stringer upper limits on power suppression. This corresponds to mass scales M_{fs}~5 10^8 $M_\odot$

$$r_{fs} \approx 0.2 \left[\frac{\Omega_X\, h^2}{0.15}\right]^{1/3} \left[\frac{m_X}{rmkeV}\right]^{-4/3} \text{Mpc} \qquad \frac{P_{WDM}(k)}{P_{CDM}(k)} = \left[1+(\alpha\, k)^{2\,\mu}\right]^{-5\,\mu}$$

$$\alpha = 0.049 \left[\frac{\Omega_X}{0.25}\right]^{0.11} \left[\frac{m_X}{\text{keV}}\right]^{-1.11} \left[\frac{h}{0.7}\right]^{1.22} h^{-1}\ \text{Mpc}$$

WDM
particle mass
1 kev

Implementing WDM power spectrum in the galaxy formation model

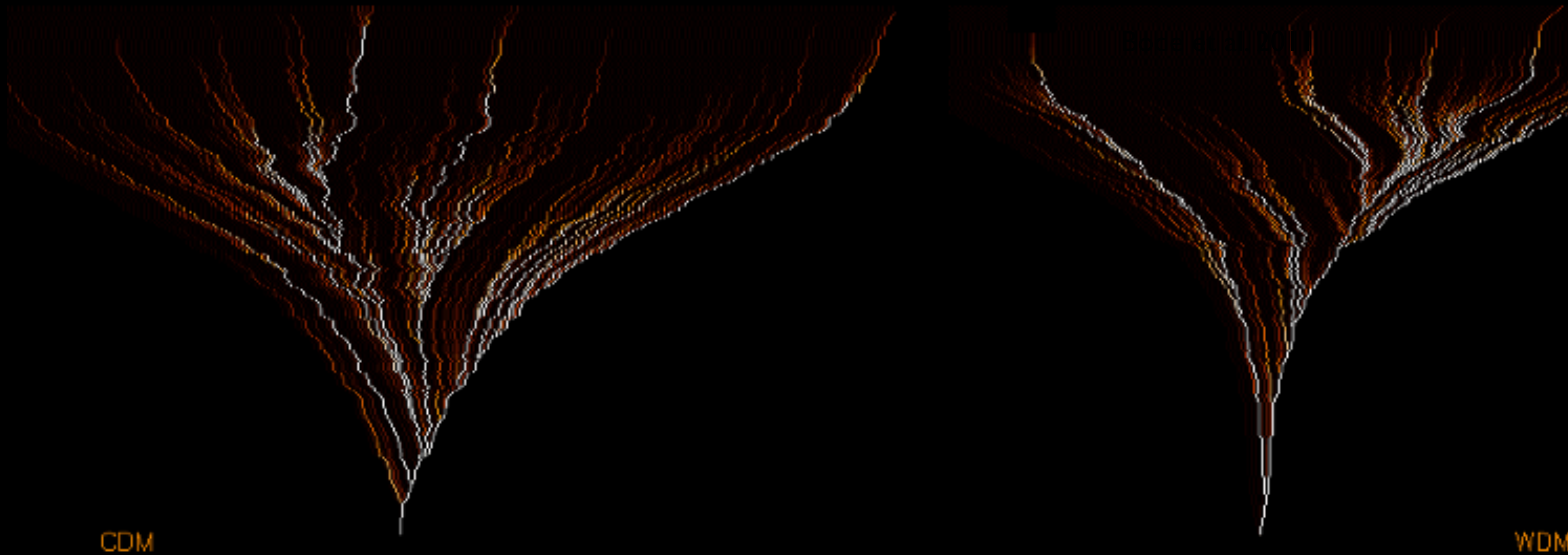

To explore the maximal effect of a power-spectrum cutoff on galaxy formation, we consider a cutoff at scales just below 0.2 Mpc, where data from Lyman-α systems (compared to N-body simulations) yields stringer upper limits on power suppression. This corresponds to mass scales M_{fs}~5 10^8 $M_\odot$

$$r_{fs} \approx 0.2 \left[\frac{\Omega_X h^2}{0.15}\right]^{1/3} \left[\frac{m_X}{rmkeV}\right]^{-4/3} \text{Mpc} \qquad \frac{P_{WDM}(k)}{P_{CDM}(k)} = \left[1 + (\alpha\, k)^{2\,\mu}\right]^{-5\,\mu}$$

$$\alpha = 0.049 \left[\frac{\Omega_X}{0.25}\right]^{0.11} \left[\frac{m_X}{\text{keV}}\right]^{-1.11} \left[\frac{h}{0.7}\right]^{1.22} h^{-1}\ \text{Mpc}$$

WDM
particle mass
1 kev

Implementing WDM power spectrum in the galaxy formation model

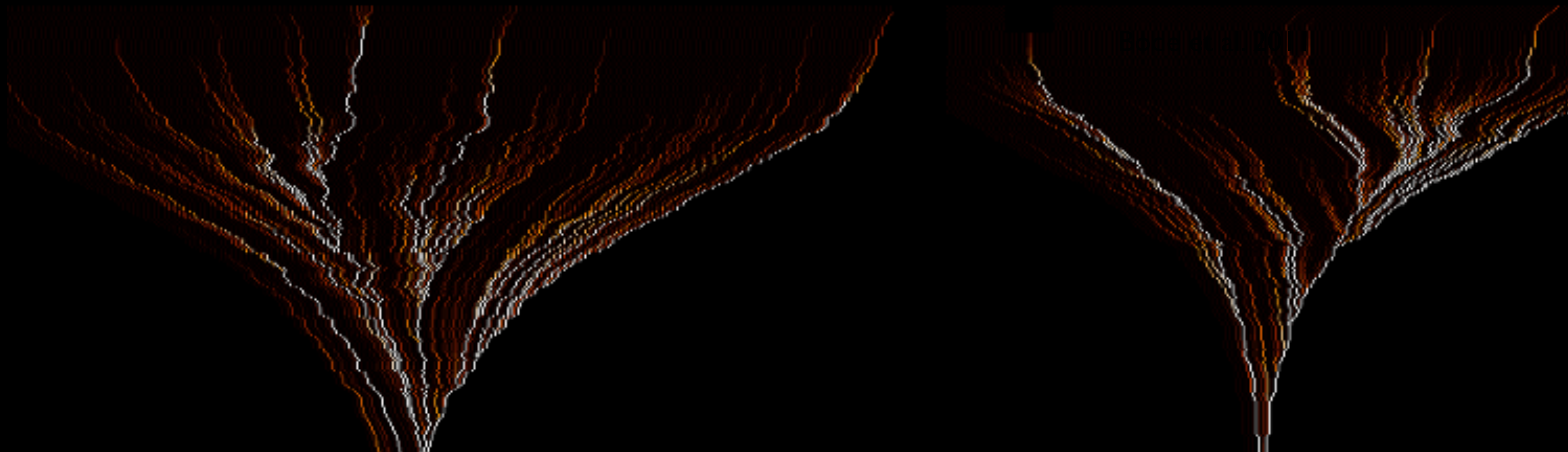

WDM

Halo Properties	Gas Properties	Star Formation	Gas Heating (feedback)	Evolution of stellar populations
Density Profiles	Profiles		SNae	
Virial Temperature	Cooling - Heating		UV background	
	Collapse			
	Disk formation			

Galaxy formation in WDM implies computing how modifications of the power spectrum propagate to the above processes

$$r_{fs} \approx 0.2 \left[\frac{\Omega_X h^2}{0.15}\right]^{1/3} \left[\frac{m_X}{rmkeV}\right]^{-4/3} \text{Mpc}$$

$$\frac{P_{WDM}(k)}{P_{CDM}(k)} = \left[1 + (\alpha\, k)^{2\,\mu}\right]^{-5\,\mu}$$

$$\alpha = 0.049 \left[\frac{\Omega_X}{0.25}\right]^{0.11} \left[\frac{m_X}{\text{keV}}\right]^{-1.11} \left[\frac{h}{0.7}\right]^{1.22} h^{-1}\ \text{Mpc}$$

WDM
particle mass
1 kev

Galaxy Formation in WDM cosmology (m_{WDM}=1 keV)

NM et al. 2012-2013

local lum. and stell. mass distributions

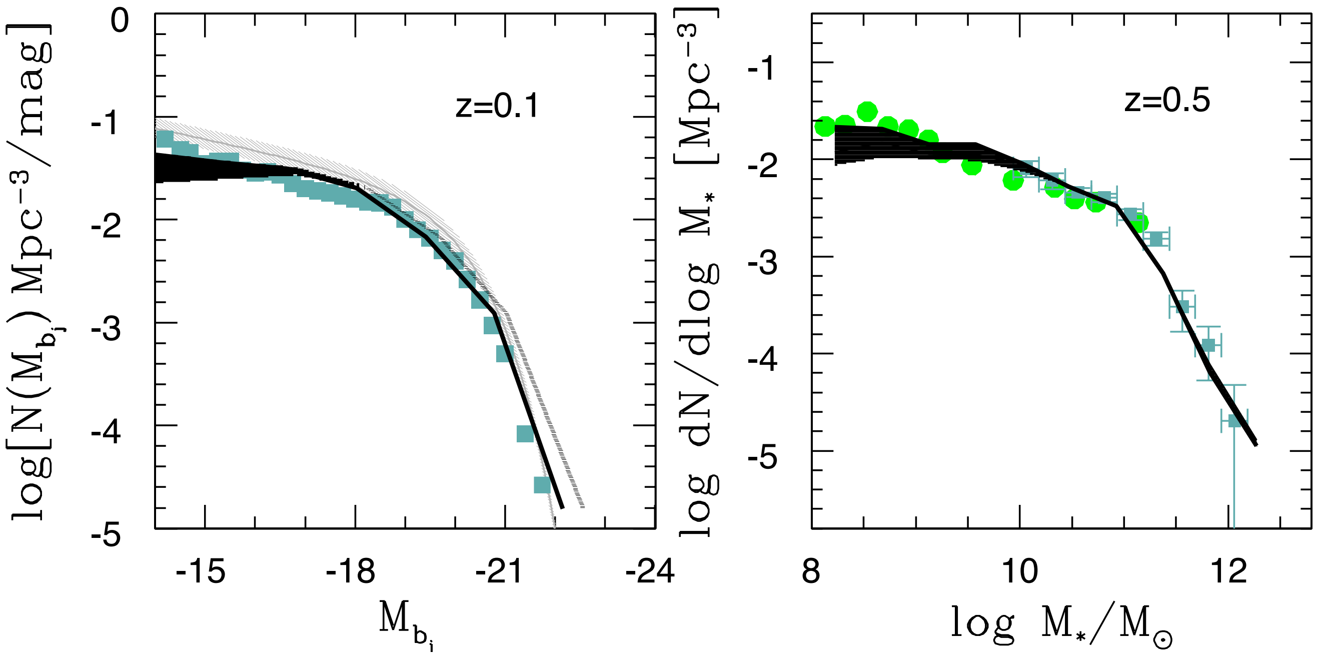

Evolution

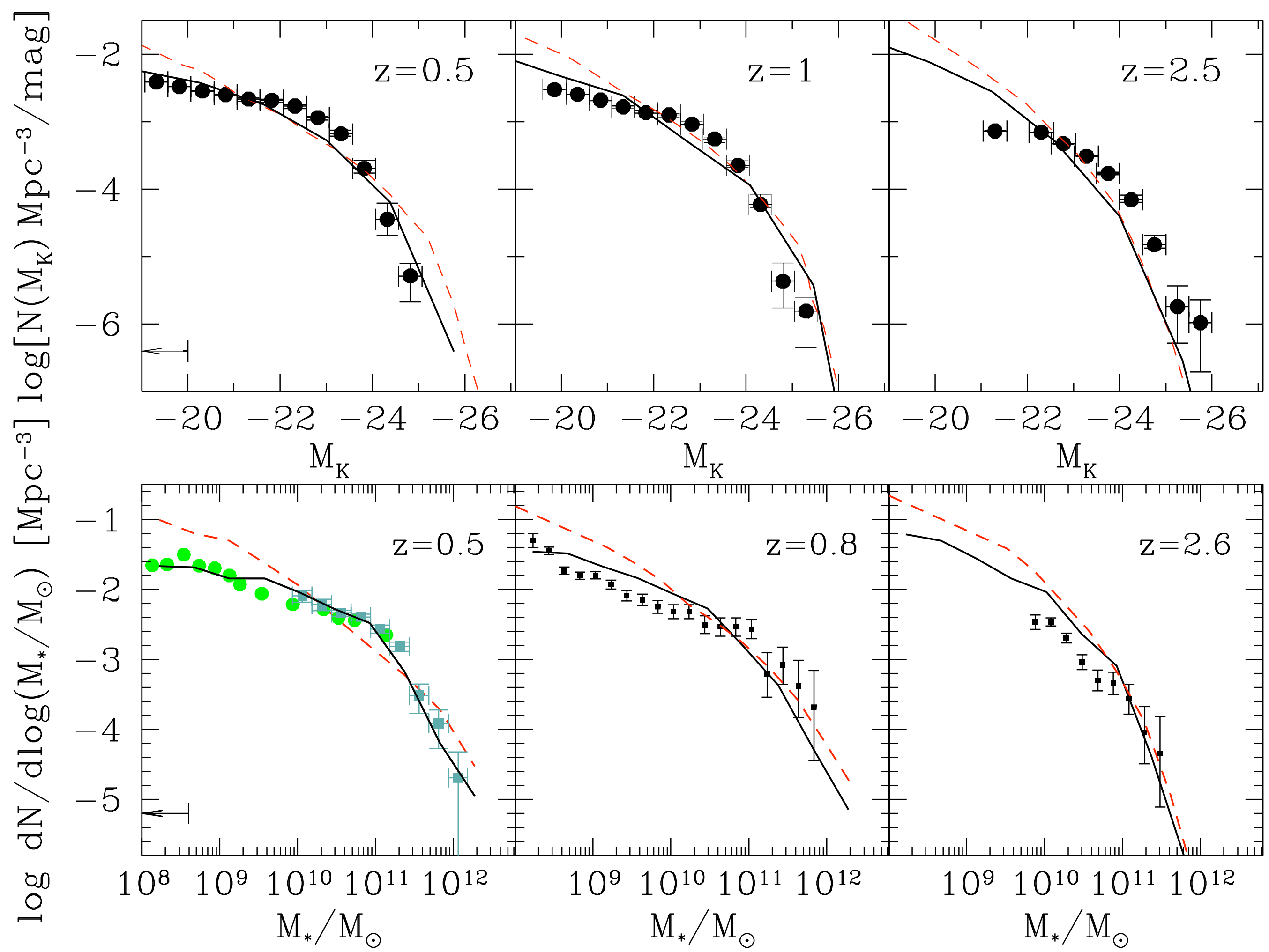

High-z (z=4) lum. distributions

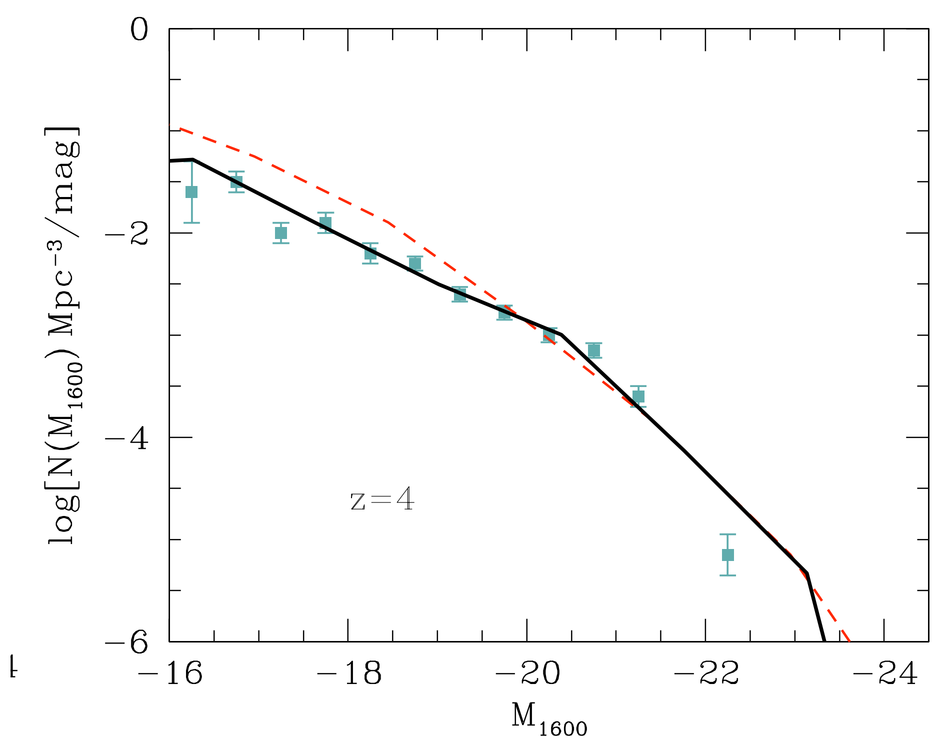

color distributions

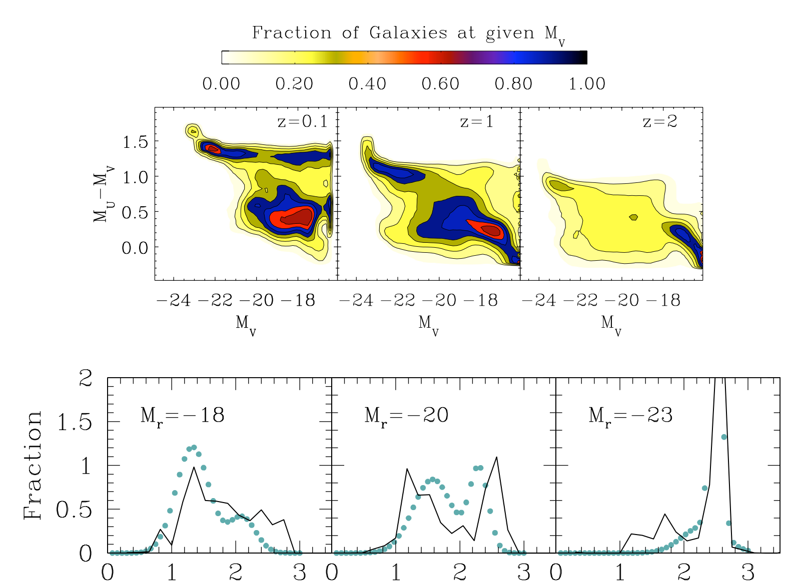

The AGN luminosity Functions

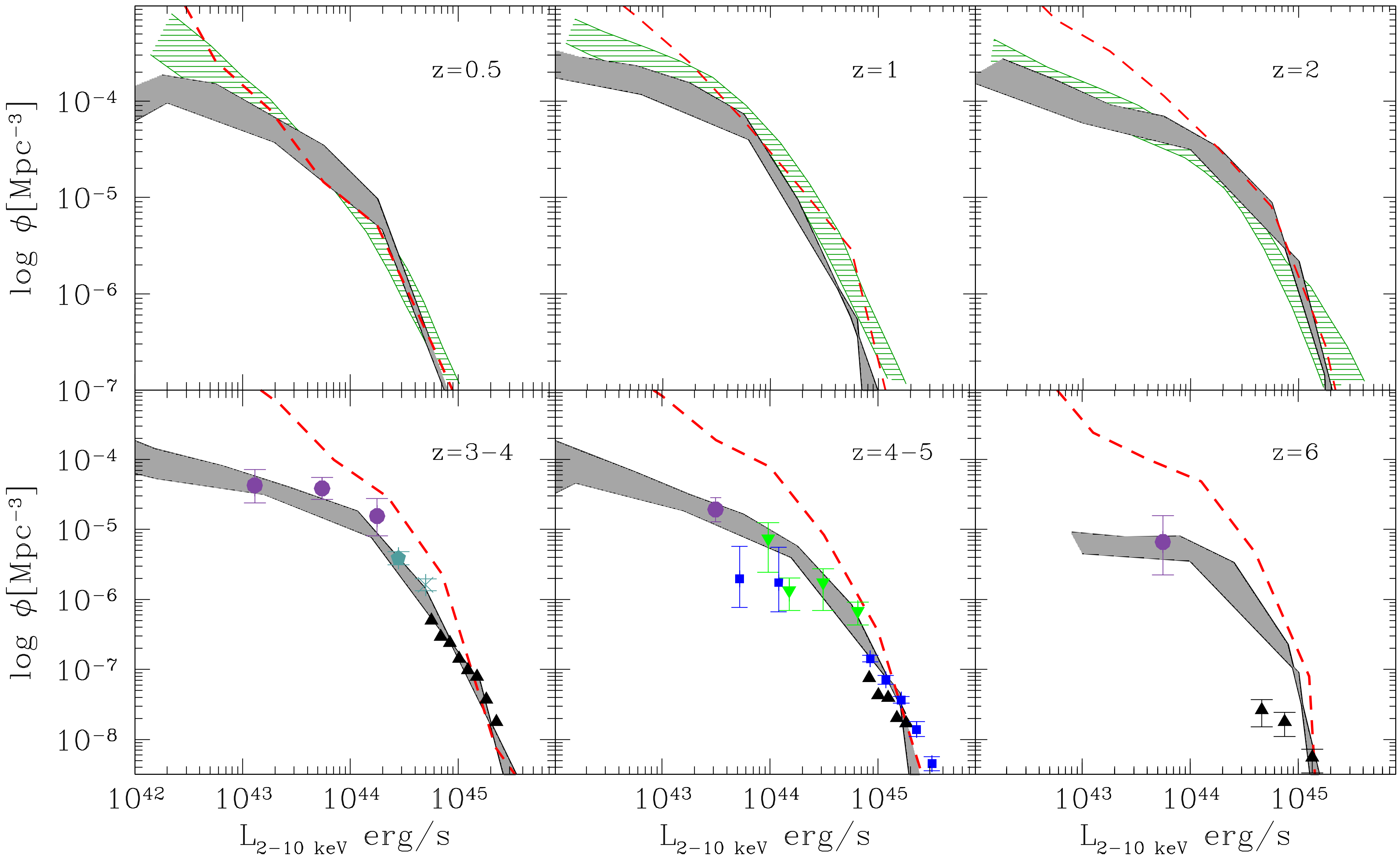

A few caveats

$$\sigma^2(M) = \int \frac{dk\,k^2}{2\,\pi^2} P(k) W(kr)$$

The above results have been obtained
changing only the
power spectrum P(k)
P(k) → σ(M) → merger trees

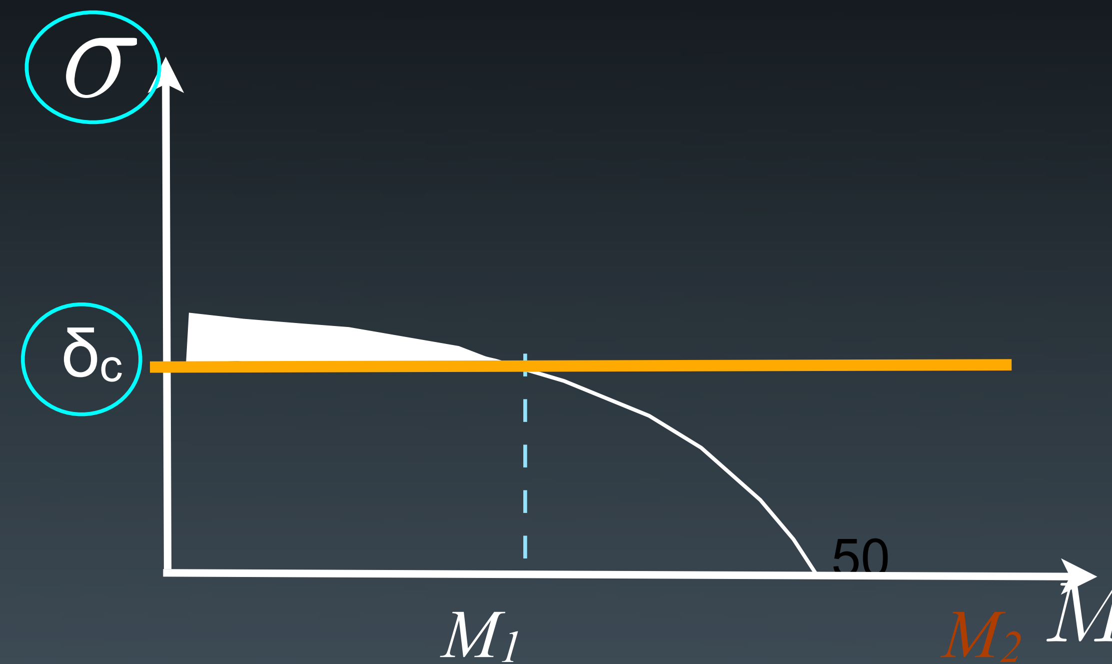

Recent analysis by Benson et al. (2012) show that:

i) the relation P(k) → σ(M) (window function)

ii) the collapse threshold δ_c

change in WDM cosmology: further suppression *below the free streaming scale*

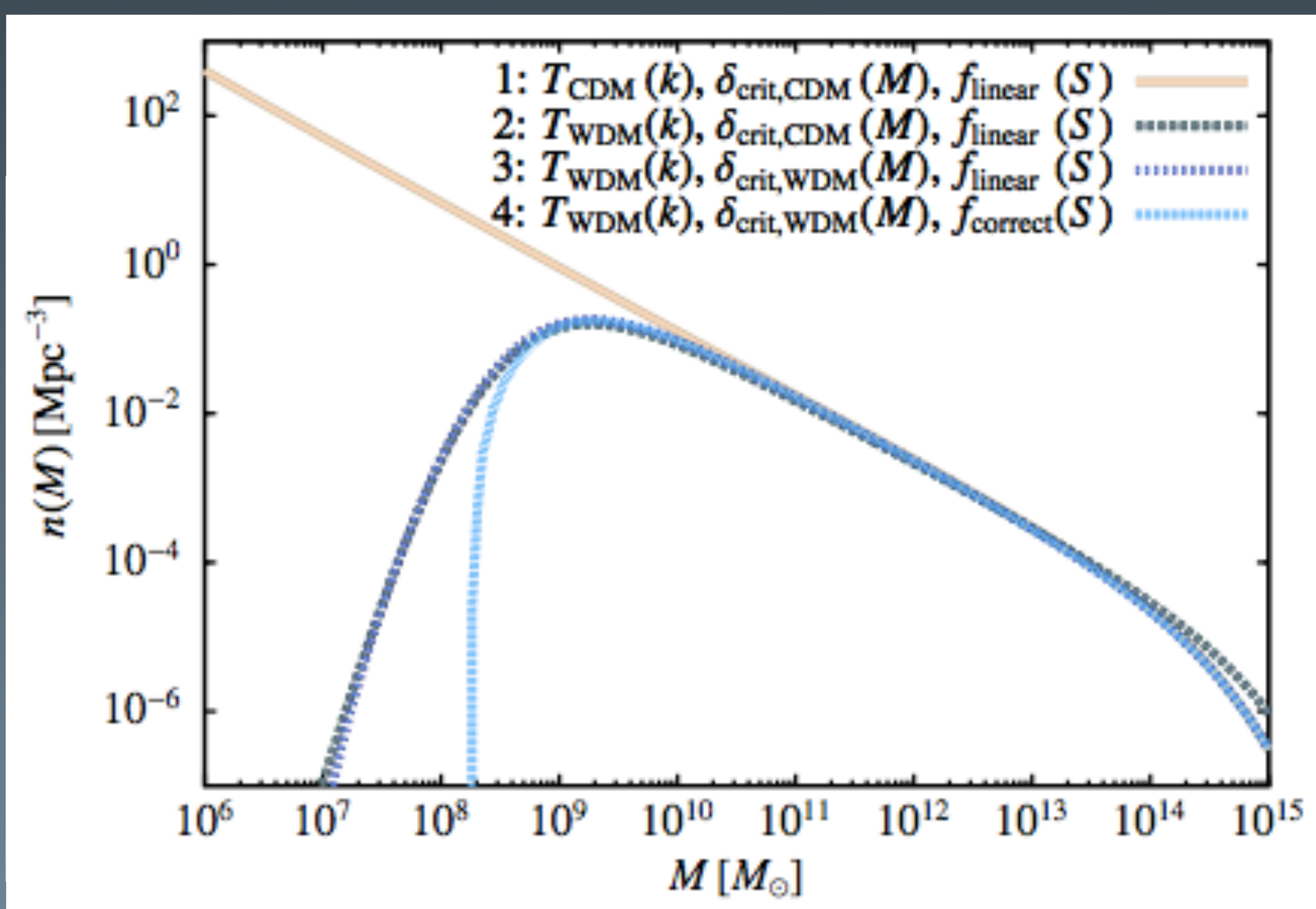

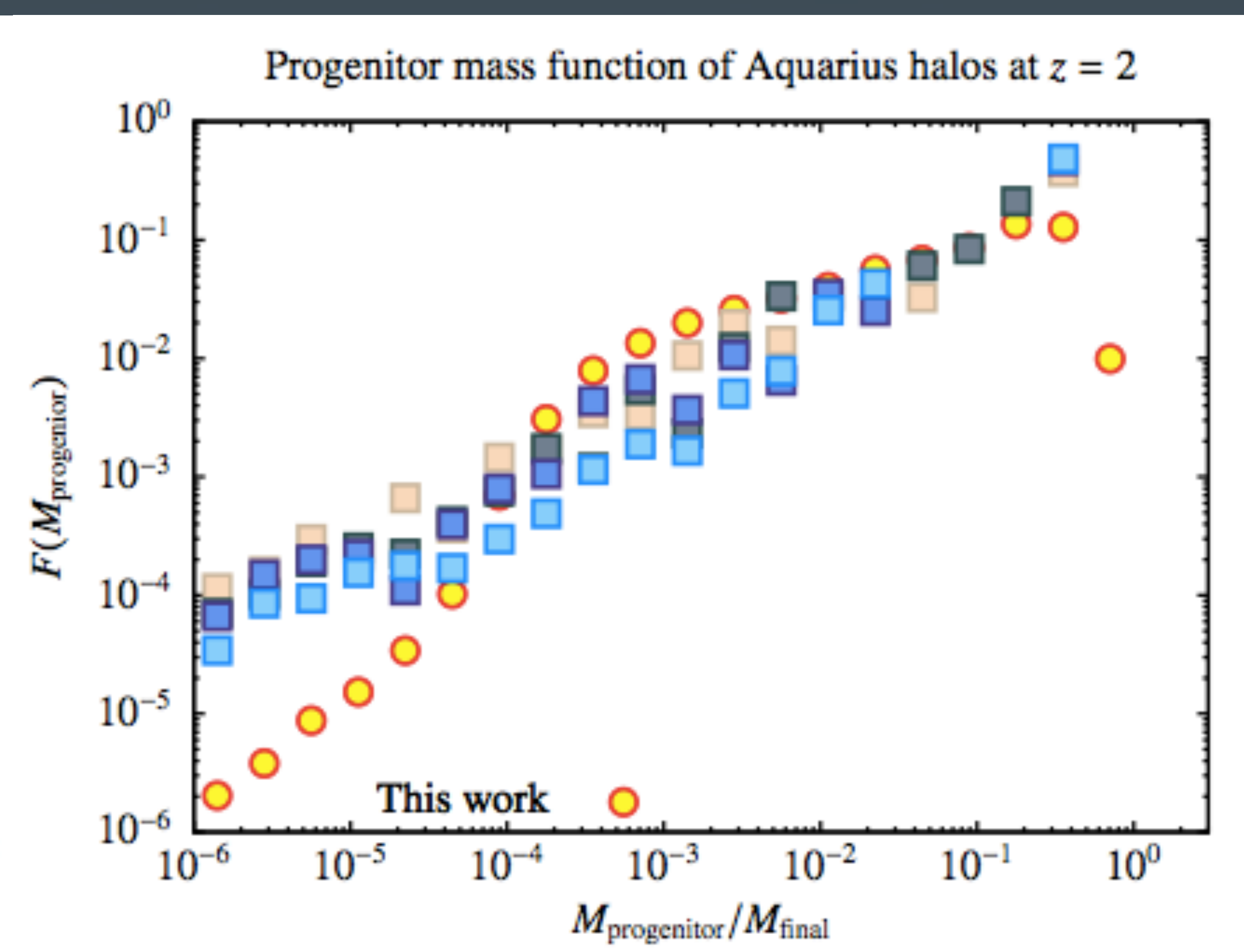

A few caveats

The above results have been obtained changing only the power spectrum P(k)
P(k) → σ(M) → merger trees

$$\sigma^2(M) = \int \frac{dk\, k^2}{2\,\pi^2} P(k) W(kr)$$

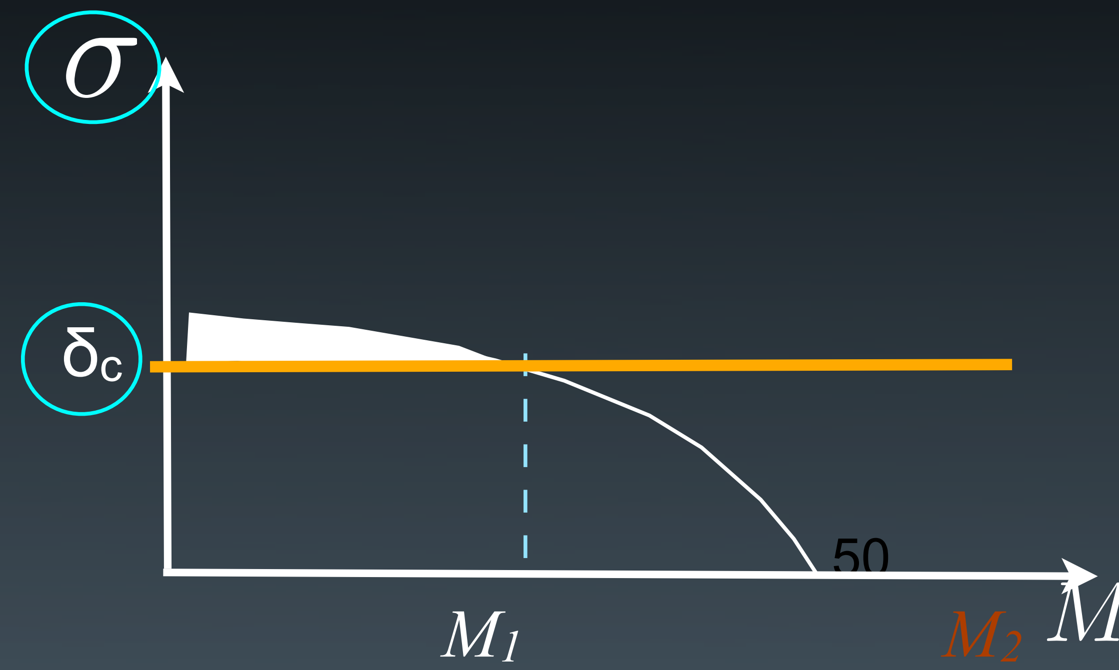

Recent analysis by Benson et al. (2012) show that:

i) the relation P(k) → σ(M) (window function)

ii) the collapse threshold δ_c

change in WDM cosmology: further suppression *below the free streaming scale*

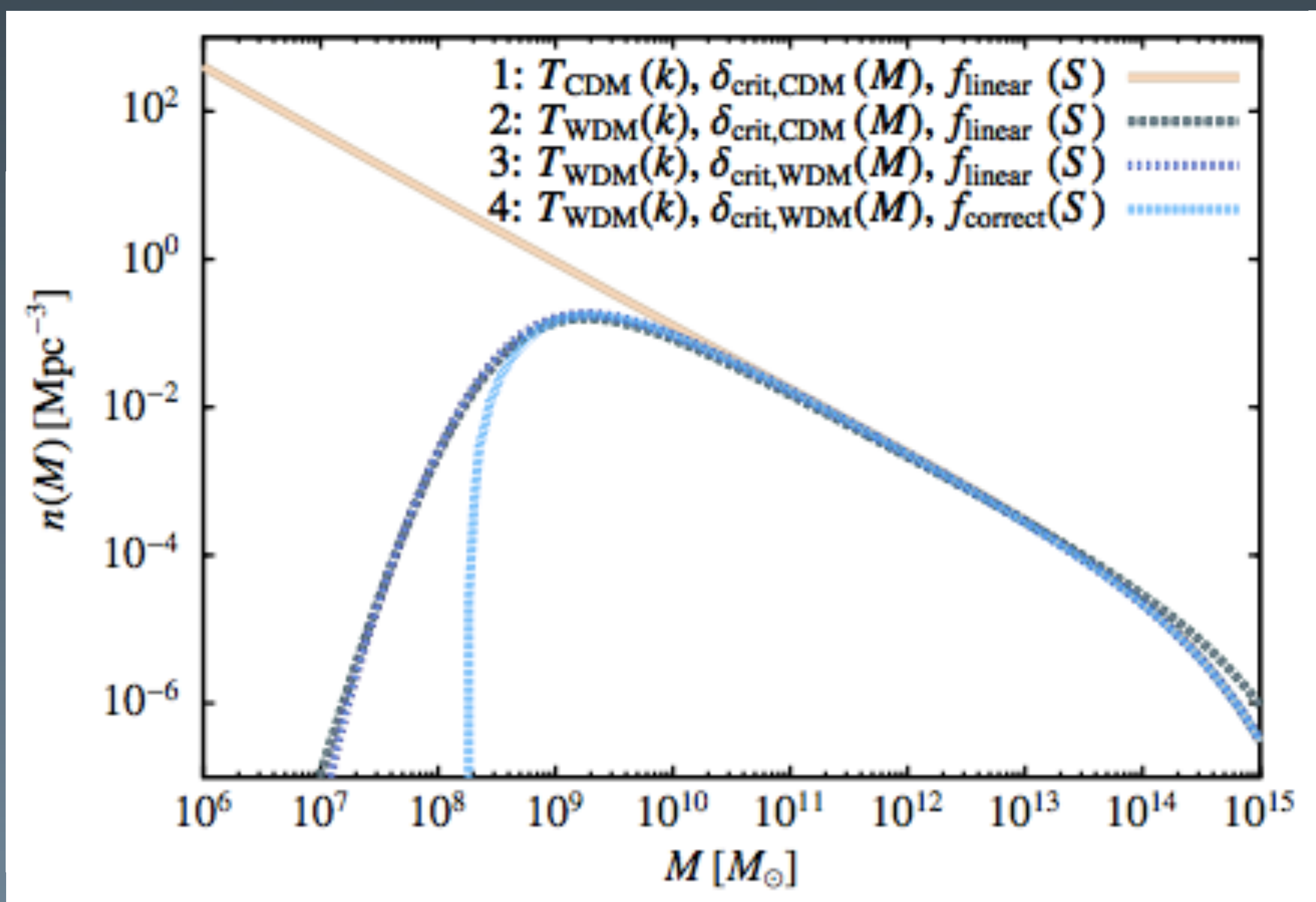

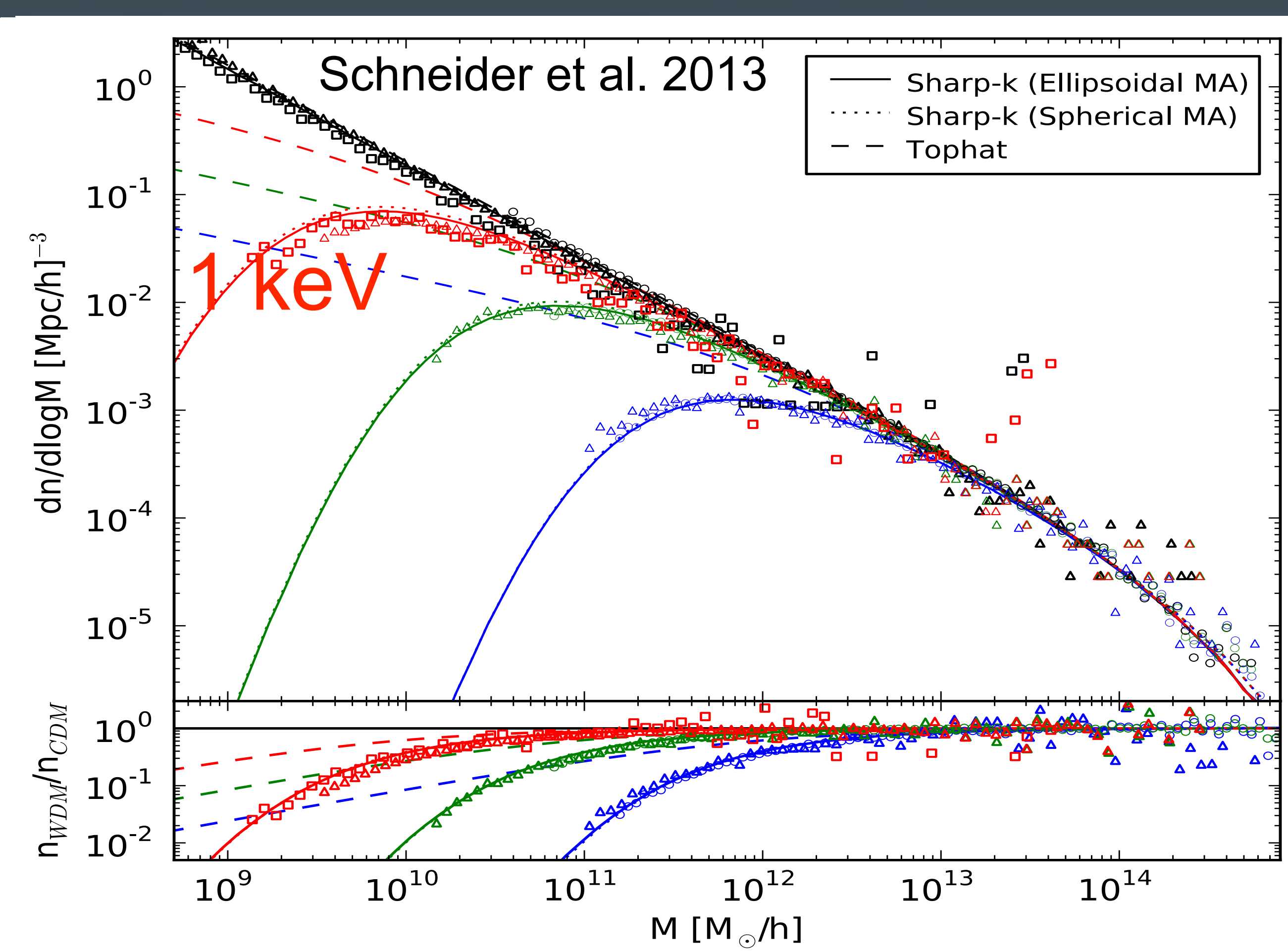

A few caveats

The above results have been obtained changing only the power spectrum P(k)

P(k) → σ(M) → merger trees

$$\sigma^2(M) = \int \frac{dk\,k^2}{2\,\pi^2} P(k) W(kr)$$

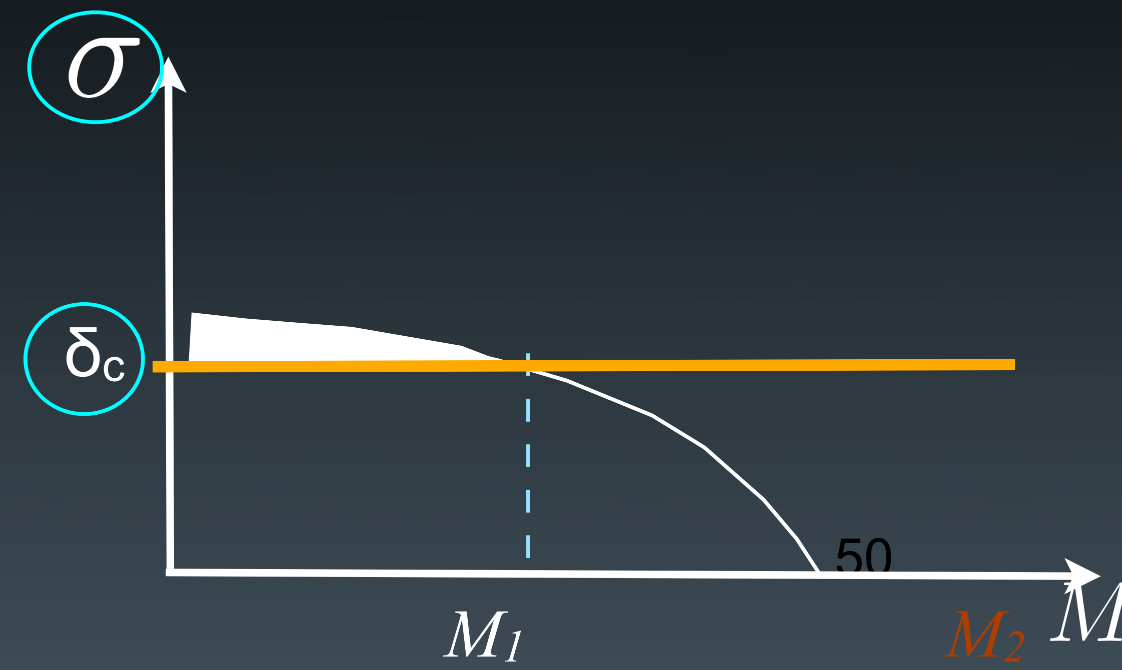

Recent analysis by Benson et al. (2012) show that:

- i) the relation P(k) → σ(M) (window function)
- ii) the collapse threshold δ_c

change in WDM cosmology: further suppression *below the free streaming scale*

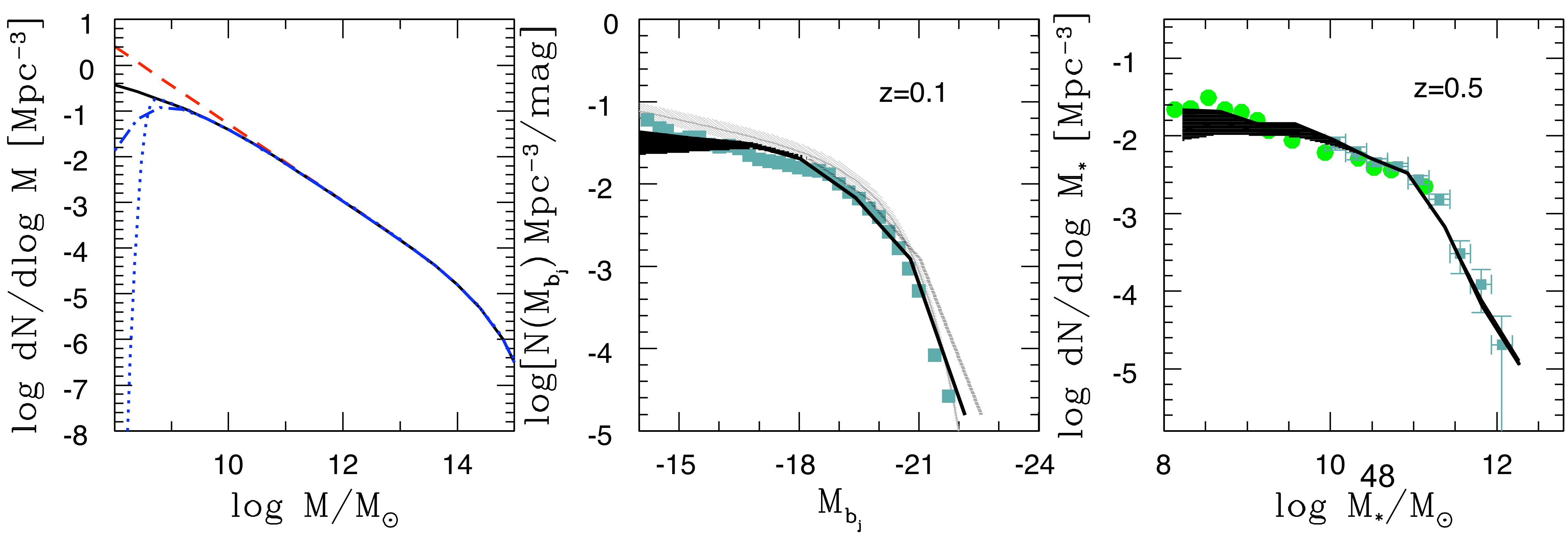

Substructure and Distribution of Rotation Velocities

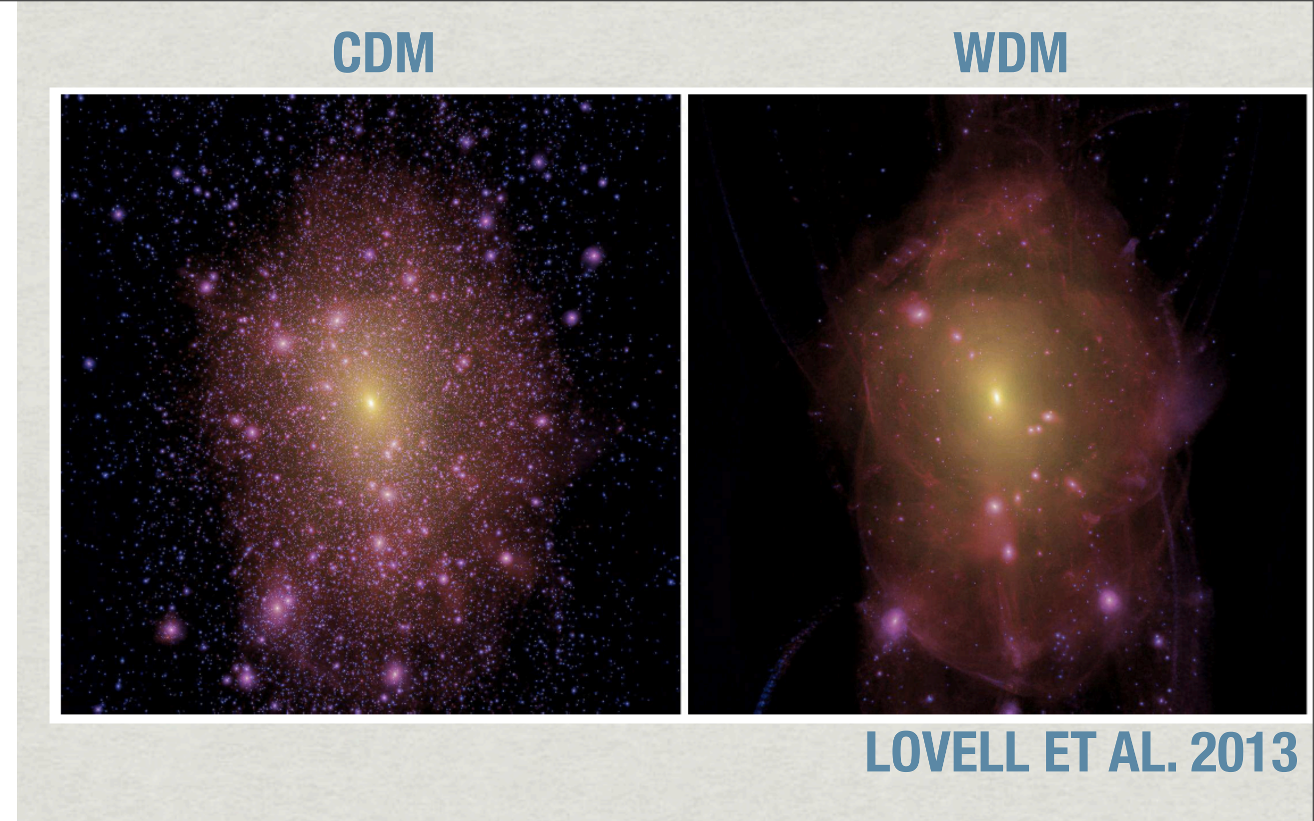

m_{wdm}=1 keV

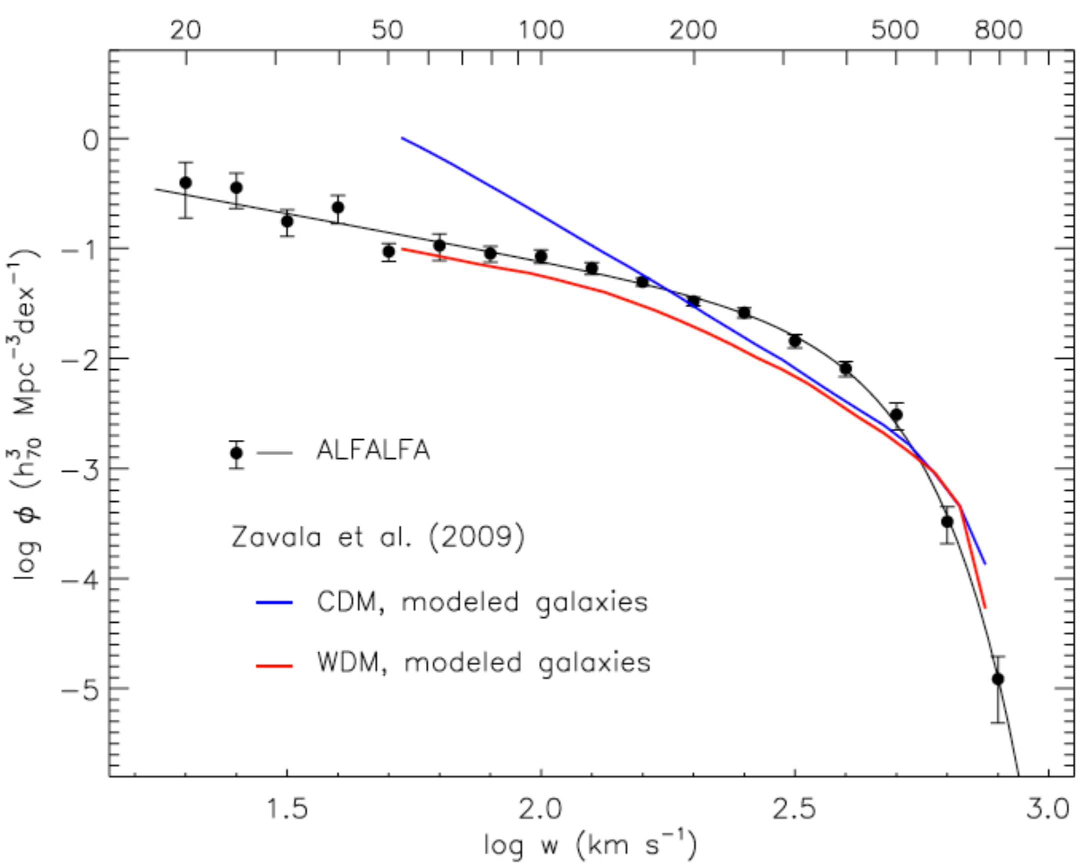

Papastergis+ (2011)

modeling: Zavala+ (2009)

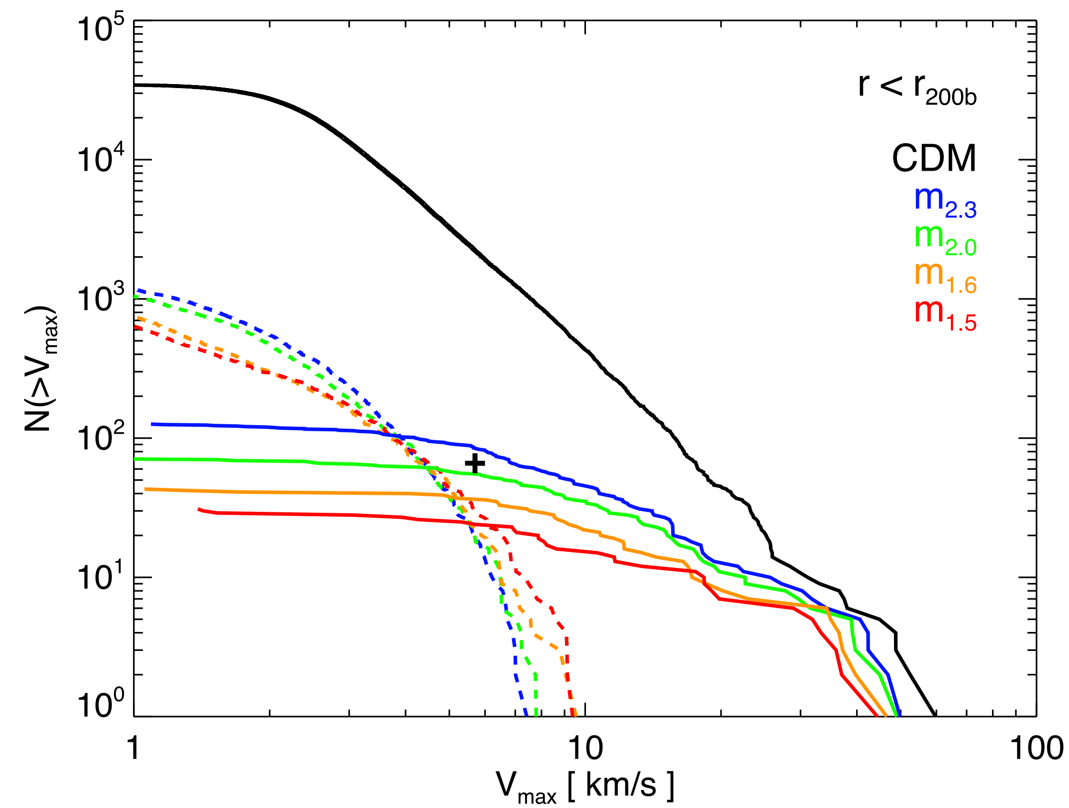

Figure 11. Cumulative subhalo mass, M_{sub}, (top panel) and V_{max} (bottom panel) functions of subhaloes within $r < r_{200b}$ of the main halo centre in the HRS at $z = 0$. Solid lines correspond to genuine subhaloes and dashed lines to spurious subhaloes. The black line shows results for CDM-W7 and the coloured lines for the WDM models, as in Fig. 1. The black cross in the lower panel indicates the expected number of satellites of $V_{max} > 5.7\,\mathrm{km\,s^{-1}}$ as derived in the text.

Luminosity Function of Satellite Galaxies

Is Milky Way representative of $M_{halo} \approx 10^{12}\ M_\odot$?

Compare with a wide set of satellites/host halos through the satellite luminosity function

ACS F814W imaging of the COSMOS field,

identify satellites as much as a thousand times fainter than their host galaxies and as close as 0.3 (1.4) arcsec (kpc)and as close as 0.3 (1.4) arcsec (kpc)

Hundreds of hosts

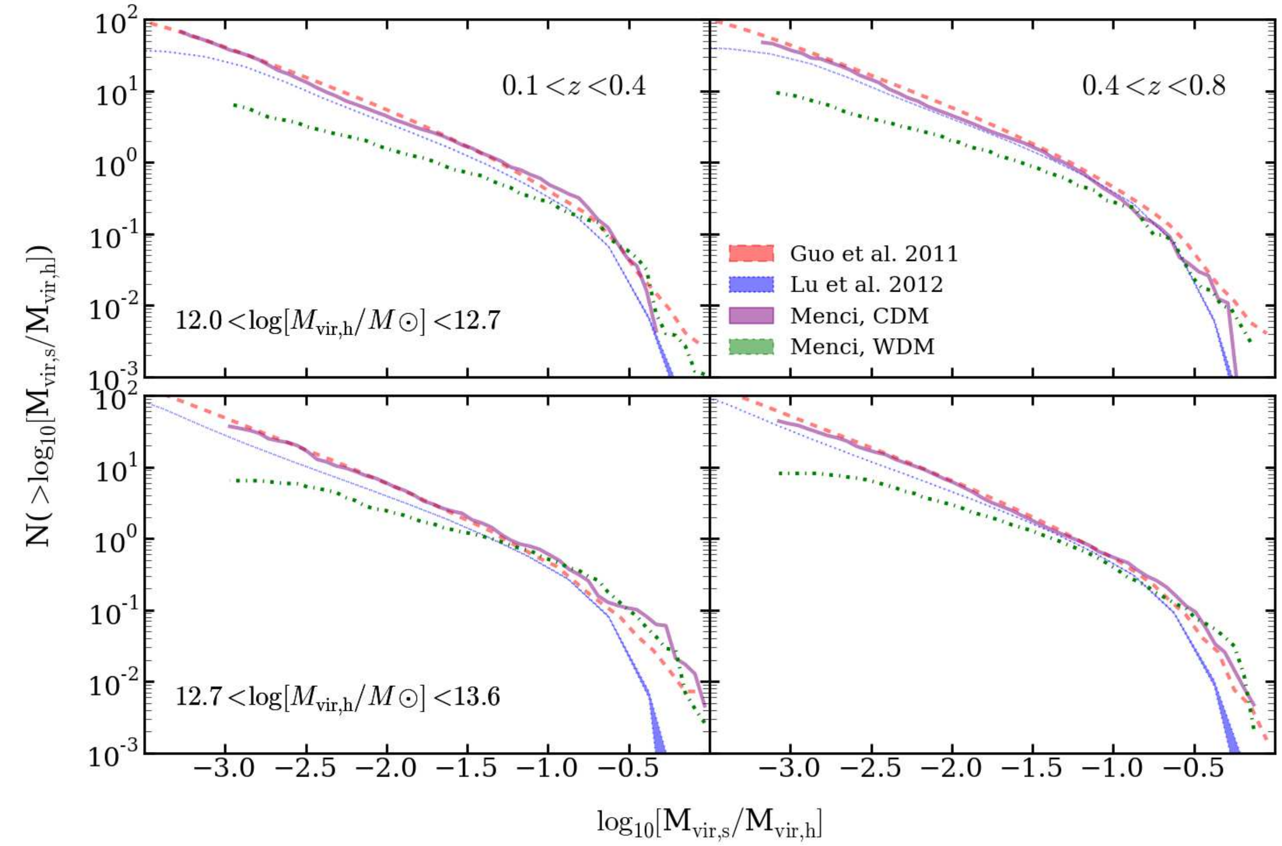

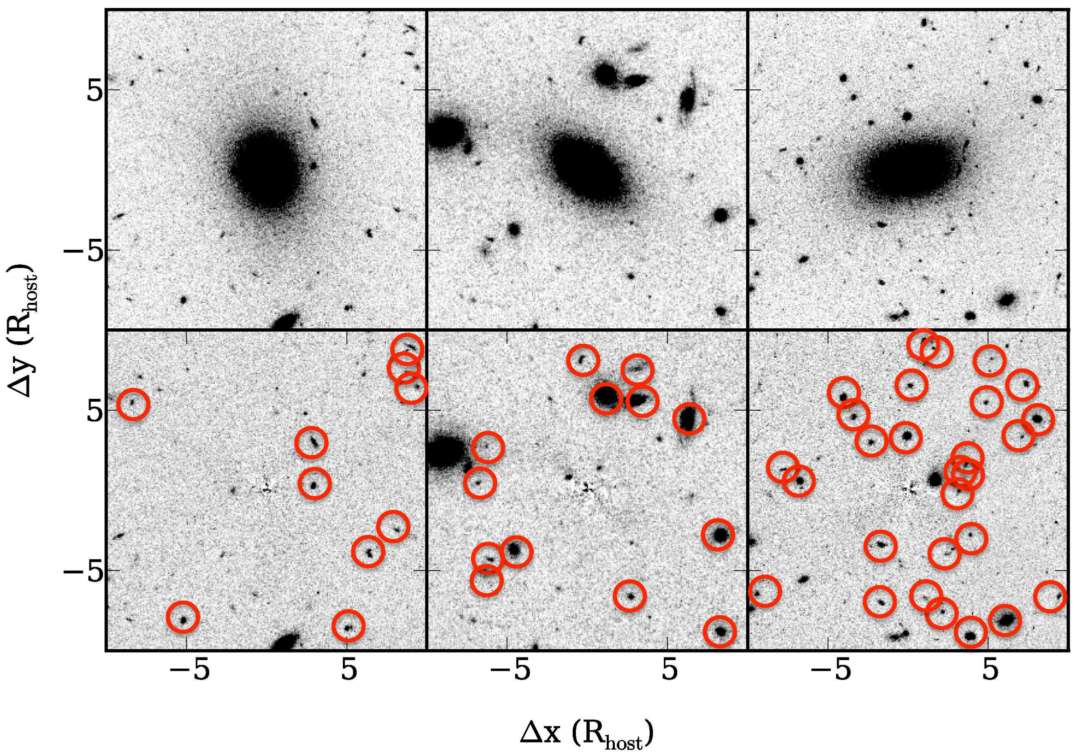

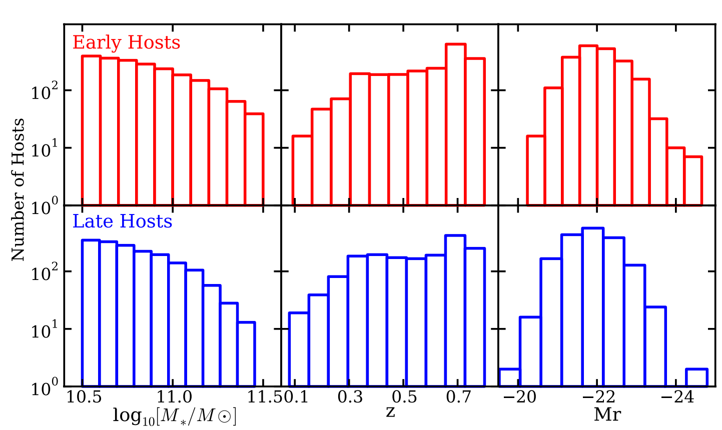

The luminosity distribution of Satellite Galaxies
Nierenberg, Treu, NM 2013

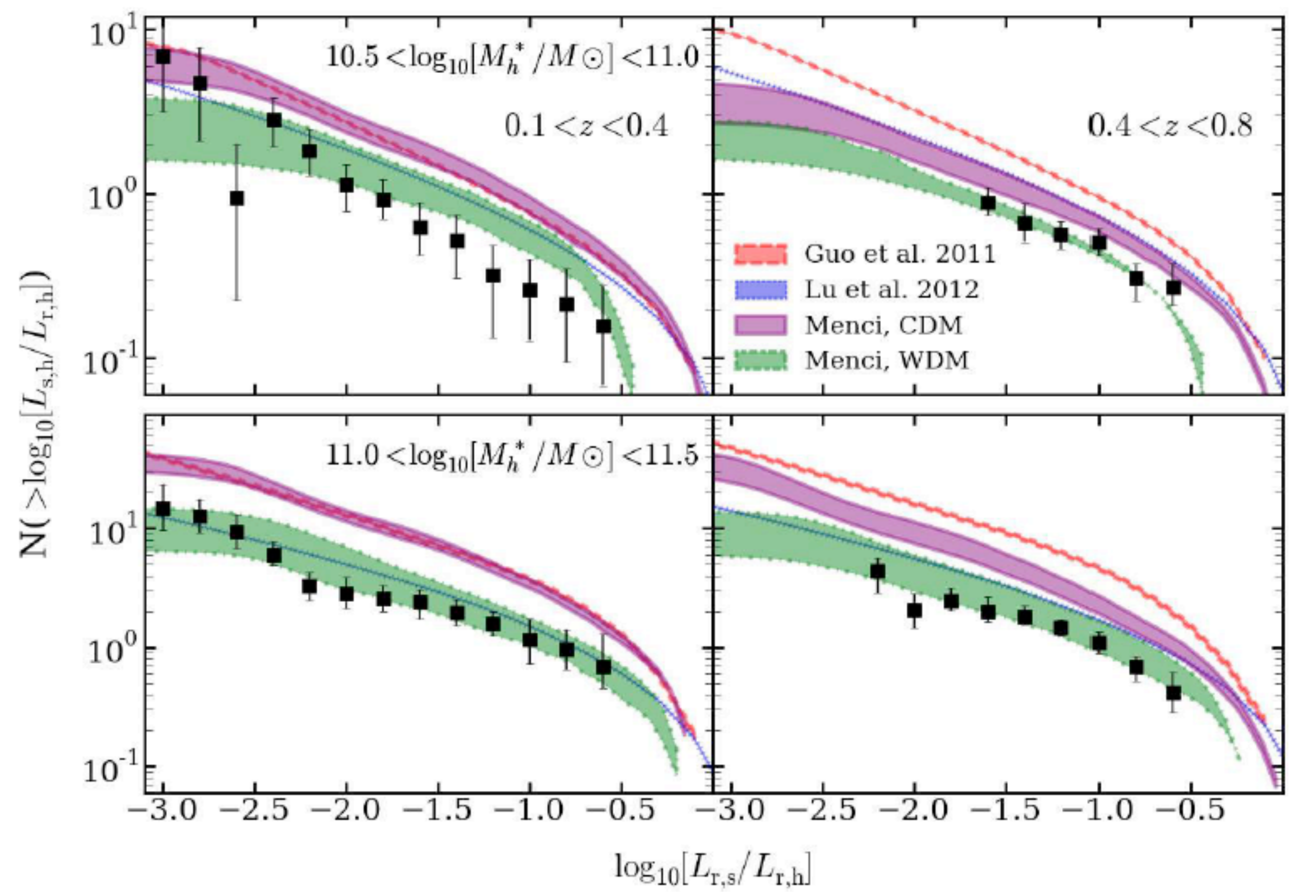

The Age of stellar populations in low-mass galaxies

CDM predicts early collapse of a huge number of low-mass halos, which remain isolated at later times retaining the early-formed stellar populations; as a result, CDM-based SAMs generally provide flat age-mass relations (Fontanot et al. 2009; Pasquali et al. 2010; De Lucia & Borgani 2012).

Increasing the stellar feedback worsen the problem

Early SF: WDM induces delay in star formation, affects small-mass objects(see, e.g., Angulo et al. 2013)

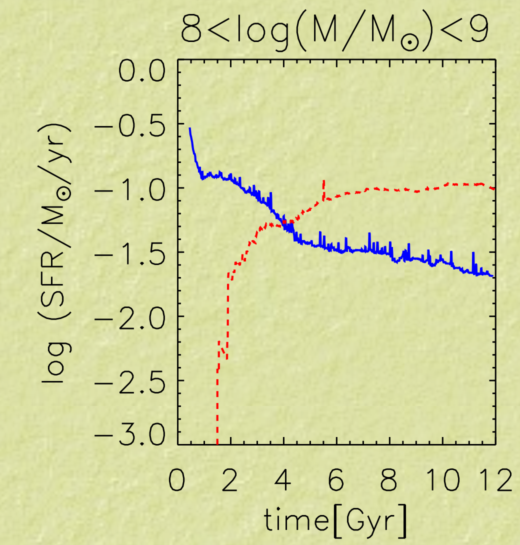

$$Age(t_0) = \frac{\int_0^{t_0} (t_0 - t)\,\psi(t)\,dt}{\int_0^{t_0} \psi(t)\,dt}$$

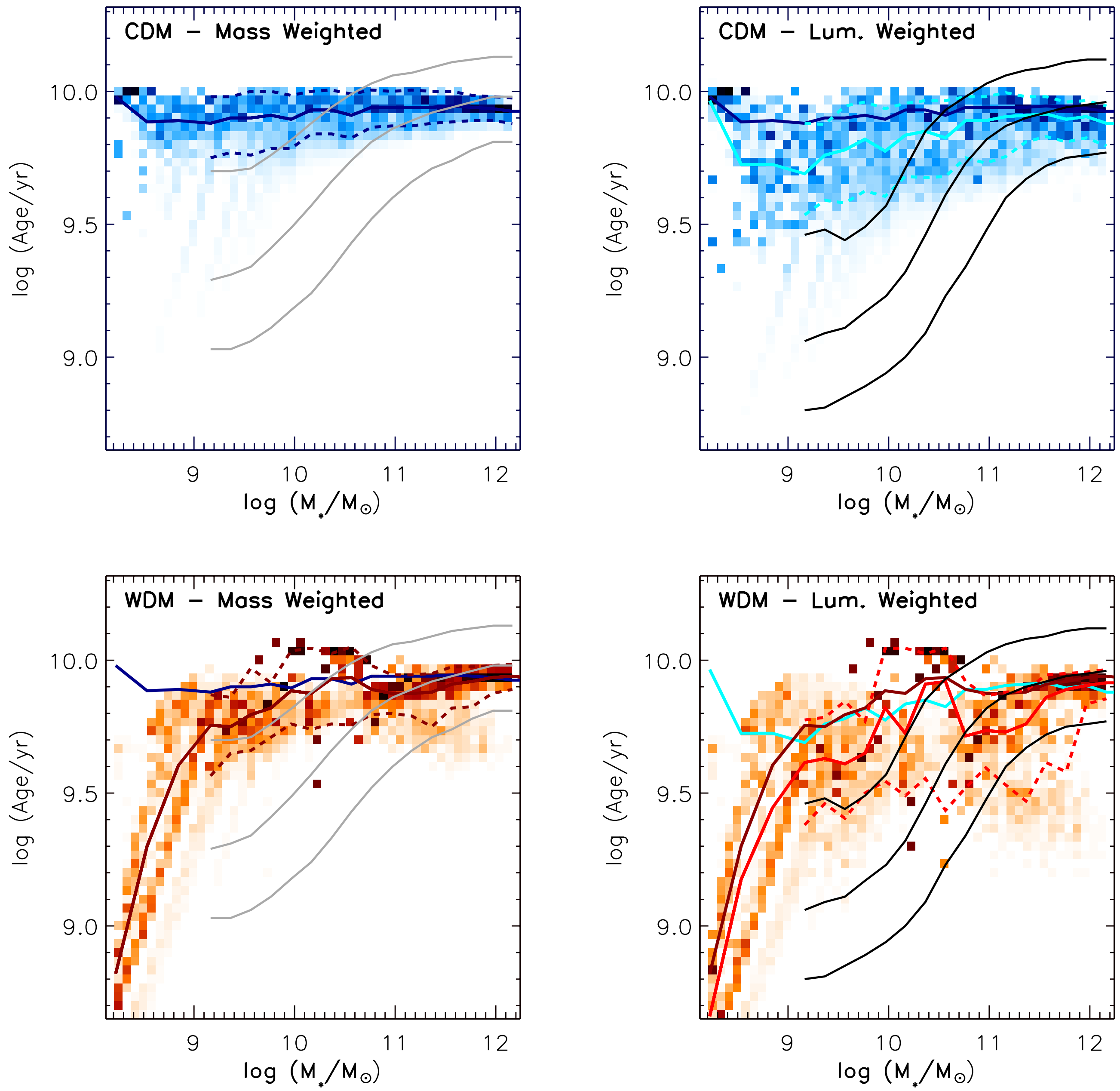

Calura, NM, Gallazzi 2014

The upper, the middle and the lower grey (black) curves represent the 16th, the 50th (median) and the 84th percentiles of the observed distribution in mass-(light-)weighted stellar age (Gallazzi et al. 2008)

Matching the V_{max}-M_* relation

A semi-empirical approach (Shankar, NM et al. 2014) in progress

1. select a sample of DM haloes
2. associate to each halo a galaxy of a given stellar mass according to an abundance matching relation
3. compute rotation velocity curves for each DM halo (for WDM adopt the $c(M_h)$ relation by Schneider et al 2012 for 1 keV thermal relic DM)
4. infer predicted V_{MAX}-M_* relation (computed at maximum of the rotation curve)

Matching the V_{max}-M_* relation

A semi-empirical approach (Shankar, NM et al. 2014) in progress

1. select a sample of DM haloes
2. associate to each halo a galaxy of a given stellar mass according to an abundance matching relation
3. compute rotation velocity curves for each DM halo (for WDM adopt the $c(M_h)$ relation by Schneider et al 2012 for 1 keV thermal relic DM)
4. infer predicted V_{MAX}-M_* relation (computed at maximum of the rotation curve)

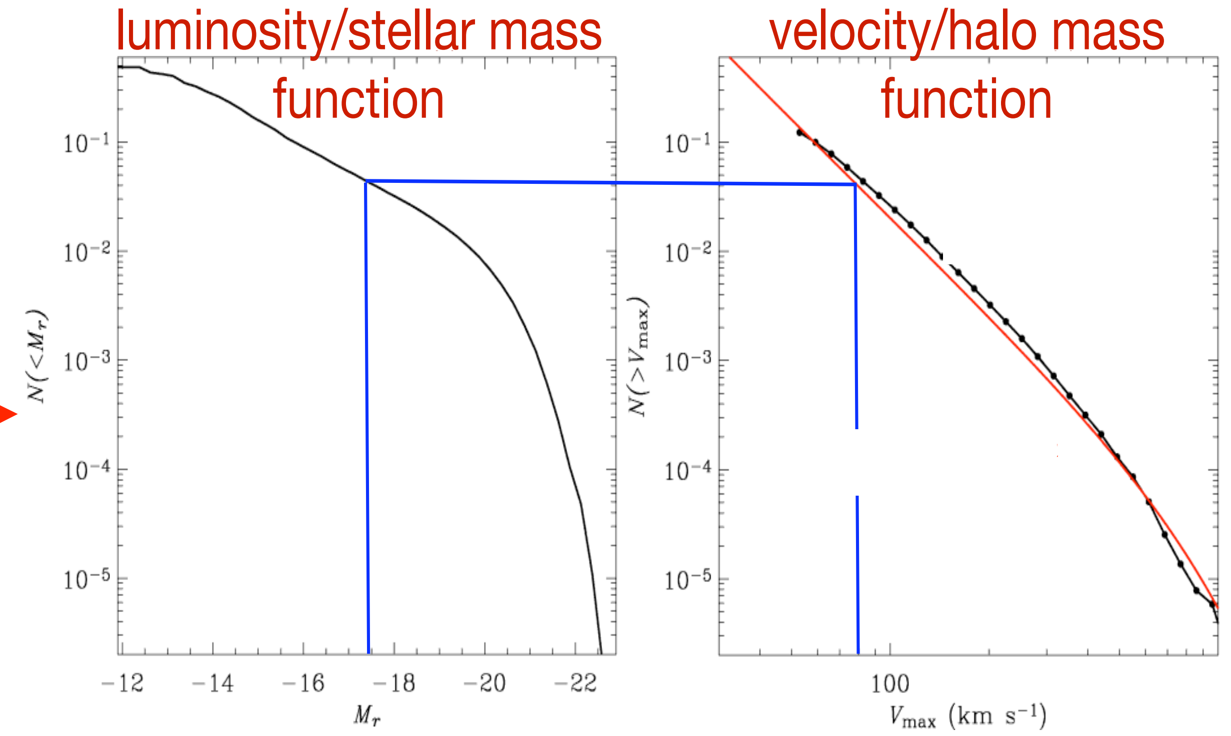

Matching the V_{max}-M_* relation

A semi-empirical approach (Shankar, NM et al. 2014) in progress

1. select a sample of DM haloes
2. associate to each halo a galaxy of a given stellar mass according to an abundance matching relation
3. compute rotation velocity curves for each DM halo (for WDM adopt the $c(M_h)$ relation by Schneider et al 2012 for 1 keV thermal relic DM)
4. infer predicted V_{MAX}-M_* relation (computed at maximum of the rotation curve)

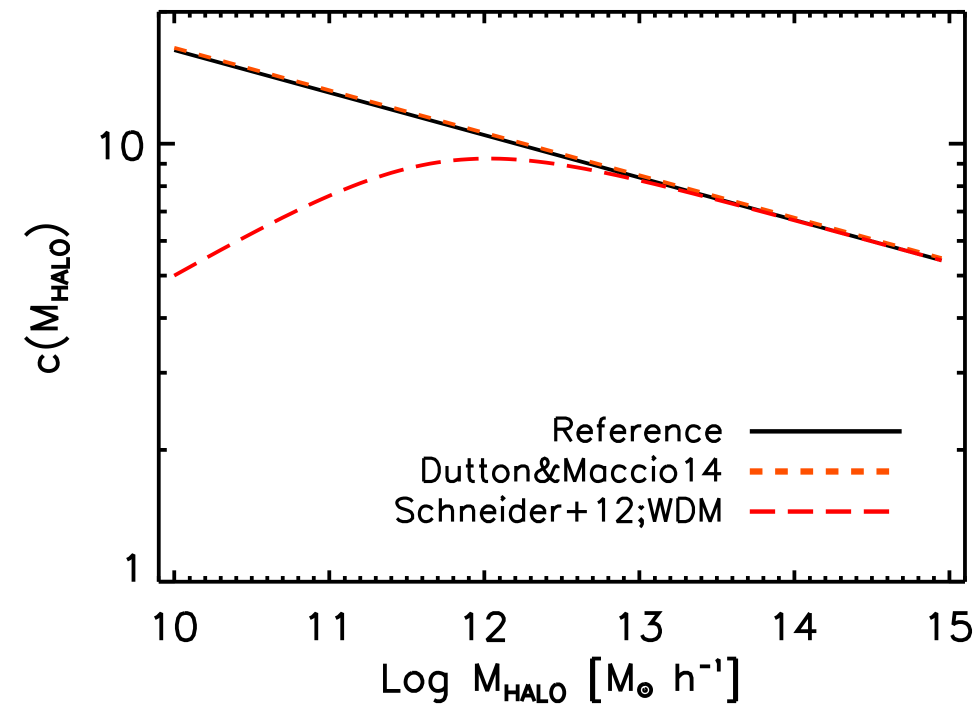

Matching the V_{max}-M_* relation

A semi-empirical approach (Shankar, NM et al. 2014) in progress

1. select a sample of DM haloes
2. associate to each halo a galaxy of a given stellar mass according to an abundance matching relation
3. compute rotation velocity curves for each DM halo (for WDM adopt the $c(M_h)$ relation by Schneider et al 2012 for 1 keV thermal relic DM)
4. infer predicted V_{MAX}-M_* relation (computed at maximum of the rotation curve)

Feedback profile from Di Cintio et al. 2014
hydro-simulations baryons+stellar feedback

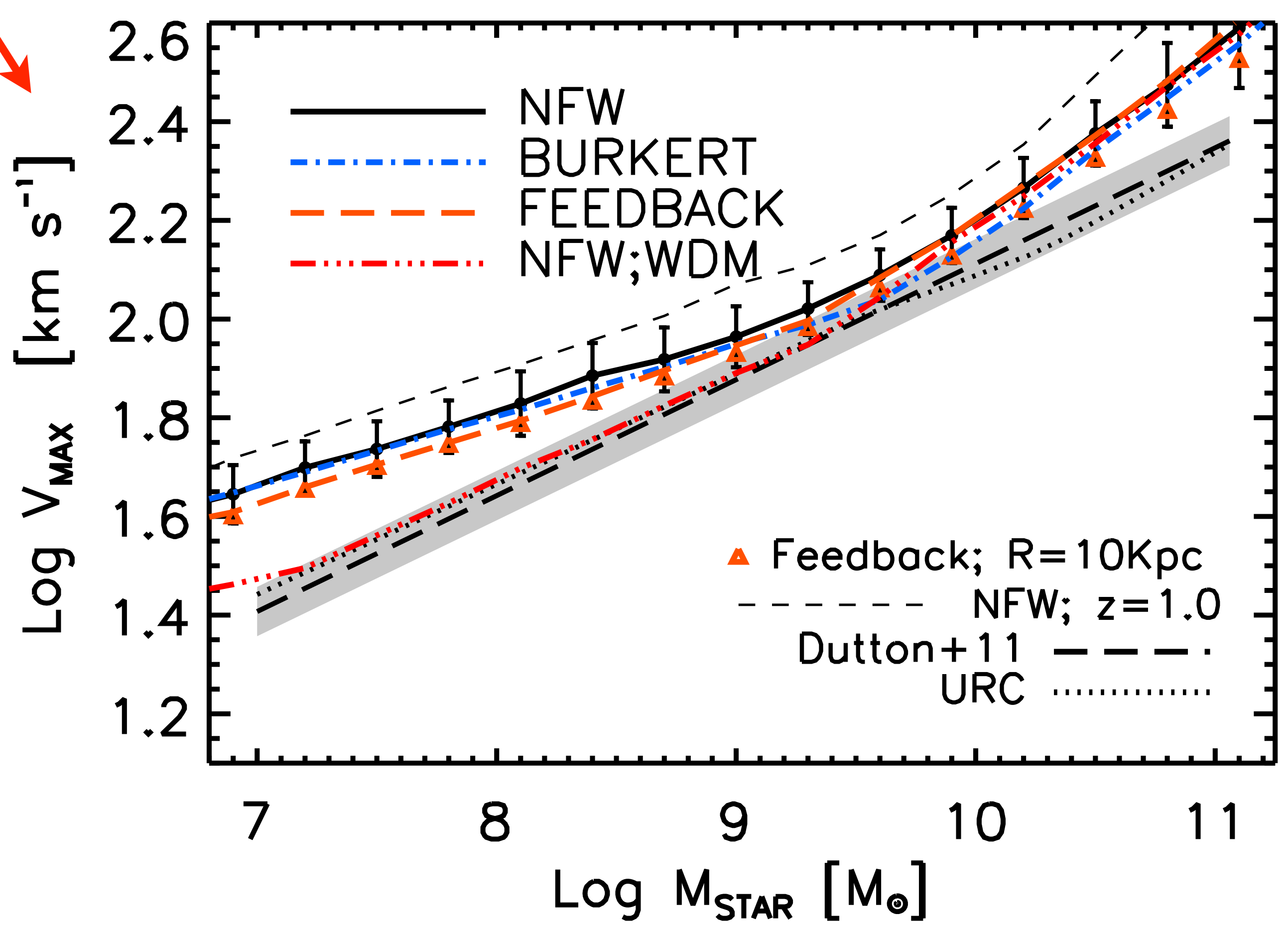

Summary

The mass of DM particles has a major impact on galaxy formation (suppression of small-scale perturbations due to free-streaming)
CDM is the limit of M_{fs}<< masses of cosmological interest

CDM problems on small scales:
- cusps
- number of satellite galaxies
- abundance of low-mass (faint) galaxies at low and high redhsifts

Baryonic physics can hardly solve all the problems if we consider ab abundance of high-z low-luminosity objects

Galaxy formation in WDM cosmology is a viable solution if the spectrum is like that corresponding to a thermal relic DM with m<2 keV (analogous to that corresponding to sterile neutrino produced according to Dodelson & Widrow with m_ν<8 keV)

There is a tension with current limits from high-z structure (Lyman-a forest)

Summary

The mass of DM particles has a major impact on galaxy formation (suppression of small-scale perturbations due to free-streaming)
CDM is the limit of M_{fs}<< masses of cosmological interest

CDM problems on small scales:

- cusps
- number of satellite galaxies
- abundance of low-mass (faint) galaxies at low and high redhsifts

Baryonic physics can hardly solve all the problems if we consider ab abundance of high-z low-luminosity objects

Galaxy formation in WDM cosmology is a viable solution if the spectrum is like that corresponding to a thermal relic DM with m<2 keV (analogous to that corresponding to sterile neutrino produced according to Dodelson & Widrow with m_ν<8 keV)

There is a tension with current limits from high-z structure (Lyman-a forest)

Summary

Schneider et al. 2013

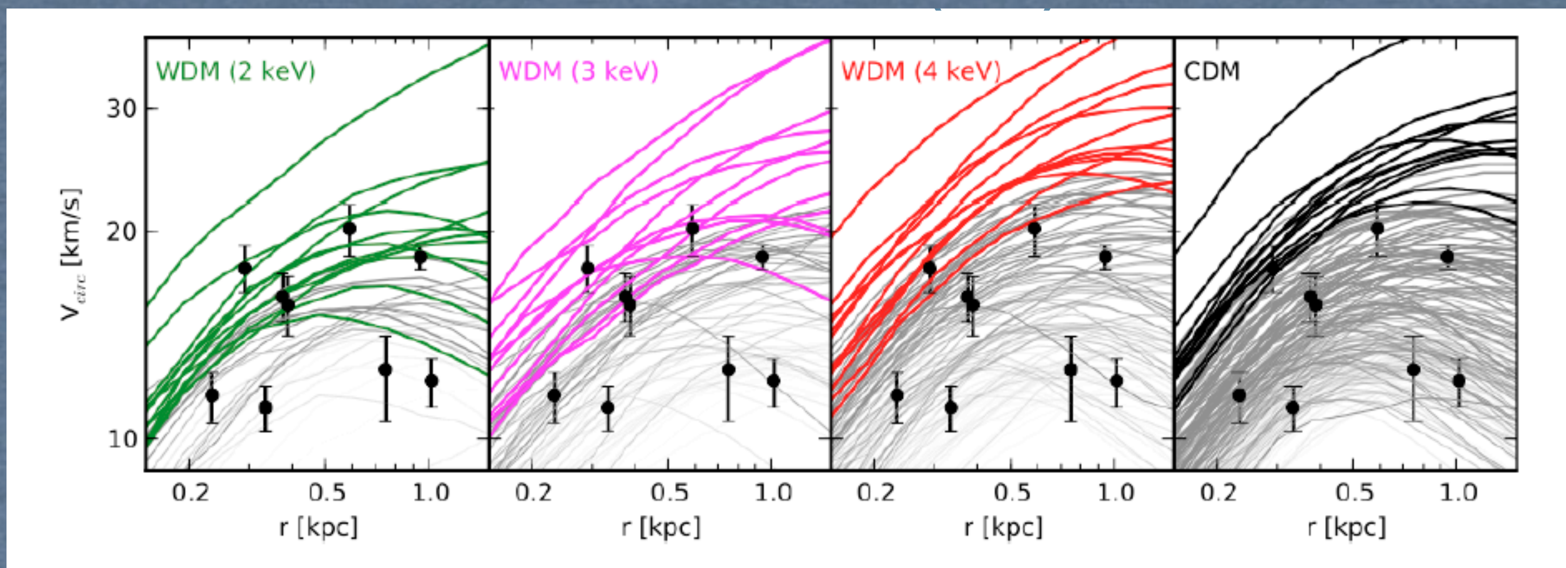

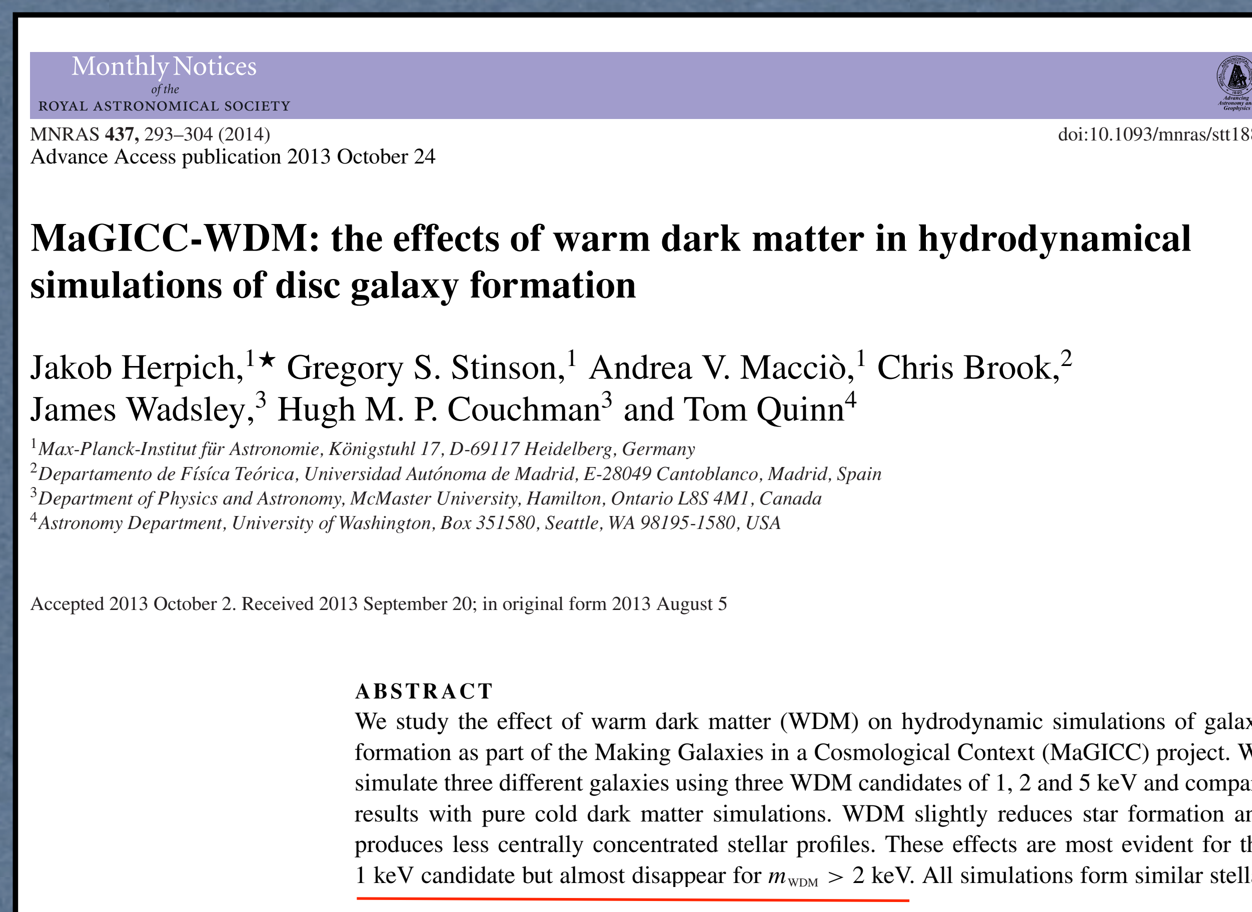

Monthly Notices of the ROYAL ASTRONOMICAL SOCIETY

MNRAS **437**, 293–304 (2014) doi:10.1093/mnras/stt188

Advance Access publication 2013 October 24

MaGICC-WDM: the effects of warm dark matter in hydrodynamical simulations of disc galaxy formation

Jakob Herpich,[1]★ Gregory S. Stinson,[1] Andrea V. Macciò,[1] Chris Brook,[2] James Wadsley,[3] Hugh M. P. Couchman[3] and Tom Quinn[4]

[1] *Max-Planck-Institut für Astronomie, Königstuhl 17, D-69117 Heidelberg, Germany*

[2] *Departamento de Física Teórica, Universidad Autónoma de Madrid, E-28049 Cantoblanco, Madrid, Spain*

[3] *Department of Physics and Astronomy, McMaster University, Hamilton, Ontario L8S 4M1, Canada*

[4] *Astronomy Department, University of Washington, Box 351580, Seattle, WA 98195-1580, USA*

Accepted 2013 October 2. Received 2013 September 20; in original form 2013 August 5

ABSTRACT

We study the effect of warm dark matter (WDM) on hydrodynamic simulations of galax formation as part of the Making Galaxies in a Cosmological Context (MaGICC) project. We simulate three different galaxies using three WDM candidates of 1, 2 and 5 keV and compare results with pure cold dark matter simulations. WDM slightly reduces star formation and produces less centrally concentrated stellar profiles. These effects are most evident for the 1 keV candidate but almost disappear for $m_{WDM} > 2$ keV. All simulations form similar stella

th m<2 keV

ording to

-a forest)

Summary

The mass of DM particles has a major impact on galaxy formation (suppression of small-scale perturbations due to free-streaming)
CDM is the limit of M_{fs}<< masses of cosmological interest

CDM problems on small scales:
- cusps
- number of satellite galaxies
- abundance of low-mass (faint) galaxies at low and high redhsifts

Baryonic physics can hardly solve all the problems if we consider ab abundance of high-z low-luminosity objects

Galaxy formation in WDM cosmology is a viable solution if the spectrum is like that corresponding to a thermal relic DM with m<2 keV (analogous to that corresponding to sterile neutrino produced according to Dodelson & Widrow with m_ν<8 keV)

There is a tension with current limits from high-z structure (Lyman-a forest)

Summary

The mass of DM particles has a major impact on galaxy formation
(suppression of small-scale perturbations due to free-streaming)
CDM is the limit of $M_{fs} \ll$ masses of cosmological interest

CDM problems on small scales:
- cusps
- number of satellite galaxies
- abundance of low-mass (faint) galaxies at low and high redhsifts

Baryonic physics can hardly solve all the problems if we consider
ab abundance of high-z low-luminosity objects

Galaxy formation in WDM cosmology is a viable solution
if the spectrum is like that corresponding to a thermal relic DM with $m<2$ keV
(analogous to that corresponding to sterile neutrino produced according to
Dodelson & Widrow with $m_\nu<8$ keV)

There is a tension with current limits from high-z structure (Lyman-a forest)

Summary

The mass of DM particles has a major impact on galaxy formation
(suppression of small-scale perturbations due to free-streaming)
CDM is the limit of M_{fs}<< masses of cosmological interest

CDM problems on small scales:
- cusps
- number of satellite galaxies
- abundance of low-mass (faint) galaxies at low and high redhsifts

Baryonic physics can hardly solve all the problems if we consider
ab abundance of high-z low-luminosity objects

Galaxy formation in WDM cosmology is a viable solution
if the spectrum is like that corresponding to a thermal relic DM with m<2 keV
(analogous to that corresponding to sterile neutrino produced according to
Dodelson & Widrow with m_ν<8 keV)

There is a tension with current limits from high-z structure (Lyman-a forest)

Mass should be m<2 keV (thermal relics)

Schneider et al. 2013

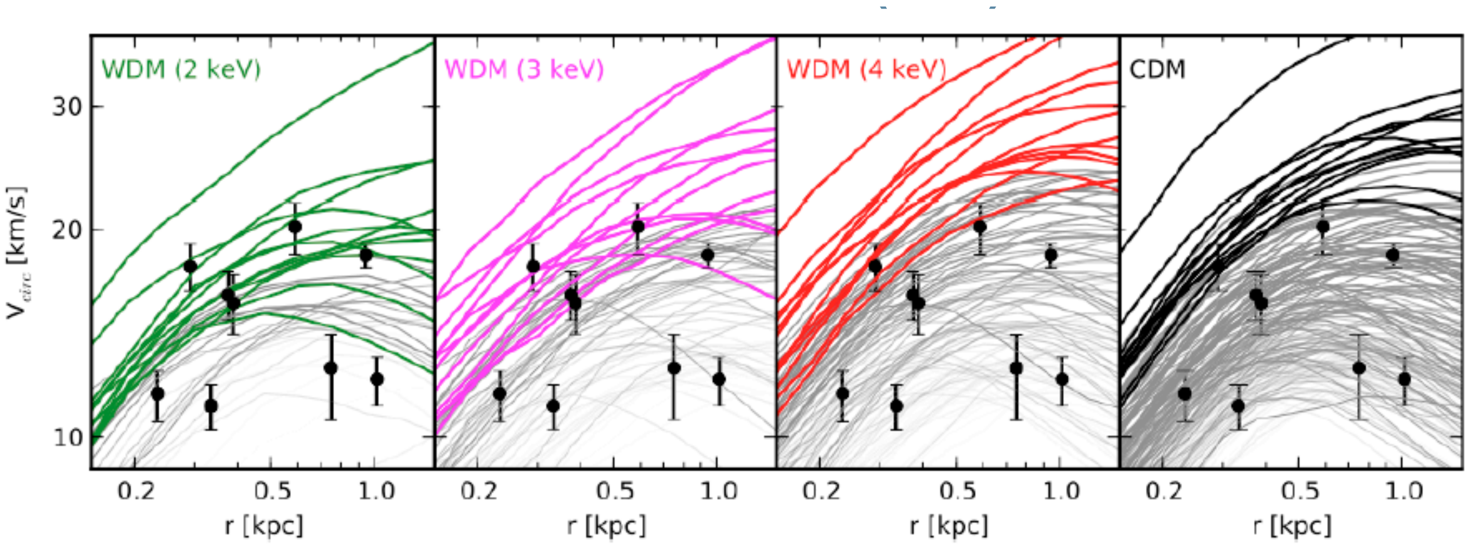

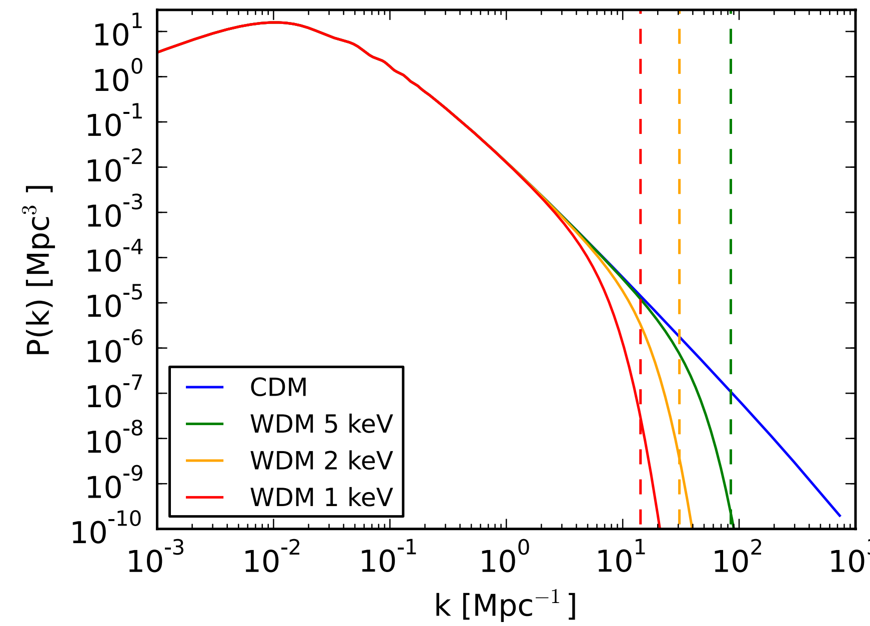

Monthly Notices of the ROYAL ASTRONOMICAL SOCIETY

MNRAS **437,** 293–304 (2014) doi:10.1093/mnras/stt1883
Advance Access publication 2013 October 24

MaGICC-WDM: the effects of warm dark matter in hydrodynamical simulations of disc galaxy formation

Jakob Herpich,[1★] Gregory S. Stinson,[1] Andrea V. Macciò,[1] Chris Brook,[2] James Wadsley,[3] Hugh M. P. Couchman[3] and Tom Quinn[4]

[1] *Max-Planck-Institut für Astronomie, Königstuhl 17, D-69117 Heidelberg, Germany*
[2] *Departamento de Física Teórica, Universidad Autónoma de Madrid, E-28049 Cantoblanco, Madrid, Spain*
[3] *Department of Physics and Astronomy, McMaster University, Hamilton, Ontario L8S 4M1, Canada*
[4] *Astronomy Department, University of Washington, Box 351580, Seattle, WA 98195-1580, USA*

Accepted 2013 October 2. Received 2013 September 20; in original form 2013 August 5

ABSTRACT

We study the effect of warm dark matter (WDM) on hydrodynamic simulations of galaxy formation as part of the Making Galaxies in a Cosmological Context (MaGICC) project. We simulate three different galaxies using three WDM candidates of 1, 2 and 5 keV and compare results with pure cold dark matter simulations. WDM slightly reduces star formation and produces less centrally concentrated stellar profiles. These effects are most evident for the 1 keV candidate but almost disappear for $m_{\rm WDM} > 2$ keV. All simulations form similar stellar

WDM particle mass: limits from the Ly-α forest

Viel et al. 2005-2013

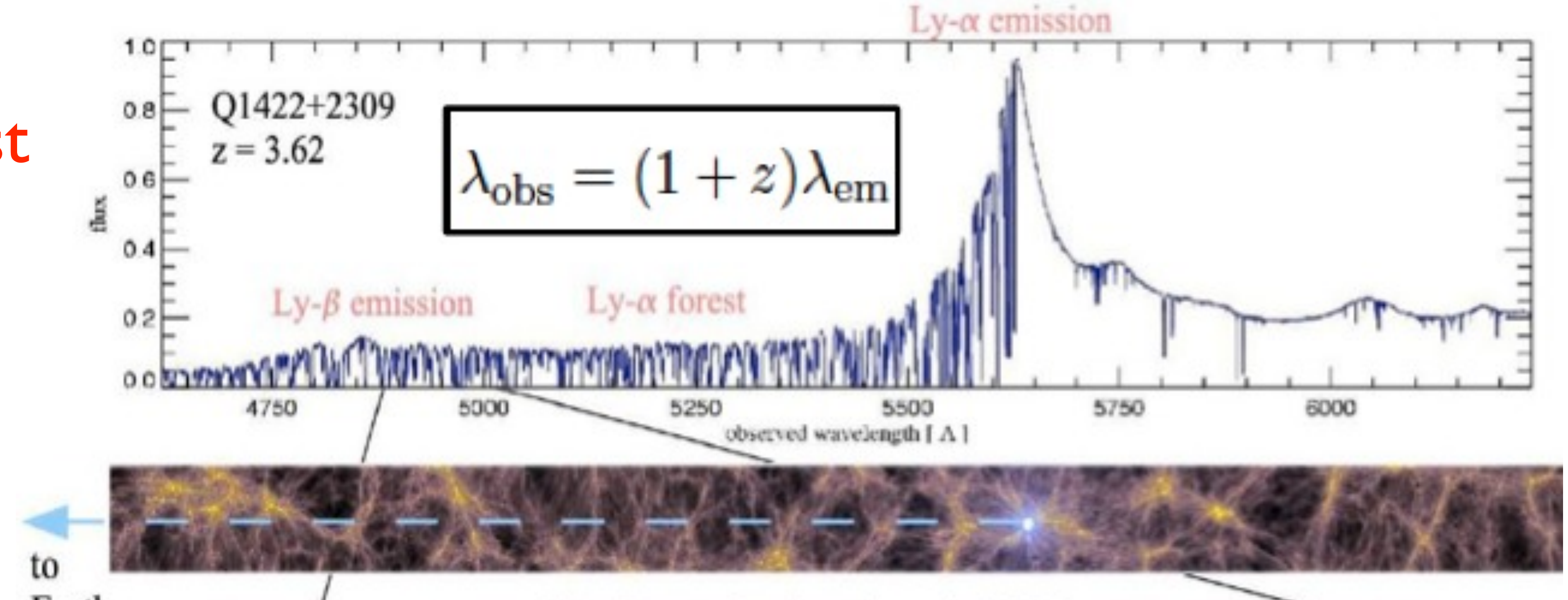

Fig. From Springel et al. 2006

$m_{WDM}>1$ keV	Thermal relics WDM
$m_\nu>4$ keV	Sterile ν WDM (DW) **Dodelson-Widrow**

↓

$m_{WDM}>4$ keV	Thermal relics WDM
$m_\nu>12$ keV	Sterile ν WDM (DW) **Dodelson-Widrow**

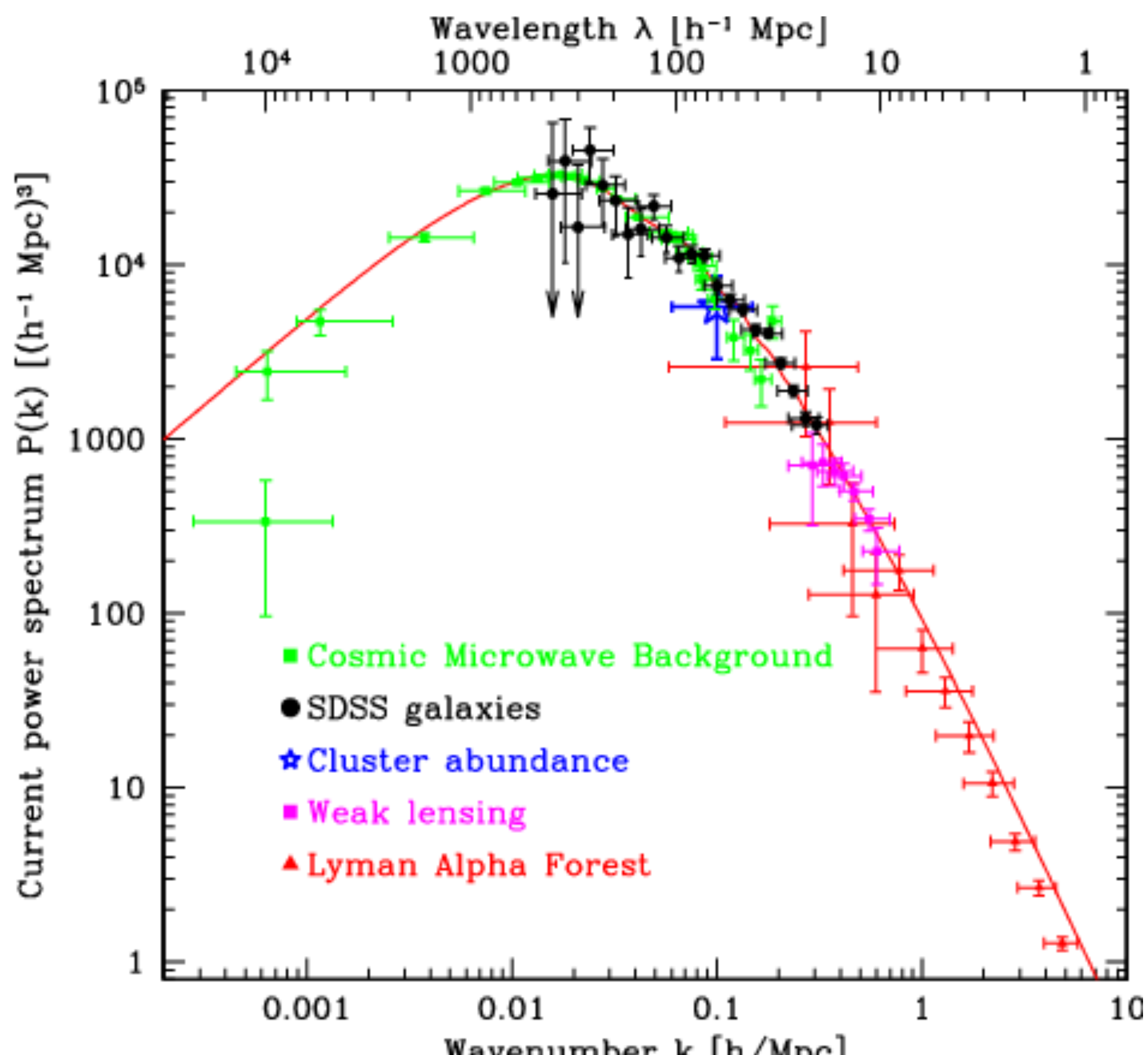

Constraints from X-ray emission from clusters and galaxies

if $m_s > m_\alpha$ the radiative decay $\nu_s \rightarrow \nu_\alpha + \gamma$ becomes allowed

$$E_\gamma = \frac{1}{2} m_s \left(1 - \frac{m_\alpha^2}{m_s^2}\right) .$$

Emission lines in X-rays from DM concentrations:
- clusters (large signal but also large background)
- galaxies

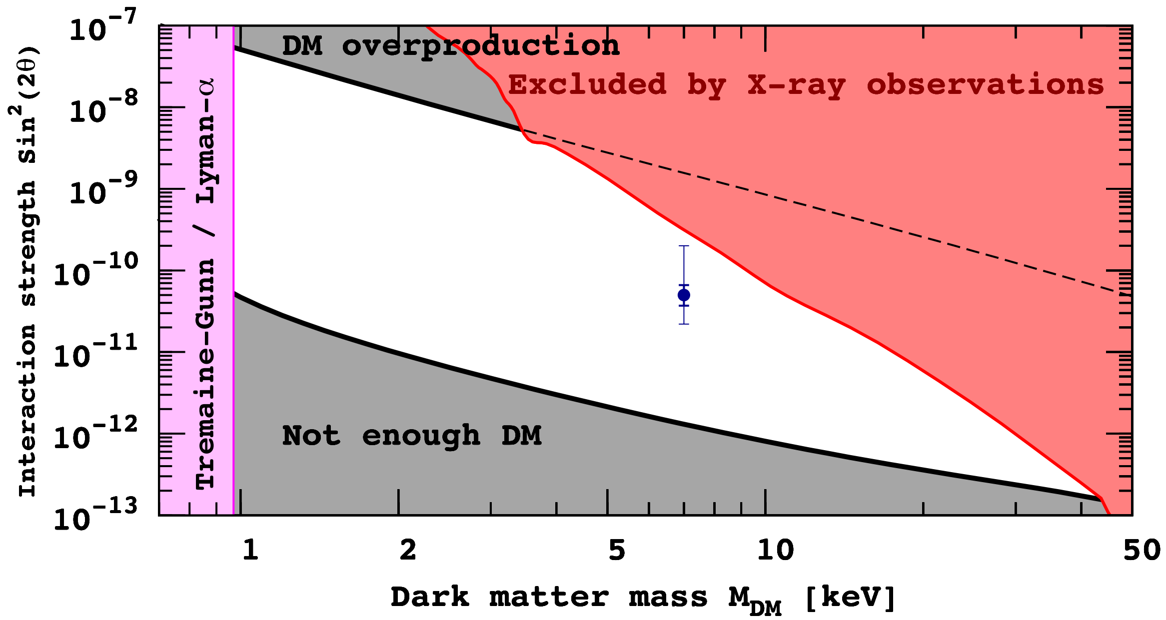

FIG. 4: Constraints on sterile neutrino DM within νMSM [4]. The blue point would corresponds to the best-fit value from M31 if the line comes from DM decay. Thick errorbars are $\pm 1\sigma$ limits on the flux. Thin errorbars correspond to the uncertainty in the DM distribution in the center of M31.

Boyarsky et al. 2014

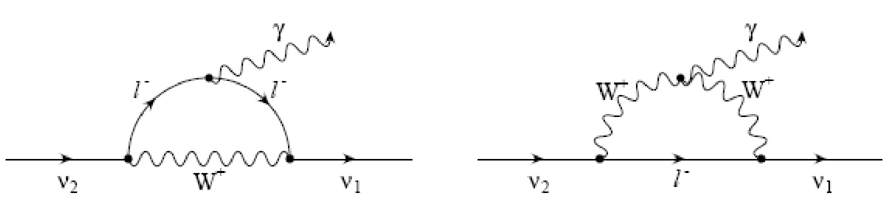

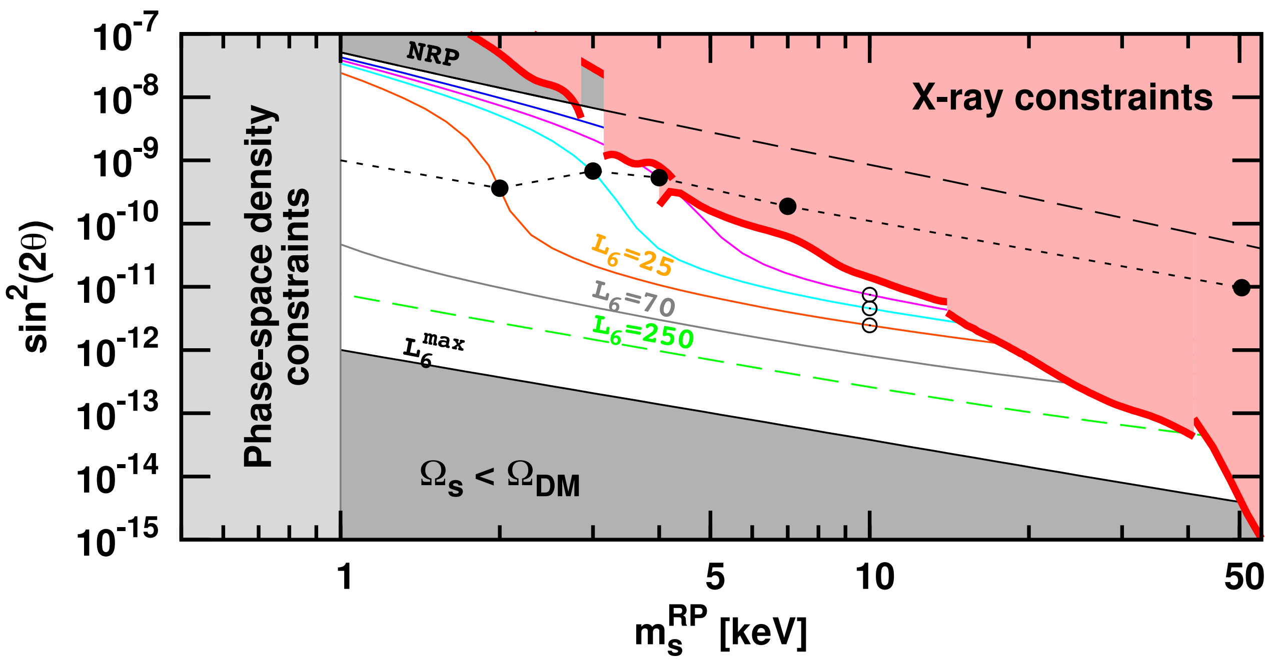

Abazajian et al. 2001-2005

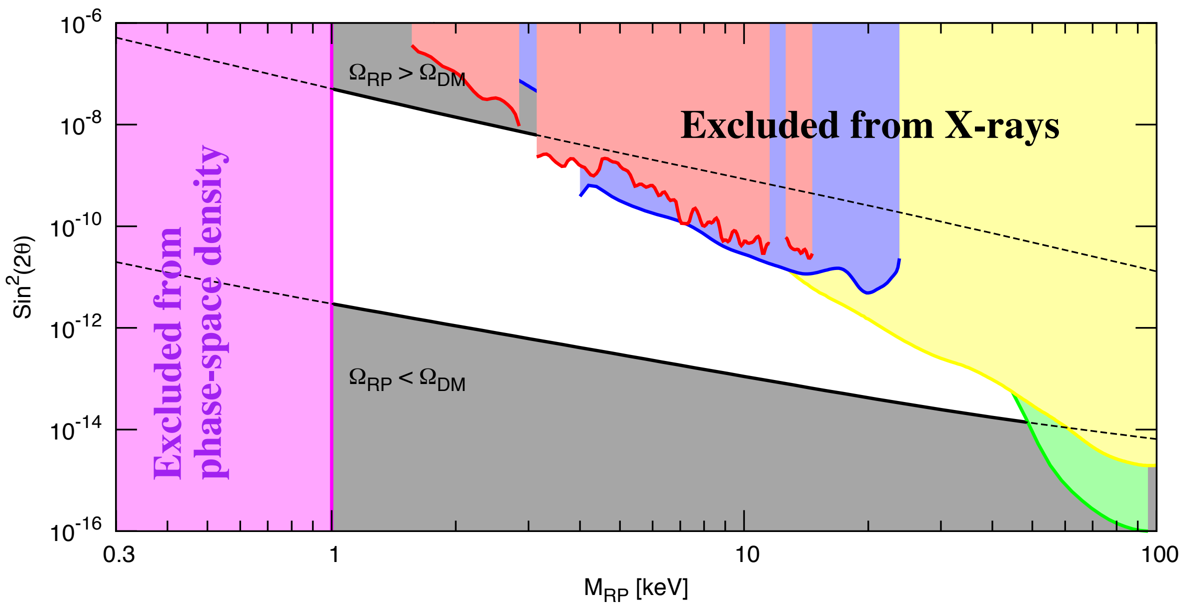

Window corresponds to resonant production

Upper boundary - zero lepton asymmetry

Lower boundary - maximal lepton asymmetry

Boyarsky et al 2009

6 – Sterile neutrino resonant production

In presence of a large lepton asymmetry, $\mathcal{L} \equiv (n_\nu - n_{\bar{\nu}})/n_\gamma$, matter effects become important and the mixing angle can be resonantly enhanced. [Shi, Fuller, 1998; Abazajian et al., 2001

$$\sin^2 2\theta_m = \frac{\Delta^2(p)\sin^2 2\theta}{\Delta^2(p)\sin^2 2\theta + D^2 + (\Delta(p)\cos 2\theta - \frac{2\sqrt{2}\zeta(3)}{\pi^2} G_F T^3 \mathcal{L} + |V_T|)^2}$$

The mixing angle is maximal $\sin^2 2\theta_m = 1$ when the resonant condition is satisfied (with $\Delta(p) \equiv m_4^2/(2p)$)

$$\Delta(p)\cos 2\theta - \frac{2\sqrt{2}\zeta(3)}{\pi^2} G_F T^3 \mathcal{L} + |V_T| = 0$$

$$\left(\frac{m_4}{1\mathrm{keV}}\right)^2 \simeq 0.08 \frac{p}{T} \frac{\mathcal{L}}{10^{-4}} \left(\frac{T}{100\,\mathrm{MeV}}\right)^4 + 2\left(\frac{p}{T}\right)^2 \frac{B}{\mathrm{keV}} \left(\frac{T}{100\,\mathrm{MeV}}\right)^6$$

Sterile neutrinos are produced in primordial plasma through

• off-resonance oscillations. [Dodelson, Widrow; Abazajian, Fuller; Dolgov, Hansen; Asaka, Laine, Shaposhnikov et al.]

• oscillations on resonance, if the lepton asymmetry is non-negligible [Fuller, Shi]

• production mechanisms which do not involve oscillations
– inflaton decays directly into sterile neutrinos [Shaposhnikov, Tkachev] – Higgs physics: both mass and production [AK, Petraki]

Watson et al. 2012

Limits from the X-ray emission from clusters and galaxies

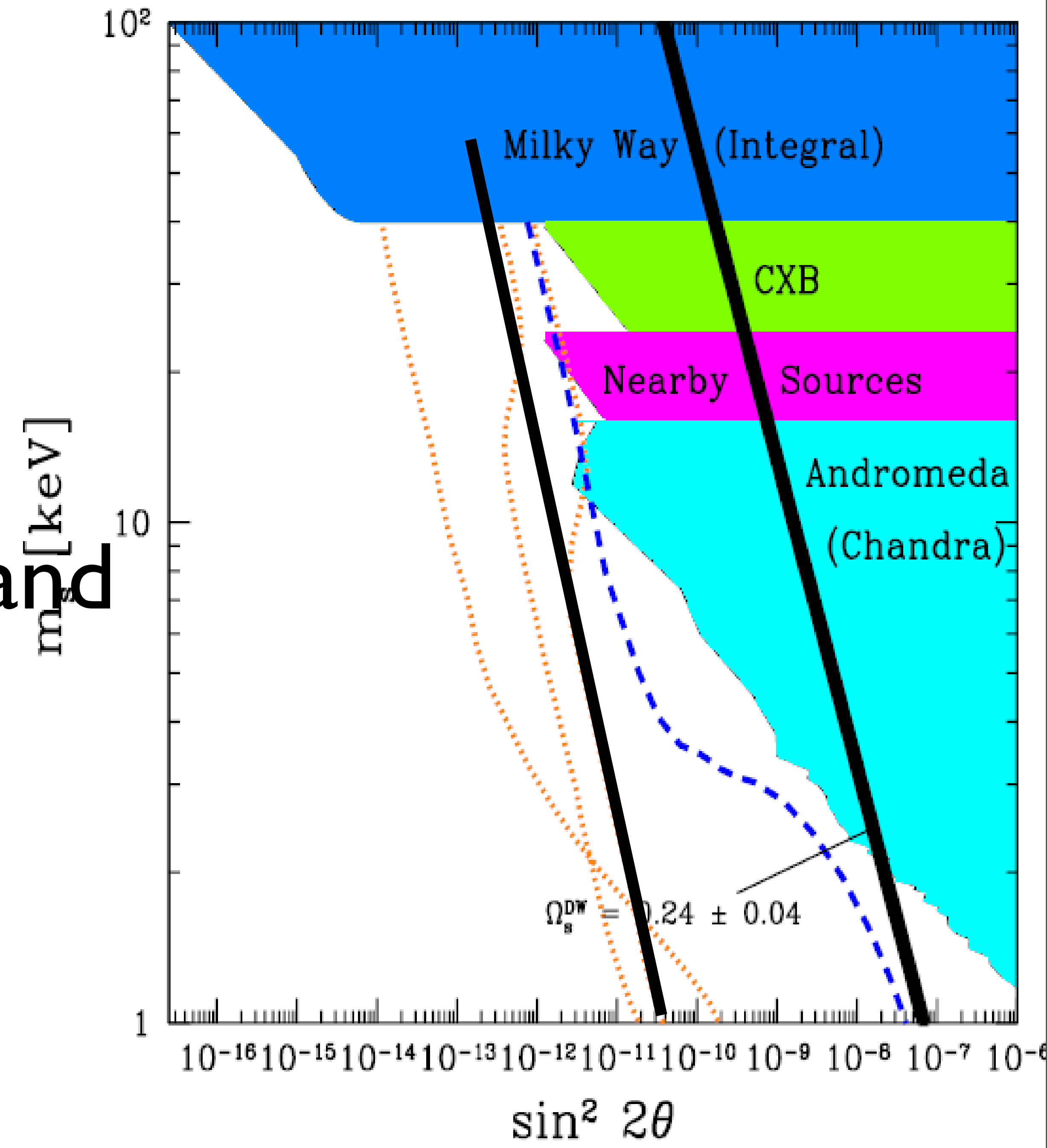

Very small **mixing** $(\sin^2 2\theta \lesssim 10^{-7})$ **between**

mass $|\nu_{1,2}>$ **&**

flavor $|\nu_{\alpha,s}>$ **states:**

$$|\nu_\alpha\rangle = \cos\theta|\nu_1\rangle + \sin\theta|\nu_2\rangle$$
$$|\nu_s\rangle = -\sin\theta|\nu_1\rangle + \cos\theta|\nu_2\rangle$$

For $m_s < m_e$,

3ν Decay Mode Dominates:

$$\Gamma_{3\nu} \simeq 1.74 \times 10^{-30} s^{-1} \left(\frac{\sin^2 2\theta}{10^{-10}}\right)\left(\frac{m_s}{\text{keV}}\right)^5$$

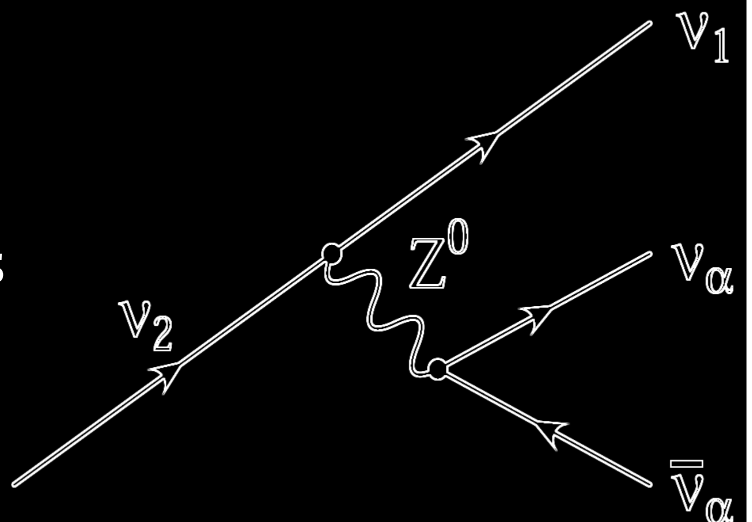

Radiative Decay Rate is:

$$\Gamma_s \simeq 1.36 \times 10^{-32} s^{-1} \left(\frac{\sin^2 2\theta}{10^{-10}}\right)\left(\frac{m_s}{\text{keV}}\right)^5 \quad \nu_s \to \nu_\alpha + \gamma$$

WIMP

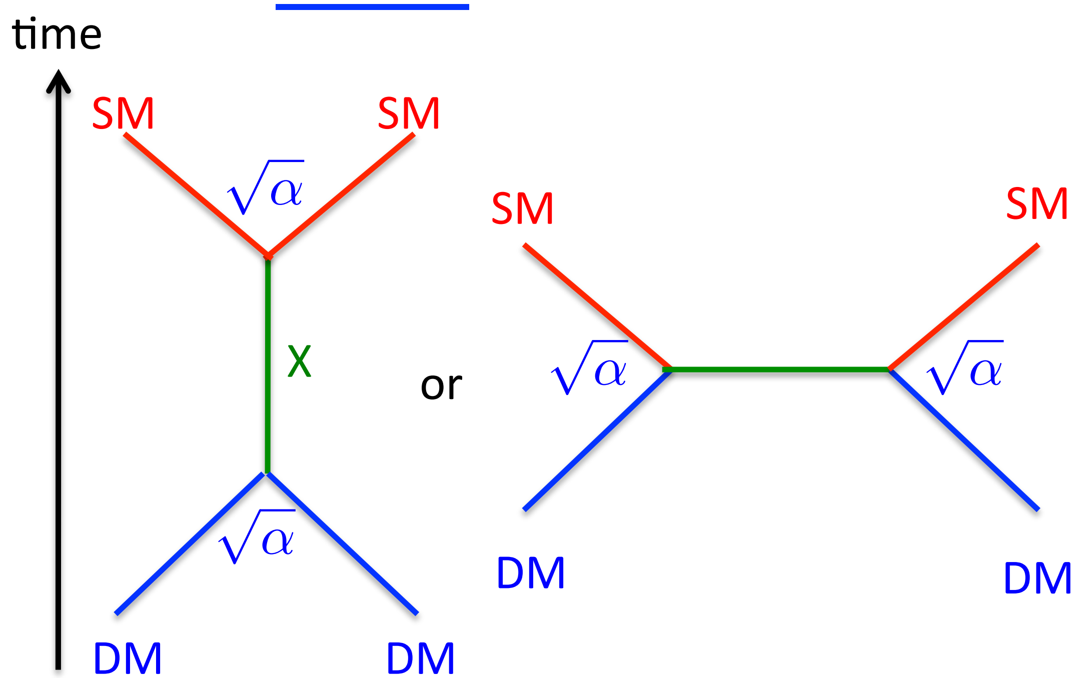

self-annihilation

freeze out

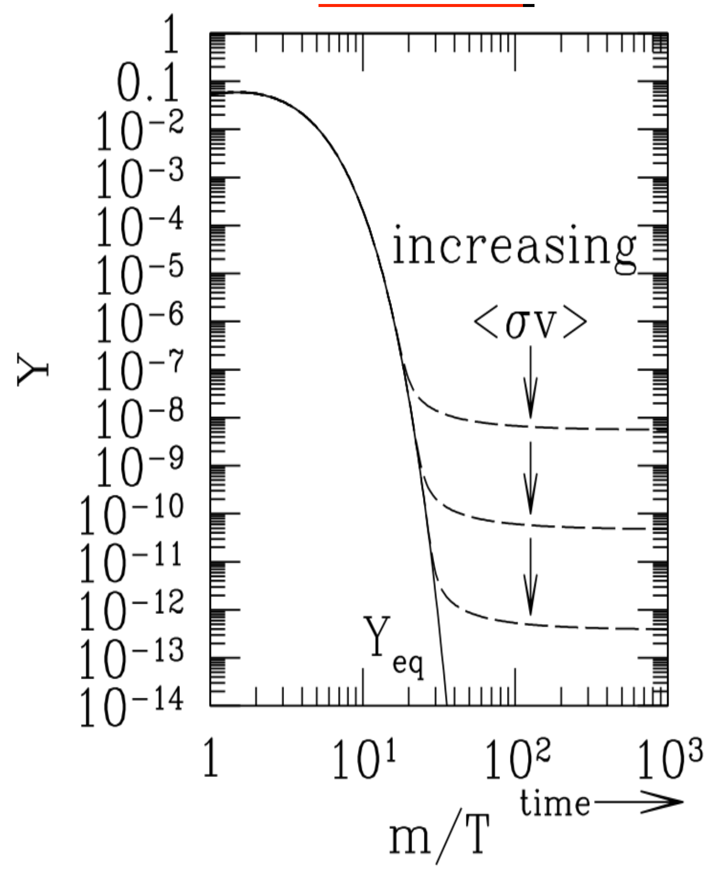

$$\Omega h^2 \approx \frac{3 \times 10^{-27}\ \mathrm{cm^3/s}}{\langle \sigma_{\mathrm{ann}} v \rangle}.$$

$$\langle \sigma_{\mathbf{ann}} \mathbf{v} \rangle \sim \mathbf{10^{-25}} \mathrm{cm^3 s^{-1}} \left(\frac{\alpha}{\mathbf{10^{-2}}} \right)^{\mathbf{2}} \left(\frac{\mathbf{100GeV}}{\mathbf{m_X}} \right)^{\mathbf{2}}$$

➡ Electro Weak Scale(∼100GeV) WIMP naturally explains the relic abundance.

TeV scale SUSY & neutralino dark matter

Dispersional relations for active and sterile neutrinos (from real part)

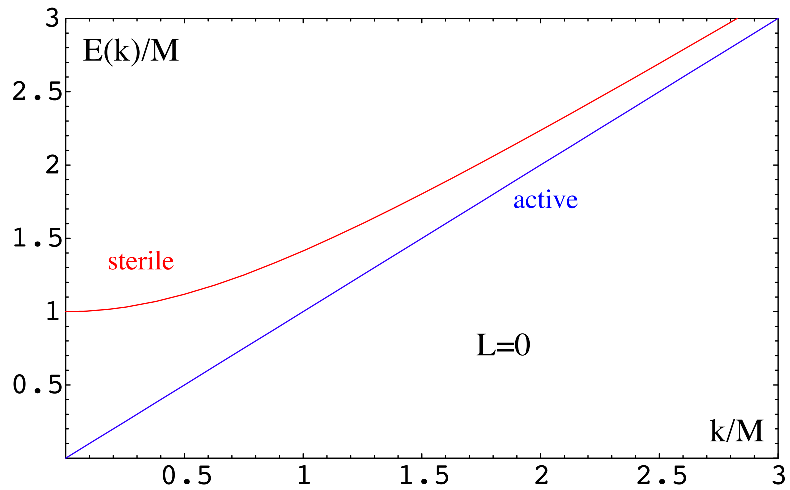

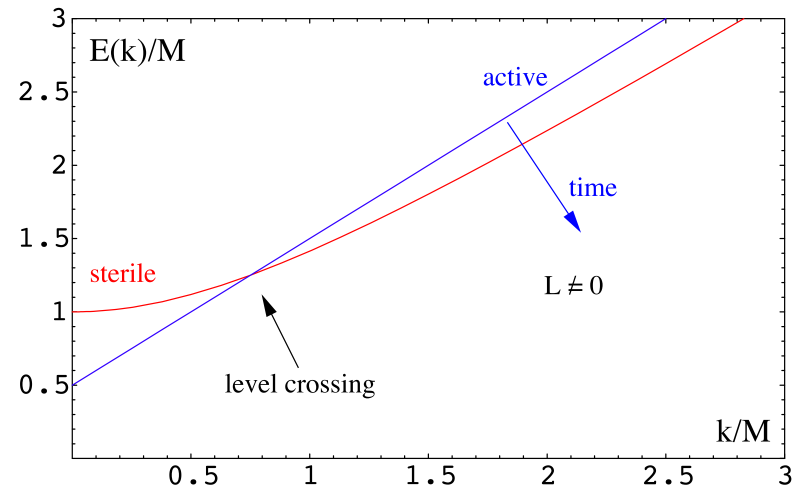

Transitions $\nu \to N_1$

Dodelson-Widrow

Zero lepton asymmetry

Resonant transitions

Shi-Fuller

Lepton asymmetry

created in $N_{2,3}$ decays

Dark matter and the Lyman-α forest.

The bounds depend on the production mechanism.

$$\lambda_{FS} \approx 1\,\mathrm{Mpc}\left(\frac{\mathrm{keV}}{m_s}\right)\left(\frac{\langle p_s\rangle}{3.15\,T}\right)_{T\approx 1\,\mathrm{keV}}$$

The ratio

$$\left(\frac{\langle p_s\rangle}{3.15\,T}\right)_{T\approx 1\,\mathrm{keV}} = \begin{cases} 0.9 & \text{for production off} - \text{resonance} \\ 0.6 & \text{for MSW resonance (depends on L)} \\ 0.2 & \text{for production at T} > 100\text{ GeV} \end{cases}$$

- Photon energy:

$$E_\gamma = \frac{M_1}{2}$$

- Radiative decay width

$$\Gamma = \frac{9\alpha_{\mathrm{EM}} G_F^2}{256\pi^4}\,\theta^2\,M_1^5$$

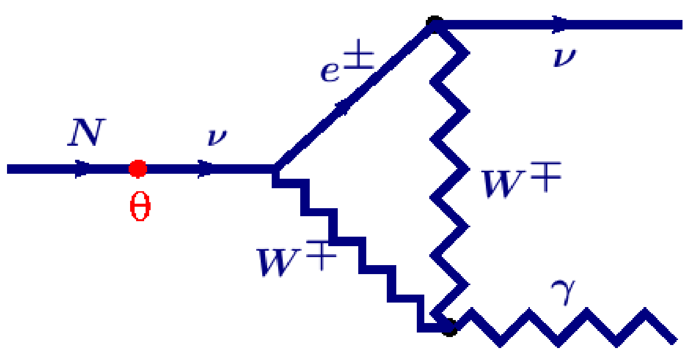

Dark matter made of sterile neutrino is not completely dark

Dolgov & Hansen (2000)

Where to look for DM decay line?

Extragalactic diffuse X-ray background (XRB)	Dolgov & Hansen, 2000; Abazajian et al., 2001 Mapelli & Ferrara, 2005; **Boyarsky et al. 2005**
Clusters of galaxies	Abazajian et al., 2001 **Boyarsky et al. astro-ph/0603368**
DM halo of the Milky Way. Signal increases as we increase FoV!	**Boyarsky et al. astro-ph/0603660** Riemer-Sørense et al. astro-ph/0603661 **Boyarsky, Nevalainen, O.R.** (in preparation)
Local Group galaxies	**Boyarsky et al. astro-ph/0603660** Watson et al. astro-ph/0605424
"Bullet" cluster 1E 0657-56	**Boyarsky, Markevitch, O.R.** (in preparation)
Cold nearby clusters	**Boyarsky, Vikhlinin, O.R.** (in preparation)
Soft XRB	**Boyarsky, Neronov, O.R.** (in preparation)

Need to find the best ratio between the DM decay *signal* and object's X-ray emission

CDM as particle Dark Matter

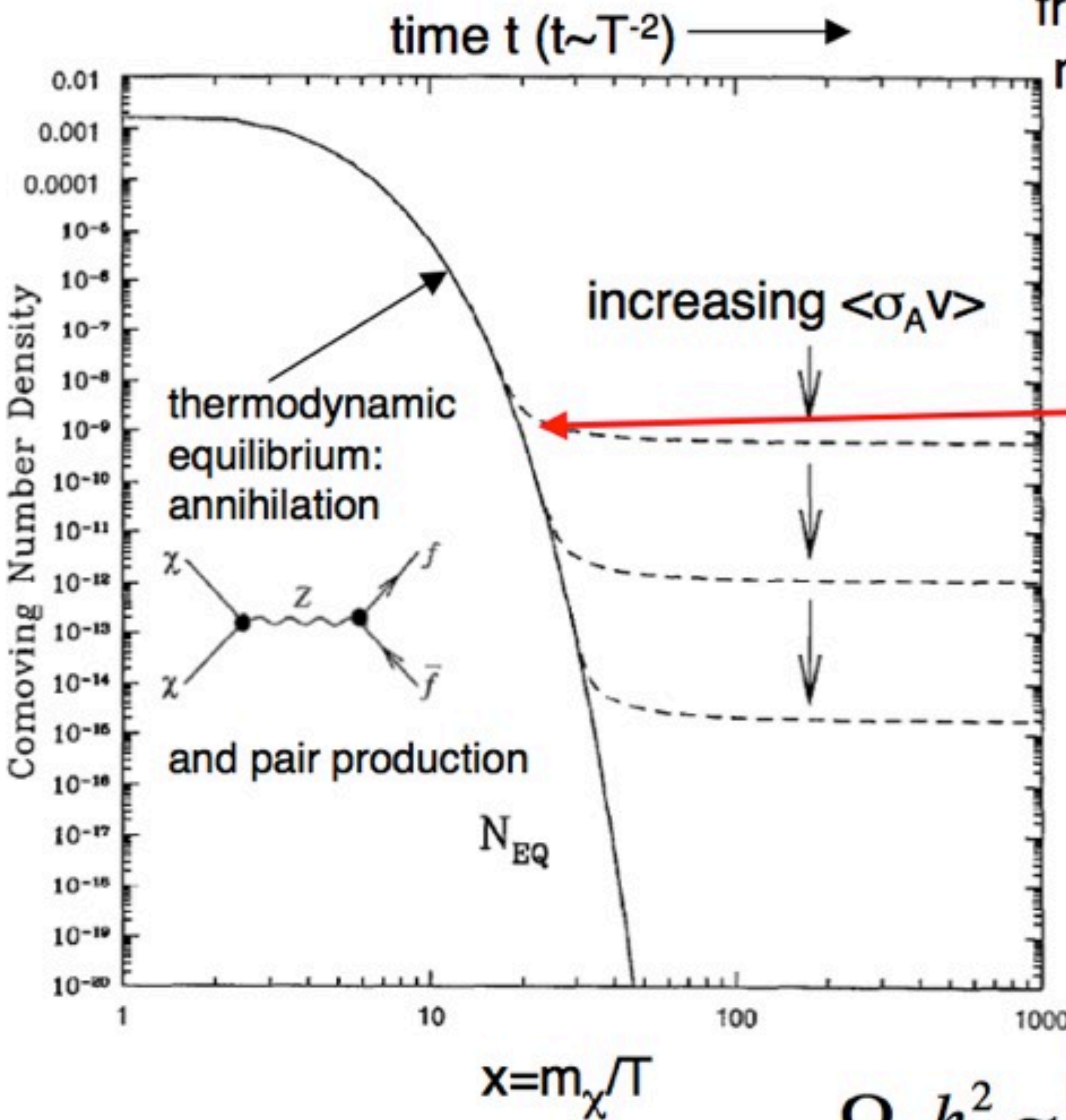

freeze-out of a weakly interacting massive particle (WIMP χ) when reaction rate drops below expansion rate

$T_{freeze-out}$~ 1/20 x m(WIMP)

Cold Dark Matter:

- non-relativistic

"survival of the weakest"

At or below the weak scale

$$\Omega_\chi h^2 \approx \frac{m_\chi n_\chi}{\rho_c} \approx \frac{3\times10^{-27}\,\mathrm{cm}^3/\mathrm{sec}}{\langle\sigma_A v\rangle}$$